RADIO METEOR ASTRONOMY

by

G. Gartrell, B.Sc. (Hons.)

A thesis
presented for the degree of

DOCTOR OF PHILOSOPHY

in the

UNIVERSITY OF ADELAIDE
(Physics Department)

May 1971

TO MY WIFE LESLYE

CONTENTS

SUMMARY

This thesis describes an investigation of the orbits of meteors detected at Adelaide (latitude 35°S) using a combined multi-station c.w. and pulse radar system. The orbit survey described is the only radio survey conducted in the Southern Hemisphere to measure the orbits of individual meteors down to a limiting radio magnitude of + 8. The equipment was operated for one week each month from December 1968 to June 1969 with a further run during October 1969. To date 1667 orbits have been determined from six months of data.

Reflections from a minimum of three and a maximum of five points along the trail were used to determine the radiant and velocity. A long-distance outstation enabled occasional measurements of reflection point separations as large as 16 kms., although the majority of reliably determined separations were of the order of 6 kms. or less. The equipment was simultaneously used to measure meteor region winds and wind shears, enabling account to be taken of these factors in the determination of the radiant and velocity data.

Distributions of the various geocentric and heliocentric quantities show broad agreement with those from other surveys conducted along similar lines, although the present data contain a significantly larger proportion of high velocity meteors than other surveys to a comparable limiting magnitude. This is attributed to a selection effect in data reduction as well as the use of the extremely clear pre-specular reflection point diffraction waveform available in a coherent phase system for the determination of velocity.

Measurements of deceleration have been carried out for each meteor of the survey. Although a wide range of decelerations and even accelerations was observed, no doubt in part due to velocity measurement errors combined with small reflection point separations, the longer reflection point separations afforded by the distant outstations have enabled computation of surface area/mass ratios from measured mean decelerations. Estimates of the average mass, size and density of the meteors detected have been made, dependent upon assumptions regarding the ablation energy, the ionizing efficiency and the magnitude. The action of a height selection effect acting on meteor density is apparent.

Comparison of the present density estimates with other data indicates that average meteor bulk densities increase with decreasing mass. This gives support for an agglomeration model of meteor formation, although fragmentation does not seem to be pronounced amongst the present radio meteor population.

In addition to the well-known helion, antihelion and apex concentrations of apparent meteor radiants this survey confirms the existence of a lesser concentration centred on the longitude of the apex at ecliptic latitude - 60°. Both this and the apex concentration are virtually removed when account is taken of observational and astronomical selection factors although a strong extended high latitude concentration remains. Comparison of the radiant distributions with similar distributions for Northern Hemisphere data shows marked symmetry about the ecliptic.

The data has been systematically searched for stream meteors and the significance of minor associations has been re-appraised. Altogether 40.4% of the orbits were found to be associated with at least one other orbit within the limits of resolution of the measurement technique. This figure drops to 29.8% when associations of pairs only are excluded. Numerous minor streams with high inclination and low eccentricity have been found at deep Southern declinations from December to March, with little activity in this quarter during June and October.

In addition to several previously established cometary associations a comprehensive search has indicated that 34 of the meteor associations found may be related to 17 comets. Associations between several long-period comets and low eccentricity high inclination streams appear indisputable and confirm the origin of the 'toroidal group' meteors, previously a matter of some doubt.

Preface

This thesis contains no material which has been accepted for the award of any other degree or diploma in any University. To the best of the author's knowledge and belief, this thesis contains no material previously published or written by another person, except where due reference is made in the text of the thesis.

(Grant Gartrell)

Acknowledgements

The project described in this thesis was carried out within the Department of Physics of the University of Adelaide under the supervision of Dr. W. G. Elford. The author would like to thank Dr. Elford for suggesting the project, for helpful discussions and particularly for his reassurance and encouragement throughout the course of the work. The author would also like to thank Dr. C. S. Nilsson for suggestions during the latter stages of the project.

The building, operation and maintenance of the radio meteor system was very much a cooperative concern. Without the assistance of a number of people the work outlined in this thesis would have been impossible. The author is indebted to his colleague Dr. B. J. McAvaney, who, in collaboration with Mr. J. W. Smith, designed some of the outstation and tape delay system equipment. Dr. McAvaney also shared with the author the responsibility for operation and maintenance of the multi-station system. Thanks are also due to Mr. N. Brown for assisting with the equipment operation. Mr. E. J. Welsby is to be complimented on his craftsmanship in construction of the equipment, and his careful maintenance of the transmitters. Mr. Welsby could be relied upon to give cheerful assistance with equipment operation and repairs during times when lesser spirits would surely have faded.

Some of the basic data reducing computer programs were formerly created by Dr. Nilsson and have been extensively modified by Dr. McAvaney and the author for use with this project. Dr. Elford supplied

the Southworth and Hawkins stream sorting program, which required only minor modifications in adaptation to the local computing facilities.

The author would like to thank the Director, Weapons Research Establishment, Salisbury, for making facilities available for film-reading, and Miss N. Mott for her advice and help during this seemingly endless task.

Misses Janice Gordon, Judy Hearse, Rille Walshe and Suzanne Spain were involved with the preparation and processing of the recording films.

Finance for the radio-meteor project was provided by the National Aeronautics and Space Administration, U.S.A. (Grant NGR 52-042-004), Australian Research Grants Committee (Grant No. B66-16370), Radio Research Board, Australia and the University of Adelaide. The author is grateful to the University of Adelaide for a University Research Grant in the early stages of the work. The major portion of the work was carried out while the author was employed as a Demonstrator in the Department of Physics. The author would like to thank the Director, Weapons Research Establishment, Salisbury, for granting leave of absence to undertake the study, and for providing support which has enabled the completion of this thesis.

CHAPTER I

INTRODUCTION

At the end of the eighteenth century Brandes and Benzenburg in Germany observed meteors simultaneously from locations several kilometres apart, and for the first time established that these objects were travelling with velocities of planetary magnitude and appeared about 100 kilometres above the surface of the Earth. During the intense Leonid shower of 1833 numerous observers noted that the meteors appeared to be radiating from a point. Olmsted is accredited with the deduction that the meteors of this shower were therefore travelling in parallel paths, with the divergence a result of perspective.

The elliptic nature of meteor shower orbits was confirmed by the predicted return of the Leonids in 1866, and associations between several streams and comets were noted. The disintegration of Biela's comet in the mid-nineteenth century and the subsequent spectacular enhancement of the Bielid stream gave further strong evidence to suggest that stream meteors may be fragments from comets.

Visual observations are still an important section of meteor astronomy today, and photographic recording of meteor trails is a natural extension of this. Improvements in film emulsions and camera design, in particular the development of the Super-Schmidt camera, have enabled the photographic recording of meteors only about one magnitude brighter than the normal limit for unaided visual observation. Öpik (1934) designed a rocking mirror device to improve the

accuracy of visual determinations of meteor velocity. The observer looked at the meteor trails in the mirror, which superposed circular motion of known frequency on the uniform motion of the meteor, producing an apparently cycloid path of characteristic shape. A calibrated rotating shutter performs the same function in the majority of meteor cameras today. A recently developed sensitive optical method for meteor observation is that of electronic image amplification using the Image Orthicon camera (Hicks et al. 1967)

The advent of radio meteor astronomy, like that of meteor astronomy itself, is linked with the confirmation of theories by observations of the Leonid shower. In the period 1929 - 1930 a number of radio researchers noticed transient ionization changes in the night-time E region, which were subsequently proved to be of meteoric origin by correlation with visual observations during the 1931 and 1932 returns of the Leonid shower. Observations of meteor ionization seem to have been from the view-point of communications engineering until after World War II when serious astronomical studies were initiated. The improvement in radio detection rates over those of visual and photographic techniques, particularly for low frequency radars, was quite startling. Radio methods in addition were not restricted to clear skies and night-time observation, and quickly revealed the presence of a number of major day-time streams.

Radar frequencies higher than about a hundred megahertz were found to be unsuited to the study of meteor trails, although sufficiently powerful radars operating as high as 500 MHz have been used to detect 'head-echoes' from local ionization near the meteoroid itself.

The usual form of reflection of radio waves with wavelengths of the order of several metres is specular in nature, and reflected waves will only reach the receiver when the trail is suitably located along the particle trajectory. As discussed in §3 the application of fresnel diffraction theory in this case enables analysis of the reflected signal for determination of the meteor velocity. The velocity may also be determined for head-echoes of sufficient duration from the rate of change of the radar range with time. A variation of the latter technique was used by Evans (1966) who directed a high-power radar at the radiants of several major meteor showers and measured meteor velocity directly from the doppler shift in the radar frequency for reflections from meteors travelling radially down the beam. Further reference is made to this work in §6.4.

Early radar studies with single equipments determined range for individual meteors, but could measure radiant rate distributions only in a statistical manner from a knowledge of the directional characteristics of the aerials used. Gill and Davies (1956), by the addition of two extra receivers several kilometres away from the main station transmitter and receiver were able to extend the method to the determination of individual meteor radiants by triangulation, and individual velocities by analysis of the diffraction waveforms, thus enabling the computation of individual orbits.

Manning, Villard and Peterson (1949) pioneered the use of continuous wave (c.w.) radio systems in the detection of meteors. By locating

the receiving site in a favourable position several kilometres distant from the transmitter they were able to prevent the ground-wave from saturating the receiver, while still using it as a phase reference with which to compare the sky-wave from the meteor. The diffraction wave-forms in this case occur both before and after the specular reflection or 't_o' point, although as outlined in §3 bodily motion of the trail due to upper atmosphere winds will produce a progressive phase change between ground and sky-waves and a resultant large amplitude low frequency doppler beat which generally obscures the post-t_o diffraction pattern. The technique thus affords a method for measurement of upper atmosphere winds as well as meteor velocity.

By itself the c.w. technique does not give any indication of range. Manning et al. (1952) overcame this problem with the development of a coherent-phase pulse radar.

Robertson, Liddy and Elford (1953) at Adelaide used a c.w. system (the fore-runner of the present apparatus) with 50 Hz saw-tooth phase modulation for determination of the sense of the wind drift (§3.3.3) and a superposed 10 μ-sec pulse for range measurement. For observation of a large portion of the sky low gain dipole aerials were used and an ingenious method for determining the direction of arrival of the received signal was developed. Phase comparisons made between signals at various aerials of an array, taking advantage of the low frequency phase information in the wind doppler, were sufficient to determine unambiguously the direction of arrival of the reflected wave. This

technique is still employed in the present system (§4.2.3). Further development of the Adelaide equipment to the present multi-station system is described in §4.1.

Despite the large numbers of meteors observed with optical and radio techniques, very few meteorites are found. The majority of meteors detected by these methods are thought to vaporise almost completely before reaching the ground. Recent work (McCrosky and Ceplecha, 1969) indicates that even the brightest such meteors may generally have properties markedly different from those of the compact stony and metallic meteorites which occasionally reach the surface of the Earth.

At the other end of the scale extremely small particles will have a large surface area to mass ratio and may be decelerated effectively to rest on entering the atmosphere without being completely vaporized. Study of these particles has been made possible by the use of rocket and satellite-borne impact detectors. Sun orbiting space probes also make it possible to detect streams of meteors not intersecting the orbit of the Earth. One obvious disadvantage of such studies is the restricted size of the detecting area available, making statistically reliable and representative sampling generally beyond the life-time of the experiment. In comparison radio and optical methods have the entire world as a detector by virtue of the enveloping atmosphere.

Impact detectors may be separated into two classes, recoverable and non-recoverable, neither of which is free from problems. Recoverable rocket payloads may include devices which expose surfaces above the

atmosphere for collection and subsequent physical examination of micrometeoroids or particle impact craters. Berg and Secretan (1967) examined a specially prepared surface after flight for craters produced by micrometeoroid impacts. The inherent surface defects of even the most highly polished optical surfaces necessitated exhaustive pre-flight surface scanning to map such defects, as well as the flight of a control surface not exposed to impact.

With the collection of micrometeoroids themselves (e.g. Soberman et al., 1963) a major problem is the prevention and identification of contamination of the collecting surfaces by terrestrial dust, both in the laboratory before and after flight, and during the activation of the experiment in flight, when dust may be transferred from other portions of the rocket.

Satellite-borne non-recoverable devices must record impacts in a manner suitable for telemetry. A variety of electronic devices have been designed to record impact parameters and penetrating abilities of micrometeoroids. Thorough pre-flight testing of any detector under all possible conditions of operation is necessary to ensure that the events recorded are of meteoroidal origin. Doubts exist as to the reality of some events detected using some types of acoustic sensors (Nilsson, 1966).

Nilsson and Alexander (1967) describe the flight on the OGO-1 satellite of an array of sensors each with two detectors separated by a known distance. Velocity measurements of particles intersecting both

detectors were made by timing the particle from the first to the second. The sensor acceptance angle for such particles gave some indication of the direction of arrival, thus enabling estimates of the orbital elements to be made.

Studies of meteoroids of all sizes are of paramount importance to the planning of future space ventures as well as possible leading us to an understanding of the Solar System. Each of the branches of meteor astronomy yields important information in its own right, but each sees only a section of the picture. While this thesis describes work carried out in the field of radio meteor astronomy many of the conclusions reached come from the comparison of this work with the results of investigations in other branches of the discipline.

One should remember that the division between 'radio meteors' and 'photographic meteors' does not imply a fundamental division in the properties of meteors, but merely indicates the limits of the observing methods, which fortunately overlap to some degree. Despite this, differences in the two classes of meteors do exist. Some meteors produce easily visible trails without much ionization, and some ionize strongly without visible radiation. As will be outlined in §2. radio meteor studies can observe a class of meteors too faint for photographic observation which does appear to have properties quite distinct from the larger photographic meteors.

§2 reviews present knowledge of the astronomical significance of meteors pertinent to the study described in this thesis. An outline of

the theory of reflection of radio waves from meteor trails, upon which the data reduction techniques are based, is given in §3. while Chapters 4 and 5 respectively describe the Adelaide Radio Meteor System and the method of data reduction.

Because of a lack of information about the physical nature of small meteoroids, correction of observational data for atmospheric deceleration has generally been the area of greatest uncertainty in meteor orbit calculations. §6 is concerned with the information available from direct measurements of meteoroid retardation undertaken in this survey. As well as confirming the reliability of the orbit computations these measurements have been used to provide estimates of meteoroid densities and mass.

§7 describes a systematic search for meteor streams amongst the present data. Comparison is made with the orbits of streams found in other surveys, and with the orbits of comets listed in the index-list of predicted meteor radiants computed by Hasegawa (1958). The distribution of meteor orbits in space is examined in Chapter 8. The relationship of stream meteors and sporadic meteors is considered, as well as implications of the distributions in regard to the origin and evolution of the meteor population.

The main conclusions of this study are outlined in §9, and while the implications for cosmogony are by no means conclusive, the results of the various sections of this study do have a reassuring degree of coherence. Reference is made to recent work on comets which supports these conclusions, and suggestions are made concerning worthwhile areas for further investigation.

This study has involved the handling of large quantities of data, and being largely observational in nature this thesis is necessarily lengthy. The major portion of the data upon which the thesis is based is not included, but may be found elsewhere (Gartrell, 1971). A list of meteor associations found during the systematic stream search is included in this thesis as an appendix.

The work described is only the second radio survey of individual meteor orbits to be undertaken in the Southern Hemisphere, and the first to limiting magnitude $M_R = +8$. The previous survey (to limiting magnitude $M_R = +6$) was also carried out at Adelaide and has been described by Nilsson (1964b). Additional receivers and larger base-lines have been incorporated in the system to enable measurement of deceleration of individual meteoroids. The new information on small meteoroids provided by this survey is not only important because of its Southern Hemisphere orientation, but should add considerably to our general understanding of meteor astronomy.

CHAPTER II

RADIO METEOR ASTRONOMY - A REVIEW

The purpose of this section is to outline recent developments and current ideas in radio meteor astronomy which are pertinent to the subject matter of the research project described in this thesis. No attempt is made to review statistical methods of radiant determination, nor to consider the meteor magnitude - flux relationship beyond its application to the present survey. As noted in §8.2.2 amplitude measurements for individual echoes have not yet been undertaken for this survey, so that no direct measurement of individual meteor magnitudes is possible.

Elford (1967) compares a number of determinations of the exponent s of the incremental flux distribution function expressed as a power law

$$dN(q_Z) \propto q_Z^{-s}\, dq_Z \qquad (2.1)$$

for the numbers of meteors $dN(q_Z)$ producing zenithal electron line densities in the range q_Z to $q_Z + dq_Z$. Elford finds that for sporadic meteors fainter than radio magnitude $M_R = +9$, where $M_R = 40.0 - 2.5 \log_{10} q_Z$, the value of s is 2.0 ± 0.05 and increases by about 0.5 for brighter magnitudes.

A similar comparison for major meteor showers shows the value of s to drop well below 2 for faint magnitudes, indicating that these showers become relatively less important with increasing magnitude.

The main consequence of such a flux law for the present survey is that the great majority of meteors detected will have electron line

densities near the equipment threshold, so that the properties of the meteors observed will be representative of the faintest meteors detectable by the apparatus.

Lebedinets and Sosnova (1968,1969) analyze in detail the interaction of radio waves with ionized meteor trails, and find that velocity determinations from the fresnel diffraction pattern may be seriously in error if the effects of ambi-polar diffusion are not taken into account. For the reasons outlined in §3.3.5 their conclusions are not directly relevant to the Adelaide method of velocity determination, which uses the pre-t_o diffraction pattern and is much less sensitive to the vagaries of diffusion than the more common use of the post-t_o diffraction pattern.

Brown and Elford (1970) have determined theoretically that the rate of decay of an ionized trail may be strongly affected by wind shear without affecting the exponential form of the decay. This may result in serious errors where decay rates are used to determine reflection point heights, and may introduce further errors into the determination of velocity from the post-t_o diffraction pattern. The Adelaide system determines wind shear for each echo and allowance is made for this in the analysis.

Verniani (1969) has recently reviewed the present knowledge on the structure of meteoroids. He finds that there is evidence to suggest that fragmentation is widespread even amongst faint radio meteors. The same conclusion has not been reached in the present survey although it is doubtful whether fragmentation can be readily recognized from the diffraction patterns alone.

Jones and Kaiser (1966) have shown that thermal shock from atmospheric heating may cause fracture of dense solid meteoroids with radii larger than 0.1 cm. While their results do not appear to be applicable to the majority of meteors detected in the present survey, it is probable that thermal shock is a contributing factor in the fragmentation of low density meteoroids.

Verniani finds the average bulk density of photographic meteors to be about 0.3 gm cm^{-3} whereas the median value of density for 320 radio meteors detected at Havana, Illinois, was close to 0.8 gm cm^{-3} (Verniani, 1966). Ceplecha (1967) has approached the problem of meteoroid density determination from quite a different stand-point to Verniani, and from a consideration of meteoroid thermal conductivity in relation to the temperature at which ablation becomes pronounced, has arrived at density estimates an order of magnitude higher. Ceplecha has demonstrated that meteors may be classified into three distinct groups on the basis of beginning height as a function of meteor velocity. The three groups apparently correspond to different classes of physical properties of the meteoroids, and Ceplecha's criterion has been applied with some success to the classification of meteor stream members by Cook (1970).

Results of density determinations in the present survey, however, are in excellent agreement with those of Verniani (1966). Verniani's median radio meteor density of 0.8 gm cm^{-3} is slightly higher than that for the Adelaide meteors of 0.65 gm cm^{-3} consistent with the magnitude differences between the Adelaide and the fainter Havana meteors.

Accurate and routine height measurements for each echo have enabled the present survey to show a dependence of meteoroid density on height which indicates that Ceplecha's density estimates may be too high.

McCrosky and Ceplecha (1969) consider the observed properties of bright fireballs in terms of a number of variations of the single body meteor theory. They conclude that fireballs must also have low densities, and find that it is unlikely that fragmentation or spallation could seriously influence the bulk density estimates. They also reject a model proposed by Allen and Baldwin (1967) of a high density meteoroid frothing due to the release of occluded gas on ablation and so having the appearance of a low density meteoroid. For a different reason the results of the present survey also suggest that frothing cannot be significant for faint radio meteors (§6.4).

Observations of faint radio meteors at Jodrell Bank (Davies and Gill, 1960) have indicated in addition to the predominantly direct orbits of low inclination the presence of a large number of meteors in orbits of low eccentricity and high inclination not apparent at brighter magnitudes. In contrast Nilsson (1964b) at Adelaide in a survey to $M_R = +6$ observed few orbits of this type and virtually none with eccentricities less than 0.6.

Davies and Gill suggested that these meteors may be derived from a hypothetical dust cloud beyond the orbit of Jupiter, with the Poynting-Robertson effect (Poynting, 1903; Robertson, 1937) causing sufficiently

rapid orbit evolution in the case of small particles to enable them to pass the 'Jupiter barrier' at high inclinations.

Hawkins (1962) reported that this class of 'toroidal' meteor orbits was detected during the Harvard Radio Meteor project. Lebedinets and Kashcheev (1967) have also detected these orbits amongst meteors brighter than magnitude + 7 at Kharkov. Lebedinets (1968) shows that the dust-cloud source proposed by Davies and Gill (1960) for these orbits is not consistent with the observed distribution, which points rather to a connection with the long-period comets.

Southworth (1968) in discussing the results presented by Lebedinets (1968) notes that although the Harvard-Smithsonian observations are similar to those from Kharkov, the conclusions are very different, no doubt because of different corrections for observational selection.

Kashcheev and Lebedinets (1967) classify orbits observed during their radio survey into four basic types:

(1) Orbits similar to those of long-period comets, with high a values and arbitrary inclinations.

(2) Orbits similar to the short-period comets with $a < 5$ a.u. and small inclinations.

(3) Orbits with small eccentricities and large inclinations.

(4) Orbits similar to type (2) but with smaller perihelion distances and sizes ($a \lesssim 3$ a.u.).

Types (3) and (4) are pronounced at faint radio magnitudes and virtually absent from bright photographic meteor observations, although the Geminids and δ-Aquarids are exceptions to the rule, having orbits of

type (4). All four orbit types have been observed during the 1969 Adelaide survey.

Whereas Lebedinets (1968) finds notable differences between the distributions of shower and sporadic radar meteors the present survey has found the distributions to be similar, possibly as a result of different criteria used for meteor association.

The former sharp distinction between shower and sporadic meteors amongst bright photographic meteors may account for Davies and Gill (1960) considering only 2% of their radio meteors to be of stream origin. Systematic stream searches (Southworth and Hawkins, 1963; Nilsson, 1964b; Baker and Forti, 1966; Kashcheev and Lebedinets, 1967) have found between 25% and 36% of the meteors observed to belong to streams of some kind. The concept of minor streams and 'associations' has been introduced, and stream searches have been made using electronic computers on the basis of an idealized model of stream dispersion (Southworth and Hawkins, 1963) for accurately reduced photographic orbits, and measurement error (Nilsson, 1964b) for less accurate radio data. The results of recent stream searches based upon versions of the Southworth and Hawkins D-criterion by Lindblad (Lund Observatory, Sweden) and Sekanina (Smithsonian Astrophysical Observatory) (Ceplecha, 1970) are not yet available to the author.

The Southworth and Hawkins D-criterion has been applied in a stream search amongst meteors of the present survey. Results are in general agreement with other such stream searches, but indicate that a flexible

approach to stream definition is desirable. Definite serial associations have been found departing radically from idealized models of stream formation and dispersion, indicating that much more consideration must be given to the mechanisms of meteor ejection from comets.

Numerous streams have been found amongst the 'toroidal' meteors with orbits of type (3), and the link between this class of meteors and the long-period comets has been confirmed. The Southern Hemisphere Puppid/Velid stream complex and the Northern Hemisphere Quadrantids are examples of 'toroidal group' meteor streams.

Lovell (1954) compares an orbit for a photographic Quantrantid calculated by Jacchia with the radio observations of Hawkins and Almond. Agreement is excellent, although the eccentricity of the radio Quadrantids is much lower than that for the photographic meteor orbit, in keeping with the mass dependent action of the Poynting-Robertson effect.

Hamid and Youssef (1963) demonstrate that secular perturbations may induce large changes in meteor orbits. They find that the Quadrantid stream has changed in inclination from 13° to 72° and in perihelion distance from 0.07 to 0.98 a.u. during the last 1700 years. The large increase in perihelion distance is particularly surprising. Their calculations indicate another possible source of toroidal group meteors. It is evident that meteors in low inclination orbits are more likely to be perturbed into orbits of high inclination than vice-versa. One argument against the present configuration of the Quadrantids resulting from secular perturbations is that Southworth and Hawkins (1963) have found

the Quadrantids to be a particularly active stream photographically, with an internal dispersion comparable to the Geminids and smaller than almost all other streams observed. Such a small internal dispersion in a stream which has undergone changes of the magnitude suggested by Hamid and Youssef (1963) seems most unlikely. It is also apparent that secular and periodic perturbations should act differentially on the photographic and smaller radio meteor orbits once differences in these orbits become established through differential action of the continuously-present Poynting-Robertson effect. Thus the observed close agreement in inclination and orientation of the orbits for the two types of observation, considered in the light of smaller dimensions of the radio meteor orbits again casts some doubt on the contribution of secular perturbations to the present Quadrantid stream. Further detailed studies of this stream, particularly at faint radio magnitudes, may provide the answers to this problem.

Kresák (1968) surveys modern knowledge of the structure and evolution of meteor streams. He shows that association tests based upon radiant data will favour retrograde orbits whereas those based upon orbital elements will not be similarly biassed. He is thus able to account for the discrepancy in the results of Kashcheev et al. (1967) who find a prevalence of retrograde orbits amongst shower meteors larger than $M_R = +7$, and the results of Nilsson (1964b) who finds the inclination to be less than 50° for 90% of radio shower meteors larger than $M_R = +6$.

Kresák (1968) in considering the proportions of stream and sporadic meteors dispersing and spiralling towards the Sun under the influence of the Poynting-Robertson effect finds that "it appears inevitable to conclude that most of the meteoroids capable of producing visual meteors do not accomplish the whole cycle of spiralling but are destroyed at larger distances from the Sun".

Three destructive processes for meteors are considered by Kresák (1968), all involving collision of some kind.

(1) Erosion by interplanetary dust and sputtering by solar protons.

(2) Destructive collision in one impact between two meteoroids of similar size.

(3) Intermediate cases of hyper-velocity impact breakage combined with mass losses due to evaporation.

Eventual bursting as a result of solar radiation induced accelerating rotation has been proposed as another means of destruction of meteoroids (Radzievskii, 1954; Paddack, 1969). The practical contribution of such rotational mechanisms to the depletion of the meteoroid population is a matter of some doubt.

In a comprehensive theoretical analysis of the present observational evidence Dohnanyi (1970) finds the distribution of sporadic meteoroids in the photographic and radio ranges to be unstable. He shows that collisional processes would rapidly change the distribution of these particles unless they are replenished by a source. Meteor

showers are found to be a suitable source provided that the population index $\alpha = 13/6$, where $N \propto m^{-\alpha+1}$ is the influx rate into the earth's atmosphere (m^{-2} sec^{-1}) of objects having a mass of m (Kg) or greater.

Following Wyatt and Whipple (1950), Dohnanyi computes the time required for a shower particle to change the true anomaly of the intersection of its orbit with the earth's orbit by 5° through the action of the Poynting-Robertson effect. Comparison with the expected lifetime for an equivalent particle through collision processes indicates that radiation damping plays only a minor role in determining the mass distribution of photographic and radio meteors.

Terenteva (1967) in examining the distribution of minor streams of optical meteors finds a tendency for symmetrical disposition of radiants across the plane of the ecliptic at much larger distances even than the well-known Northern and Southern branches of the Taurids, δ- and i-Aquarids. Perturbations and erosion by interplanetary dust will be most pronounced near the ecliptic plane, and thus such branching of a low-inclination stream may give an indication of its age.

Terenteva notes such symmetrical radiants may be separated by as much as 50°. This is apparently evidence for the reality of secular perturbation such as that proposed by Hamid and Youssef (1963) for the Quadrantids, since for a meteor stream initially spreading across the ecliptic plane those meteors spending most of their time below the ecliptic would be perturbed in the opposite sense to those spending most time above. A division of the stream into Northern and Southern branches

could thus come about even without erosion near the ecliptic plane by interplanetary dust.

The delineation in the present survey of a large number of minor streams including many in the 'toroidal group' is particularly interesting in view of the agreement between a number of the latter and some long-period comets.

The questions raised in this survey by apparent anomalies in the relation of high inclination meteors to long-period comets, in general as well as in particular cases, may be of fundamental cosmogonic importance. Further consideration is given to these questions in Chapter 9.

CHAPTER III

RADIO REFLECTION FROM METEOR TRAILS

3.1 INTRODUCTION

An adequate understanding of the process of reflection of radio waves from meteor trails is a vital pre-requisite to the implementation of the survey described in this thesis. A brief summary of the pertinent points of the theory is presented here. McKinley (1961) gives a more detailed account.

The main points to be considered are the interaction of the meteoroid with the atmosphere which produces an ionized column, the effect of any subsequent motion of the column, and the interaction of radio waves with the ionized column.

3.2 TRAIL FORMATION

Observed meteoroids generally enter the atmosphere with highly supersonic velocities, between 10 kms/sec and 70 kms/sec. Collisions with air molecules result in a loss of forward momentum accompanied by a heating effect. Öpik (1958) discusses in detail the interactions possible for various combinations of meteoric and atmospheric properties. In the main, neutral atoms of the meteor are ablated from its surface by the heating effect and travel with thermal energies relative to the meteor until colliding with surrounding relatively stationary air atoms with resultant ionization, both of meteor and air atoms. The mean free path of air molecules determines the probable distance travelled by a

meteor atom before ionizing collision and hence the initial radius of the ionized column produced by the meteor at any height.

The initial radius at a height of 100 kilometres is of the order of 1 metre or slightly larger (Greenhow and Hall, 1960; Bayrachenko, 1965) while the mean free path at this height is of the order of 10 cms (U.S. Standard Atmosphere, 1962).

Once formed the ionized column will eventually decay through the effects of ambi-polar diffusion, and to a lesser extent, recombination and attachment. Meteors have been suggested as a source of ionization for the night-time E layer (Nicolet, 1955). A meteoric origin seems probable for long-lived metallic ions associated with the occurrence of sporadic E (Young et al., 1967), and a correlation has been noted between sporadic E occurrences and the Leonid meteor shower of November, 1965 (Wright, 1967).

Since ablation results in a decrease in the mass of the meteoroid and since the atmospheric properties change markedly with height, it is apparent that the production of ionization along the trail will be far from constant. In general this reaches a maximum shortly before either strong deceleration or more commonly complete vaporization terminate the observable trail. Verniani (1961) outlines in detail the equations describing the behaviour of an ablating meteor in the atmosphere.

Perhaps the greatest limitation in this work is the lack of knowledge of the actual form of the meteoroid itself. Modern thought generally favours the idea of a fairly low density porous fragile

structure for the majority of small meteoroids (Verniani, 1964) and even for large fire-balls (McCrosky and Ceplecha, 1969). This structure is thought to account for the observed fragmentation of some meteors, although the incidence of fragmentation does not appear to be an important factor amongst faint radio meteors according to Weiss (1960a) and the present survey (§6.4).

3.3 REFLECTION OF RADIO WAVES BY METEOR TRAILS

The basic feature of reflection of radio waves by meteor trails which makes the Adelaide radio technique so useful is the specular nature of the reflection process. This enables us to use fresnel diffraction theory to determine meteor velocity at the reflection point. and to determine the orientation of the trail from geometrical constraints.

It should be mentioned that while reflection of radio waves from meteor trails is generally specular in form this need not always be the case. Barber, Sutcliffe and Watkins (1962) at Jodrell Bank have observed at frequencies of several hundred MHz a class of echoes in which the specular condition for reflection is relaxed. These would appear to be some form of head echo. McIntosh (1962, 1963) discusses observations of head echoes with the 32 MHz Springhill meteor radar, and notes that there has been some confusion and uncertainty in the past as to what constitutes a true head echo. A recent survey of various types of radio reflections from meteor trails has been made by Millman (1968).

A number of workers including Lovell and Clegg (1948), Herlofson (1951), Kaiser and Closs (1952), and Lebedinets and Sosnova (1968, 1969)

have considered the nature of scattering of radio waves by ionized meteor trails. The predominant radio reflection is from the trail electrons rather than the ion component, and the strength of the reflected signal is dependent upon the electron line density as well as the polarisation and wavelength of the incident radiation. Kaiser and Closs (1952) and Lebedinets and Sosnova (1968) give formal derivations of the reflection coefficients.

3.3.1 Phase Angles

The main advantage of the CW method lies in the phase information which is retreived in addition to the variations in power of the reflected signals. In the CW system the receiving sites detect a small portion of the transmitted radiation directly along a ground-path. This signal is then used as a reference against which the reflected sky-wave is compared. The separation between transmitter and receiving sites must be such that the receivers are not overloaded by the direct radiation; for optimum operation the ground wave signal strength at any receiving site should be half that necessary to produce receiver overload with the receiver gain adjusted so that galactic background or receiver noise is just perceptible at the receiver output.

If the wave at the transmitting aerial has the form

$$A_T = F_T\, e^{i\omega t} = F_T\, e^{i\phi}$$

for the simple case of coincident transmitter and receiver, the wave at the receiver from an element ds of trail at a point P has the amplitude

$$dA_R = \frac{A_T G \lambda \sqrt{2\rho}}{4\pi R^2}\, g(s)\, e^{i\psi_P}\, ds \qquad (3.1)$$

where A_T is the amplitude of the transmitted wave; G is the gain of the receiving antenna; ρ is the input resistance of the receiver; g(s) is the reflection coefficient at the point P; R is the distance from the transmitter to the point P on the trail.

For reflection from a stationary trail the phase angle of the reflected wave at the receiver is

$$\psi_P = \omega t - \frac{4\pi R_P}{\lambda} - \beta \qquad (3.2)$$

where β is the phase change on reflection and $\frac{4\pi R_P}{\lambda}$ is the phase angle due to the length of the path travelled by the wave.

Should the trail have a radial component of velocity u towards the transmitter-receiver site we should include an additional time-dependent term such that

$$\psi_P = \omega t - \frac{4\pi R_P'}{\lambda} - \beta + \frac{4\pi u}{\lambda}(t - \tau) \qquad (3.3)$$

where $\tau = 0$ when $R_P' = R_P$.

This expression is given since it clearly shows the relative senses of the various contributory phase terms. However, because of additional complications concerning the motion of the trail as a whole under the influence of a wind it is simplest to investigate the properties of a stationary trail first and then take account of the effects of wind and wind shears (Kaiser, 1955).

It should be noted that some workers (e.g. Kaiser, 1955; McKinley, 1961; Kashcheev and Lebedinets, 1961) have employed the

optics convention for describing phase, in which phase angle increases with optical path length. In the present (electrical engineering) convention, however, all phases are regarded at an instant in time, and the increase in path length then corresponds to a phase lag.

The distinction between the two systems has not been made clear in the past and has led to some confusion. Provided that one consistently adheres to one convention the terms on the right-hand side of eqn 3.3 will have the same relative sense irrespective of which convention is employed, and the difference between the two amounts merely to the substitution of $-\psi$ for ψ on the left-hand side.

3.3.2 The Cornu Spiral

Integrating the contributions from all elements ds up to the point P (at a distance s_1 along the trail, see Fig. 3.1) the total received amplitude

$$A_R = \frac{A_T G \lambda \sqrt{2\rho}}{4\pi R^2} \int_{-\infty}^{s_1} g(s)\, e^{i\psi}\, ds \qquad (3.4)$$

where the lower limit of the integral may be taken as $-\infty$ since $d A_R \to 0$ as $s \to -\infty$.

It is assumed that the reflection coefficient g(s) varies sufficiently slowly with s in the region of P_o to justify its removal from under the integral for simplification of analysis, although the method of velocity determination used in this survey is quite insensitive to variations in g as well as irregular ionization (see §3.3.4).

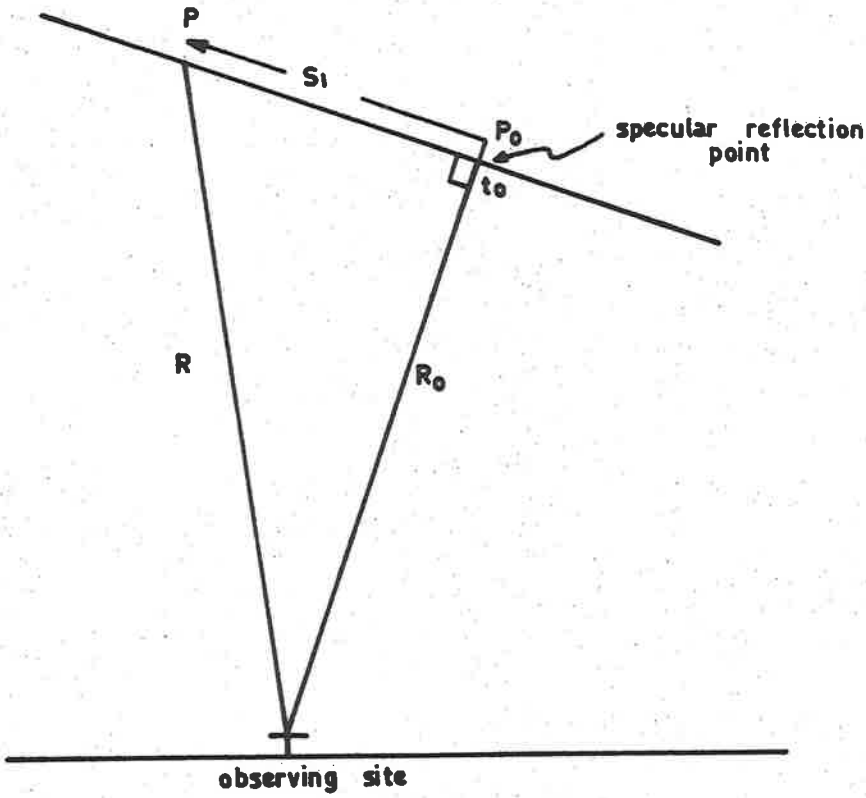

FIG. 3·1 REFLECTION GEOMETRY FOR THE CASE OF COINCIDENT TRANSMITTER AND RECEIVER.

Using the approximation $R = R_o + \frac{s^2}{2R_o}$ we may write 3.4 as

$$A_R = F_R \, e^{i\psi_o} \, (C - iS) \qquad (3.5)$$

where

$$C = \int_{-\infty}^{x_1} \cos \frac{\pi x^2}{2} \, dx, \quad S = \int_{-\infty}^{x_1} \sin \frac{\pi x^2}{2} \, dx$$

are a form of the fresnel integrals.

$$x = \frac{2s}{\sqrt{R_o \lambda}} \; ; \quad F_R = \frac{A_T G \lambda \sqrt{2\rho}}{4\pi R_o^{\,2}} \, \frac{\sqrt{R_o \lambda}}{2} \, g$$

and

$$\psi_o = \omega t - \frac{4\pi R_o}{\lambda} - \beta \; .$$

The representation of the bracketed term (C - iS) on an Argand diagram is a Cornu spiral, inverted from the optics Cornu spiral which corresponds to the function (C + iS). Figure 3.2 shows the function (C - iS) with the origin moved to the point (½ - ½i) in the usual manner. Distance along the trail corresponds to distance along the spiral, and the relative amplitude and phase contributions of any segment of the trail may be found by joining the two representative points with a straight line, the length of which gives amplitude and the argument of which gives phase. The absolute scale of the Cornu spiral is given by the magnitude of F_R which corresponds to $\frac{1}{\sqrt{2}}$ of the distance between the points (½ - ½i) and (- ½ + ½i)(= $\sqrt{2}$ reduced units). The term $e^{i\psi_o}$ gives the relative phase of the reflection from the specular reflection point R_o. In an absolute reference frame the time dependent portion ωt of ψ_o represents an anticlockwise rotation of the entire spiral about the point (½ - ½i) with angular velocity ω.

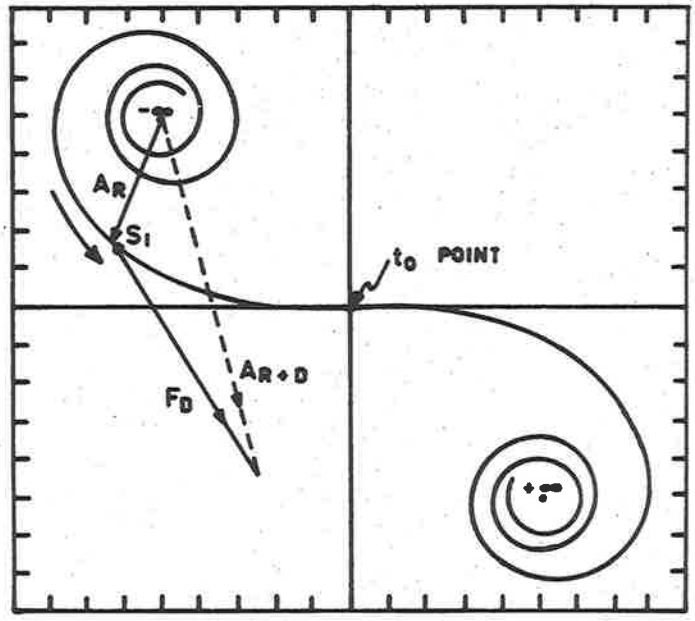

FIG. 3·2 THE CORNU SPIRAL. THIS IS VERTICALLY INVERTED FROM THE CONVENTIONAL OPTICS CORNU SPIRAL. THE ORIGIN HAS BEEN MOVED TO THE POINT $(1/2 - 1/2\,i)$.

In the CW case addition of the ground-wave causes total power at the receiver to be given by the expression

$$P_{R+D} = F_R^2(C^2 + S^2) + F_D^2 + 2F_R F_D(C \cos \psi + S \sin \psi) \qquad (3.6)$$

where

$$\psi = \frac{2\pi D}{\lambda} - \frac{4\pi R_o}{\lambda} - \beta$$

is the phase angle of the skywave relative to the ground-wave; D is the distance of the direct radio ground-path; F_D is the amplitude of the ground-wave at the receiver input. In general the time dependent variation of skywave phase keeps pace with that of the ground-wave and the time dependence may be ignored.

The resultant amplitude and phase at any time may then be found by vector addition of the ground-wave vector to the skywave vector (see Fig. 3.2). McKinley (1961) calculates theoretical amplitude-time curves for various values of the skywave phase relative to the ground-wave and $\sqrt{2}\ F_R = F_D$. These are shown in Fig. 3.3.

Since considerable use is made of the Cornu spiral and the related amplitude-time diagram, although the reverse is the true case it is convenient to regard the Cornu spiral as having the invariant phase and consider the relative phase of the ground-wave from this reference. The specular reflection point is the natural origin of the time scale for any calculations and is referred to as the 't_o' point. The preceding fresnel diffraction pattern is commonly referred to as the 'whistle' since it generates a characteristic descending audio tone when a loud-speaker is connected to the receiver output. Furthermore, in considering

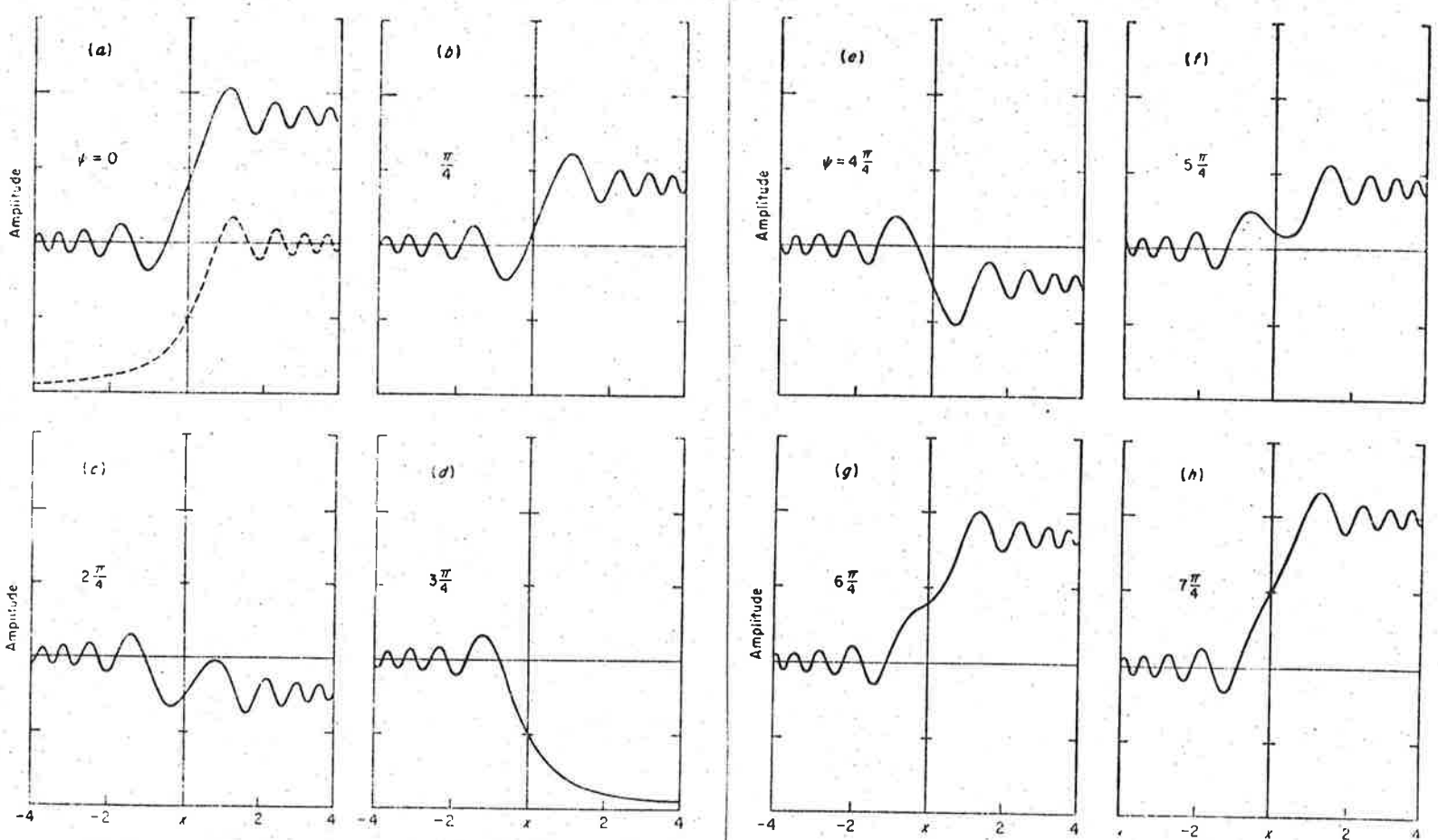

Theoretical amplitude-time curves of meteor echoes based on the diffraction theory. Receiver output voltage is plotted against the argument x of the Fresnel integrals, which is directly proportional to time. The dashed curve in graph (a) is for the noncoherent radar case. The solid curves are computed for the cw or coherent-pulse radar case, for selected values of ψ, and for equal strengths of the reference voltage and the final meteor-echo voltage.

FIG 3 . 3 AFTER Mc KINLEY (1961) .

relative times of events in the pre-t_o whistle, it is convenient to reverse the normal time scale so that these events take place at times which may be regarded as positive with respect to the t_o point as origin.

3.3.3 The Effect of Wind and Wind Shear

For a stationary meteor trail the point of closest approach and the t_o point coincide. However, when the trail is formed in a uniform wind field this condition is no longer true. Fig. 3.4 illustrates the effect of a uniform wind in changing the orientation of the ionized column from the meteoroid path AA´ to the line BB´ with a resultant shift of the t_o point from A_o to B_o. Let velocity of meteoroid be V and wind velocity u. Since $\theta = u/V$ this displacement amounts to a distance $R_o\ u/V$ or a time delay of $R_o\ u/V^2$ seconds.

Bodily motion of the ionized column also introduces a time dependence into the phase of the ground-wave relative to the skywave, causing rotation of the ground-wave vector of Fig.3.2 about the tip of the skywave vector (or vice-versa). The variation in amplitude of the resultant vector amounts to a doppler beat, the frequency of which is related to the line-of-sight wind velocity at the trail.

It should be emphasized here that the statement made by Kaiser (1955) that for a uniform wind the form and magnitude of the echo remains unchanged, and that the pattern is simply displaced in time, is only applicable to echoes from pulse-type equipments. In the case of CW equipments with some ground-wave present at the receiver the steady phase shift

$$\frac{d\psi}{dt} = \frac{4\pi u}{\lambda}$$

will result in some modification of the pre-t_o diffraction pattern, for the same reason that it produces a doppler beat between ground and sky-waves after the t_o point.

This effect is graphically demonstrated by reference to the Cornu spiral. Fig. (3.5) shows the displacement of diffraction maxima x_1, x_2, x_3 to x_1', x_2', x_3' as a result of such a phase variation. The effect is generally rather small, due to the difference of several orders of magnitude between typical meteor and wind velocities. In extreme cases, however, the degree of 'winding-in' of the spiral (or 'winding-out') could cause a displacement in the position of a diffraction maximum by as much as one cycle within the first half-dozen cycles of an amplitude-time plot.

With the Adelaide system the doppler information is used to determine the line-of-sight component of the wind at each reflection point. Knowing the phase at the t_o point, the phase information from the wind determination is extrapolated into the pre-t_o diffraction pattern so that correction for this effect is possible. (see §5.2).

The presence of wind-shear introduces further complication. In general the ionized column will become deformed and curved. The effect in most cases does not limit the accuracy of the interpretation of the amplitude-time records, particularly when dealing with the pre-t_o pattern. At the specular reflection point the angle θ of Fig. 3.4 is still given by u/V.

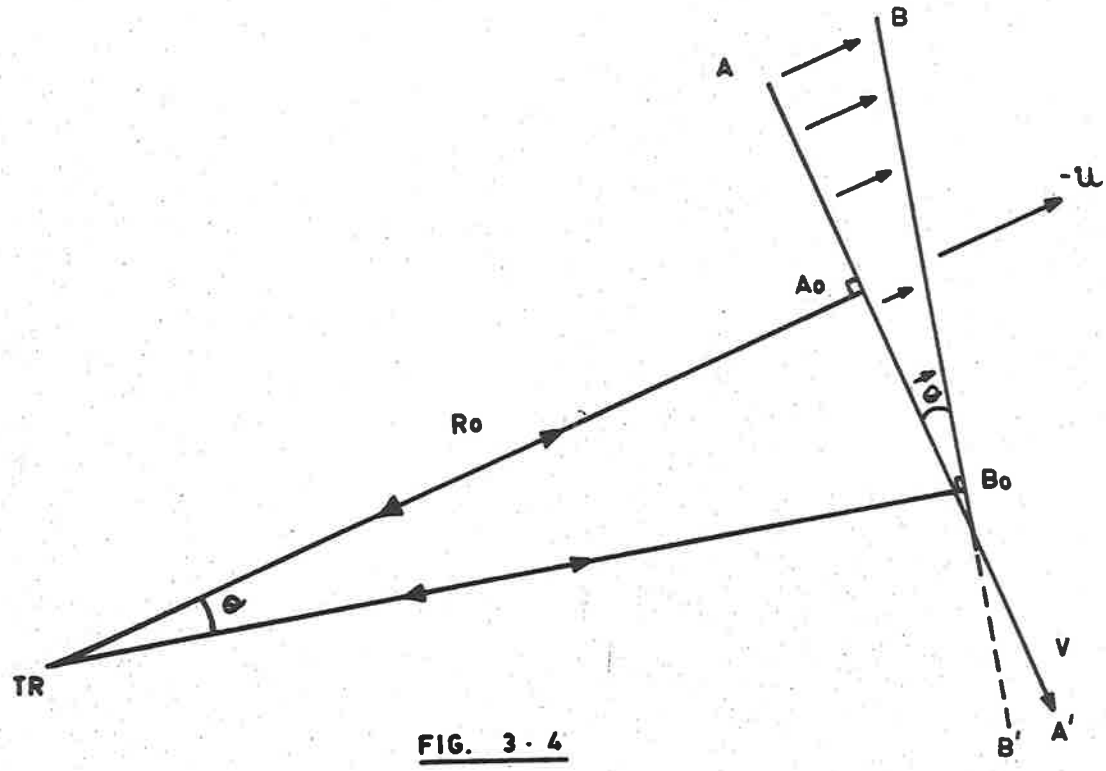

FIG. 3·4

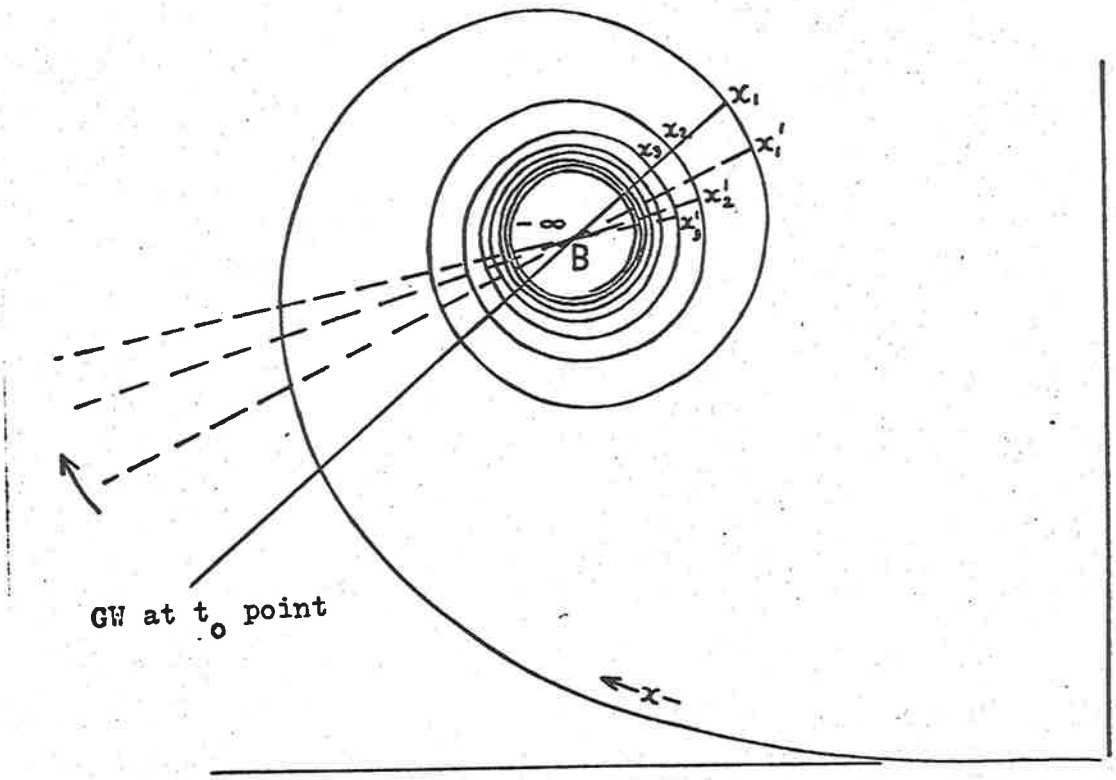

FIG. 3·5 THE EFFECT OF A RECEDING WIND ON SUCCESSIVE DIFFRACTION MAXIMA AND MINIMA. AFTER NILSSON (1962).

Wind shear is measured with the Adelaide system, since line-of-sight wind velocities are measured at a number of spaced points on the trail. No attempt is made to correct the velocity determination for the effect of shear, if present, as the correction in most cases is insignificant. Strong wind shear will make interpretation of the body doppler pattern difficult and rejection of the echo probable.

The saw-tooth phase modulation of the CW transmitter described in §4.2.1 results in the retardation of the ground-wave phase by 90° approximately 1 millisecond before the similarly retarded skywave arrives at the same aerial.

On arrival of the retarded skywave the relative phase of ground and skywave reverts to normal. In general the vector sum of the 90° phase-shifted skywave and the ground-wave will have a different amplitude from the vector sum of the normal skywave and ground-wave, so that the brief phase jump will appear as a brief amplitude increase or decrease on the amplitude-time record. These will be referred to as "phase spikes". Fig. 3.6 represents such a case where F_D' represents F_D retarded by 90° and F'_{r+D} the new resultant.

The post-t_o phase spikes will delineate a 'phantom' doppler beat pattern phase shifted 90° (+ or -) from the main pattern. Whether the shifted pattern leads or lags the main waveform depends upon whether the trail is advancing or receding, and hence the sense of the line-of-sight drift is determined.

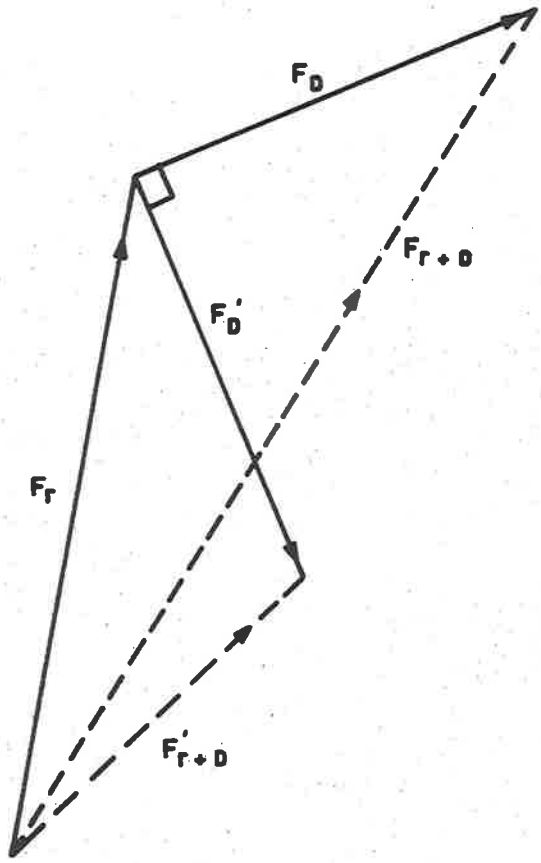

FIG. 3·6 CHANGE IN AMPLITUDE OF RESULTANT DUE TO 90° CHANGE OF PHASE OF GROUND WAVE ARRIVING AT AERIAL IN ADVANCE OF SKY - WAVE.

3.3.4 Irregular Ionization

The analysis of the meteor orbit films involves determination of the relative positions of consecutive diffraction extrema preceding the t_o point (see §5.2). One of the assumptions made in deriving eqn 3.5 is that the reflection coefficient only varies slowly in the region near the t_o point. In terms of the Cornu spiral this restriction implies that each contribution from a length of trail ds has the same amplitude as that from any other ds (apart from the R variation) and varies only in phase. Thus we may directly relate distance along the spiral to distance along the trail.

The Cornu spiral is, however, only a special case of a general vector phase-amplitude diagram, in which the amplitudes from segments of trail may be allowed to vary although the relative phases of the various segments are still determined by the geometry of the meteor flight path relative to the detecting system. If irregular ionization should cause one segment of trail to reflect four times the power of another segment of similar length, the length of the representative vector on the phase-amplitude diagram would be twice as long. This would result in the type of deformation from the idealized Cornu spiral shown in Fig. 3.7. Note particularly that with this representation distance along the spiral is no longer directly proportional to distance along the trail.

However, distance along the trail is still directly related to phase on the diagram, and in the presence of a ground-wave for all

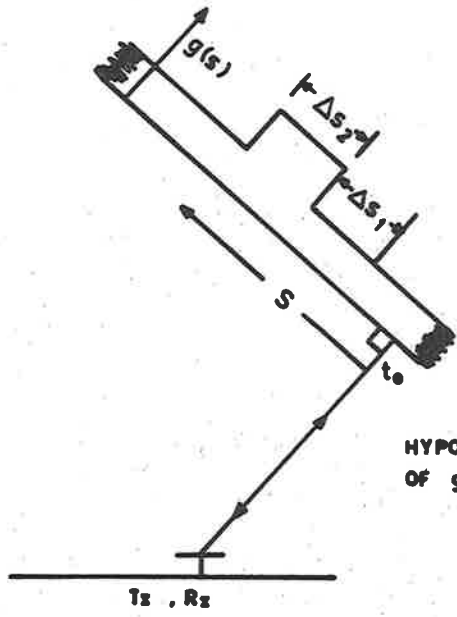

HYPOTHETICAL VARIATION OF g(s) ALONG TRAIL.

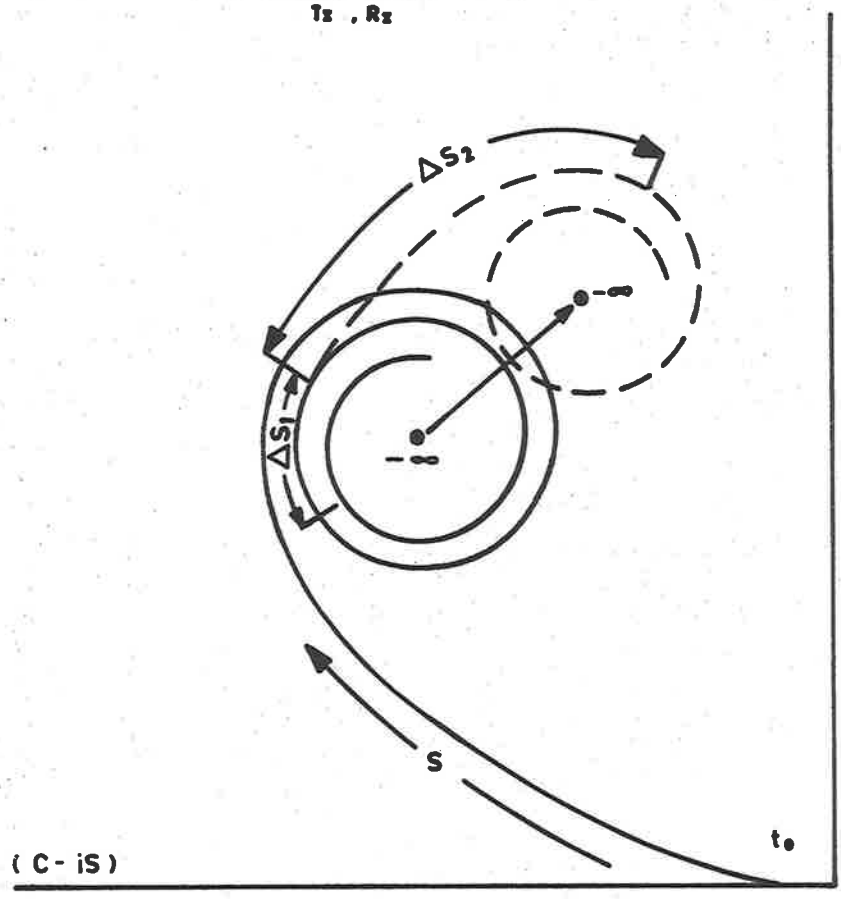

FIG. 3 · 7

SOLID CURVE IS NORMAL CORNU SPIRAL FOR UNIFORMLY IONIZED TRAIL. DOTTED CURVE SHOWS EFFECT OF HYPOTHETICAL g(s) VARIATION ABOVE ON PHASE - AMPLITUDE DIAGRAM.

likely variations of g(s) the relative times of occurrence of the diffraction amplitude extrema should be unchanged from those predicted by the ideal Cornu spiral with the assumption of constant g.

3.3.5 Diffusion

Lebedinets and Sosnova (1969) analyse in detail the errors which may arise in a velocity determination from a diffraction record if the effect of ambi-polar diffusion is ignored. They find that the error may be of either sign and in extreme cases may be as high as 30%.

While their work is certainly generally applicable, the estimate of percentage error in velocity is based upon the determination of velocity from consideration of the post-t_o diffraction pattern. In the Adelaide survey, where velocity is determined from the pre-t_o whistle, the effects of diffusion are far less significant. Each pre-t_o diffraction extremum is recorded at the instant the meteor produces the ionization contributing the greatest amount of the reflected signal. Whereas, the amplitudes of post-t_o extrema decrease as the trail extends to higher order zones, and are increasingly dependent upon the constancy of the preceding major portion of the total reflected signal.

Diffusion of earlier sections of the trail in the pre-t_o case is thus both less important and less advanced than for the equivalent post-t_o pattern. For this reason the Adelaide method of velocity determination using the pre-t_o diffraction pattern is less sensitive to trail irregularities and inherently less subject to error than use of the post-t_o pattern.

CHAPTER IV

THE ADELAIDE RADIO METEOR SYSTEM

4.1 INTRODUCTION

The present radio-meteor system has evolved over a number of years from that first described by Robertson, Liddy and Elford (1953). In its initial form the system was used for the study of winds in the meteor region by the measurement of drifts of meteor trails.

The addition of spaced receiving sites in 1959 (Weiss and Elford, 1963; Roper, 1962; Nilsson, 1962) enabled the measurement of individual meteor orbits and a study of atmospheric turbulence to be undertaken.

Further extensions and refinements of the system, in particular a substantial increase in transmitter power and the addition of two more receiving sites at greater distances, have been implemented in the years 1967 - 1969.

Meteor winds are still measured for one week each month on a routine basis. Increased echo rates as a result of increased transmitter power have greatly improved the resolution of this study. Concurrently with the orbit survey which is described in this thesis an investigation of small scale motion of the atmosphere was carried out. Apart from its own merit this study enables positive corrections to be made to the orbit data for the effects of atmospheric wind drift and shear, thus improving their overall accuracy. A study of the distri-

bution of ionization along meteor trails was also undertaken during part of the orbit survey, and a combination of these data with the orbit data could prove fruitful at a later date.

In its present form the Adelaide meteor system consists essentially of two transmitters, one CW and one pulsed, located at the same site, and operating on similar but distinct frequencies. A network of receivers is located at distances in excess of 20 km from these transmitters. There is one main receiving station at which all recording is carried out. The other stations are designed to run unattended. Information from these sites is telemetered to the main station for concurrent recording.

4.2 EQUIPMENT

4.2.1 Transmitters

Two transmitters are located on the top floor of one of the buildings of the Department of Physics at Adelaide. The CW transmitter has an output power of 1.5 kW at 26.773 MHz and the pulse transmitter produces 8 μ sec. pulses at a frequency of 200 sec^{-1}, with peak power 65 kW at 27.540 MHz.

The output of the CW transmitter is phase modulated by a mains-locked 50 Hz saw-tooth waveform which retards the phase by 90° in 80 μ sec. and restores it to zero over 20 millisec. This device produces 'sense spikes' at the receivers in the manner described in §3.3.3. These spikes are used in the determination of the sense of the observed winds as well as for timing in the analysis of the orbit data.

Figure 4.1 shows a block diagram of the transmitters, which are described in greater detail by Roper (1965).

4.2.2 Transmitting Aerials

Aerials for both transmitters are simple half-wave dipoles mounted one quarter-wave above the flat metal roof of the transmitter room, which serves as a ground plane. Interaction between the two aerials should not be significant since they are separated by a distance of the order of a wavelength and are almost co-linear. During the latter stages of the survey a reflector was incorporated in the CW aerial to decrease the ground-wave at the main receiving site to the optimum level. This adjustment was not critical to the sensitivity of the survey, but rather enabled fuller use to be made of the dynamic range of the receivers after changes in ground-wave strength caused by an increase in the transmitter power.

It has not been possible to measure the directional variation of gain for these aerials, but since they are accurately situated with respect to an excellent ground-plane it is felt that their properties would be adequately described by the theoretical configurations. The dangers of making assumptions in regard to aerial polar gain configurations are well appreciated for high gain directional aerials. Fortunately the same problems are of much less significance when dealing with low gain aerials as used in the present survey, and particularly in the present application. In all cases we are actually concerned with the product of the directional gains for transmitting and receiving aerials

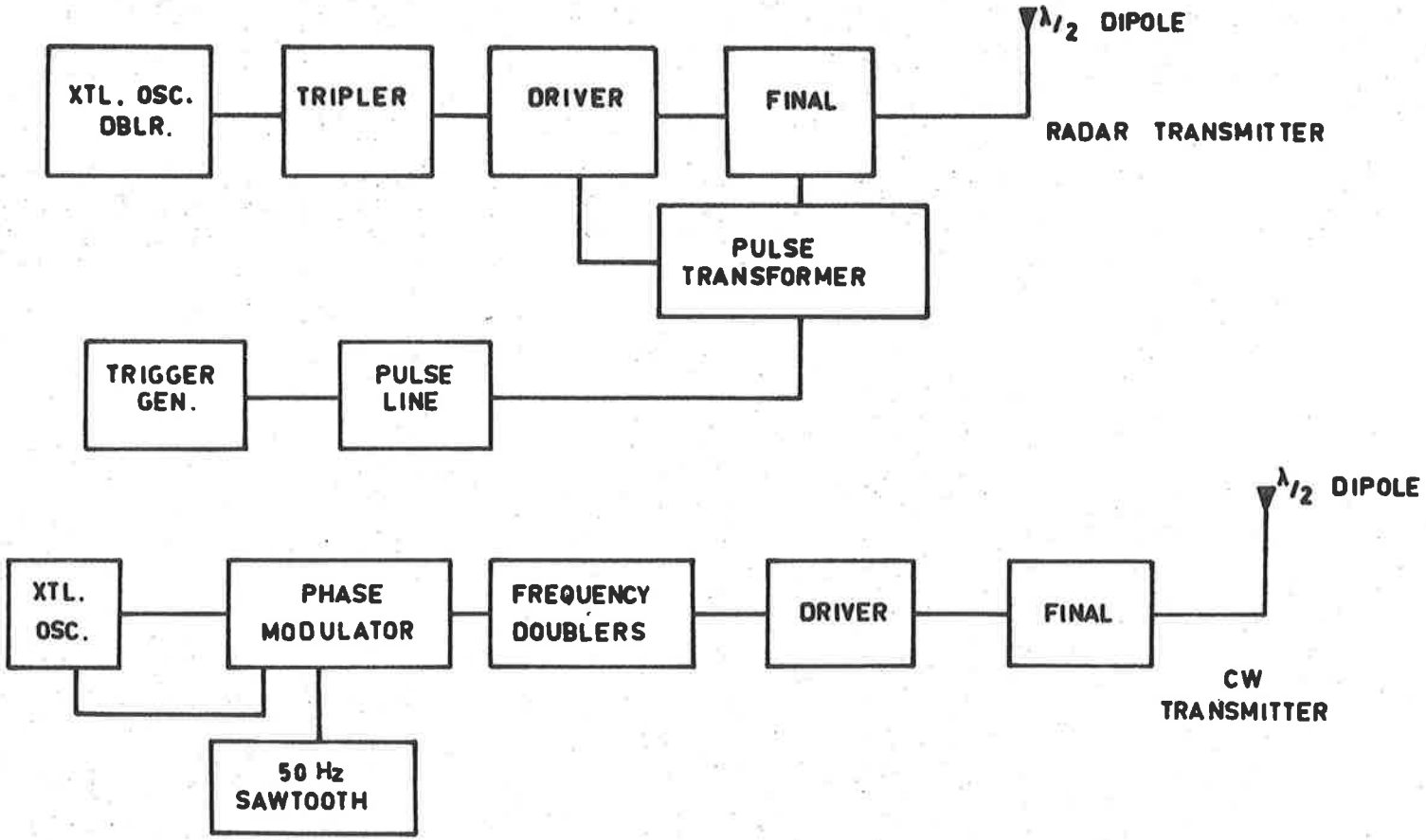

FIG. 4 · 1 : Block diagram of the radar and CW transmitters.

($G_R \cdot G_T$) and minor departures from theory at low elevations become of little consequence.

This is confirmed by the observed distribution with zenith angle for reflection points in this survey (Fig. 4.2.)

Further justification for this is seen in the fact that for most of the radiants observed meteors may be expected to occur over large portions of the visible sky. Calculation of response of the system as a function of radiant azimuth and elevation is therefore dependent upon integration of the probability of detection, itself a function of the product $G_R \cdot G_T$, over the entire sky. This integration will minimise the effect of minor variations in the aerial polar diagrams.

4.2.3 Main Station Receiving Aerials

Altogether seven 27 MHz receiving aerials are located at the main receiving site. One of these is a three element half-wave Yagi directed horizontally towards the transmitter to detect the radar ground-wave pulse which is used to trigger the radar ranging equipment. Of the other six aerials, all of which are standard half-wave dipoles one quarter-wave above ground, one is connected to the pulse radar receiver. Figure 4.3 shows the configuration of the remaining 5 aerials which are used as a direction finding array. An analysis of phase diagrams for each aerial shows that the four possible measurements of relative phase are sufficient to determine unambiguously the direction of arrival of the sky-wave. These phase comparisons are obtained in practice by rapid switching

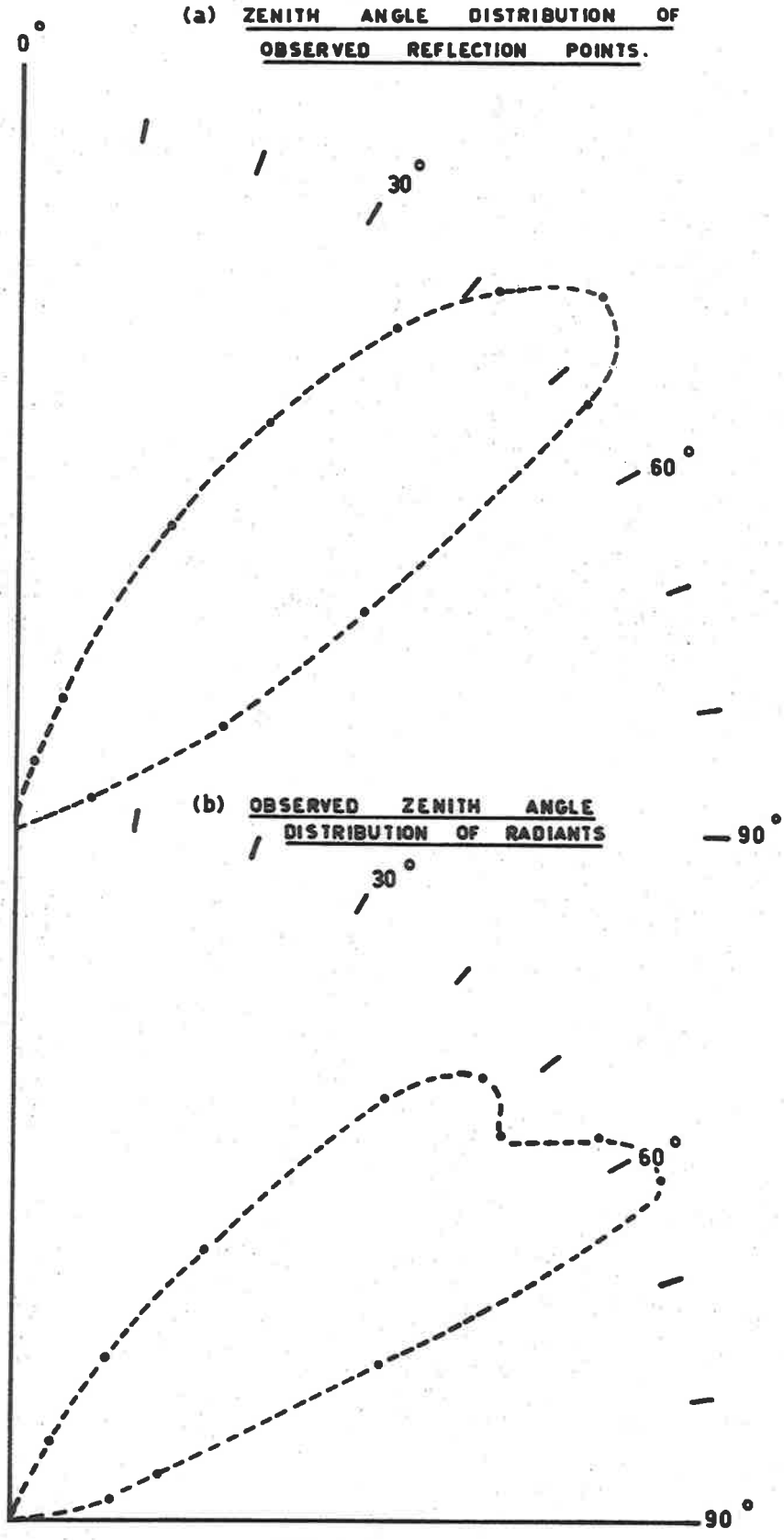
(a) ZENITH ANGLE DISTRIBUTION OF OBSERVED REFLECTION POINTS.
0°
30°
60°
(b) OBSERVED ZENITH ANGLE DISTRIBUTION OF RADIANTS
90°
30°
60°
90°

FIG. 4·2

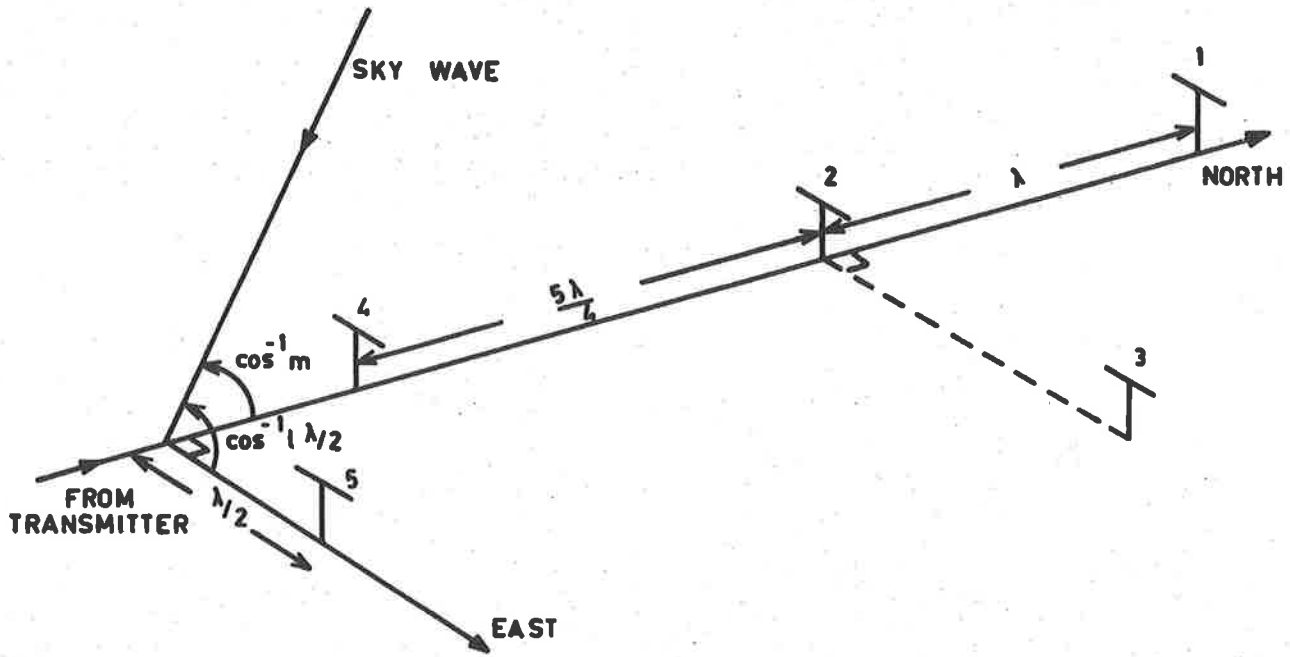

LAYOUT OF DIRECTION FINDING AERIALS AT ST. KILDA.

FIG. 4·3 : The layout of the antennae used for determining the direction of arrival of the sky wave. The transmitter is 23 km to the south.

between aerials at inputs to receivers. This technique has been employed for some years in the routine recording of mean winds.

4.2.4 27 MHz Receivers

The nature of the signals reflected from meteor trails determines the necessary features of the detecting receivers. The body doppler is in general a large amplitude low frequency variation, whilst the diffraction whistle may be of small amplitude with frequencies as high as 300 Hz. For reasonable reception of the sense spikes a bandwidth of at least 2 kHz is desirable.

Essentially the receivers require low noise figures with adequate bandwidth and a large dynamic range. The use of logarithmic receivers has been considered and rejected. For recognition and analysis of the features of the reflected signals it is desirable that these be recorded in linear form. The possible benefits from logarithmic receivers coupled with a subsequent exponentiating procedure to recreate linearity appear to be outweighed by the degree of sophistication required of the circuitry.

The main station receivers have a noise figure of less than 2 db, bandwidth ± 4.0 kHz between 3db points and linear response to inputs up to 30 μ volts with smooth overload up to 55 μ volts.

The outstation receivers have an additional requirement, that of good reliability under reasonably severe operating conditions. This reliability has been obtained through all solid-state construction, although slightly at the expense of the other factors. The receiver

bandwidth at ± 3.0 kHz is set by a mechanical filter. Noise figures for these receivers are higher than those of the base station, being between 2.8 and 3.4 db, and the overload condition occurs for inputs in excess of 25 μV. Nevertheless, degradation of the outstation signals is mainly due to the telemetry links, and these receiver figures are quite acceptable for the majority of echoes.

With receiver noise less than 3 db, galactic noise provides the lower limit to the detectability of signals. For a 27 MHz receiver with a bandwidth of ± 3 kHz this represents a noise power of approximately 3×10^{-15} watts. For the Adelaide system in its present form this sets a lower limit of just under 10^{13} electrons per metre for the line density of a meteor trail for which the diffraction pattern is observable. This corresponds to an average limiting radio magnitude, given by

$$M_R = 40 - 2.5 \log_{10} q \qquad \text{(McKinley, 1961)}$$

of + 8. (The commonly accepted electron line density for transition from underdense to overdense reflection is 2.4×10^{14} electrons/m.)

4.2.5 The Outstations and Telemetry Links

Figure 4.4 is a block diagram of the equipment comprising each outstation. The 27 MHz receiving aerial is a half-wave dipole situated one quarter wavelength above ground. The specifications of the 27 MHz receiver have been outlined in Section 4.2.4. A clock drive switches the receiver input to a crystal controlled 26.773 MHz oscillator once per hour providing a 10 μV reference input for system calibration.

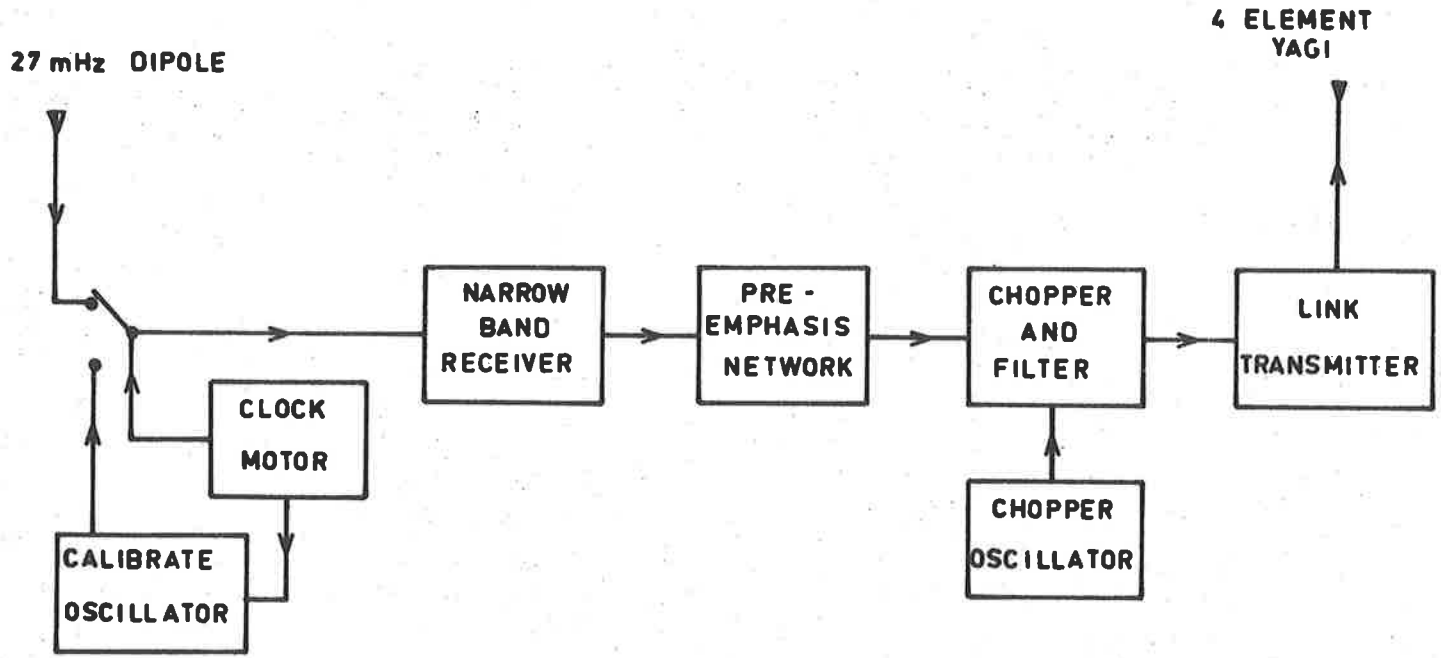

FIG 4·4 : Block diagram of the equipment installed at each outstation.

The level of the ground-wave at the receiving site should ideally be half of the maximum input before overload, or approximately 12 μV, and where possible receiving sites have been chosen in relation to local features by testing ground-wave strength variation from point to point to achieve this figure. The addition of a sky-wave to the ground-wave may cause both positive and negative variations in this voltage level, depending upon relative phases, and it is important that this D.C. voltage as well as frequency variations from almost D.C. up to the maximum necessary for transmission of the sense spikes be relayed to the main recording station. This is effected by feeding the receiver detector output into a diode ring modulator which chops the output to ground potential at a pre-determined frequency. The chopped signal is then passed through a band-pass filter centred on the chopping frequency (either 2.0 kHz or 3.5 kHz) and the resultant sub-carrier is used to frequency modulate the telemetry transmitter.

The telemetry links, operating in the 160 MHz band, are restricted by local regulations to maximum deviations of ± 5 kHz. Resultant noise levels are unavoidably high and may represent an equivalent modulation of the sub-carrier of 2%. This is the same order of magnitude as the modulation produced by the faintest meteors detectable in the present survey, namely those producing electron line densities of the order of 10^{13} electrons/metre.

To make best use of the available bandwidth the low amplitude diffraction information is amplified at the output from the 27 MHz

receiver, prior to transmission over the telemetry link, by an amount such that the amplified receiver noise level produces a sub-carrier modulation somewhat in excess of the 2% modulation due to link noise. Since the post-t_o doppler signal is typically an order of magnitude larger in amplitude than the pre-t_o diffraction whistle it is not possible to amplify this portion of the echo waveform proportionately without over-modulating the sub-carrier. Fortunately the doppler information is usually of much lower frequency than the 30 - 600 Hz range for the diffraction whistle, making it possible to use a frequency dependent amplifier to boost the higher frequency diffraction signal without amplifying the doppler.

Fig. 4.5 shows the construction of the housing and aerials for the two short distance outstations (Sheedys and Direk). These are enclosed in the same underground metal boxes used in a previous survey (Nilsson, 1964b). A greater degree of protection has been provided against extremes of weather and the possibility of vandalism (one balun transformer acquired a bullet hole early in the setting-up period). All aerial connections are fully enclosed and where possible encased in epoxy resin.

The medium and long distance outstations (Buckland Park and Glenthorne) are less prone to vandalism, being located within research establishments. The chief distinguishing feature of these outstations is that the 27 MHz aerials are free-standing at distances of approx. 70 metres from the electronic packages. At Glenthorne a tower has been constructed and at Buckland Park use has been made of an existing aerial

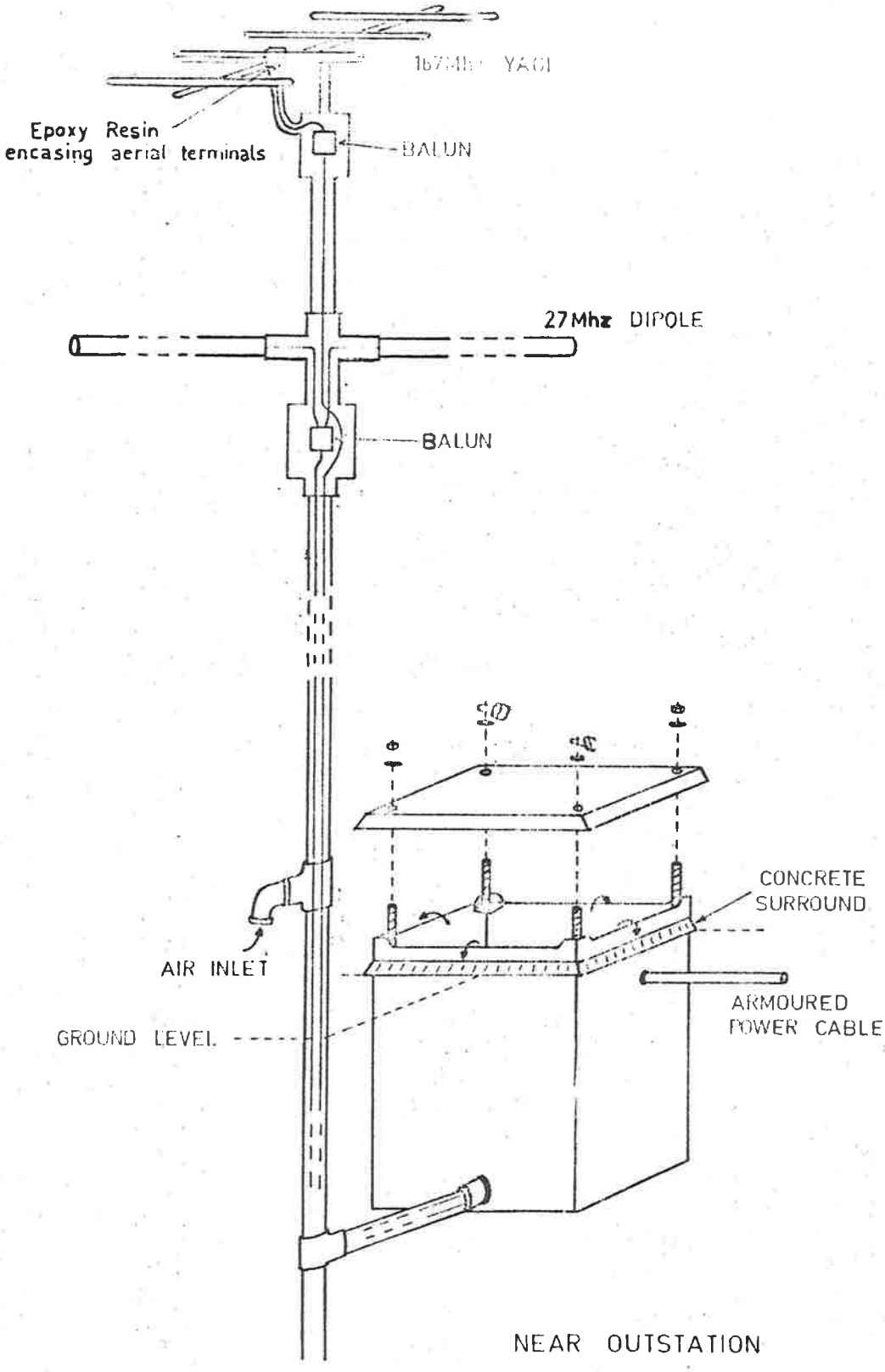

FIG. 4·5 Schematic diagram of the method of construction at the Direk and Sheedys outstation sites.

pole in each case to raise the link transmitter aerial 35 feet above the ground to enable strong reception at the main station.

Commercial FM transmitters and receivers are used in the telemetry system. Modifications have been made to improve linearity and to enable the transmitters to operate at a continuous output of up to 10 watts.

The telemetry aerials are 4 element Yagis. Table 4.1 shows the various parameters of the telemetry network.

Telemetry Link	Frequency (MHz)	Polarisation	Sub-Carrier Frequency (kHz)	Height of Tx Aerial Above Ground (Feet)
Buckland Park	162.34	Horizontal	2.0	35
Sheedys	167.02	Horizontal	2.0	10
Direk	167.02	Horizontal	3.5	10
Glenthorne	162.34	Vertical	3.5	35

TABLE 4.1 PARAMETERS OF TELEMETRY SYSTEM

The Sheedys and Direk links share the same frequencies but since the paths are at right angles, the front to side rejection ratio of 36 db for the aerials ensures that the appropriate FM receiver limiter only operates for the desired signal. Buckland Park and Glenthorne also share a frequency. Vertical polarization of one set of aerials re-inforces the rejection of the unwanted signal in this case.

The outputs of the main station telemetry receivers are passed through ± 600 Hz band-pass filters centred on the appropriate sub-

carrier frequency for each link. Table 4.1 shows that the choice of sub-carriers in relation to link transmitter frequencies ensures further rejection of the unwanted signal at this stage.

4.2.6 Main Station Recording Equipment

The output of one of the 27 MHz receivers at the main station is chopped and filtered at 3.5 kHz, and along with the signals from the outstation links fed to the channel distribution unit. Because of the different requirements of various studies undertaken with the equipment, three separate oscilloscope display units are used to record the data on 35 mm. photographic film.

The mean wind recording system is operated on a routine basis, and does not use the outstation signals. This display records the radar range information as well as the signals from the array of aerials used for direction finding (Fig. 4.3.).

The other two displays have essentially similar input, namely the information contained on the five sub-carriers from the channel distribution unit, but treat it differently. The wind shear display is recording data with the same characteristic frequencies (0.5 Hz - 20 Hz) as the mean wind display, and both use a slow speed (0.38 ins/sec.) for the film drive.

The orbit display requires a higher speed film transport to resolve the frequencies of the brief pre-t_o 'whistle' (in the region 30 Hz - 300 Hz) and for this display the Shackman Camera has been modified to give a film transport speed of 1.9 ins/sec.

Although the whistle recording sequence has the shortest duration, in a 24 hour recording period the orbit display will typically use 500 feet of film, compared with 200 feet for the other two displays combined. Economy, as well as ease of film reading makes it desirable to keep the displays separate at the present time.

To avoid the consumption of excessive quantities of film, recording only takes place when an event likely to be a meteor echo occurs. Figure 4.6 shows the relation of the various units at the main station. The sequence unit continuously monitors the output of one of the main station mean wind equipment receivers. When the signal from this receiver varies from its mean level by more than a preset amount the sequence unit initiates and controls a recording sequence. A pulse triggers monostable multivibrators which determine the duration of engagement of the respective camera clutches. The sequence unit is also responsible for incrementing the six digit counters in each display and firing electronic flash tubes which illuminate them. The duration of the mean wind and wind shear recording period can be adjusted at the sequence unit. Because of the frequency of day-time air-traffic over the station the sequence unit has been designed to hold the recording cycle in an inoperative state at the end of one sequence for a persistent echo until the signal level reverts to normal, thus avoiding considerable film wastage. Inevitably some meteor echoes are lost. Increasing intermittent interference is not overcome by this device, and an echo recognition unit is planned, using logic circuitry to initiate the recording sequence

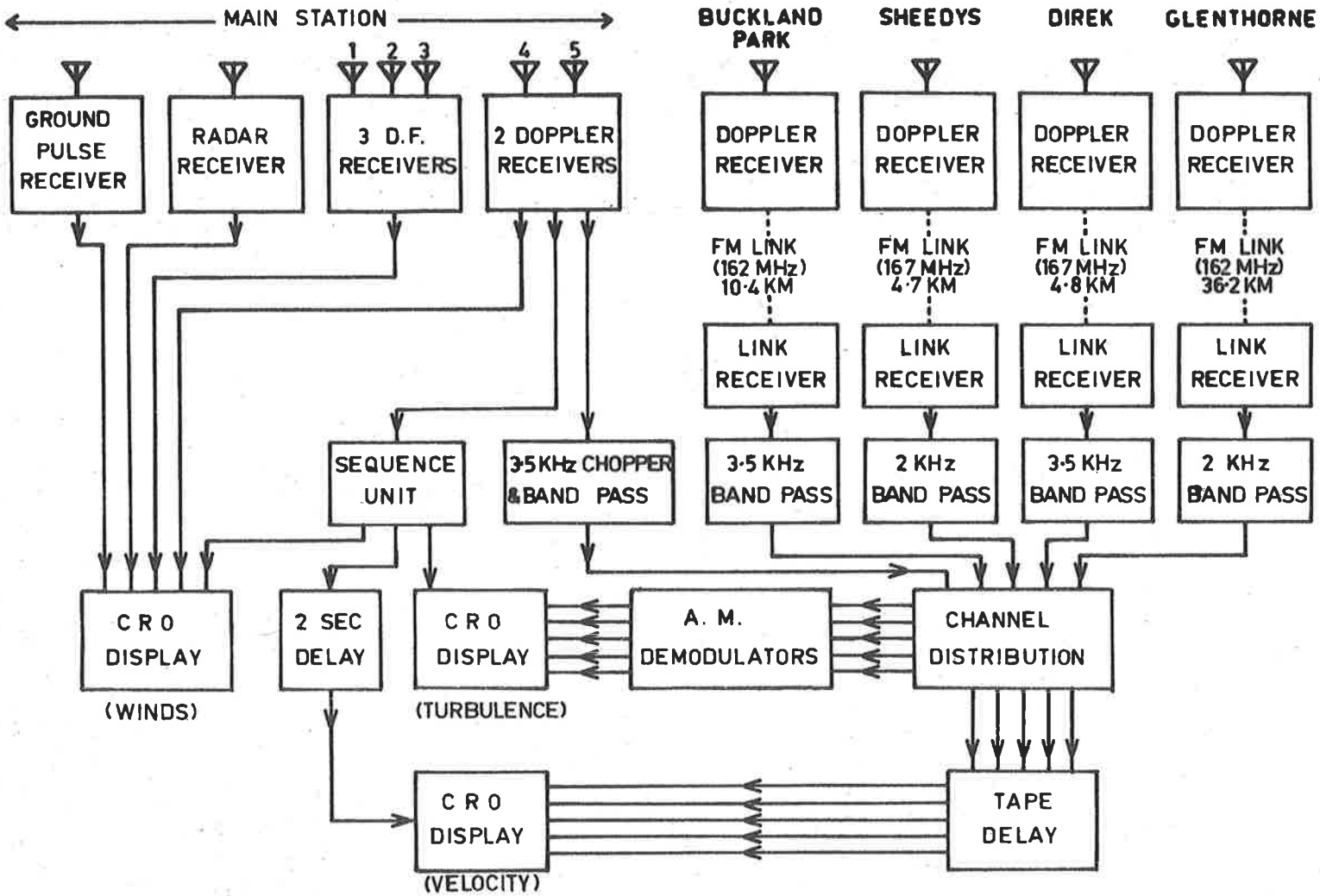

FIG. 4 · 6 BLOCK DIAGRAM OF MAIN RECEIVING STATION

only if a pre-determined number of consecutive pulses, presumably reflections from the pulse radar, are received with suitable and similar range. The present survey has shown that such a unit is essential if a reasonable proportion of the day-time meteors are to be observed.

The orbit display has a subsidiary sequence unit of its own. Since the sudden change in amplitude which triggers the main sequence unit only occurs in the vicinity of the t_o point, the pre-t_o information used for orbit determination would be lost with direct recording. To recover this the five channels are continuously recorded on a tape delay which gives ample time prior to the t_o point of the delayed signals when the normal recording sequence is initiated. Figure 4.7 shows the relation of the recording periods for the various displays. During the 1.5 second delay a clock face in the orbit display is illuminated and towards the end of the period the electronic flash illuminates the counter. At the expiry of 1.5 secs. the camera clutch engages and the H.T. is applied to the oscilloscope tubes, brightening them. Recording continues for a pre-determined time, at the end of which the camera clutch disengages and the oscilloscope tubes go dark again.

Figure 4.8 shows the various components of the tape delay system. The high tape speed of 30 ins/sec is necessary to ensure an adequate frequency response to handle the frequencies as high as 20 kHz generated by the FM modulators. The signals from the channel distribution unit are first demodulated by a standard diode ring circuit, then filtered with an active low-pass network with a 1 kHz cut-off frequency

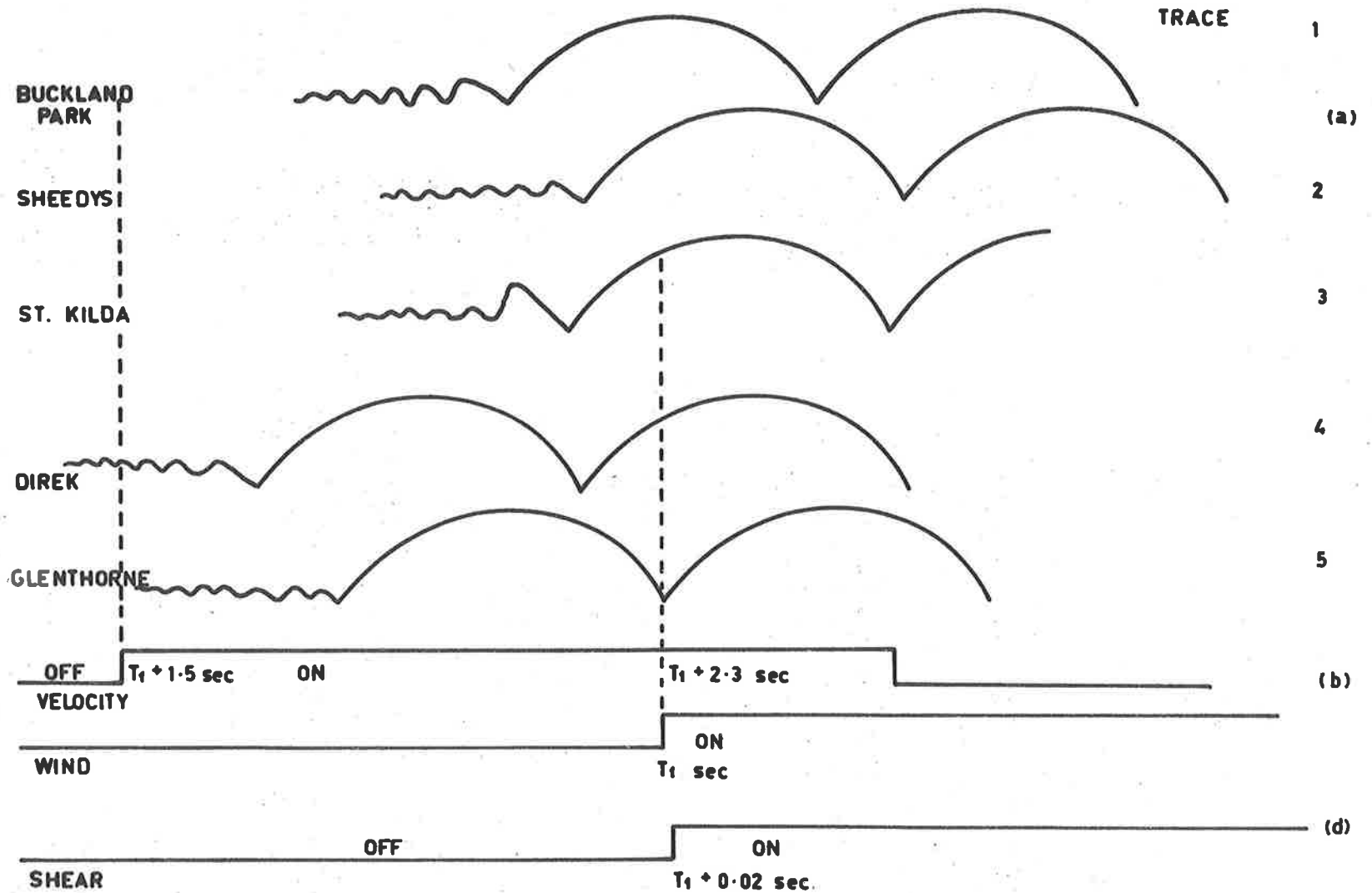

FIG. 4·7 TIMING DIAGRAM FOR RECORDING EQUIPMENT. THE SEQUENCES IN (c) AND (d) OCCUR IN REAL TIME WITH RESPECT TO (a), SEQUENCE (b) IS DELAYED BY 1·5 SEC WITH RESPECT TO (a).

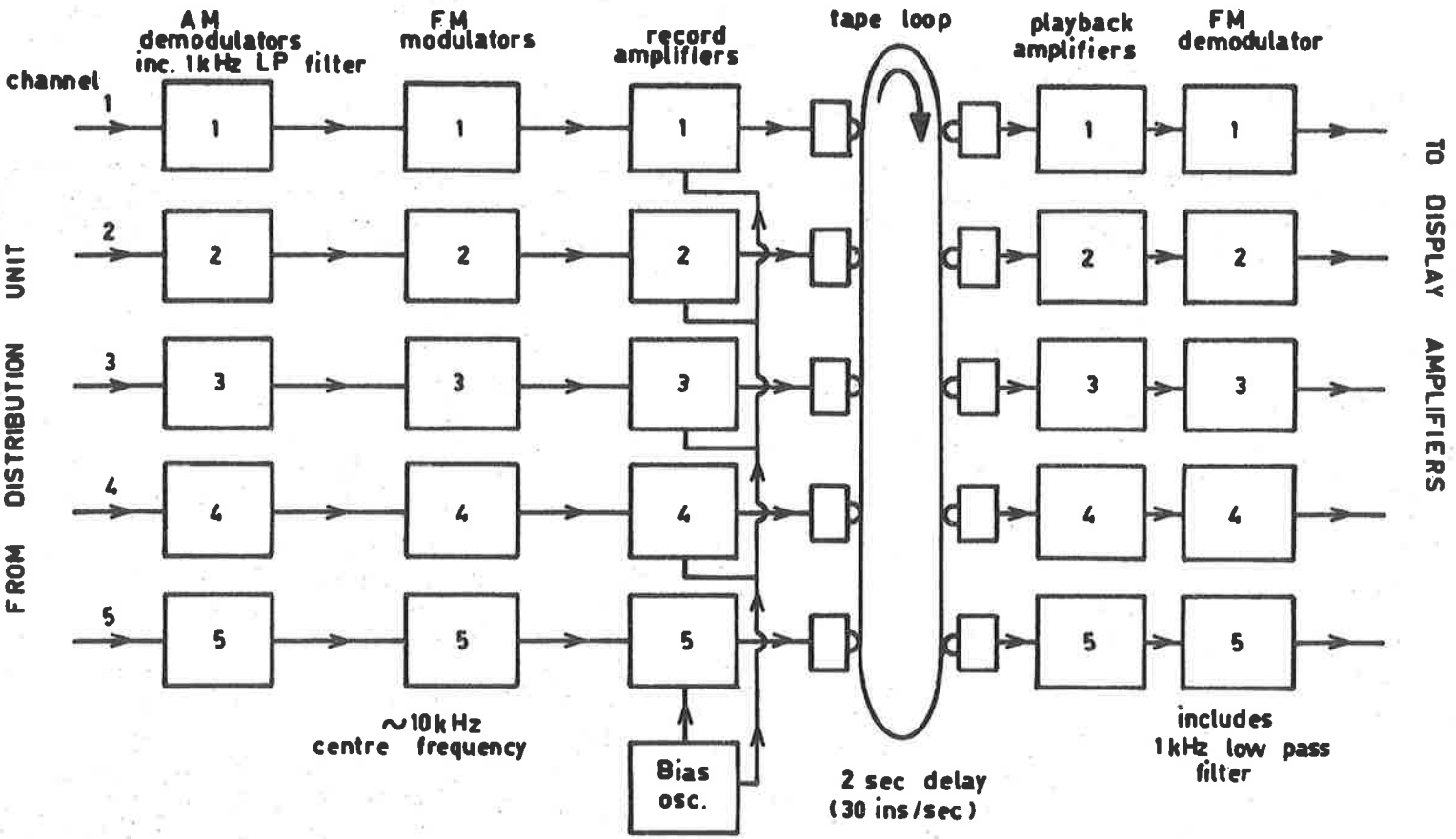

FIG. 4·8 . Block diagram of the tape delay system used in recording the whistle waveforms.

before passing through a notch filter centred on the sub-carrier frequency. The demodulated signals control the frequency of a voltage-dependent oscillator, the output from which is recorded on the tape loop by way of the record amplifiers. Early attempts at direct AM recording were not successful because of numerous partial drop-outs on the recording tape which are apparently unavoidable. Linearity of the FM system was excellent, and in general no degradation of the signals was observed through the tape unit.

The use of a tape loop rather than a long reel was found preferable, despite problems in splicing the tape. It was found that a loop bedded into the heads with age, and significantly less drop-outs occurred after half an hour of use than immediately after fitting of a new loop. Nevertheless, at the high speed of 30 ins/sec. head wear was rapid and wear of the tape required replacement of loops once every 24 hours. (In one day's operation each section of the tape passed over each of the 4 heads in excess of 40,000 times.) Splices could generally only be relied upon for the same period of time.

The tape unit used was an EMITAPE deck fitted with 8 channel heads on 1 inch tape. This machine has an electronic speed sensor to ensure constant speed of the capstan. The alignment of the heads is sufficiently accurate to make timing errors negligible. A more probable source of error would lie in poor tracking of the tape, however, the use of carefully made tape-loops did not introduce any significant errors of this kind.

Although the recording system has not been calibrated in toto for phase shifts, all the individual units have separately been checked for frequency-dependent phase variation. The only significant phase variation occurs in the tape delay system, and this amounts to less than 20° over the frequency range of interest.

No measurable degradation of the signals occurs in the main station recording equipment. The limiting factor in the case of the outstation signals is the high noise of the telemetry links. The noise level of the main station velocity record is mainly due to the galactic background noise at the receiver input.

4.3 FILM RECORDS

Film records for one echo from the three displays are shown in Figure 4.9. The velocity record (a) and the shear record (b) show traces corresponding to the five channels, Buckland Park, Sheedys, St. Kilda, Direk and Glenthorne (in that order from top to bottom of the film). The Glenthorne channel shows only noise for this record since the telemetry link was inoperative at the time. The sixth trace on the velocity record shows an inverted duplicate of the St. Kilda channel, while the sixth trace on the shear record shows the variation in amplitude of the echo received by the radar receiver.

The radar range and mean wind record (c) shows (from top to bottom) a series of dotted lines representing intervals of 20 km on which the reflection from 150 km slant range shows clearly. The next two traces show the output from the 'doppler' receivers used to determine the

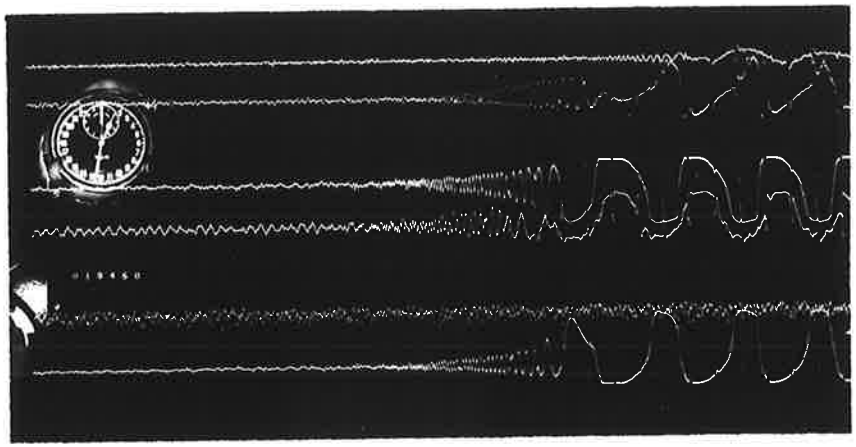

a

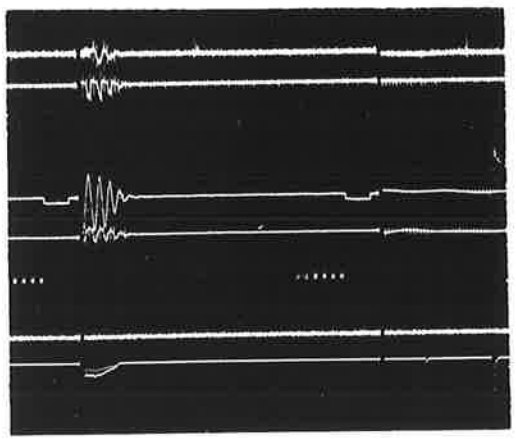

b

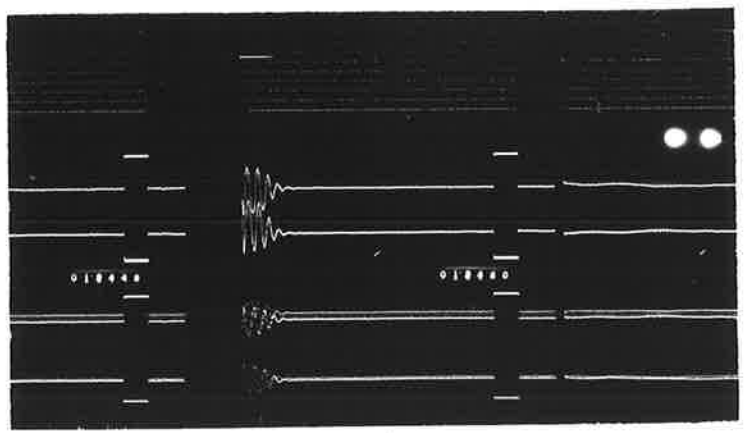

c

Figure 4·9 Films from; (a) velocity display showing whistles, (b) mean wind display showing doppler waveforms at each outstation, (c) wind display.

magnitude and sense of the line of sight wind, while the remaining traces are used in the determination of reflection point direction.

The sense spikes can barely be resolved in the photograph (b) but can be seen clearly in (a). Some distortion of these is unavoidable in the various filter networks throughout the recording system since the spikes contain frequencies much higher than it is necessary to pass to adequately record the velocity whistle. Consideration of the echo shown indicates that the t_o point was reached by the meteor on the Direk trace first, followed in order by St. Kilda, Sheedys and Buckland Park. The sense spikes are used as concurrent time references for the various traces, as well as for temporal calibration of distance along the recording.

4.4 GROUND GEOMETRY AND REFLECTION POINT DETERMINATION

4.4.1 Location of Outstations

A number of factors have led to the present arrangement of outstations, including the availability of power at the site, security, and local geography. The level of the ground-wave signal strength was a particularly important consideration. Figure 4.10 shows the resulting disposition of outstations.

The relative positions of the main station, the Adelaide transmitters and the Sheedys and Direk outstations were determined for a previous survey (Nilsson, 1964b) by means of a tellurometer link between the various sites and a prominent local co-ordinated trigonometric station. The positions of the Glenthorne and Buckland Park outstations

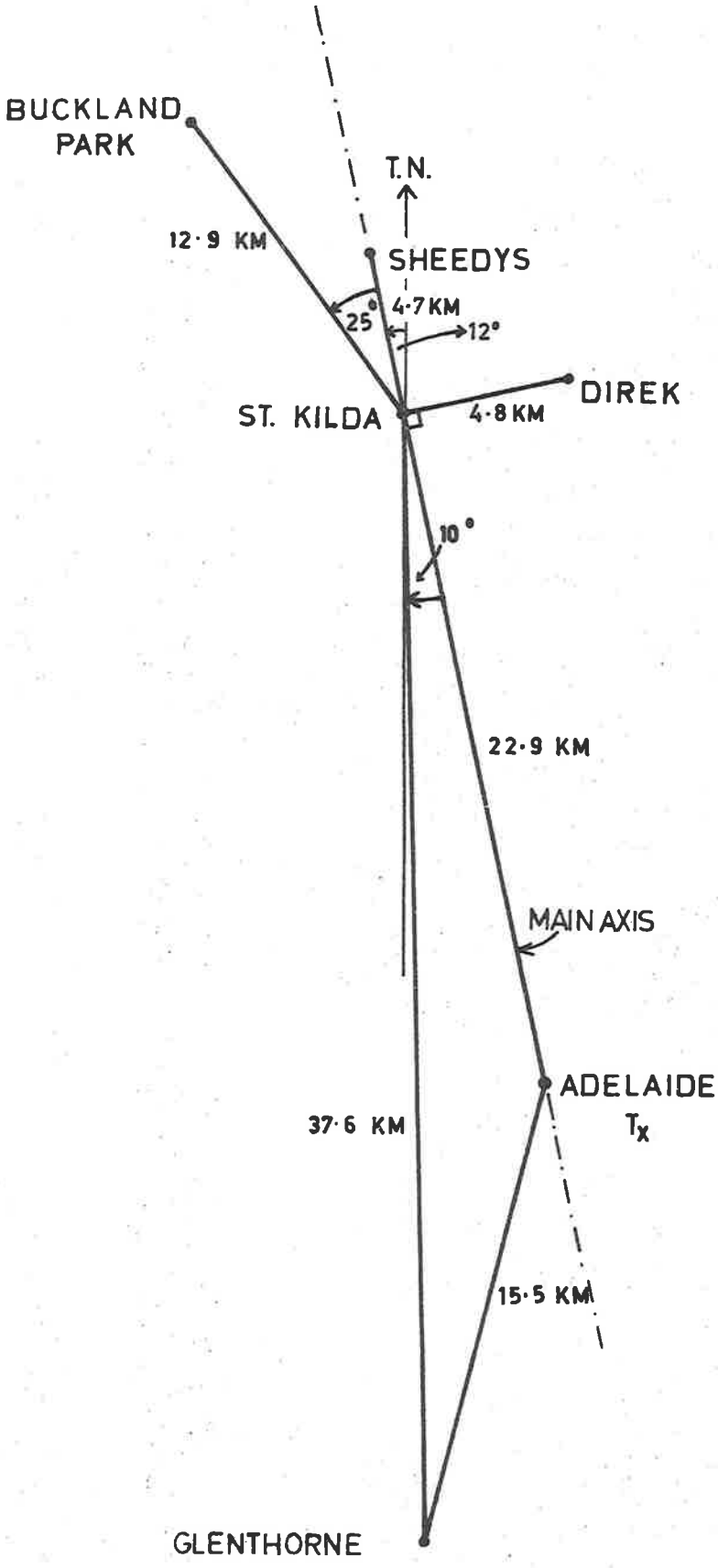

FIG. 4 · 10 : Plan of Transmitting and Receiving sites.

were related to the St. Kilda station by more conventional means (since the tellurometers were not available) using a theodolite, heliographs, and radio-telephone communication. Triangulation to the nearest visible co-ordinated trigonometric stations involved sighting distances of as much as 15 miles. Measurements were only possible in near-perfect atmospheric seeing conditions, but despite these difficulties location of the various survey points was achieved to within one metre for the Glenthorne station and with slightly less accuracy at the Buckland Park site. The accuracy of the survey was more than sufficient in terms of the resolving capability of the system which is practically determined by the RF wavelength of 11 metres.

Co-ordinates of the main receiving site including the most up-to-date corrections available from satellite determinations of the shape of the earth are:

Longitude: 138° 33' 40"
Latitude : -34° 42' 15" .

4.4.2 Location of Reflection Points

Figure 4.11 shows the paths of specularly reflected waves from the trail of a meteor whose direction of arrival would produce echoes similar to those of Figure 4.9(a.). The symbols T_G, T_E, T_M, T_N, and T_B denote the times at which the meteoroid generates the t_o reflection at the appropriate receiving sites. The position in space of the main station t_o point is determined by combining the radar range information with the direction of arrival of the reflected radiation at the

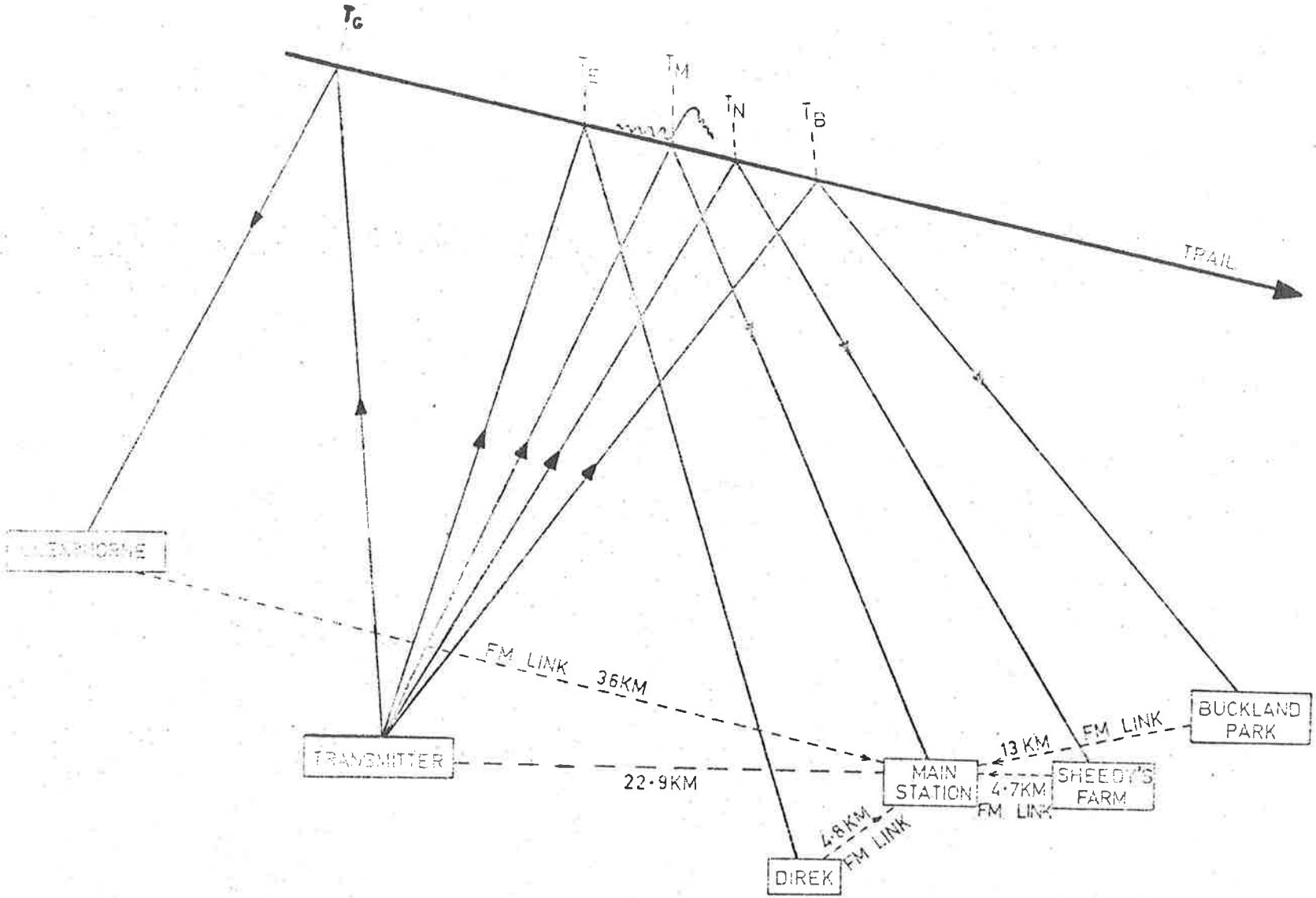

FIG. 4 · 11 : Schematic diagram (not to scale) of the site locations and geometry of the Adelaide Radio Meteor System. The times T_G, T_E, T_M, T_N, T_B refer to the times when the meteoroid passes the specular reflection points for each site.

main station direction finding array described in Section 4.2.3.

Knowledge of the radar range makes possible determination of the meteor velocity from the diffraction whistle on each trace (in the manner outlined in §5.2), and with this knowledge the time differences ($T_B - T_M$) etc., may be related to distance along the meteor trail. The specular reflection constraint then enables us to determine from the ground geometry the orientation of the trail necessary to produce the measured separation distances. The method of calculation of trail direction cosines follows that described by Nilsson (1964b), appropriately extended to include the Buckland Park station. Too few echoes were received from Glenthorne to warrant their use in the determination of trail orientation. Direction cosines of the reflection points are determined first in a frame of reference for which the Adelaide - St. Kilda - Sheedys outstation line provides one axis and the St. Kilda - Direk outstation line an axis at right angles. If the trail direction cosines are given by (λ, μ, ν) it is apparent that λ may be determined by consideration of the Sheedys and Main Station reflection points only, and μ by consideration of the Direk reflection point once λ is known. Similarly if Direk does not return an echo μ may be found from the Buckland Park echo with λ determined as before. In the event that the echo from Sheedys is not reducible λ and μ may be determined by solving the pair of simultaneous equations describing the Buckland Park and Direk reflection points with the additional information from the main station reflection point.

Usually readable echoes were received from the four stations and it was thus possible to calculate three sets of direction cosines using different combinations of the stations (the St. Kilda reflection being common to the three sets). In this case the adopted values for the direction cosines were found by taking the average of the three sets weighted according to measured trail separation distances.

A check on the consistency of the data is available since between the knowledge of the direction of arrival of the reflected wave at the main station, the radar range, the calculated trail direction cosines and the condition of specular reflection there is an item of redundant information. Nilsson (1964b) describes in detail a method used also in the present survey of optimising the data by treating the cosine of the zenith angle of the main station reflection point as the redundant item.

This method essentially involves adjustment of the measured mean value of velocity by a small amount (within the measurement error) to the value for which re-calculated trail direction cosines are most consistent with the rest of the data. Echoes for which the closest allowable agreement falls within prescribed limits have been assigned a quality marker and the remainder retained for checking. It is re-assuring to note that the mean resultant height adjustment arising from this optimization process over any large number of echoes is close to zero, ruling out the possibility of any systematic error in the velocity reduction technique.

CHAPTER V

DATA REDUCTION

5.1 FILM READING

The meteor wind equipment is run for one week each month on a routine basis, and the reading of the wind films is carried out by trained computing assistants on a specially designed film-reader (Stone, 1966) which punches the information in digital form on computer cards. This film-reader is also used to reduce the wind shear films. The velocity films require better resolution and have been read on either a Telereader or a Boscar by the author at the Weapons Research Establishment, Salisbury. In a CW system the shape of the recorded waveform is a function of the relative phases of the ground-wave and the sky-wave (see §3.3.2) and with the additional complications of sometimes fast line-of-sight winds further altering the recorded waveform it was felt that the degree of physical interpretation required in reading the velocity records demanded an operator well versed in the theory. Output from both the latter film-readers was in the form of punched paper tape, from which the information was subsequently transferred to computer cards, and collated with the appropriate range, wind and shear data, before finally being written on to magnetic tape for reduction on a CDC 6400 computer at the University of Adelaide.

Consideration is being given to the possibility of direct digital magnetic recording to avoid the circumlocutory data handling that currently limits the amount of data which may be usefully recorded.

Direct digitization of the wind and shear records is a straight-forward matter and the only obstacle to its implementation is at present a financial one. Automatic digitization of the velocity information is far from straight-forward, however. The information is of higher frequency and the amplitude generally much less. Visual recovery of the positions of the various extrema is possible even when the signal is comparable with the noise. To handle the data with the same resolution on a computer would make an absorbing study in programming.

The resolutions of the Telereader and Boscar were both more than adequate in terms of the time scale of the meteor film records, being 1/15 millisecond per unit and 1/20 millisecond per unit respectively. Temporal calibration of the film records was determined by the interval between the 'sense spikes', which are locked to the 50 Hz mains frequency so that on average, reading over various times of the day, five spikes (actually the interval between six spikes) represent 100 msec. Relative times of events only have been read from all films. To date no amplitude measurements have been undertaken.

Film reading was automated as much as possible for speed, but nevertheless using the Telereader it was still generally only possible to read between thirty and forty records in one day before fatigue necessitated a halt in the interests of reading accuracy. Slightly more could be read on the Boscar which is a faster machine although it was not as frequently available.

It was found early in the reduction stages that not all velocity records which appeared suitable for reduction were also suitable for wind film reduction, and vice versa, and the following method of selection of suitable records for detailed analysis was developed for maximum efficiency of effort.

(i) The films from the mean wind were read in the usual manner. This routine wind patrol does not rely upon the other records, and rates for echoes suitable for wind reduction are many times higher than those suitable for velocity reduction. In order for an echo to be acceptable for reduction the presence of at least one cycle of doppler beat was necessary so that phase differences at the direction finding aerials could be determined uniquely.

(ii) The velocity films were scanned and a note taken of echoes for which there was a readable whistle on at least three traces. At this stage echoes for which the wind film had also been read were analysed in detail.

(iii) The shear film was read for the echoes analysed in stage (ii), since the shear study also required a knowledge of the trail orientation and reflection point positions.

(iv) The wind film was re-examined to try to recover wind information where possible for those echoes noted in stage (ii) as suitable for reduction.

The method of film-reading of suitable velocity records is as follows:

The various waveforms are inspected and an estimate is made of the approximate location of the t_o point in each case. A card is punched with echo number, time of echo from display clock, and five numbers, one for each trace, to indicate whether the first extremum prior to the t_o point is a maximum (1) or a minimum (2). In the absence of a reducible waveform the number for that trace is 0.

Five other cards are then punched, one for each receiving site, giving relative positions of up to 17 (this number is chosen for convenience in punching the information on to the computer cards) consecutive fresnel half-cycle maxima and minima, with a further number locating a simultaneous time marker (usually a convenient phase-spike) the purpose of which is to reference all recorded points on each separate trace to a common point in time. The use of phase spikes as simultaneous time markers eliminates errors which could arise from misalignment of the display oscilloscope traces. This form of calibration also obviates the need to know the display camera film transport speed accurately.

The film readers were calibrated by taking measurements of the distances between up to twenty consecutive phase spikes on each trace at the beginning of each film, the interval between phase spikes being determined by mains frequency which generally varies by much less than 1% and over a day is controlled to average 50 Hz exactly.

In digitizing the waveforms the positions of the diffraction extrema only are measured since these will be least affected and most readily distinguishable in the presence of noise.

5.2 DETERMINATION OF VELOCITY AND POSITION

As mentioned in §5.1 the initial digital data for each trace includes the time displacements of up to 17 diffraction extrema, the time of one reference marker and a number indicating whether the first item is a maximum or a minimum. Also known is the line-of-sight wind velocity for that reflection.

§3.3.3 describes the effect of a line-of-sight wind on the location of successive diffraction extrema. To correct for this we use the method described by Mainstone (1960) of extrapolating the phase from the t_o point back into the diffraction pattern.

Let the time of the i^{th} item be t_i and its phase be P_i. In the computer the time zero is shifted to the point $(3t_1 - t_2)/2$ which serves as the first guess for the position of the t_o point. The initial estimate of phase at this point (ψ_o) is 2π if the first item is a minimum and π if it is a maximum.

If we consider time as increasing in the direction of higher order pre-t_o fresnel zones, then relative to this new zero, the phase at a time t is given by

$$\psi(t) = \psi_o \pm \left[\begin{matrix} A \\ R \end{matrix}\right] 2\pi ft \qquad (5.1)$$

where the letters A and R indicate that the positive sign is chosen for an advancing wind and the negative sign for a receding wind.

We may consider the phase in units of π and substitute numerical values in (5.1) to yield

$$P_i = \left[\begin{matrix} 2 \\ 1 \end{matrix}\right] \pm \left[\begin{matrix} A \\ R \end{matrix}\right] \cdot |u| \cdot t_i/2.8 \qquad (5.2)$$

where u is the wind drift velocity in metres/sec and is related to the doppler frequency f and the R.F. wavelength λ by

$$u = f \cdot \lambda/2 \ .$$

Since the diffraction extrema correspond to successive additions and subtractions of the ground-wave and sky-wave vectors the phase of the i^{th} item corresponding to the distance of the reflecting zone along the trail from the t_o point and corrected for the phase change due to the wind will be given by

$$Z_i = i - P_i \qquad (5.3)$$

Z_i is thus the resultant phase of the wave which would have been returned from the trail up to the i^{th} section were the trail stationary.

Returning to the original approximation for the variation in path length R of reflected waves as a function of the distance s along a stationary trail of the reflection point from the t_o point we have

$$R = R_o + s^2/2R_o \qquad \text{(see §3.3.2).}$$

The difference in radio path length is $x = 2(R - R_o) = s^2/R_o$. Substituting $\psi - \psi_o = 2\pi x/\lambda$ we get

$$\psi = \psi_o + \frac{2\pi s^2}{\lambda R_o} \qquad (5.4)$$

where the sense of the phase change is consistent with the reversed time scale and is of opposite sign to that considered in §3.3.1.

For computation we consider (5.4) in the form

$$s = s(\psi)$$

and calculate the points $s_i = s(Z_i)$. Since $Z_i = Z_i(t_i)$ (eqns 5.2 and 5.3), a plot of s_i against the corresponding t_i should be a straight line with slope V for a meteor of constant velocity.

In fact we would expect the velocity to vary along the meteor path due to the action of atmospheric drag, so that the slope of the curve should change. Over the limited length of trail considered (17 diffraction extrema represent a distance of several kilometres for an average range trail) a small but significant deceleration may occur, resulting in a slight systematic tendency to overestimate the phase and the velocit at the t_o point as well as the height of the t_o point itself. Since it is expected that the reflections will be from the vicinity of the point of maximum ionization for the majority of the meteors observed it is considered that the approximation of constant velocity and the resulting straight line fit to the points (s_i, t_i) is adequate for the determination of the mean velocity in most cases.

Fig. (5.1) shows the variation of position of consecutive diffraction maxima with respect to the t_o point as a function of the phase of the ground-wave relative to the sky-wave at the t_o point. The points are plotted against the argument of the fresnel integrals which is directly proportional to distance along the trail, and for a meteor with constant velocity, directly proportional to time.

Note that as the ground wave phase advances the maxima move towards the t_o point. When the ground-wave has advanced by 2π the n^{th} maximum becomes the $(n - 1)^{th}$. The case considered represents a stationary

trail in the absence of wind drift. Fig. 5.1 shows that the relative positions of the lower order extrema vary much more rapidly with variation in ψ_o than do the higher order extrema.

Thus for an incorrect estimation of ψ_o the calculated s_i will be displaced from their true positions, the sense of the displacement depending upon the sense of the error in ψ_o. Since the displacement of the lower order s_i is much more sensitive to variations in ψ_o than that of the higher order s_i the plot of the points (s_i, t_i) will be a curve which approaches the straight line for correct choice of ψ_o asymptotically with increasing s_i. The sense of the curvature will again depend upon the sense of the error in ψ_o.

In the computer the slope of the best fit straight line to the first three calculated (s_i, t_i) is compared to the slope of the best fit straight line to the remaining data points. This technique requires a minimum of seven diffraction extrema to be present before a trace is considered to be readable. The estimate of ψ_o is varied in discrete steps $(\pi/20^c)$ until agreement between the two slopes lies within specified error limits. The permissible range of variation of ψ_o is sufficiently large to allow for the possibility that the first item read may not in fact be the first diffraction extremum, since as may be seen from Fig. 5.1 the variation of the second and higher order extrema is still a reasonably sensitive guide to the choice of ψ_o even without the first extremum. This was found to be quite useful in the recovery of the echo in the presence of rapid wind doppler beats which may considerably

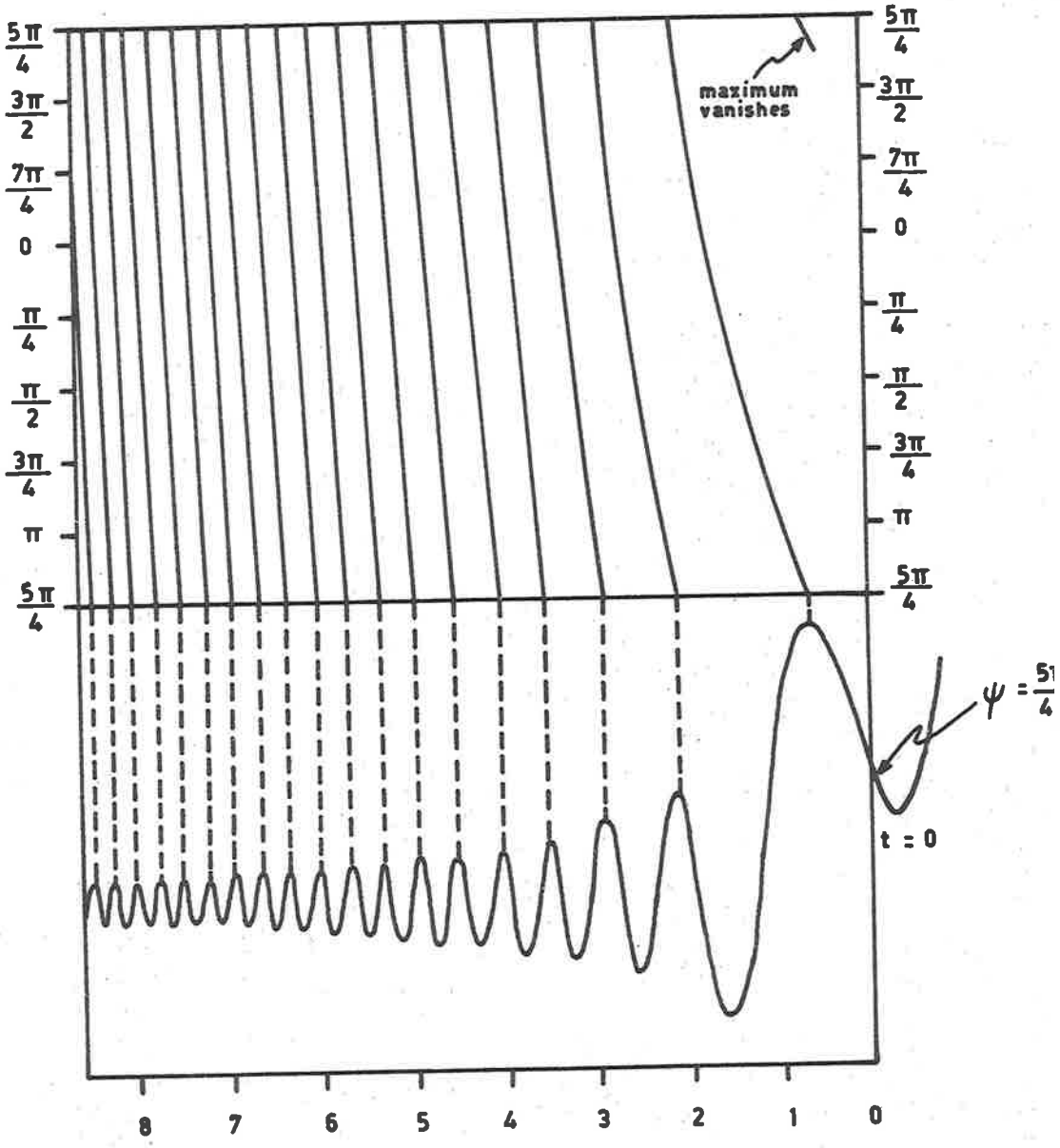

FIG. 5·1 VARIATION OF POSITION OF PRE - t_o DIFFRACTION MAXIMA AS A FUNCTION OF THE PHASE OF THE GROUND - WAVE RELATIVE TO THE SKY WAVE AT THE t_o POINT.

distort the diffraction waveform in the vicinity of the t_o point and make identification of the first extremum unreliable.

The slope of the best fit straight line gives a measure of the meteoroid velocity at that outstation while the intercept on the time axis gives a measure of the time of the t_o point. A mean velocity for that meteor is found by averaging the velocities determined for each outstation weighted according to the number of diffraction extrema used in each case. Time differences between the various calculated t_o points are determined by referring them to the time of the phase spike used as a simultaneous time marker on each trace.

The separation along the trail of the various reflection points from the main station reflection point are given by

$$S_j = V(T_j - T_3), \quad j = 1,2,4,5 \ .$$

Where V is the velocity of the meteoroid and the T_j are the times of the various t_o points relative to the common simultaneous time marker.

5.3 ACCURACY OF RESULTS

The main factor determining the accuracy of the radiant and velocity measurements is the method of interpretation of the fresnel diffraction waveforms. Expected errors in other data used in the reductions are:

(i) The direction cosines (l, m, n) of the specular reflection point from the main receiver (error ± 0.02).

(ii) The height of the reflection point (± 2 km).

(iii) Local civil time of echo recording (± 1 minute).

Reduction programs employed were checked against those used in a previous Adelaide survey (Nilsson, 1964b) by a comparison run using Nilsson's data with the new reduction. Results were virtually identical. Lack of time has prevented complete reduction of the data recorded during the present survey to date, with the months of April and May not even sampled yet. Consequently there has been insufficient time to consider reading a large number of records twice for estimation of film-reading errors. However, a small batch of records was read twice as a spot check. Results of this check are consistent with those of a larger sample carried out by Nilsson, and on this basis Nilsson's estimates of R.M.S. error for his results are equally applicable to the present survey where the closest three stations only are used, and certainly provide an upper limit to the expected errors of the present survey due to the increased accuracy afforded by the redundancy of 4-station echoes (in some cases 5) and the longer base-lines available.

Estimates of standard deviation for the various astronomical quantities are:

$$\text{R.A.} \pm 2.7^{\circ} \quad \text{Dec.} \pm 2.2^{\circ} \quad \text{Vel.} \pm 2.1 \text{ km sec}^{-1}.$$

$$e \pm 0.05 \quad i \pm 4^{\circ} \quad \omega \pm 6^{\circ} \quad 1/a \pm 0.12$$

It is evident from Table 5.1 that there is in general better agreement between the two velocity determinations for any one station than between the values of velocity measured at the various stations for any one record. Inspection shows this trend to be general for all the data and not merely a feature of the particular echoes shown. If we were to

TABLE 5.1

Echo No.		North	Sheedys	St. Kilda	Direk
18262	(a)	54.3	51.8	54.0	-
	(b)	51.8	50.6	54.6	-
	|Δ|	2.5	1.2	.6	-
18266	(a)	69.2	74.5	66.7	65.2
	(b)	68.9	72.6	65.6	66.9
	|Δ|	.3	1.9	1.1	1.7
18327	(a)	18.0	16.2	18.6	-
	(b)	17.3	17.6	18.6	-
	|Δ|	.7	1.4	.0	-
18404	(a)	62.9	61.1	61.7	59.6
	(b)	62.9	58.4	61.1	56.4
	|Δ|	.0	2.7	.6	3.2
18431	(a)	32.7	32.2	31.8	-
	(b)	32.5	32.1	31.7	-
	|Δ|	.2	.1	.1	-
18556	(a)	45.5	43.7	47.7	47.2
	(b)	45.7	45.3	44.9	46.3
	|Δ|	.2	1.6	2.8	.9

Table 5.1 compares the value of meteor velocity determined for each trace for 6 meteors which passed all stages of the reduction program on both readings.

The letters (a) and (b) denote the first and second reading of the data. $|\Delta|$ is the absolute value of the velocity difference between the two readings. Velocity is in km sec^{-1}. A histogram of the values $|\Delta|$ from Table 5.1 is given in Fig. 5.2.

assume that the velocity differences from trace to trace on any one record were entirely due to recorded noise and that the true velocity was constant and the mean of the various estimates for that record then it would be possible to assess the additional uncertainty in velocity from this effect in normal statistical terms. However, as the velocities may in certain conditions be expected to have true differences through deceleration it is not possible to readily assess independently the contribution of noise to the uncertainty in any velocity measurement. The R.M.S. deviation of the measured fresnel pattern from the best fit theoretical pattern is calculated separately for each trace. (See Figs. 8.10 - 8.11.) Generally this shows good agreement between measurement and theory. The phase spikes which serve the dual purpose of time reference and calibration markers in addition to their use in determining direction of motion of the line-of-sight wind are a necessary evil, since with the limited bandwidths available in the system some loss of sharpness of these features is inevitable and small local interruptions in the diffraction pattern commonly result.

Table 5.2 compares the two sets of observed trail separation distances of the various reflection points from the main station reflection point (kms). The letters (a) and (b) distinguish between first and second readings of the same echo. $|\Delta|$ is the absolute value of the difference between the two readings. A histogram of the differences is shown in Figure 5.3 showing a standard deviation of the order of ± .2 kms for the effects of film reading on estimation of separation.

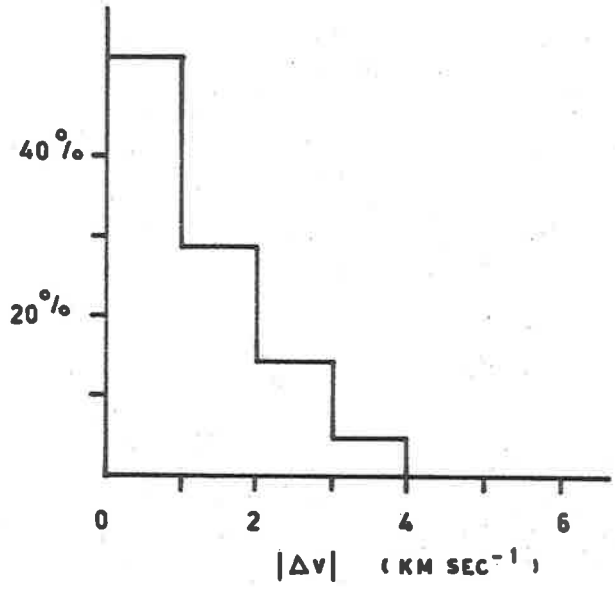

FIG. 5·2 HISTOGRAM OF $|\Delta|$ FROM TABLE 5·1.

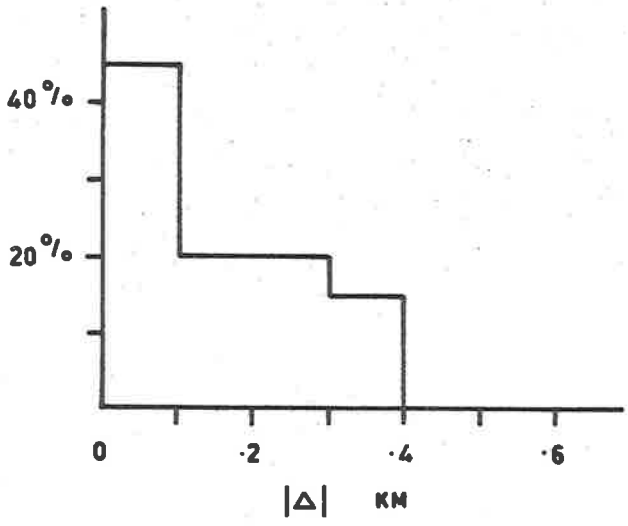

FIG. 5·3 HISTOGRAM OF $|\Delta|$ FROM TABLE 5·2.

It should be remembered that these separation distances are not directly measured, but must be inferred from measured time displacements between t_o points, assuming a constant average velocity along the trail.

Irregular ionization along the meteor train will affect the amplitude rather than the phase of the reflected signal and will not alter the positions of the diffraction extrema. Additional uncertainties in the measurement of reflection point separation which will arise from departures of the recorded diffraction whistles from the theoretical waveforms come from noise, mainly introduced by the telemetry links from the outstations.

These distortions to the recorded waveform effectively cause the least squares fit straight line to lie away from its proper position, thus introducing error into the estimates of velocity and the position of the t_o point. The diffraction extrema corresponding to the fresnel zones near the t_o point are the most sensitive guide to phase and hence the location of the t_o point. These zones also have the broadest extrema, and hence the greatest probability of error in determination of positions.

As can be seen from Fig. (5.1) small errors in estimation of position of a low order extremum will produce only a small shift in phase, as the spacing of the points giving best fit corresponds to a small vertical displacement of a horizontal line intersecting the loci of the various extrema with changing phase. It is also apparent that it is not strictly necessary to include the first fresnel zone in fitting

TABLE 5.2

Echo No.		North	Sheedys	Direk
18262	(a)	- 4.75	- 1.13	-
	(b)	- 4.47	- 1.03	-
	|Δ|	.28	.10	
18266	(a)	- 3.95	- 1.25	1.86
	(b)	- 3.96	- 1.20	1.82
	|Δ|	.01	.05	.04
18327	(a)	- .36	- .59	-
	(b)	- .11	- .79	-
	|Δ|	.25	.20	
18404	(a)	- 3.90	- .82	1.74
	(b)	- 3.54	- .48	1.93
	|Δ|	.36	.34	.19
18431	(a)	- 4.58	- 1.51	-
	(b)	- 4.60	- 1.49	-
	|Δ|	.02	.02	
18556	(a)	- 5.87	- 1.51	1.38
	(b)	- 5.96	- 1.75	1.27
	|Δ|	.09	.24	.11

the points to the theoretical pattern, although some accuracy may be lost without it. In certain cases, notably where the presence of an unusually rapid body doppler has caused distortion of the first pre-t_o zone beyond recognition, it is still possible to recover the necessary information from the echo for orbit determination purely by consideration of the second and higher order extrema.

With the present records it is generally possible to determine easily the relative positions of many more than the 17 such extrema

handled by the data reduction program. (On rare occasions echoes with in excess of 50 distinguishable fresnel zones may be observed.) It is apparent from Fig. (5.1) that with the 17 extrema read it would be most unlikely that distortion of the recorded waveform would result in the best fit to the theoretical pattern in such a manner that the two could be an entire zone out of step. In general this would only be likely to occur where the record quality was so poor that the computer program processing the data would reject the record as unsuitable for further analysis anyway. There is a possibility, although only slight, that a record with such an error could have sufficient other complementary errors to enable apparently reasonable values to be computed from it.

For the majority of echoes, however, the worst error likely to be encountered in estimation of the t_o position should be much less than the length of the first fresnel zone, which for the Adelaide survey amounts to a distance of approximately 0.7 kms for an echo of average range. The expected error will lie somewhere between this value and that of 0.2 kms introduced by film reading. The ability of the system to measure to within a few degrees the radiant positions of known meteor streams using computed reflection point separations of only approximately 2 kms indicates that the overall expected error is nearer 0.2 kms than 0.7 kms.

CHAPTER VI

ATMOSPHERIC RETARDATION

6.1 INTRODUCTION

The computation of a meteor orbit from the initial observation may be divided into three sections, namely calculation of the observed velocity and radiant from observational data, extrapolation of the observed velocity to a geocentric velocity outside the earth's atmosphere, and finally conversion from geocentric to heliocentric coordinates for determination of the orbital parameters.

The last stage of this computation presents no problem (see, e.g. Porter, 1952) and the first is limited only by the quality of the observational data. It is the allowance for the retarding effect of the atmosphere wherein the greatest uncertainty lies. To some degree this is due to a lack of knowledge of the properties of the atmosphere at meteor heights, but primarily the uncertainty is due to a lack of knowledge of the structure and composition of the small meteoroids comprising the major portion of the radio meteor population.

Various workers have approached the problem in different ways. Gill and Davies (1956) estimated the velocity decrease due to retardation from a consideration of the correlation between the scatter in measured velocities of members of known meteor streams and the reflection point heights. Lebedinets (1968) has employed a correction of the form $\Delta v \sim \frac{1}{v}$. Evans (1966) describes an experiment in which a narrow-beam high power radar operating at 68 cm. wavelength was directed at the radiants of a number

of intense meteor showers. Head echoes were detected from meteors travelling radially along the beam and Evans was able to measure velocities and decelerations accurately by means of the doppler shift in the radar frequency. Unfortunately this method, being restricted to head echoes, is limited to investigation of the members of major streams. Its undeniable advantage is the great accuracy of the direct measurement of velocity afforded by the doppler shift technique, enabling sensitive measurement of small velocity differences.

With the addition of long-distance outstations to the Adelaide meteor system we hoped to be able to follow a meteor over a path of sufficient length to observe distinct decelerations despite the relatively large probable measurement errors of the reduction procedure. From such observations one would be able to improve the accuracy of orbit computations, as well as learning something of the properties of the meteoroids themselves. Despite poorer accuracy this method has the advantage over that of Evans in that it is equally applicable to sporadic meteors, and that data may be collected on a routine basis.

6.2 DERIVATION AND SOLUTION OF THE DRAG EQUATION

With the Adelaide system we are able to determine:-

(1) The position in space of a point on the meteor trail.

(2) Direction cosines (orientation) of the trail.

(3) The meteor velocity at up to five reflection points on the trail.

(4) The time taken for the meteor to travel between these points.

(5) The separation along the trail of the reflection points (inferred from 3. & 4. - maximum separation possible approximately 20 km).

(6) Limiting observable trail electron density.

With this information it should be possible to measure decelerations at least for some meteors on a routine basis. From the deceleration the surface area/mass ratio for the meteoroid can be computed and if we make some assumptions concerning the ionizing efficiency the meteoroid density may be deduced.

First it is necessary to assume suitable models for the meteor and the atmosphere through which it passes. The atmospheric model assumed is the U.S. Standard Atmosphere (1962). About meteors we know less. We are uncertain of their shape, composition, and likelihood of fragmentation. It is necessary to consider an "effective spherical meteor" with an "equivalent radius", and indirectly gain information about the true meteoroid properties from an analysis of the deviations of measured results from predictions.

From a consideration of the conservation laws involved in the ablation process Verniani (1961) finds that the acceleration due to atmospheric drag can be expressed as

$$a = \frac{-3F\gamma}{4\rho_m gH} \cdot \frac{v^2}{r} \cdot p \qquad (6.1)$$

where

g = gravitational acceleration

H = atmospheric pressure scale height

p = atmospheric pressure

ρ_m = meteor bulk density

r = equivalent radius of meteor (defined through the relation $m = \frac{4}{3}\pi r^3 \rho_m$, where m is the meteor mass)

v = meteor velocity (with respect to a stationary atmosphere)

γ is the drag coefficient of Verniani (equivalent to the K of Öpik (1958)).

F is a shape factor defined by $\sigma = F4\pi r^2$, where σ is the meteor cross-sectional area (Note: $F = 4J$ where J is Öpik's shape factor).

Following Evans (1966) we take the value $J \sim 0.5$ ascribed by Öpik to an "average solid meteoroid of not too unusual shape" and consider that $\gamma = 1$ in this case, since it is thought that the majority of meteors detected with our system are small compared with the mean free path of air molecules at the heights considered, so that air-caps would generally not be formed. With these assumptions (6.1) becomes

$$a = \frac{-3}{2\rho_m} \frac{v^2}{r} \rho \qquad (6.2)$$

where $\rho = \frac{p}{gH}$ is the air density.

A more complete expression for the acceleration should include gravitational acceleration, but for all but the slowest meteors at the upper limit of the meteor height range (v and ρ both small)

$$|g| << \left[\frac{3}{2} \cdot \frac{v^2}{\rho_m r} \cdot \rho\right]$$

and g can safely be ignored. This is clear from Fig. (6.1) which shows the variation of $|a|$ with height for various meteor velocities and a likely range of values of G (the surface area/mass ratio).

It should be emphasized that account is taken elsewhere of the prolonged gravitational acceleration acting upon the meteor outside the atmosphere which produces the phenomenon known as zenith attraction (see, e.g. McKinley, 1961).

Rotation of the earth about its axis introduces the need for a further correction of the meteor radiant position and velocity for diurnal motion. This rotation of the axes of observation makes it necessary to consider also pseudo (coriolis and centrifugal) forces acting upon the particle in any complete description of the equations of motion, but for all likely meteor velocities the resulting apparent accelerations are small compared with g and once again may safely be omitted from the drag equation.

From the laws of conservation of energy and momentum Verniani (1961) shows that

$$m = m_\infty \exp\left[\frac{v^2 - v_\infty^2}{4\xi}\right]$$

and hence

$$r = r_\infty \exp\left[\frac{v^2 - v_\infty^2}{12\xi}\right] \qquad (6.3)$$

where

m_∞, r_∞ are mass and equivalent radius of the meteoroid before ablation .

ξ is the ablation energy per unit mass and can be written as $\frac{\gamma\ell}{\Lambda}$.

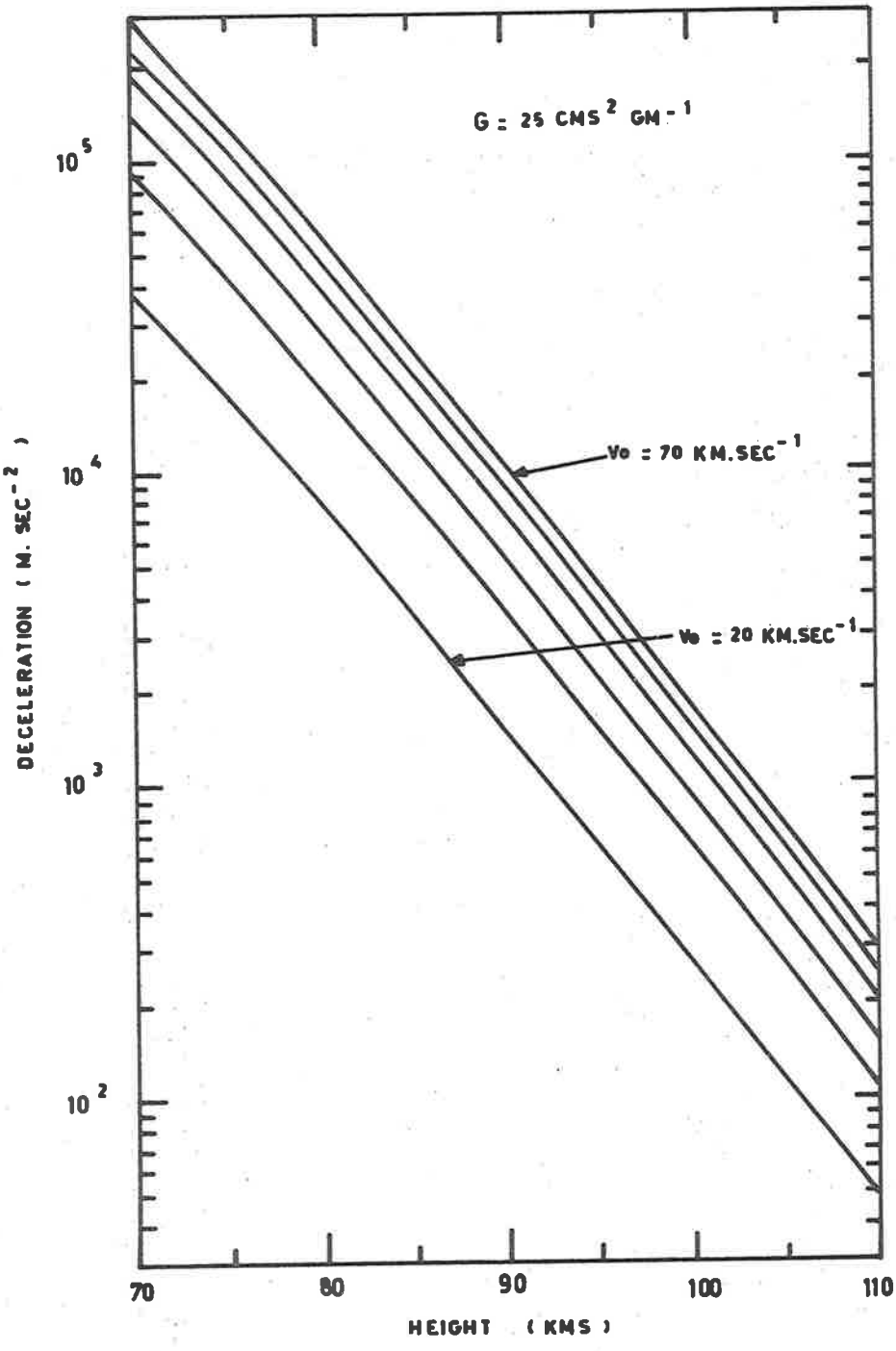
G = 25 CMS^2 GM^{-1}
V_o = 70 KM.SEC^{-1}
V_o = 20 KM.SEC^{-1}
DECELERATION (M. SEC^{-2})
10^5
10^4
10^3
10^2
70
80
90
100
110
HEIGHT (KMS)

FIG. 6 · 1 (a)

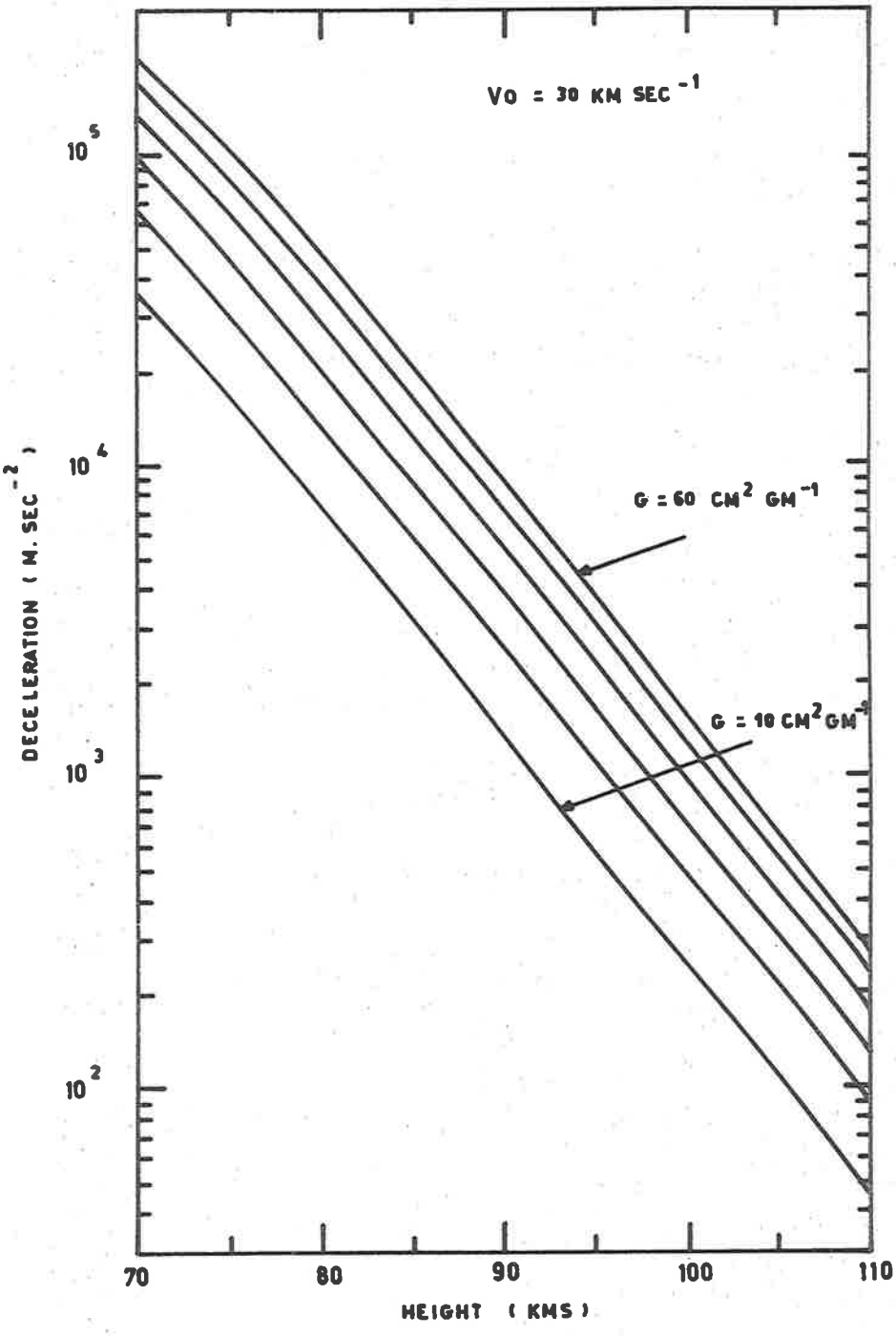
Vo = 30 KM SEC $^{-1}$
10^5
10^4
10^3
10^2
DECELERATION (M. SEC $^{-2}$)
G = 60 CM^2 GM^{-1}
G = 10 CM^2 GM^{-1}
70
80
90
100
110
HEIGHT (KMS)

FIG. 6 · 1 (b)

ℓ is the latent heat of vaporization of the meteoroid.

Λ is the coefficient of heat transfer.

Jacchia (1949) gave a value of 30 km^2 sec^{-2} for ξ. Evans (1966) found ξ to have an average value of 15.4 km sec^{-2} for some Geminid and Quadrantid meteors. Further, Jacchia (1958) has observed a slight increase in ξ during the ablation of photographic meteors. However, for the present purposes we may assume that it will remain reasonably constant over the trail separation distances usually observed.

Verniani (1961) derives from eqn (6.1) an explicit form for the acceleration

$$a = \frac{\cos \chi}{2H} v^2 \exp\left[\frac{-v^2}{12\xi}\right] \cdot \left[E_i\left(\frac{v_\infty^2}{12\xi}\right) - E_i\left(\frac{v^2}{12\xi}\right)\right] \qquad (6.4)$$

where $E_i(x)$ is the exponential integral

$$\int_{-\infty}^{x} \frac{e^t}{t}\, dt \ , \ x > 0 \ .$$

If v_∞ is known, a comparison of (6.4) with (6.1) shows that we have sufficient information to deduce the surface area/mass ratio G. However, since v_∞ is not directly measured in this survey, we find it useful instead to develop eqn (6.2) in the following manner.

Consider a meteoroid travelling through the atmosphere. We may assume without loss of accuracy that, over the length and height range to be considered, the path is a straight line. Let the angle of the path to the zenith be χ. In general the meteor will be approaching the earth so that $\chi > \frac{\pi}{2}$ and $\cos \chi < 0$. Let the quantity x be the position

vector of the meteoroid along the trajectory, defined so that x becomes increasingly positive as the meteor progresses. Fig. 6.2 shows two points on a meteor trajectory. The meteor arrives at the point P_o, position vector x_o, height h_o, at time t_o, and reaches P, position vector x, height h, at time t. Then

$$(x - x_o) = (h - h_o) \sec \chi \text{ which is } > 0 \text{ for } t - t_o > 0.$$

The meteor velocity is positive in this reference system. The deceleration due to drag is in opposition to the velocity.

The notation employed is such that

$$v = \dot{x} = \frac{dx}{dt}$$

and

$$a = \dot{v} = \ddot{x} = \frac{d^2x}{dt^2}$$

Let H_o be the atmospheric scale height at h_o and assume it to be constant over the limited height range involved. We have assumed F and γ to be constant for all meteors under consideration, and throughout the ablation period. In addition we must assume that ρ_m and ξ are constant for a particular meteor during the ablation process.

Since the atmospheric pressure scale height is assumed to be constant over the limited height range under consideration we may write

$$\rho = \rho_o \exp\left[(x_o - x)\frac{\cos \chi}{H_o}\right] \qquad (6.5)$$

In the same manner that eqn (6.3) was derived we may show that

$$r = r_o \exp\left(\frac{v^2 - v_o^2}{12\xi}\right) . \qquad (6.6)$$

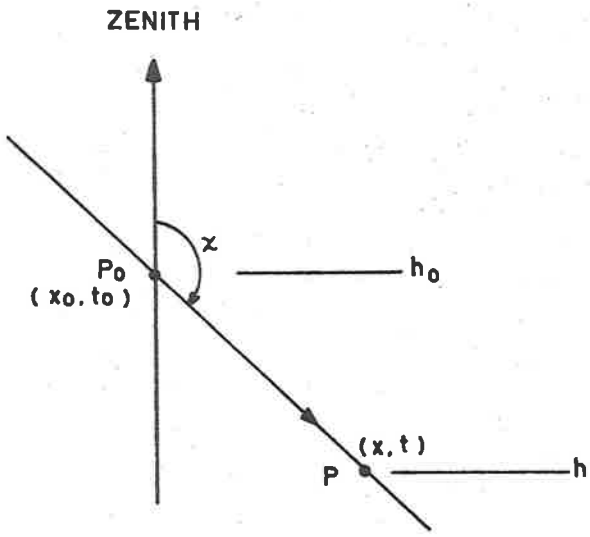

FIG. 6 · 2

Substitution of (6.5) and (6.6) in (6.2) gives

$$\ddot{x} = - \frac{3}{2} \frac{v^2 \rho_o}{\rho_m r_o} \exp \left[(x_o - x) \frac{\cos \chi}{H_o} + \frac{(v_o^2 - v^2)}{12\xi} \right] \qquad (6.7)$$

i.e.

$$\ddot{x} = - Av^2 \exp \left(- \frac{v^2}{12\xi} - Bx \right)$$

where

$$B = \frac{\cos \chi}{H_o} \qquad (6.7a)$$

and

$$A = \frac{3}{2} \frac{\rho_o}{\rho_m r_o} \exp \left(x_o B + \frac{v_o^2}{12\xi} \right)$$

Putting $\dot{v}$ for $\ddot{x}$ and using the relation $\frac{\dot{v}}{v} = \frac{dv}{dx}$ we may rearrange (6.7a) to give

$$\exp \frac{v^2}{12\xi} \frac{dv}{dx} = - Ae^{-Bx} \qquad (6.8)$$

which may then be integrated to give

$$\int_{v_o}^{v} \exp \frac{v^2}{12\xi} \, dv = - A \int_{x_o}^{x} e^{-Bx} \, dx \qquad (6.9)$$

On making the substitution $z = \frac{v^2}{12\xi}$, whence $dz = 2z \frac{dv}{v}$ (6.9) becomes

$$\left\{ E_i \left(\frac{v^2}{12\xi} \right) - E_i \left(\frac{v_o^2}{12\xi} \right) \right\} = \frac{2A}{B} \left[e^{-Bx} - e^{-Bx_o} \right]$$

In full, this expression is:

$$\left\{ E_i \left(\frac{v^2}{12\xi} \right) - E_i \left(\frac{v_o^2}{12\xi} \right) \right\} = G_o \rho_o \exp \left(\frac{v_o^2}{12\xi} \right) \cdot \frac{H_o}{\cos \chi} \cdot \left[\exp \left(\frac{\cos \chi}{H_o} (x_o - x) \right) - 1 \right] \qquad (6.10)$$

where $G_o = \frac{3}{\rho_m r_o}$ is the surface area/mass ratio at the point x_o.

Theoretical curves describing the relationship between the various quantities in Eqn (6.10) have been computed and are shown in Figures 3(a) - (d). These curves clearly illustrate the advantages of large outstation separations for this work, although it should be realized that very few meteors produce trails which are detectable over lengths greater than 20 km. Assuming that the measurement errors in velocity and time are nearly independent of separation distance and reflection point height it can be seen that the probability of reliable deceleration measurement increases with increasing reflection point separation, and most strongly with decreasing reflection point height.

6.3 ACCURACY OF RESULTS

Fig. (6.4) shows the variation of error in the measurement of the surface area/mass ratio (which will arise from errors in measurement of velocity and position) as a function of the height of the upper reflection point. The error has been calculated for two representative velocities, 30 km sec^{-1} and 60 km sec^{-1}, assuming an absolute error in measuring the difference of the velocities at two reflection points of 3 km sec^{-1}. The dependence of error in G upon error in measurement of trail separation distance is such that the curve for v=30 km sec^{-1}, D=20 km is equally applicable for any $d + d' = D$ where d is the true separation distance and d' is the absolute error in d. Thus the 20 km curve represents a separation distance of 20 km assuming no measurement error, or equally well a separation of 18 km with an error of 2 km.

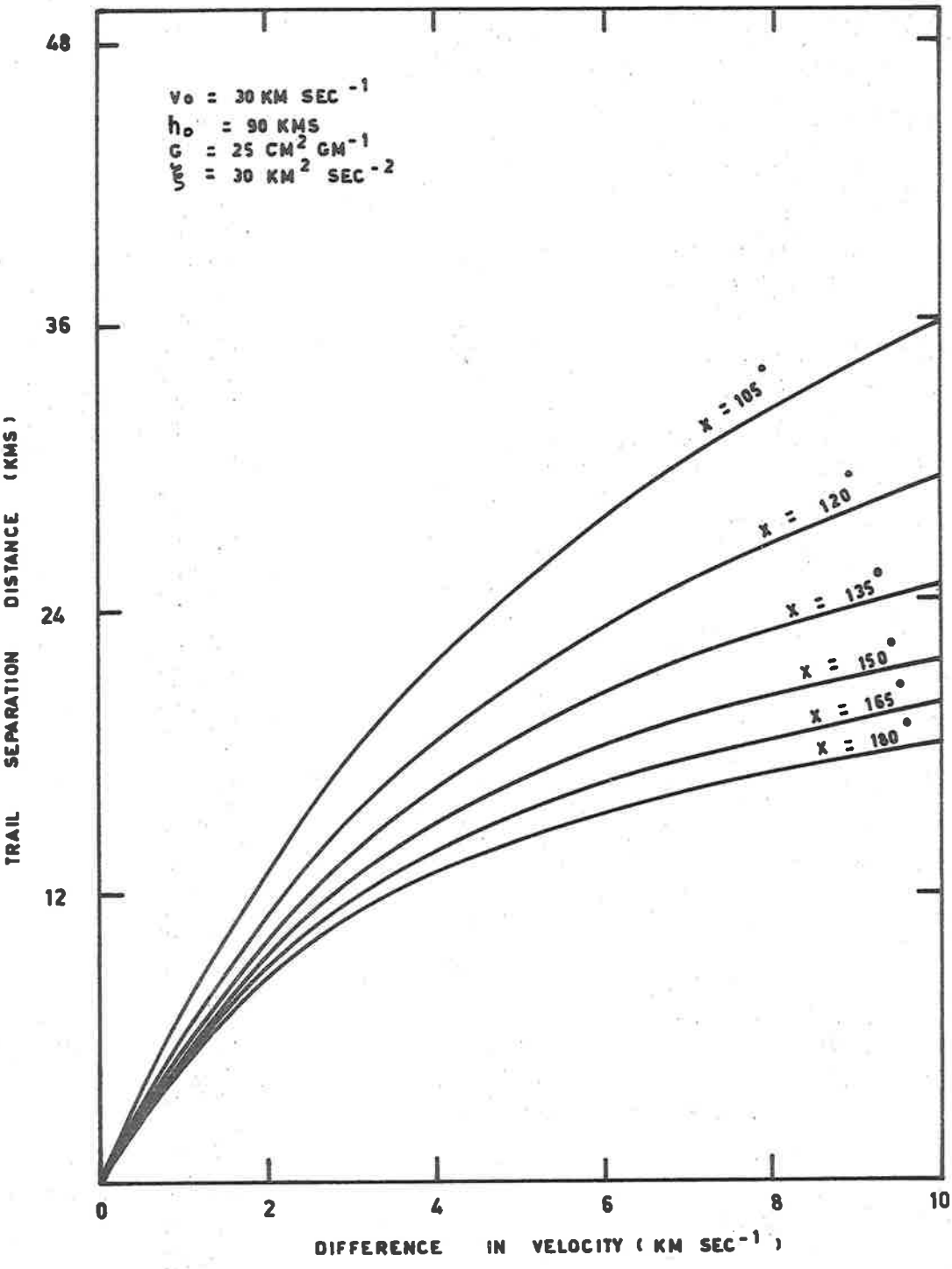
Vo = 30 KM SEC -1
ho = 90 KMS
G = 25 CM2 GM-1
ξ = 30 KM2 SEC-2
χ = 105°
χ = 120°
χ = 135°
χ = 150°
χ = 165°
χ = 180°
48
36
24
12
0
2
4
6
8
10
TRAIL SEPARATION DISTANCE (KMS)
DIFFERENCE IN VELOCITY (KM SEC-1)

FIG. 6·3 (a)

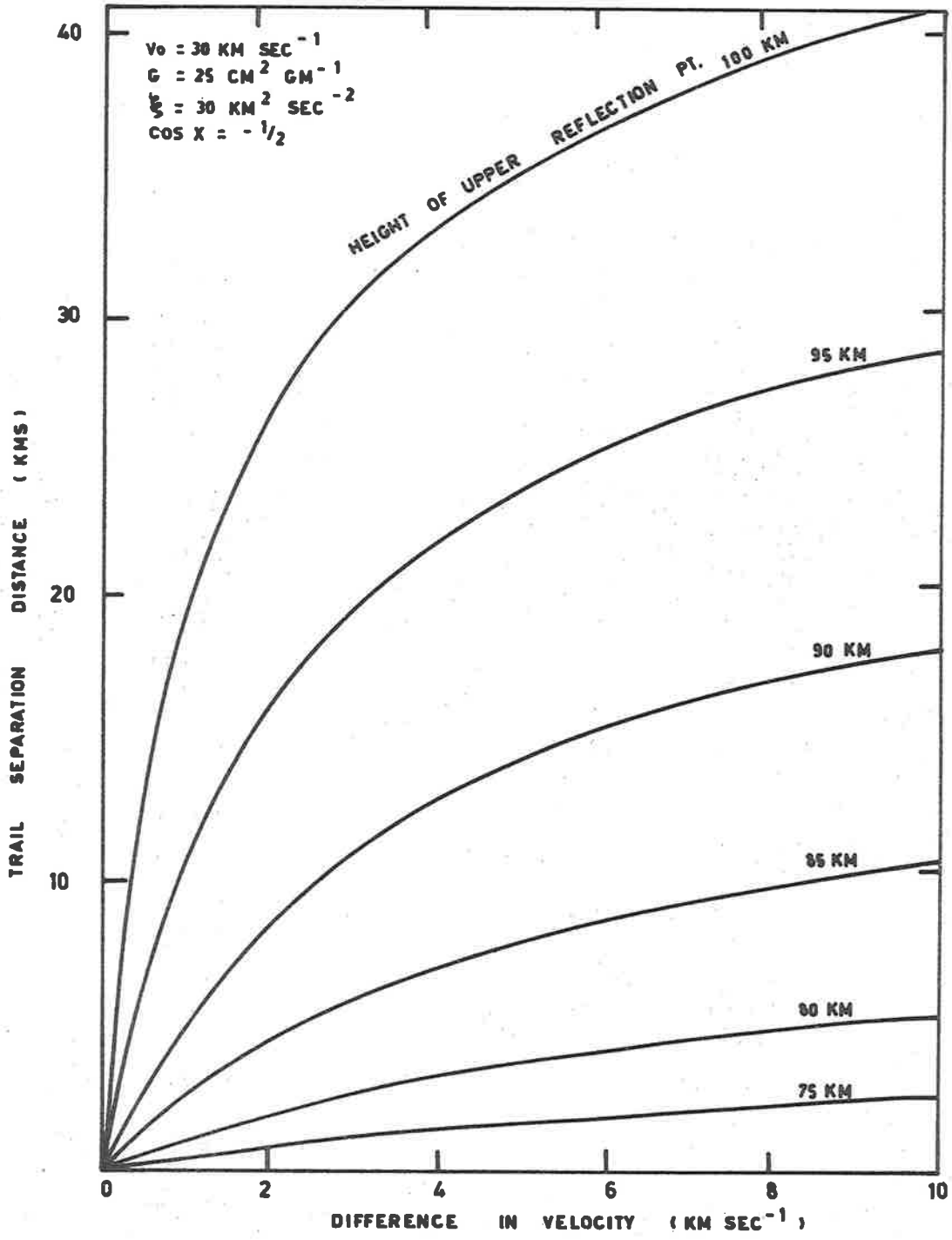
Vo = 30 KM SEC⁻¹
G = 25 CM² GM⁻¹
ξ = 30 KM² SEC⁻²
COS X = -1/2
HEIGHT OF UPPER REFLECTION PT. 100 KM
95 KM
90 KM
85 KM
80 KM
75 KM
TRAIL SEPARATION DISTANCE (KMS)
DIFFERENCE IN VELOCITY (KM SEC⁻¹)
40
30
20
10
0
2
4
6
8
10

FIG. 6·3 (b)

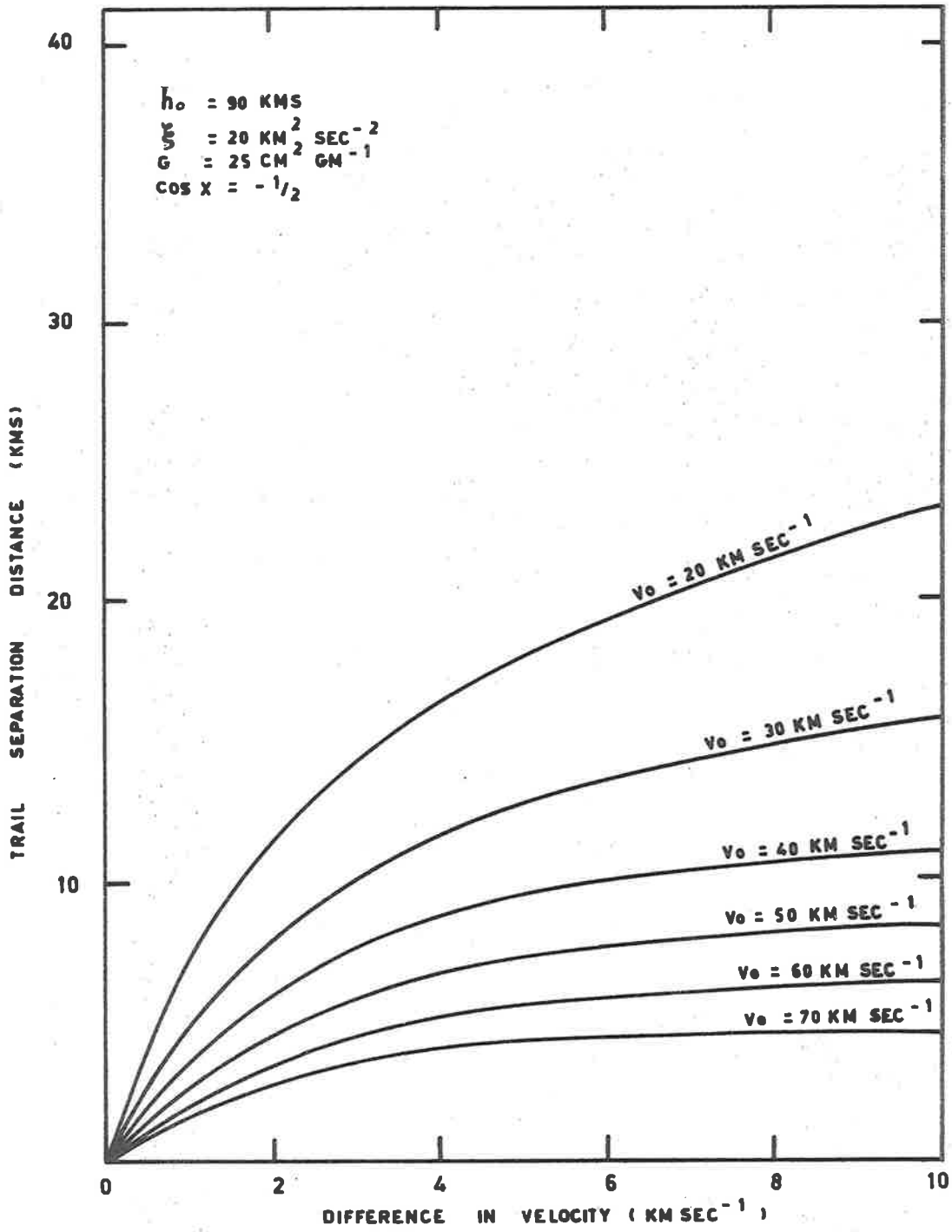
h_o = 90 KMS
ξ = 20 KM^2 SEC^{-2}
G = 25 CM^2 GM^{-1}
cos X = $-1/2$
Vo = 20 KM SEC^{-1}
Vo = 30 KM SEC^{-1}
Vo = 40 KM SEC^{-1}
Vo = 50 KM SEC^{-1}
Vo = 60 KM SEC^{-1}
Vo = 70 KM SEC^{-1}
TRAIL SEPARATION DISTANCE (KMS)
40
30
20
10
0
2
4
6
8
10
DIFFERENCE IN VELOCITY (KM SEC^{-1})

FIG. 6·3 (c)

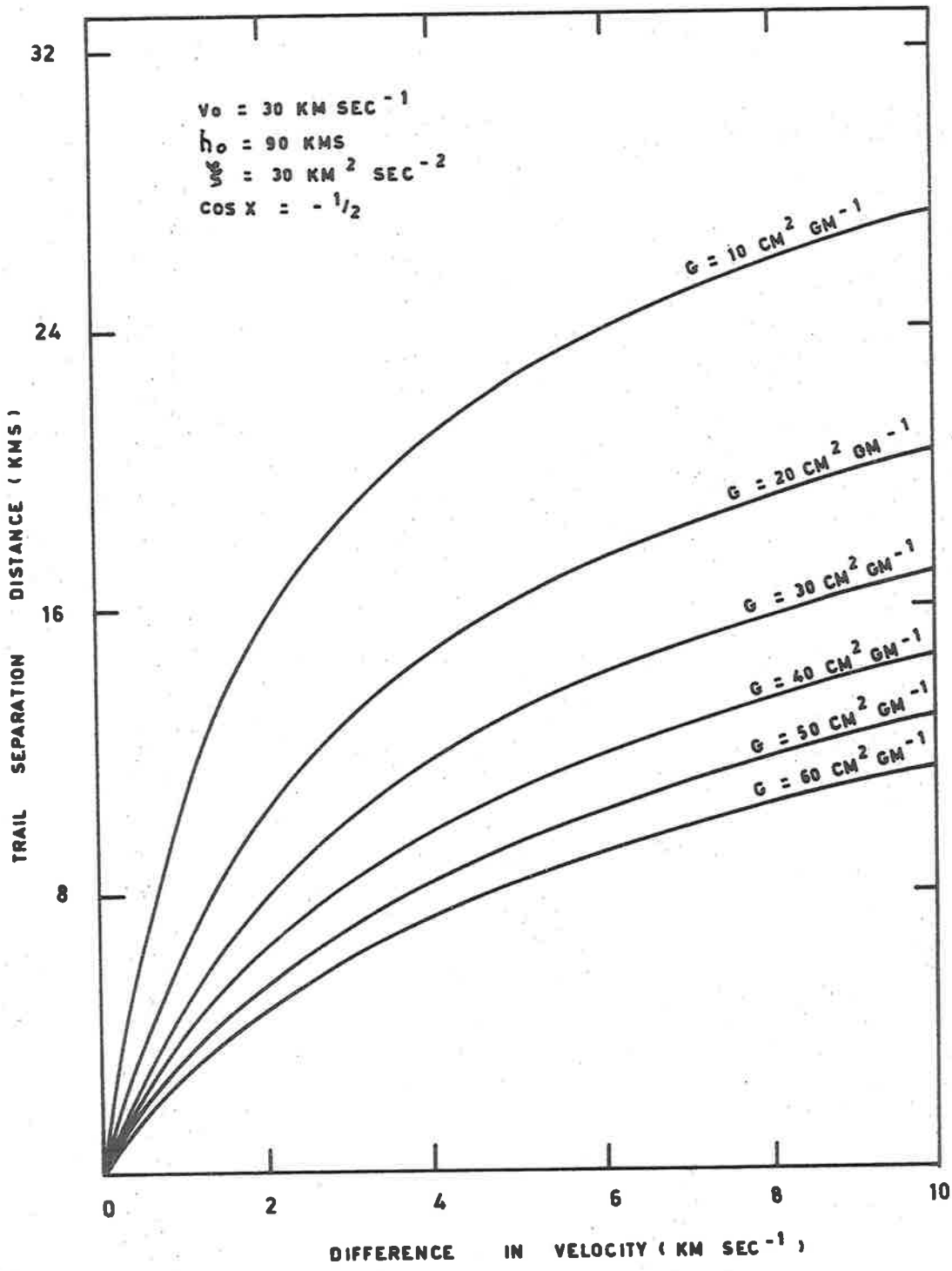
32
24
16
8
V_o = 30 KM SEC^{-1}
h_o = 90 KMS
γ = 30 KM^2 SEC^{-2}
COS X = $-\frac{1}{2}$
G = 10 CM^2 GM^{-1}
G = 20 CM^2 GM^{-1}
G = 30 CM^2 GM^{-1}
G = 40 CM^2 GM^{-1}
G = 50 CM^2 GM^{-1}
G = 60 CM^2 GM^{-1}
TRAIL SEPARATION DISTANCE (KMS)
0
2
4
6
8
10
DIFFERENCE IN VELOCITY (KM SEC^{-1})

FIG. 6 · 3 (d)

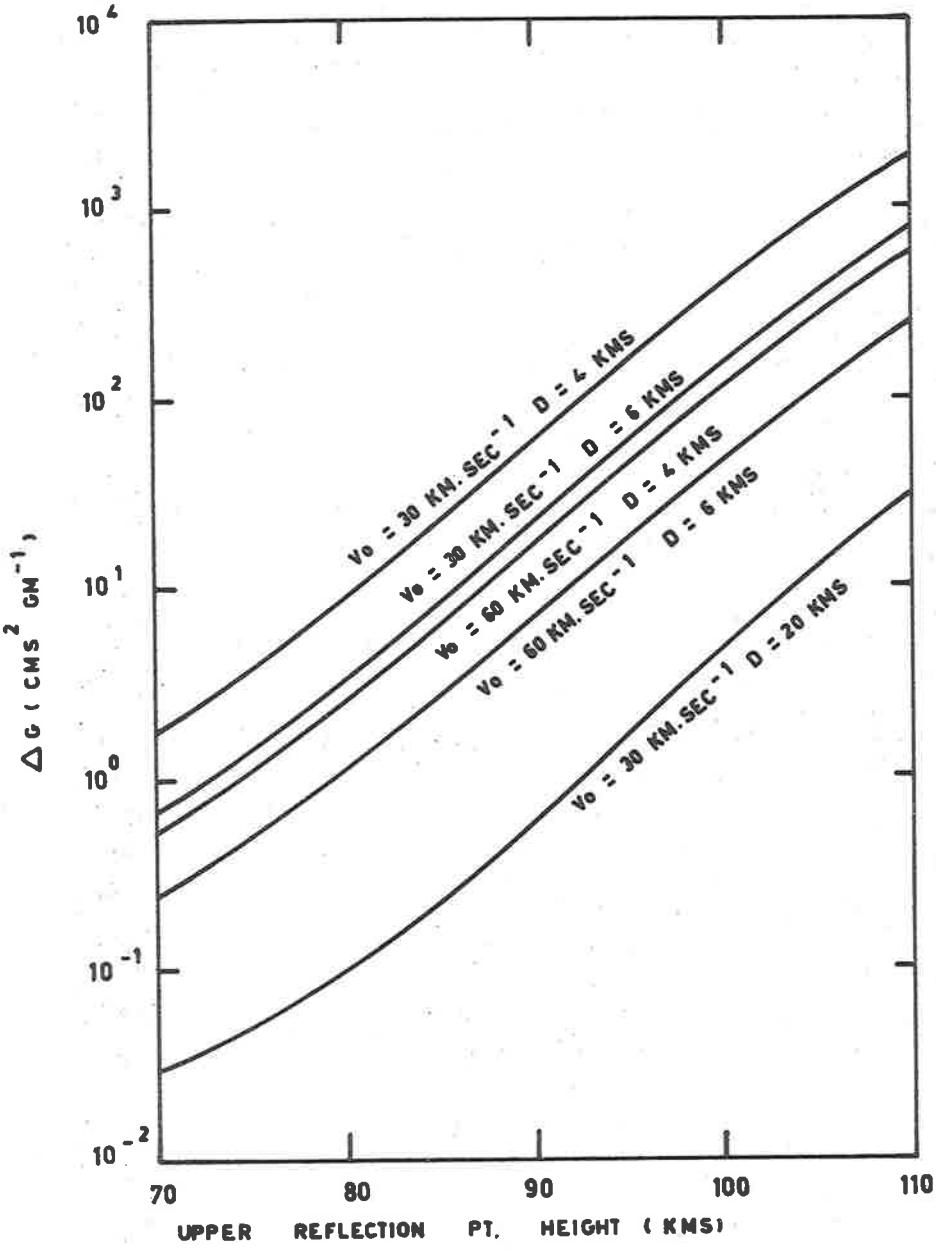
10^4
10^3
10^2
10^1
10^0
10^{-1}
10^{-2}
ΔG (CMS^2 GN^{-1})
V_o = 30 KM. SEC^{-1} D = 4 KMS
V_o = 30 KM. SEC^{-1} D = 6 KMS
V_o = 60 KM. SEC^{-1} D = 4 KMS
V_o = 60 KM. SEC^{-1} D = 6 KMS
V_o = 30 KM. SEC^{-1} D = 20 KMS
70
80
90
100
110
UPPER REFLECTION PT. HEIGHT (KMS)

FIG. 6·4

6.4 MEASURED VALUES OF SURFACE AREA/MASS RATIO

With the Adelaide system we have enough information to solve (6.10) for G_o for each meteor for which an orbit can be calculated. This calculation has been made for all the meteors in the present survey. The range of computed values for G_o extends from very large negative numbers (indicating a measured acceleration) through to very large positive numbers. However, the majority of the extreme values are attributable to differences in measured velocity at closely spaced reflection points, giving the appearance of rapid decelerations (or accelerations).

At least two estimates of G_o were available for each meteor reduced. Average values for G_o were calculated for each meteor, rejecting outright any measurement with a separation distance of less than 1 kilometre, and weighting the remaining values exponentially in proportion to separation distance and inversely according to height of the reflection point relative to the main station reflection point.

Histograms of distribution of measured values of G for 5 km. intervals in height are given in Figs. 6.5(a) - (f). The distributions in each case have the appearance of an error scatter centred around a central peak. Small sample sizes in some cases make statistical interpretation difficult, but nevertheless in addition to corroborating the estimates of error shown in Fig. 6.4 a comparison of the various histograms reveals clear trends in the data.

For $\Delta v = v_1 - v_0 \ll v_0$

$$E_i\left(\frac{v_1^2}{12\xi}\right) - E_i\left(\frac{v_0^2}{12\xi}\right) \approx \frac{12\xi}{v_0^2}\left[\exp\left(\frac{v_1^2}{12\xi}\right) - \exp\left(\frac{v_0^2}{12\xi}\right)\right].$$

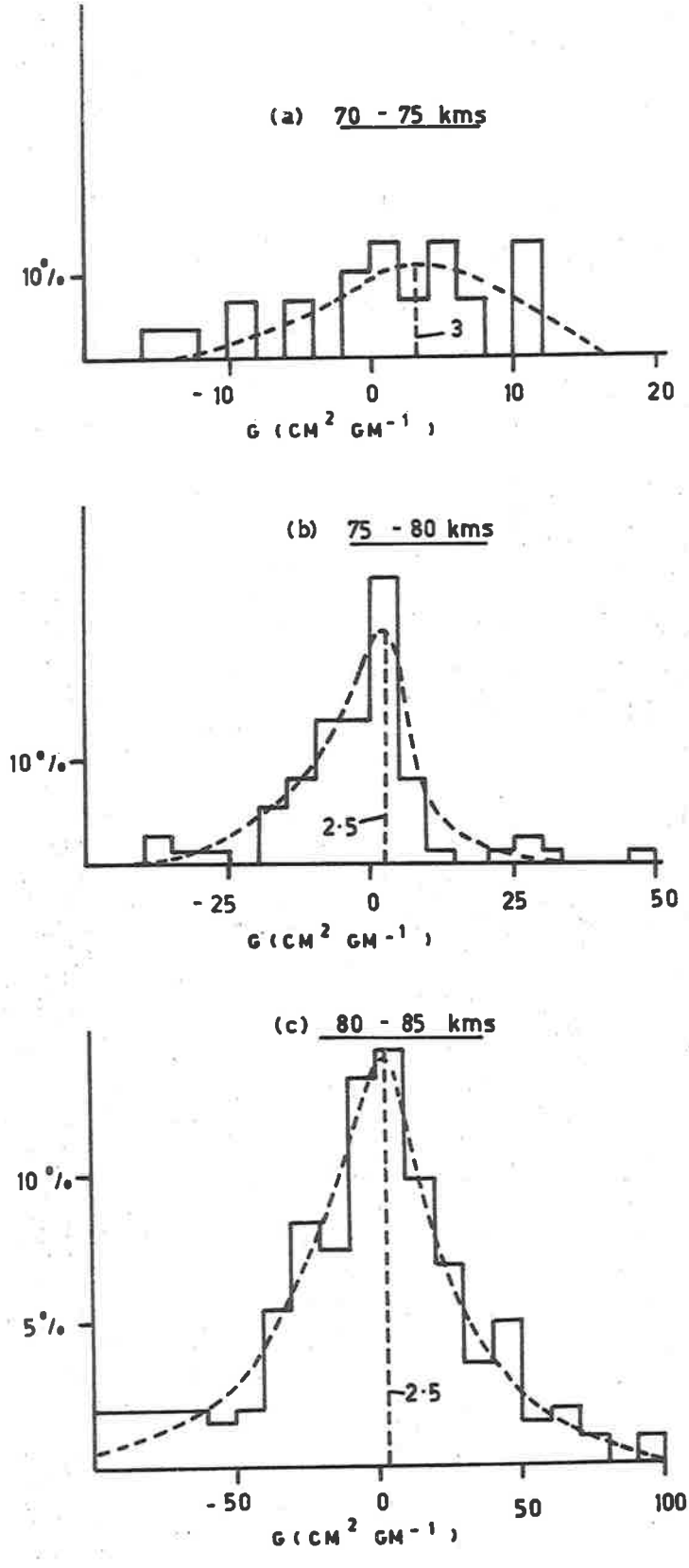

FIG. 6·5 DISTRIBUTION OF MEASURED VALUES OF SURFACE AREA / MASS RATIO FOR VARIOUS INTERVALS OF REFLECTION POINT HEIGHT.

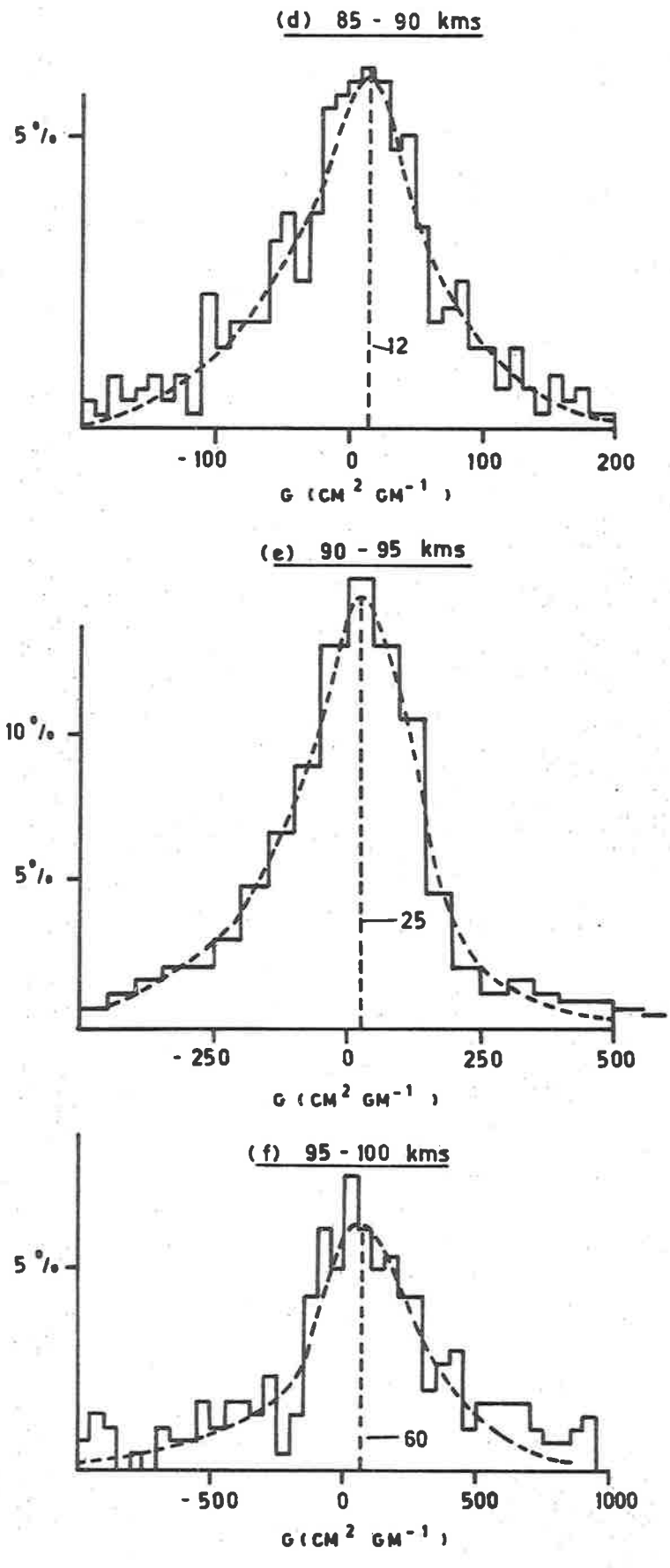
(d) 85 - 90 kms
5 %
12
- 100
0
100
200
G (CM 2 GM-1)
(e) 90 - 95 kms
10 %
5 %
25
- 250
0
250
500
G (CM 2 GM-1)
(f) 95 - 100 kms
5 %
60
- 500
0
500
1000
G (CM 2 GM-1)

FIG. 6·5 (cont.)

Using this approximation it can be shown that

$$G \propto \left\{\exp\left\{\left(\frac{\Delta v}{12\xi}\right)\left(\frac{2v_0 + \Delta v}{12\xi}\right)\right\} - 1\right) \exp\left\{\frac{\cos \chi}{H_o} \Delta x\right\} \qquad (6.11)$$

where $\Delta x = x_1 - x_0$. Errors in the determination of G arise primarily from errors in Δv and Δx.

From this it follows that whereas we can expect errors in Δv and Δx to be distributed normally in the statistical sense, errors in G will be exponentially dependent upon these original errors so that the spread of values of G will not follow a normal distribution. To produce a histogram of normal distribution for G it would be necessary to first locate the mean and then logarithmically contract the deviations about the mean in a suitable manner. Since the value of the mean is dependent upon the measured deviations it would be difficult to apply this procedure to the analysis of the present distributions.

It is not possible to calculate simply the logarithmic mean for G since the calculated values of G may be positive, negative or zero.

Additional problems should be considered in the treatment of the data. It is certainly reasonable to expect that there will be some true variation amongst the values of G in any sample, even assuming that the majority of the meteors observed have the limiting magnitude for the survey.

Pokrovskiy (1964) postulates a number of mechanisms whereby the atmospheric interaction could even cause meteoroid acceleration. Possibly then not all of the measured accelerations in the present survey, represented as negative G values, are attributable to error alone.

The range of 5 km. from which data was drawn for each histogram is a large fraction of an atmospheric scale height, and significant changes in atmospheric conditions will be evident over this range. Finally, there is some uncertainty as to the randomness of the error distribution. It is likely, in view of the ability of the reduction program to optimise data with small initial errors more effectively than other data with slightly greater errors, that the reliability of the more central portions of the histograms is significantly greater than that of the limbs. These considerations are given weight by the similarities of the histograms themselves. All have positive modal values, and positive mean values for the central portions. The inclusion of extreme values in determination of the mean without any weighting to subdue their influence can significantly alter the mean, in two of the distributions even making it slightly negative.

The various difficulties and uncertainties outlined above severely limit the amount of information available from the data as well as making rigorous statistical treatment impracticable. Nevertheless broad trends in the data are clearly apparent and are worth presenting.

Smooth curves have been fitted to the various histograms on the assumption that the true distribution of G in any height range is unimodal. The peak value of the fitted curve is then taken as the representative value of G for that distribution. The curves have been fitted visually and have no mathematical significance. Their purpose is to give some weight to the values near but not included in the modal value of the

histogram, and so compensate for bias in the results which could occur through choice of the grouping interval if the middle value of the mode alone were taken.

Fig. 6.6 shows the relation of the modal values thus obtained for the various height ranges. The quantity plotted is $r\rho = \frac{3}{G}$ for ease of comparison with values obtained by Evans (1966) for some individual Geminid and Quadrantid meteors.

The basic agreement between the present results and those of Evans is clearly apparent. Evans' data shows the same tendency for increasing $r\rho$ with decreasing height, and as he mentions, some of this spread could be due to inaccurate measurement of height. Nevertheless the variation in height range shown is certainly far too great to be entirely attributable to error and the described trend is clearly real. The Adelaide data has extremely reliable height measurement for a meteor radar system (within ± 2 km). Evans estimates his apparatus to have a limiting magnitude sensitivity of $M_v = +5$ for directly approaching meteors whereas the Adelaide survey has a limiting magnitude near $M_R = +8$.

Evans estimates the mean value of the ablation energy for his meteors to be 15.4 $km^2\ sec^{-2}$, whereas the value used in the calculation of G for the present data is 30 $km^2\ sec^{-2}$. Adoption of Evans' value for the Adelaide data would result in even closer agreement between the two sets of observations than at present.

The observed variation of $r\rho$ with height which is also apparent in Evans' data is the reverse of what would be expected for a population of

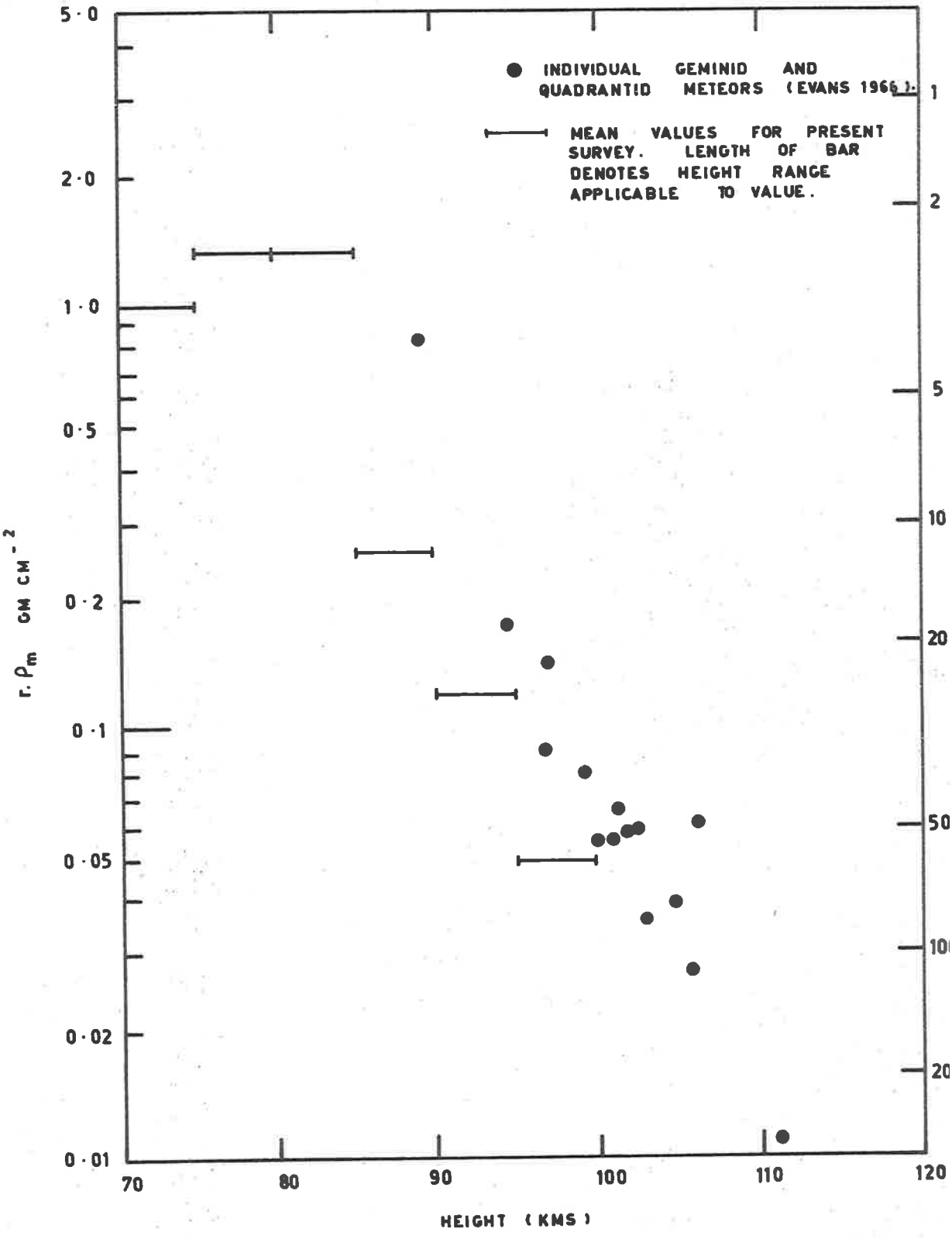
INDIVIDUAL GEMINID AND QUADRANTID METEORS (EVANS 1966).
MEAN VALUES FOR PRESENT SURVEY. LENGTH OF BAR DENOTES HEIGHT RANGE APPLICABLE TO VALUE.
r. ρm GM CM⁻²
5·0
2·0
1·0
0·5
0·2
0·1
0·05
0·02
0·01
1
2
5
10
20
50
100
200
70
80
90
100
110
120
HEIGHT (KMS)

FIG. 6·6

meteors with identical properties (in which we would expect ablation to decrease r_ρ with decrease in height) and is evidently due to the operation of a strong selection effect on a meteor population with a wide variation in properties.

The notion that the selection could be related to limiting magnitude with the smaller, fainter, larger G meteors being arrested at the greatest heights is irreconcilable with the differential mass flux law $N(m) \propto m^{-s}$, $s \sim 2$ and the observed frequency distribution of reflection point height.

It is apparent that the selection effect operates on the meteor density variation. Verniani (1964) finds a similar variation of density with height of maximum light for photographic meteors from the data of Hawkins and Southworth (1958), although the range of variation is not as great as for the present data.

While one should guard against trying to read too much from subtle variations in data originally based upon rather sweeping assumptions, and while Evans' estimate of limiting magnitude is certainly derived in a different manner to that of the present data, it does seem reasonable to assume that the Adelaide meteors have a smaller mean mass than those of Evans.

We may determine the meteor mass from the relation

$$m_\infty = \frac{1}{12} \mu H f^{-2} (1 + 2f)^3 \frac{q_m}{\beta} \sec \chi \qquad (6.12)$$

in which

$$f = 1 + 3(2 + \eta)\xi V_\infty^{-2} \qquad \text{(Weiss, 1958; Verniani, 1961)}$$

where β is the probability of ionization of a meteor atom, μ is the mass of a meteor atom, H is the atmospheric scale height, q_m is the maximum electron line density along the trail, χ is the zenith angle of the trail and ξ is the ablation energy per unit mass. η is the exponent of the relation

$$\beta = \beta_0 v^\eta \qquad (6.13)$$

and from Verniani and Hawkins (1964) we take $\beta_0 = 1 \times 10^{-20}$; $\eta = 4$. If we assume that the majority of meteors are observed near maximum trail electron line density q_{max}, then for a typical meteor of magnitude $M_R = +7$ at 90 km height with $v = 40$ km sec^{-1} and $\cos \chi = 0.6$, eqn (6.12) predicts $m_\infty \approx .01$ gm ($M_R = +8$ is the limiting magnitude of this survey and the majority of meteors detected would be slightly brighter). The value of $r\rho = .1$ gm. cm^{-2} for this height range in the present survey then yields, taking

$$m_{max} = \frac{8}{27} m_\infty \qquad \text{(Verniani, 1961)}$$

$$r_{eff.} \sim .15 \text{ cm}$$

$$\rho \sim .65 \text{ gm. cm}^{-3}$$

which is in good agreement with the tentative estimates of density obtained by Verniani (1964) for the $M_p = +8$ radio meteor data of Hawkins and Southworth (1963), as well as the more precise estimates of Verniani (1966).

These results are based upon the same basic assumptions as those of Verniani (1964, 1966) and agree with those results rather than the higher density estimates of Ceplecha (1967). Thus Ceplecha's criticism of Verniani's assumptions which he suggests lead to an underestimation of the density by a factor of five applies equally to the present results.

If the majority of meteors observed are near the limiting magnitude for the survey, then from eqn (6.12), assuming $\eta \sim 4$, we see that even the slight tendency to smaller observed velocities at the lowest height ranges apparent in Fig. 8.1 will be sufficient to require meteors observed at lower heights to have larger masses than those observed at greater heights. Nevertheless the density selection effect apparent in the variation of r_p with height will yield density estimates much closer to those of Ceplecha for meteors observed at lower reflection point heights.

Ceplecha (1970) notes that air densities at meteor heights may vary over a short period of time by as much as 60% from the standard atmosphere. This alone can cause order of magnitude errors in applications of the theory in individual cases. The mean values of surface area/mass ratio calculated in the present survey, however, are from data collected over continuous recording periods of a week or more for 6 months and as such, provided that the standard atmosphere represents the true mean, should be insensitive to air density fluctuations of this order.

Certainly the best we can do in the light of the necessary assumptions is to compare our measurements with those made elsewhere using

similar assumptions. Until more is known of the composition of the various types of meteors and the nature of the atmospheric interaction, mass and density estimates by the present method can be no more than a comparative guide.

Ceplecha (1967) approached the problem from thermodynamic considerations, and found that if the temperature for all meteors was raised to the same value at the beginning of light emission a parameter k_B could be defined where

$$k_B = \log \rho_B + \frac{5}{2} \log v_\infty - \tfrac{1}{2} \log \cos \chi \qquad (6.14)$$

where v is velocity above the atmosphere; χ is the radiant zenith angle; ρ_B is atmospheric density at the beginning height.

The quantities on the R.H.S. of (6.14) are all measurable and thus k_B may be determined for meteors for which these quantities are known. From the relation generating (6.14) comes the more "physical" definition of k_B,

$$k_B = \log \frac{2\tau_B}{\Lambda} + \tfrac{1}{2} \log \lambda \delta c b \qquad (6.15)$$

where τ_B is the temperature at beginning of light (assumed constant), Λ is the heat-transfer coefficient, λ the heat conductivity, δ the density, c the specific heat of the meteor and b the air density gradient (which only varies slowly over the height range considered).

Thus it may be seen that, apart from any dependence on τ_B and b, k_B is determined by entirely intrinsic properties of the meteoroidal material. Ceplecha has measured the distribution of k_B for a number of

samples of meteors and has found the existence of three distinct maxima representing three distinct types of meteor composition. The positions of these maxima are independent of the velocity range of the sample used. By calibrating the k_B factor against meteors of known composition, including an artificial iron meteoroid (McCrosky and Soberman, 1963), Ceplecha determined approximate densities of 4.0 gm cm^{-3}, 2.2 gm cm^{-3} and 1.4 gm cm^{-3} for the three compositional types.

In an attempt to relate the present meteor sample to the samples measured by Ceplecha a k factor has been determined for each meteor by assuming (for lack of a better assumption) that the observed reflection point height for the majority of meteors is related in some simple way to the height of commencement of pronounced ionization. However, the distribution of k so obtained has a single peak the value of which depends on the velocity range considered. This is apparent from a consideration of Fig. 8.1 which shows only a very slight dependence of the mean reflection point height on meteor velocity for the present meteor sample, in contrast to the discrete bands of beginning height which should depend quite distinctly on velocity and which are implied by the three distinct k_B values observed by Ceplecha (1968).

There are several possible explanations for the failure of the present sample to agree with Ceplecha's results. Strong height selection may overwhelm any tendency for the observed distribution to vary as $\rho_B \sim v_\infty^{-2.5}$ and even more so for the suggested variation $\rho_B \sim v_\infty^{-3.5}$ proposed by Verniani (1967). Even for a limited velocity range the

accuracy of the data may not be sufficient to resolve two or three distinct peaks. Possibly in any of the velocity ranges considered only one of the three types predominates. It is possible that the specular reflection constraint effectively obscures any simple relation between beginning heights and observed reflection point height.

Verniani (1964) notes an increase in average densities of radio meteors over those of photographic meteors by a factor of 2. The present results corroborate this trend for increasing density with decrease in mass, as do comparisons of the present results with those of Evans (1966) if the magnitude estimates of both sets of data are reliable.

Since it does not seem likely that material of higher density should have a greater probability of forming smaller meteoroids an explanation of this trend is proposed in which it is assumed that (at least for the magnitude ranges under discussion) the chemical composition of a meteoroid is independent of its size. The basic proposition of this model is that the small meteors are more regular in shape than the large ones. Even amongst ices the densities suggested by Verniani seem inapplicable to compact objects. It seems possible therefore that there exists some extremely small but macroscopic range of compact particles which may be considered as the 'building blocks' for agglomerations of irregular shape which constitute the larger meteors. The average density of these larger accumulations would be lower than that of the contributing particles. Such a model, depending on the formation of the basic particles themselves, could also explain the observed differential

number mass law in terms of the relative probabilities of formation of accumulations of certain numbers of particles.

Comets would fit into this scheme as rare and extremely great agglomerations or concentrations of agglomerations of the same particles, whether of the form of a dense cloud or of particles actually joined together or a combination of the two. The formation of a meteor stream from total or partial disintegration of a comet under the action of strong forces close to the sun would be merely the break-up of one large agglomeration into many smaller ones, or the 'stripping off' of some smaller agglomerations from the central swarm.

There is considerable uncertainty as to the origin of the cometary constituents leading to gas production, and while Richter (1963) considers it most probable that gases have been formerly occluded and adsorbed into the dust particles of comets he finds the mechanism of solar heating with the re-emission of such gases to be inadequate to explain the observed life-times of comets. The recent discovery of immense atmospheres of hydrogen surrounding Comet Tago-Sato-Kosaka 1969 and Comet Bennett (Bertaux and Blamont, 1970) gives strong support for the 'icy comet' model of Whipple (1950,1951). Condensation of gas molecules onto the particles in the form of a surface ice may be a continuing process at large distances from the sun. The origins and rates of condensation of such gases are shrouded in doubt.

The observation of occluded gases in meteorites (Richter, 1963), although these bodies are presently thought to have properties distinct from their less dense meteoric counterparts, raises the question of the

possible significance of gases in much smaller meteoroids, particularly in the light of the inadequacy of the solar heating model to explain cometary gas emission life-times.

Some features of the orbital distributions discussed later in this thesis suggest that comets may have originated within the solar system, and that comets and meteors may be largely composed of pumice-like material. It is possible that collision between pumice-like particles in a comet would release considerable quantities of trapped gas, and that such a mechanism could explain the observed cometary gas emission life-times.

The intra-solar system origin at the same time implies the ejection of material from the solar system in hyperbolic orbits, suggesting that particles of similar composition might be expected according to the accretion theory of Lyttleton (1948). Lyttleton suggests that particles may be gathered by collision processes due to gravitational focussing in the wake of the sun as the solar system passes through an interstellar dust cloud.

It should be emphasized that the above discussion does not preclude the existence of meteors from other sources, as evidenced by meteorites of possibly asteroidal, lunar and terrestrial origin, nor does Lyttleton's theory preclude the existence of comets such as the Jupiter family which appear (Marsden, 1969) to be related to asteroids of the Apollo type or vice-versa.

Ceplecha (1967) suggests that 54% of the Super-Schmidt meteors of McCrosky and Posen (1961) are of asteroidal origin whereas Jacchia, Verniani and Briggs (1965) find only one out of 413 precisely reduced Super-Schmidt meteors to have an appearance consistent with asteroidal origin despite an observational bias in favour of such meteors.

It is difficult to reconcile the observed variation of G as a function of reflection point height with the density estimates of Ceplecha (1967). The higher densities apparently observed at lower reflection point heights would need to be increased proportionately if the upper height range densities were scaled to correspond to those of Ceplecha, and would then become improbably large.

The agglomeration or fragile structure meteor model implied by the low density measurements of the present survey suggests a high probability of fragmentation. However Weiss (1960a) does not find fragmentation to be pronounced for faint radio meteors. A high probability of fragmentation should be observed as a positive skew of the histograms of measured G (Fig. 6.5). No such skew is apparent, indicating that the probability of fragmentation is at least sufficiently small to escape detection in this way. Occasionally during film-reading the pre-t_o diffraction waveform was observed to have a well-defined beat frequency envelope. This could be the result of one particle breaking into two particles of slightly differing velocity.

No such diffraction pattern was considered suitable for reduction. The incidence of fragmentation on this basis also is thought to be small,

although it is doubtful whether it could commonly be recognized in this manner.

It is possible that the observed density variation with height is merely a selection effect acting upon a range of densities occurring naturally amongst the particles before entering the atmosphere. The observed frequency distribution with height would then be related to a probability distribution of meteoroid density centred near the value of .65 gm cm^{-3} found for this survey for meteors near 90 kms height.

An alternative or additional mechanism for the observed density variation with height might be possible if we consider that the initial meteoroid has a low density porous or extended structure. Since heating takes place very rapidly on collision with the atmosphere it does not seem reasonable to assume that the meteoroid will heat through evenly in a time much shorter than its time of atmospheric flight except in the case of extremely small particles.

Jones and Kaiser (1966) have shown that solid meteoroids of radius greater than 0.1 cm may develop a marked radial thermal gradient with resulting stresses sufficient to produce fracture before ablation commences. McCrosky and Ceplecha (1969) find that fragmentation due to thermal shock of this kind becomes decreasingly important as the body size increases.

The present density estimates indicate that the majority of meteoroids observed to $M_R = +8$ cannot be of homogenous solid composition. Nevertheless, it is evident that thermal gradients will still be

generated even in extended structures and may still be important in the fragmentation process.

It is possible that heating initially melts only the outside layers of the meteoroid, which in a porous or cellular structure would cause part of the material of these layers to collapse inwards with resultant increase in the apparent overall meteoroid density, at the same time as other material from these layers is ablated. The observed density variation with height would be attributed to the progressive nature of this molten collapse as heating continued. It is interesting to note that the proportionate change in density with height noted by Verniani (1964) for larger meteors than observed in the present survey is somewhat smaller, consistent with this theory.

Since eqn (6.10) has been formulated on the assumption of constant bulk density it is not strictly valid if the bulk density of individual meteoroids varies. However, in view of the other uncertainties of our basic meteor model there seems to be little point at present in mathematically considering a more complex model. Certainly since the majority of deceleration measurements were made over distances of only a few kilometres it is reasonable to assume that over these distances the density variation may be small enough to still permit sensible application of eqn (6.10). In this event there would be a systematic tendency for the measurements of bulk density thus obtained to be too large.

The change in properties provided by a molten or plastic outer layer could well be sufficient to impede fragmentation of small meteor-

oids while not being adequate to contain the stronger mechanical forces which might be expected in a larger body.

The concept of individual meteoroid density variation does not explain the observed frequency distribution with height, and it seems likely if this effect does occur at all, that it must occur in conjunction with the initial density variation which is the dominant factor.

It should also be pointed out that the observed density variations with height are the reverse of what might be expected if the frothing mechanism proposed by Allen and Baldwin (1967) contributed significantly. McCrosky and Ceplecha (1969) outline some of the uncertainties of the classical theory of meteors and consider the application of a number of models to the observed behaviour of bright fire-balls. Despite the initial appeal of the model of Allen and Baldwin of a dense object which appears to be less dense because of surface frothing on heating (a phenomenon which may be observed when a substance with occluded gases is melted in vacuo) McCrosky and Ceplecha do not consider the magnitude of such a frothing effect to be great enough to explain the observed properties of fire-balls and find most evidence to support mean densities of 0.1 gm cm^{-1} for group C and 0.6 gm cm^{-1} for group A fire-balls. Thus their analysis indicates meteoroid densities consistent with those apparent from the present survey.

6.5 CALCULATION OF UNRETARDED GEOCENTRIC VELOCITY

For a given value of G_o we may write

$$\ddot{x} = -\frac{G_o}{2}\rho_o v_o^2 \quad \text{at } x = x_o .$$

Thus eqn (6.4) becomes

$$-\frac{H_o\rho_o G_o}{\cos\chi} = \exp\left(-\frac{v_o^2}{12\xi}\right)\cdot\left(E_i\frac{v_\infty^2}{12\xi}\right) - E_i\left(\frac{v_o^2}{12\xi}\right)\Big) \qquad (6.16)$$

Assuming the same (constant) value for ξ used to calculate G_o we may solve (6.16) for v_∞ .

This can only be accomplished readily if the term involving exponential integrals is replaced by an approximate form. We assume (as will generally be true) that the percentage difference between v_∞ and v_o is small, so that

$$\left\{E_i\left(\frac{v_\infty^2}{12\xi}\right) - E_i\left(\frac{v_o^2}{12\xi}\right)\right\} \sim \frac{12}{v_o^2}\left[\exp\left(\frac{v_\infty^2}{12\xi}\right) - \exp\left(\frac{v_o^2}{12\xi}\right)\right]$$

and (6.16) becomes approximately:

$$-\frac{H_o\rho_o G_o}{\cos\chi} = \frac{12\xi}{v_o^2}\left[\exp\left(\frac{v_\infty^2 - v_o^2}{12\xi}\right) - 1\right] \qquad (6.17)$$

which yields

$$v_\infty' = \left(v_o^2 + 12\xi \ln\left[1 - \frac{v_o^2\rho_o G_o H_o}{12\xi\cos\chi}\right]\right)^{\frac{1}{2}} \qquad (6.18)$$

Since the estimate v_∞' of v_∞ is not quite correct and since (6.17) is only an approximate form of

$$-\frac{H_o\rho_o G_o}{\cos\chi} = \frac{12\xi}{v^2}\left[\exp\left(\frac{v_\infty^2 - v_o^2}{12\xi}\right) - 1\right]$$

we could improve upon this with a one step iteration by putting

$$v_\infty^2 = v_o^2 + 12\xi \ln \left[1 - \frac{(v_o^2 + v_\infty'^2)\rho_o G_o H_o}{24\xi \cos \chi}\right] \qquad (6.19)$$

where the approximation

$$\overline{v^2} = \frac{v_o^2 + v_\infty'^2}{2}$$

should be good for all likely decelerations, i.e.

$$v_\infty^2 = v_o^2 + 12\xi \ln \left[1 - \frac{v_o^2 + 6\xi \ln \left(1 - \frac{v_o^2 \rho_o G_o H_o}{12 \cos \chi}\right) \rho_o G_o H_o}{12\xi \cos \chi}\right] \qquad (6.20)$$

From this value of v_∞^2 it is possible to determine G_∞,

$$G_\infty = \frac{G_o r_o}{r_\infty} = G_o \exp \left(\frac{v_o^2 - v_\infty^2}{12\xi}\right) . \qquad (6.21)$$

Combining (6.20) and (6.21) we get

$$G_\infty = G_o \left\{1 - \frac{v_o^2}{12\xi} \frac{\rho_o G_o H_o}{\cos \chi} - \tfrac{1}{2} \frac{\rho_o G_o H_o}{\cos \chi} \ln \left[1 - \frac{v_o^2}{12\xi} \rho_o \frac{G_o H_o}{\cos \chi}\right]\right\}^{-1} .$$

In view of the inability of the present survey to measure G with suitable accuracy for each meteor detected, it has been necessary to assume a value for G_o in computing the geocentric velocity of the meteor above the atmosphere. Calculations have been made for all meteors for two values of G_o, 5 $cm^2\ gm^{-1}$, and 50 $cm^2\ gm^{-1}$.

Further analysis (see §6.4) suggests that this correction would best be made employing a continuously varying G which increases with reflection point height. Lack of time has not permitted general recalculation of the meteor orbits using this form of the deceleration, however recalculation of the orbits from two months of data showed

little overall difference between the orbits determined by assuming $G = 5$ cm^2 gm^{-1} for all meteors and those determined with the variable G. The majority of the features of the general orbital parameter distributions are not sensitive to the different values of G employed, though the choice can certainly have a significant effect on some meteors, particularly those at low reflection point heights. The results of §6.4 certainly indicate that the adoption of the value of $G = 50$ cm^2 gm^{-1} for all meteors would lead to significant errors in the computation of v_∞. Fig. 6.7 shows the frequency of the various velocity corrections for the two values of G used. For $G = 5$ most meteor velocities were altered by less than 1 km/sec, whereas for $G = 50$ the bulk of the meteors had velocity corrections in the range of 1 km sec^{-1} to 4 km sec^{-1}.

As indicated in §6.4 measured values of G at low heights in general may be smaller than 5 cm^2 gm^{-1} by as much as 50%. This is corroborated by the distribution of hyperbolic meteors found as a function of height. The hyperbolic orbits contributing to Fig. 8.3 were computed with $G = 5$, and the bulk of these above 80 kms in height would have had little or no velocity correction for atmospheric retardation. A comparison with Fig. 8.2 , which shows the distribution of reflection point height for all meteors detected in the present survey, shows clearly an anomalously high percentage of hyperbolic meteors with low reflection point heights, particularly for the underdense and intermediate type meteors. This indicates that the cause of apparent hyperbolicity for some of these meteors may be that the assumed surface area/mass ratio of 5 cm^2 gm^{-1} at low heights is probably still too high.

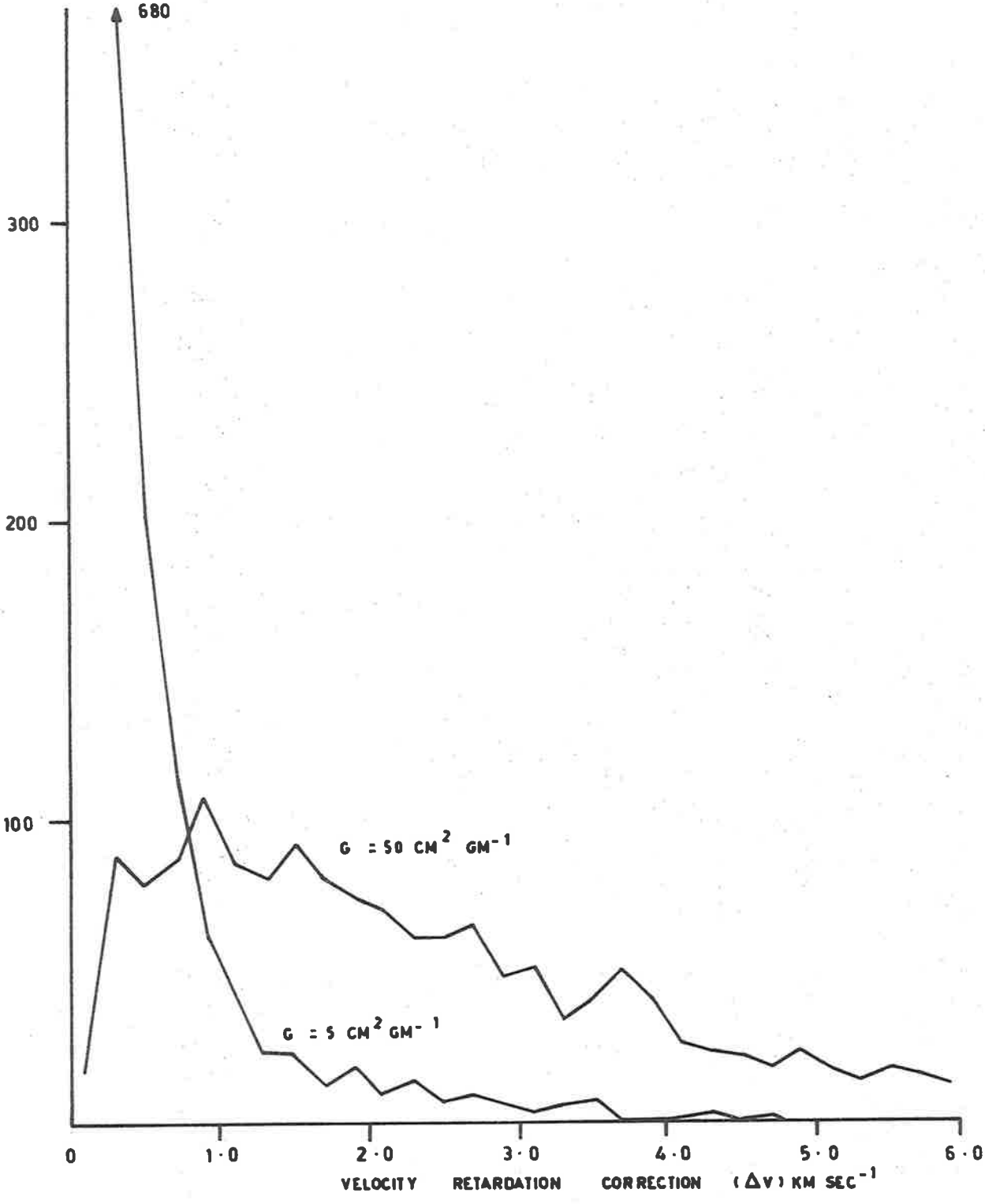

FIG. 6·7 DISTRIBUTION OF THE ATMOSPHERIC RETARDATION CORRECTION ΔV FOR TWO VALUES OF SURFACE AREA / MASS RATIO.
$G = 50\ CM^2\ GM^{-1}$, $G = 5\ CM^2\ GM^{-1}$.

One of the fundamental assumptions made in using the drag equation to determine G is that the mean free path of air molecules at the height considered is large compared with the meteoroid dimensions. At the lowest reflection point heights this condition may no longer be met, particularly by larger meteoroids, and an air-cap may be formed reducing the drag coefficient from an assumed unity value to as little as .5 (see Öpik, 1958). Failure to account for air-cap formation could thus result in underestimation of G by as much as a factor of 2.

6.6 SUMMARY

The purpose of this chapter has been to analyse the information available from observations of atmospheric retardation. The measured variation of surface area/mass ratio for meteoroids with height of observation is in good agreement with that found by Evans (1966) and is the reverse of that expected for a sample of meteoroids of uniform size and homogeneous composition.

Independent confirmation of the measurements of surface area/mass ratio comes from the calculation of unretarded geocentric velocity for all meteors assuming G = 5 $cm^2\ gm^{-1}$ at the reflection point height. This assumption results in an anomalously high number of hyperbolic orbits for meteors with reflection point heights below 83 km in good agreement with the measured value of G for this height, and confirming that the average value of G at lower heights is less than 5 $cm^2\ gm^{-1}$.

An estimate of the density for the present meteors observed near 90 km is in good agreement with measurements of Verniani (1964, 1966) and

suggests that the majority of meteoroids are of low density, with a tendency for bulk density to increase toward fainter magnitudes.

Further support for the reality of these density estimates comes from the apparent variation of density as a function of height in the present survey. The estimates of density corresponding to meteors observed at the low end of the height range are sufficiently high to indicate that the low values of bulk density found for meteors at greater heights must be real.

The apparent density variation with height does not favour the frothing model of Allen and Baldwin (1967) and suggests that the meteoroids may be initially extended agglomeritic or pumice-like structures. Pumice-like composition seems most probable, since it is consistent with the inferences of the observed meteor orbit distribution discussed in the following chapters, and summarized in Chapter 9.

CHAPTER VII

METEOR STREAMS

7.1 INTRODUCTION

This chapter describes the delineation of meteor streams in the data from the present survey. Sections 7.2, 7.3 and 7.4 discuss problems concerning the definition and identification of meteor associations, while the remainder of the chapter examines the relation of specific streams found in this survey to other streams observed at Adelaide and elsewhere.

A search for possible cometary associations with the present meteor streams has revealed a number of associations which raise interesting questions as to the mechanism of ejection of meteoric material from comets. These questions are discussed in §7.8 and further in Chapter 9.

It should be noted that not all the data recorded in the present survey has yet been analysed. Table 7.1 lists the overall recording periods and shows for which of these the data has been analysed to date. It is apparent that the observed durations of a number of streams are limited by the recording periods and do not indicate the true duration of stream detectability. An example of this is given by the ζ-Perseid stream, at present detected only in June. It is anticipated that more members of this stream will be found amongst the May data when that is analysed.

	Data	
	Recorded	Analysed
1968 December	9 - 16	9 - 16
1969 January	20 - 25	21 - 23*
" February	10 - 17	10 - 17
" March	16 - 22	16 - 22
" April	13 - 20	-
" May	11 - 18	-
" June	7 - 14	7 - 14
" October	5 - 9 15 - 19	- 15 - 19

TABLE 7.1

*The echoes from the latter stages of the January recording period were rendered unsuitable for analysis by electrical storms and persistent interference.

7.2 ASSOCIATION TESTS FOR STREAM METEORS

A major problem in the analysis of distributions of meteor orbits concerns the differentiation of stream meteors from the sporadic background. Several workers have attempted to find some objective criterion for testing the association of two meteors (Southworth and Hawkins, 1963; Nilsson, 1964b), and indeed such a criterion, with the assistance of an electronic computer, is almost essential for the comparison of the large numbers of meteors detected by a radio survey such as the present one.

Southworth and Hawkins devised an association test which amounts to a measure of the distance between two orbits in a 5-dimensional space, based upon the five independent elements specifying the orbit, suitably weighted. For two meteors (A & B) to be considered associated the distance D(A,B) between their orbits in this space must be less than some pre-determined value D_s where

$$D(A,B) = \left\{ \sum_{j=1,5} c_j^2 \left[C_j(A) - C_j(B) \right]^2 \right\}^{\frac{1}{2}} \qquad (7.1)$$

in which the C_j are suitable independent functions of the orbital elements and the c_j are normalizing functions which should be inversely proportional to the expected standard deviation of the corresponding C_j in a stream.

Nilsson's association test required agreement between each of the orbital elements of two meteors in turn to within two standard deviations for that element. It can be seen that this test is similar in many ways to that of Southworth and Hawkins but differs in that it considers each orbital element entirely on its own, whereas the latter test allows slightly larger differences in one element if agreement between the other elements is particularly close.

The second basic difference between the two tests lies in the choice of the association limits. Southworth and Hawkins devised their test for application to the orbits of accurately reduced photographic meteors and considered the observed spread in the orbits of stream meteors as being generated by some idealized dispersing mechanism,

whereas Nilsson's association limits assumed identical orbits for stream meteors and were based upon the larger expected observational errors of a radio survey.

Observational errors notwithstanding the major problem in detecting meteor associations is to determine how wide to cast the net. What should we regard as acceptable differences between meteors classed as members of the same stream? The meteor population is a dynamic and evolving entity. It is apparent that streams are formed at different times and that members gradually disperse under the influence of both the spread in energies of the member particles at stream formation and the subsequent action of various external perturbing forces. It is natural therefore to expect a greater dispersion of orbital elements amongst members of an old stream than amongst those of more recent origin.

The question of separate or common origins for stream and sporadic meteors is itself an important consideration. Are sporadic meteors the remnants of streams dispersed beyond recognition? Could they be members of a vast background of as yet unresolved minor streams? It is evident that some sporadic meteors belong to each of these categories. One of the questions we seek to answer is whether all sporadic meteors have originated this way, or whether in fact there exists a class of truly sporadic meteors with origins quite distinct from the stream meteors.

Hawkins (1962) discusses the "toroidal group" of sporadic meteors of high inclination and low eccentricity which becomes increasingly

apparent at fainter magnitudes, and suggests that intensive study of this system with high-power radar equipments is necessary to determine its cosmogonic significance.

Kascheev and Lebedinets (1967) and the present survey have detected a number of streams with characteristics similar to the toroidal group. The apparent absence of larger photographic meteors in these streams distinguishes them from the well-known major streams, and it is possible that they result from action of the Poynting-Robertson effect on old streams with perihelia greater than 1 a.u.

Eshleman and Gallagher (1962) from radar studies of 15th magnitude meteors (trail electron line densities 10^{10} m^{-1}) find evidence that the sporadic background is in reality a mixture of short-lived showers, with about 10 shower groupings being simultaneously present on average. These studies also show number-velocity and number-mass distributions in accord with those found for larger radar meteors. They suggest that these interplanetary dust clouds may constitute a vast family of small, dilute, subvisual comets. Such a concept is not inconsistent with the agglomeration theory of meteor composition discussed in §6.4.

Photographic meteors of various streams may sometimes be identified compositionally by characteristic light intensity profiles and spectra (McKinley, 1961) but classification of radio meteors is entirely dependent upon the comparison of orbital elements or radiant data. For the present purposes a meteor stream may be defined as a significant concentration of orbits in orbit space.

The scatter between measured orbits of stream meteors will in part be due to measurement errors as well as the true differences between the orbits. The effect of the former can be estimated, and for radio meteors will be relatively large. The true differences will depend upon the nature and duration of the dispersion mechanism. Since a stream is characterized by an increased density of orbits compared with adjacent regions of orbit space it is apparent that random observational errors where the association limits are based upon stream dispersion alone will move more true stream meteors outside the accepted limits of stream membership than the number of sporadics which through chance or error will be included in the stream classification. Increasing the association limits to include probable measurement error may recover most of these meteors but will also increase the probability of inclusion of spurious meteors in the sample.

Where a major stream is involved this effect may be estimated by varying the limits of the association factor and observing the resulting changes in the stream configuration. As the association factor is decreased in size from more than adequate down to a representative value for the particular stream only small changes in stream structure should be observed. The effect of further decreases in size from this point on should be to divide the stream into a number of smaller ones and rapidly obscure it altogether.

Southworth and Hawkins (1963) have measured a number of known streams for which they had sufficient meteors in their sample, and have

determined their D criterion for each of these streams, measuring the values D_m between the meteors in the stream and the mean orbit for the stream as well as the smallest value of D for which each member of the stream was found to be associated with at least one other member of the stream. On the basis of these measurements they chose a value for D which they applied to their sample to test for new streams.

It should be noted that there is a fundamental difference in the application of the D criterion to two meteor orbits to test for association within certain limits, and the application of the same criterion to the members of a stream. Stream meteors may be considered as either directly or serially associated. For direct association all members of the stream must lie within a certain distance D_m of the mean orbit for that stream. For serial association it is not necessary for two associated meteors to be within a distance D_s of each other, but merely that each should be a member of a group of meteors each of which is less than D_s from at least one other member of the group. The latter case thus represents a form of "chaining" where two meteors which would not be found associated by the first test are linked by an intermediate meteor. This form of the association test can be most useful, but obviously must be applied with care. For dispersing mechanisms such as the Poynting-Robertson effect which may act differentially on the mass distribution of a stream an association test of this type may be more sensitive in stream detection, and may include less spurious stream members than would be found merely by increasing the allowable D_m and testing for association with the mean.

With a sufficiently large sample of meteor orbits it could be most interesting to map the orbit association density distributions for a wide range of values of D_s. For small D_s values we would expect to delineate the streams of recent origin, and as the value of D_s is increased we might hope to resolve more diffuse and hence probably more ancient streams. To do this effectively, however, we must be able to judge whether a grouping is significant, or whether it has merely arisen from chance. The likelihood of chance grouping will certainly increase with increasing D_s. The significance of the major meteor streams is beyond doubt. We would like to be as sure of the significance or otherwise of the minor and more diffuse associations.

7.3 THE SIGNIFICANCE OF SMALL GROUPS

Southworth and Hawkins (1963) and Nilsson (1964b) determine the likelihood of spurious streams in their data by searching for streams in equivalent artificial sets of data. The artificial data was constructed in each case by shuffling and re-assigning the appropriate orbital elements. Significant numbers of spurious streams were found in this way, and these workers have all commented that the number of such streams found will be an upper limit to that in the true sample, since the artificial sample is based upon the orbital elements of a set of data containing a significant proportion of streams anyway.

Despite its obvious limitations, in view of the considerable uncertainty in our knowledge of observational selection effects, this method is probably the best available for determining the level of

stream significance in any sample. Nevertheless it is certainly necessary that we should be clearly aware of these limitations.

It is apparent that any meteor component not related to streams will still be subject to perturbing influences so that even if its distribution were to have originated in a random manner, which seems unlikely, its present distribution will favour some regions of orbit space more than others. Additionally when consideration is given to the probability of collision with Earth per unit time, and the probability of observation, it is apparent that some meteor orbits will be far more readily detected than others. Thus a pair of associated orbits detected in an observationally sparse region of orbit space will be of greater significance than a pair of associated orbits from a readily observable region.

Comparison with an artificial sample as described above may possibly yield an estimate of the total number of spurious associated pairs, triples and so on in our true sample, but certainly does not give any indication as to the degree of reality of any individual association, which will depend strongly on its orbital configuration. This is illustrated clearly by reference to the spurious streams detected by Southworth and Hawkins (1963) in their artificial sample. They found eight associations: five pairs, and one each with three, four and five orbits. The larger associations each had eccentricities near .59 and the pairs had higher values. Mean inclinations apart from one pair with a value of 10° were all 6° or less. We may infer from their test that any association in their data with higher inclination is likely to be significant, even if only for a pair of meteors.

In §8.2 a number of factors are introduced for correction of observed distributions to those actually occurring in space.

It is evident that Eqn (8.3), which is based upon the mathematical expectation of collision of a particle with Earth per unit time interval may be simply extended to represent the likelihood of collision with more than one member of a stream. The probability of collision of Earth with n meteors of a stream is given by

$$P(n,k) = \frac{kR^2V_\infty^2}{n\pi \operatorname{Sin} i \operatorname{Sin}\theta} \left(2 - \frac{1}{a} - p\right)^{-\frac{1}{2}} a^{-3/2} \qquad (7.2)$$

where θ is the angle between tangents to the orbits of the stream and Earth at intersection, and the notation is otherwise as for Eqn (8.3). The factor k takes into account quantities such as the apparent stream width and the volume number density of meteoroids within the stream at 1 a.u.

It should be noted that P(n,k) as given by (7.2) is not normalized, and in fact becomes undefined for $i = 0$ or $\theta = 0$. The original form of the mathematical expectation derived by Öpik (1951) from which a weighting factor of the form of (8.1) has been derived by Whipple (1954), is an un-normalised probability of collision between two bodies in orbits about a third body (in this case the Sun), per heliocentric revolution of either particle. This expectation is based upon many revolutions of the orbiting bodies as well as secular variation of the perihelion longitudes and nodes. It does not give the absolute normalised probability of collision in the present case with Earth during the first passage of a meteoroid within 1 a.u. of the Sun.

This limitation does not affect the validity of Whipple's use of the inverse form as a weighting factor, but does restrict practical use of (7.2) to the determination of probability ratios between different streams or stream configuraions, in which the need for normalization is eliminated.

From comparison of the relative strengths of the helion and antihelion components of the apparent radiant distribution as a function of ecliptic longitude Nilsson (1964b) deduced that the majority of associated pairs he detected were due to chance while the larger associations were probably significant. While Nilsson's conclusions may well apply to the meteors of low inclination which predominate in the helion and antihelion components and which also constitute the major streams generating the asymmetries in the relative strengths of these components, it is clear that they have little bearing on the significance of associations amongst meteors such as the toroidal group with high inclination. That Nilsson seems to have overlooked this point is understandable in view of the relatively small number of toroidal meteors observed by him at $M_R \leq +6$.

It should also be emphasized that the present well-defined streams are not an absolute yard-stick against which one can compare the significance of other associations, even though systematic searching may reveal numerous lesser streams with the same degree of association. In some conditions we might expect more diffuse associations to be just as significant, and hopefully with sufficient data we might be able to

measure evolutionary trends from a comparison of these diffuse associations with the more compact streams.

Recorded observations of various meteor streams and comets indicate that at least some streams are still being formed and that meteor streams can generally be expected to age rapidly in a time scale short compared with the apparent age of the solar system. We do not know whether comets and meteors form a steady-state system or whether they are decaying remnants from solar system formation. However we can reasonably expect that streams will become more diffuse with age and eventually become indistinguishable from the sporadic background, particularly at faint radio magnitude.

7.4 ASSOCIATION SIGNIFICANCE AND SAMPLE SIZE

Irrespective of the relative dependence of the significance of an association on its location in orbit space it is apparent that it is of benefit to a stream search to combine orbit catalogues, and search through as large a meteor sample as possible. As the sample size is increased genuine stream associations should generally become increasingly significant whereas chance associations should merge into the background.

One limitation to this procedure, however, is the probability of existence of numerous minor streams which may be strongly grouped in their orbits, like the concentration which enhances the Leonid meteor stream once every 33 years, and which would therefore tend to be made less significant by averaging over a long period.

It is apparent that the most satisfactory way of increasing the sample size is to increase the sensitivity of the radio system to record more meteors over any given period of time. An alternative and possibly most interesting way of achieving the same end and gaining further information at the same time would be to co-ordinate the recording periods for a number of radar equipments throughout the world, enabling direct combination as well as direct comparison of the catalogues.

7.5 A SYSTEMATIC STREAM SEARCH

The data obtained in the present survey has been systematically searched for streams in two ways. Sorting on each orbital element in turn, with the allowable differences for association set to slightly more than two standard deviations in each case, resulted in 32% of the meteors being associated. This figure drops to 21% when associations of pairs only are excluded.

The data was also searched for streams using the D criterion method of Southworth and Hawkins, setting $D(A,B) = 0.1$ as the association limit, and then augmenting this data with additional streams detected with the value of $D(A,B)$ set at 0.2. The latter were checked for any duplication of the $D < .1$ streams and also for associations in which 'chaining' had become obvious. This search found 40% of the meteors to be associated, or 30% excluding pairs. Generally the same streams were detected by the two methods, although in some cases there were minor variations in sub-grouping. As the latter test is apparently more sensitive, the results

from that test are presented here. It is interesting to note that proportionately less pairs were detected by the D criterion method, mainly due to the inclusion of some of the pairs into larger streams. These associations are listed in the Appendix. Pairs are included, since these may well be significant at high inclinations, but are probably less so for orbits close to the ecliptic.

7.6 DISCUSSION OF PARTICULAR STREAMS AND SOME POSSIBLE COMETARY ASSOCIATIONS

7.6.1 The Geminid Meteor Stream

The Geminid meteor stream is one of the most intense observed in the Northern Hemisphere, and has been well studied in a number of surveys. It has been observed to have a compact radiant (Weiss, 1959) and thus provides a useful check on the accuracy of radiant determination of the present survey. Table 7.2 compares the mean radiant and orbit of the Geminids observed at Adelaide during 1968 with results from other workers. The agreement is generally good. The mean declination is somewhat lower than that observed in the majority of cases, and the inclination also correspondingly lower. The low value of declination has been attributed by Nilsson (1964b) to the unfavourable location of the radiant for observation from Adelaide, resulting in larger than normal observational errors, which on the basis of the comparison of the present results would appear to have some systematic bias towards lower declinations. This is difficult to explain if the radiant is virtually a point source, but would be relatively easily explained in terms of the variation in sensitivity of the Adelaide system at low elevations if the

Geminid radiant at these magnitudes were extended. A relatively weak subsidiary radiant at lower declinations would not affect Northern Hemisphere results greatly but could significantly influence observations from Adelaide.

Association 12.15 lies close to the Geminid radiant but the velocity measurement seems significantly higher. Although small, the possibility of measurement error in the reduction cannot be ruled out entirely in this case.

Differences between the declinations of associations 12.01, 12.10 and 12.11 and the mean declination of the Geminid radiant are too great to be attributable to error alone. These associations apparently represent a weaker, diffuse stream probably associated with the Geminids but with lower inclination.

Poole (1967) reports the detection at Sheffield of a second 'early' radiant associated with the Geminids with similar declination but a value of right ascension approximately 15° less, which agrees well in R.A. with association 12.02 of this survey. It is most interesting in this regard to note the similarities between the Geminids and the 11 Canis Minorid stream recently discovered by Hindley and Houlden (1970). Table 7.3 compares visual and photographic observations of this stream with the Geminids, considering the latter with negative inclination and the nodes interchanged.

TABLE 7.2

Radiant and Orbit of Geminids

Source	N	α	δ	V_∞	$1/a$	q	e	i	ω	Ω
This Survey (1968)	20	112.3	+30.2	36.2	0.74	0.13	0.90	18.2°	326.7°	261.3°
Whipple (1954)	13	112.7	+32.4	36.4	0.73	0.14	0.90	23.9	324.4	261.2
McCrosky & Posen (1961)	72	111.3	+32.5	36.3	0.71	0.14	0.90	23.1	324.2	260.2
Jacchia & Whipple (1961)	20	111.4	+32.5	36.2	0.74	0.14	0.90	23.3	324.3	260.2
Southworth & Hawkins (1963)	16	112.6	+32.3	36.3	0.73	0.14	0.90	23.3	324.1	261.4
Nilsson (1964b)	22	109.4	+30.4	34.2	0.79	0.15	0.88	17.4	325.1	259.8
Kashcheev & Lebedinets (1967)	401	11.4	+32.6	36.0	0.76	0.14	0.89	23.7	325.8	259.6

TABLE 7.3

	α	δ	V_∞	$\frac{1}{a}$	q	e	i	ω	Ω
11 Canis Minorids	115	12		-	.04	-	89	158	78
	115	13	38	.53	.08	.96	33	151	80
Geminids	111	32	36	.73	.14	.90	-22	147	80

As Hindley and Houlden note, the new stream is only the second such found for which q < .1 a.u., the other being the δ-Aquarid/Arietid stream. Several other associations with similarly small perihelion distance have been detected amongst radio meteors by the present survey and by Kashcheev and Lebedinets (1967). Nevertheless, this type of orbit is sufficiently rare to suggest when coupled with the alignment of the nodes and arguments of perihelion that the Geminids and 11 Canis Minorids may be related in some way. It is possible too that other stream activity during the same period with radiants in the same quarter of the sky (Tables 7.11 & 7.12), including the Monocerotids, may have a related origin. Alternatively the streams may have been generated by members of a comet group. Groups of this type are not unknown, and in particular the Kreutz group of sun-grazing comets (Marsden, 1967), as the name suggests also have small perihelion distances.

Hindley and Houlden have suggested a possible association of the 11 Canis Minorids with Comet Mellish 1917 I, while extensive searching has failed to find any comet associated with the Geminids.

Whipple (1954) seems to have been the first to note the similarity between some meteor orbits and that of Comet Mellish 1917 I. His two meteors which agree with the cometary orbit particularly well are definitely Monocerotids, and it is apparent that the agreement between the Monocerotids of Table 7.11 and the orbit of the comet is even better than that of the 11 Canis Minorids.

Table 7.4 lists the orbital elements of Comet G. Kirch 1680 which shows some tendency for alignment with the Geminids and an unusually small value of q. The radiant data is that predicted by Hasegawa (1958) for a stream associated with this comet. The similarity suggests that the comet which may be responsible for the Geminids may well have been a long-period one, despite the small value of a for the stream, and could explain why the search for a comet with the stream orbit has not met with success.

TABLE 7.4

	α	δ	V_∞	a	q	e	i	ω	Ω
Comet G.Kirch 1680	133	+21	51	426.7	.006	.999	60.7	351	272

Nilsson (1964a) reports observation during September, 1961 of the Sextanid meteor stream also observed by Weiss (1960b) during 1957, and notes its similarity to the Geminids. A search amongst the present October data has not revealed any Sextanids, although the earlier October data not yet reduced may be more fruitful. However, three

associated pairs were found in October with small perihelion distances and perihelion longitudes within 30° of that for the Monocerotids. These associations are listed in Table 7.5.

TABLE 7.5

	α	δ	V_∞	1/a	q	e	i	ω	Ω
10.12	55	+18	28	1.24	.16	.80	2.6	152	24
10.14	56	+ 3	41	.49	.14	.92	45.7	143	24
10.15	58	+12	44	.64	.04	.98	48.8	162	23

Associations 10.14 and 10.15 show similarities which confirm their significance. The values of V_∞ are similar to those for the Monocerotids, although the similarity between the Monocerotid orbit and that of Comet Mellish 1917 I (Table 7.11) suggests that yet another comet may have given rise to associations 10.14, 10.15, and possibly 10.12.

The mean R.A. for the twenty Geminids of association 12.05 is

$$\alpha = 112.3 + 1.1(\odot - 261.3)^\circ$$

which corresponds more closely with the majority of measurements than Nilsson's determination of

$$\alpha = 109.8 + 1.1(\odot - 260.1)^\circ$$

The mean daily motion of the radiant coincides with that observed by Nilsson and is greater than that measured by Weiss (1959) and Kashcheev and Lebedinets (1967). Little reliance can be placed on this measurement, once again because of poor observability of the radiant

at Adelaide. The results do indicate, however, that there are no serious systematic errors in the reduction procedure, and provide a lower limit to our expectations of accuracy for radiants more suited to observation from Adelaide.

7.6.2 The Virginids

Only minor activity associated with the Virginid stream was observed during March. McKinley (1961) lists the dates in between which meteors of this stream may be detected as March 5th to April 2nd. Table 7.6 lists three associated pairs and one unassociated meteor from the present survey with other observations of this stream for comparison. Two of these associations have higher inclinations than previously observed. Of particular interest is the close similarity between the March association 3.03 and association 2.07 in February, also listed, and between these orbits and the lower inclination Virginids. If these higher inclination streams are classified as a branch of the Virginids our observations extend the dates of detection forward to February 12th. Cook (1970) refers to a stream detected by Lindblad (1970) in a stream search amongst photographic meteor orbits. Lindblad's paper is not yet available to the author, however Cook lists this stream as the Northern Virginids, with $\alpha = 173$, $\delta = +5$ and $V_\infty = 36$ km sec^{-1}, and notes that it was detected over the period Feb. 3rd to Mar. 12th. Without comparison of the orbital elements it is not possible to say how closely this stream corresponds to association 2.07 of the present survey. However, the agreement in the period of detection which is significantly earlier than

previous observations of the Virginids is some measure of independent confirmation of the existence of this stream.

TABLE 7.6

Source	N	α	δ	V_∞	$\frac{1}{a}$	q	e	i	ω	Ω
This Survey 33201	1	190	- 4	34	.40	.30	.88	1	299	357
3.17	2	183	- 3	30	.32	.41	.86	1	105	177
3.22	2	197	+ 4	31	.52	.32	.84	14	300	358
3.24	2	201	+ 9	34	.44	.30	.86	24	302	358
3.03	5	203	+ 3	33	.61	.23	.86	19	312	358
2.07	4	174	+16	33	.62	.23	.85	20	313	325
12.13	2	237	- 8	31	.85	.23	.80	18	44	261
Whipple (1954)	4	182	+ 4	32	.25	.42	.90	6	284	354
McCrosky & Posen (1961)	5	179	+ 1	29	.46	.44	.80	1	285	351
Jacchia & Whipple (1961)	3	176	0	29	.37	.45	.83	2	102	170
Nilsson (1964b)	3	189	- 4	34	.42	.26	.89	3	304	355
Kashcheev & Lebedinets (1967)	9	188	+ 1	31	.51	.36	.82	6	297	356

Nilsson (1964b) suggests a possible connection between his March Virginid data and an association of three meteors observed in December. Association 12.13 in the present survey, again only for a pair of orbits, corresponds quite well to the March associations 3.22 and 3.24 except for smaller size of orbit, and is particularly close to 3.03. Nilsson's December association similarly has a smaller mean orbit than his Virginids.

7.6.3 The Arietids

Six associations were detected during June with radiants and velocities near the generally accepted values for the Arietid stream. As can be seen from Table 7.7 four of these correspond reasonably well to observations by other workers, while two (6.07 and 6.12) have significantly lower declinations. The latter two must be considered real since each has six members. Good agreement in longitude of perihelion as well as size and shape of orbits suggest that they are genuinely connected with the Arietids.

No evidence of the progressive increase in inclination with passage through the stream noted by Lovell (1954) was found in this survey. However the considerable spread in inclination found by other workers is extended even further by our observations.

TABLE 7.7

Source	N	α	δ	V_∞	$\frac{1}{a}$	q	e	i	ω	Ω
This Survey 6.03	3	47	+18	42	.28	.04	.98	2.4	18°	82°
6.04	9	44	+19	43	.54	.02	.99	18.0	14	81
6.05	32	49	+23	41	.37	.08	.96	17.4	28	81
6.06	4	39	+19	43	.67	.02	.99	30.9	11	80
6.07	6	48	+ 9	41	.65	.06	.96	-38.2	23	81
6.12	6	47	- 2	43	.51	.12	.92	-65.3	34	81
Lovell (1954) 1950	-	44	+22	38	.67	.10	.94	18.0	29	77
Lovell (1954) 1951	-	43	+24	39	.62	.09	.94	21.0	29	77
Davies & Gill (1960)	6	50	+26	41	.75	.04	.97	46.0	19	89
Nilsson (1964b) 61.6.1	7	47	+25	44	.44	.04	.98	38.9	20	85
Nilsson (1964b) 61.6.2	8	46	+26	40	.67	.06	.96	33.4	23	85
Baker & Forti (1966)	52	36	+26	38	.36	.09	.93	31.3	27	73
Kashcheev & Lebedinets (1967) Mean	380	43	+23	39	.60	.10	.94	18.7	30	77
Kashcheev & Lebedinets (1967) June 17-20	18	52	+25	40	.60	.08	.96	22.8	25	87

7.6.4 Hyperbolic Streams

Altogether eight associations between meteors with hyperbolic orbits have been found in the present survey. Four of these are within probable measurement error of the parabolic limit for closed orbits, but the remainder are more strongly hyperbolic and seem unlikely to be entirely attributable to error. Nevertheless, similarity between some of these associations and adjacent elliptic streams suggests common origins and does not favour the possibility of interstellar origin. Babadzhanov and Kramer (1967) draw similar conclusions from observations of hyperbolic meteors amongst the Perseids. Seven of the associations are between pairs of meteors only, although two of the pairs probably belong to the one stream. The remaining association is between seven meteors all of which are hyperbolic.

Table 7.8 compares the orbital elements of association 2.37 with the nearby association 2.15 of elliptic orbits.

TABLE 7.8

	N	α	δ	V_∞	$\frac{1}{a}$	q	e	i	ω	Ω
2.15	4	250	-86	44	.08	.95	.93	70.2°	330°	144°
2.37	2	224	-85	49	-.23	.94	1.24	76.0°	337°	144°

The main complex of hyperbolic associations observed occurred in October and seems to be related to the Orionid stream. Six Orionids were observed in this survey, and the mean orbit found for this stream

is in good agreement with observations by other workers (see Table 7.9).

TABLE 7.9

Source	N	α	δ	V_∞	$\frac{1}{a}$	q	e	i	ω	Ω
This Survey 10.05	6	94	+14	68	.13	.65	.85	161.8°	76°	24°
Whipple (1954)	2	95	+16	66	.16	.54	.92	162.9	88	29
McCrosky & Posen (1961)	48	95	+15	68	.02	.58	1.01	162.8	80	31
Jacchia & Whipple (1961)	5	95	+16	68	.06	.57	.96	164.4	82	29
Southworth & Hawkins (1963)	12	96	+16	68	.05	.57	.97	164.9	83	29
Nilsson (1964b)	8	97	+14	65	.16	.50	.92	160.3	91	32
Baker & Forti (1966)	7	95	+16	65	.26	.56	.83	165.0	88	27
Kashcheev & Lebedinets (1967)	61	93	+16	66	.21	.57	.88	164.2	86	25

Table 7.10 compares the orbital elements for the October hyperbolic associations with the mean elements for the Orionids. Associations 10.09 and 10.10 were both detected on the same day and the degree of eccentricity of the orbits, if due to recent perturbation, could be related. Were the observations made five days later it might have been possible to attribute such perturbations to the close proximity of the moon to the radiant.

TABLE 7.10

	N	α	δ	V_∞	$\frac{1}{a}$	q	e	i	ω	Ω
10.05	6	94°	+14°	67	.14	.65	.85	161.8°	76°	24°
10.07	2	90°	- 0	66	- .05	.68	1.04	132.9	67	24
10.08	7	87°	+ 8°	71	- .38	.63	1.26	147.7	70	24
10.09	2	89°	+ 6	78	-1.23	.72	1.89	147.1	55	25
10.10	2	90°	+15	79	-1.10	.68	1.75	164.5	59	25

Hajduk (1970) has studied the structure of the Orionid and η-Aquarid meteor stream, and finds that the Orionid stream is filamentous with filament diameters of the order of 10^6 km. Similarities between the Orionids and the less well observed η-Aquarids appear to confirm the associations of these streams with Comet Halley.

To the best of the author's knowledge the associations 10.09 and 10.10 are the most hyperbolic meteors ever found to be related to a meteor stream associated with a periodic comet. These associations indicate conclusively that strongly hyperbolic meteors observed at Earth may be the result of recent perturbations and need not imply an interstellar origin. Possibly the hyperbolic meteors have resulted from collisions between two or more large Orionids.

7.6.5 The Monocerotid Stream

Although no Monocerotids were found to be associated by the systematic stream searches, three meteors were observed with radiants and velocities corresponding to this stream. One of these meteors is slightly hyperbolic, but the mean orbit is not. Agreement between present observations and those of past surveys is good, as shown in Table 7.11. The orbit of Comet Mellish 1917 I is also given for comparison.

TABLE 7.10

Source	N	α	δ	V_∞	$\frac{1}{a}$	q	e	i	ω	Ω
This Survey 12.09	3	106°	+ 6°	42	.13	.19	.98	39.9°	130°	82°
Whipple (1954)	2	103	+ 8	43	-	.19	1.00	35.0	128	82
Whipple & Hawkins (1959)	-	103	+ 8	43	-	.19	1.00	35.2	128	82
Southworth & Hawkins (1963)	1	102	+ 8	44	.05	.16	.99	39.8	131	78
Nilsson (1964b)	6	102	+10	42	.18	.11	.98	39.0	139	76
Comet Mellish 1917 I	-	106	+ 6	40	.04	.19	.99	32.7	121	88

Nilsson (1964b) observed in two successive years a radiant which is definitely distinct from, but may well be related to the Monocerotid stream. Association 12.02 of the present survey lies close to this radiant, and has perihelion longitude close to that of Nilsson's associations 60.12.9 and 61.12.2 as well as the Monocerotids. This suggests that the present association may also be related to this complex.

However, its mean observed velocity is 10 km sec^{-1} less than that for the other associations, so the similarity could be coincidental. Table 7.12 compares the radiant and orbit data for these associations. Further confirmation of the radiant is given by the visual observations from Waltair, India recorded by Srirama Rao, Rama Rao and Ramesh (1969) who have noted activity in two successive years.

TABLE 7.12

Source	N	α	δ	V_∞	$\frac{1}{a}$	q	e	i	ω	Ω
This Survey 12.02	6	95°	+18°	32	.37	.33	.85	7.1°	117°	82°
Nilsson (1964b) 60.12.9	4	96	+15	42	.05	.20	.99	18.7	131	77
Nilsson (1964b) 61.12.2	4	95	+15	42	.09	.11	.99	22.6	135	74
Srirama Rao et al. (1969) 1963	15	88	+22							
Srirama Rao et al. (1969) 1964	46	93	+18							

7.6.6 The Southern Taurids and ζ-Perseids

The $D(A,B) \leq .1$ stream search detected an association of 55 meteors consisting of 49 Southern Taurids and 6 ζ-Perseids. Tables 7.13 and 7.14 compare the respective components of this association with other observations. It should be noted that the mean orbits of the ζ-Perseids for the data of Nilsson (1964b) and Kashcheev and Lebedinets (1967) are for observations over May and June, whereas the observations for the present survey are limited to June only until the May data is reduced. The longitude of perihelion for this stream is observed to

increase during the period of observation, hence the higher value for the present survey. To date only half the October data has been analysed. It is anticipated that more Southern Taurids will be found amongst the remaining data.

TABLE 7.13

Source	N	α	δ	V_∞	$\frac{1}{a}$	q	e	i	Ω	π
This Survey D.01	49	44	+11	31	.58	.30	.82	7.1	24	153
Whipple (1954)	8	53	+14	30	.43	.38	.84	5.5	43	155
McCrosky & Posen (1961)	17	43	+11	29	.53	.37	.80	5.3	31	145
Jacchia & Whipple (1961)	13	38	+10	30	.55	.34	.81	5.1	25	142
Southworth & Hawkins (1963)	11	28	+ 8	30	.56	.32	.82	5.0	14	136
Nilsson (1964b)	17	59	+17	26	.48	.50	.76	4.2	56	155
Baker & Forti (1966)	61	62	+18	27	.55	.41	.76	2.9	54	165
Kashcheev & Lebedinets (1967)	73	27	+ 9	31	.48	.33	.84	2.2	15	133

Radiant and Orbit of Southern Taurids

TABLE 7.14

Source	N	α	δ	V_∞	$\frac{1}{a}$	q	e	i	Ω	π
This Survey D.01	6	65	+27	30	.58	.30	.82	7.1	81	150
Nilsson (1964b)	27	51	+22	30	.59	.31	.82	4.8	71	127
Baker & Forti (1966)	57	55	+21	29	.55	.33	.81	3.2	73	132
Kashcheev & Lebedinets (1967)	60	52	+23	30	.62	.31	.80	5.7	71	128

Radiant and Orbit of ζ-Perseids

7.6.7 The Andromedid (Bielid) Stream

Association 10.11 of two meteors only appears to belong to the formerly spectacular Andromedid stream associated with Comet Biela 1852 III. Table 7.15 compares the orbital elements of this association with observations of photographic Andromedids by Hawkins, Southworth and Steinon (1959), and Southworth and Hawkins (1963). Mean radiant data for the observations of Hawkins et al (ibid.) are not given, but the individual radiant coordinates cover a broad area in general correspondence to the other radiant data presented, including that of Hasegawa (1958) for the theoretical stream radiant associated with the comet orbit.

Analysis of the remaining October data for the present survey may possibly yield further Bielids. Agreement in inclination and longitude of perihelion of our results with the photographic observations is quite good. The present association has a mean orbit which is considerably smaller than those of the other observations listed, as well as that of the comet. This might possibly indicate that the radio meteors observed belong to an older branch of the stream at a more advanced stage of evolution.

TABLE 7.15

Source	N	α	δ	V_∞	$\frac{1}{a}$	q	e	i	Ω	π
This Survey 10.11	2	23	+ 9	22	.64	.60	.62	0.1	24	116
Hawkins et al (1959)	23	-	-	-	.29	.75	.78	6.3	224	106
Southworth & Hawkins (1963)	14	19	+ 5	22	.43	.71	.70	0.4	26	100
Comet Biela 1852 III	-	23	+29	19	.28	.86	.76	12.6	246	109

The Andromedid (Bielid) Stream

Table 7.16 compares three associations found by Nilsson (1962) in Canis Minor and Hydra with three pairs of orbits observed in this vicinity by the present survey also during October. The agreement confirms the reality of this stream.

TABLE 7.16

Source	N	α	δ	V_∞	$\frac{1}{a}$	q	e	i	ω	Ω
Nilsson (1962) 26.1	3	127	+6	69	.23	.95	.78	156	334	32
Nilsson (1962) 26.2	3	116	+2	64	.50	.97	.52	148	13	32
Nilsson (1962) 26.3	3	120	+1	67	.15	.98	.84	148	10	35
This Survey 10.16	2	117	-5	66	.17	.97	.82	136	340	25
This Survey 10.17	2	121	+5	67	.35	.92	.67	152	325	24
This Survey 10.18	2	114	+6	67	.39	1.00	.61	153	359	25

The minor radiant in Aquarius observed by Nilsson (1964b) during March was observed again in this survey. Nilsson (1962) noted activity in this radiant also during February, which he felt could correspond to the day-time appearance of a stream observed at night in

July. Although Nilsson only observed two meteors in the July radiant these correspond closely to three from the list of photographic meteors published by McCrosky and Posen (1961), confirming the stream. While the present survey did not detect the activity from the radiant in Aquarius during February, an association of 7 meteors from this radiant was observed in March. Table 7.17 compares the radiant and orbit data for these associations. The present data confirms both the March and February associations of Nilsson. There is some discrepancy in the longitude of the ascending nodes between the February-March day-time stream and the probable night-time appearance of this stream in July. However, as it is apparently a broad stream this may still be acceptable. The correspondence of the longitudes of perihelion is excellent.

TABLE 7.17

Source	N	α	δ	V_∞	$\frac{1}{a}$	q	e	i	Ω	π
This Survey 3.01	7	338	- 8	35	.60	.18	.89	1.8	359	42
Nilsson (1962) Feb. 5.2	3	317	-11	33	.32	.32	.90	6.2	329	34
Nilsson (1962) McCrosky & Posen (1961) July	5	307	-15	29	.34	.38	.87	4	217*	47
Nilsson (1964b) March 61.3.2	3	340	- 8	32	.47	.30	.86	2.5	354	53

* This might be υ instead of Ω since the inclination is small.

7.6.8 Stream Radiants Possibly Associated with Comet Lexell 1770 I

Nilsson (1964b) lists three radiants for the period 13 - 16 June, 1961 in Ophiuchius and Sagittarius which may be associated with Comet Lexell 1770 I. Nilsson (1963) previously discussed the possible association of the December Scorpids with the same comet. Southworth and Hawkins (1963) discovered a stream radiant for five meteors over the period 21 May to 16 June, which they have named the θ-Ophiuchids. More recently Cook (1970) has listed the radiant of the μ-Sagittariid stream detected by Lindblad (1970) for four meteors and has noted the association of this stream with Comet Lexell. Terenteva (1968) lists a family of six minor streams detected over the period 16 June - 16 August for which orbital elements and computed values of Tisserand's criterion suggests an association with Comet Lexell.

Cook (1970) has classified a number of meteor streams in terms of the discrete beginning height criteria of Ceplecha (1967, 1968) and has ascribed to the μ-Sagittariids a classification of type A or lower. It is most unfortunate that Cook was unable to classify the four June θ-Ophiuchids in the list of Southworth and Hawkins (1963) for comparison in view of their possible related origin.

McKinley (1961) and Ellyett and Roth (1955) also give radiants for streams in this region for which velocity measurements are not available.

Two June streams with radiants in this general vicinity were observed in the present survey. Stream D.02 with six members in June includes one meteor (No. 18043) observed on February 12th. Table 7.18 compares the radiant and orbit data for these meteors and an association (2.01) of three meteors with an adjacent radiant also from February.

TABLE 7.18

Source	No	α	δ	V_∞	$\frac{1}{a}$	q	e	i	Ω	π
6.01	4	262	-25	26	.43	.52	.77	1	260	357
D.02	6	271	-24	28	.60	.41	.75	1	261	15
18043	1	308	-21	31	.68	.28	.81	-2	323	17
2.01	3	316	-21	31	.48	.36	.82	-5	324	30

The similarities between the orbits of Table 7.18 seem too pronounced to be coincidental. The longitudes of perihelion are perhaps the most reliable guide to common origin. π for D.02 is approximately as far behind π for Comet Lexell as Nilsson's Scorpids are in front. Were it not for D.02 the longitude of perihelion of association 2.01 would not have led to the consideration of its possible association with this comet.

Table 7.19 compares the orbital elements of streams 6.01 with Comet Lexell. The agreement in π is excellent, but the discrepancy in Ω is considerable. On the other hand, since the inclination of the stream is so low, good agreement exists between the nodes of 6.01 and

Nilsson's Scorpids if we reverse the nodes of 6.01 and consider the inclination as negative.

It is unfortunate that the present observations have done little to solve the problems outlined by Cook (1970) in connection with this stream complex. Certainly, however, these observations give further confirmation to the existence of the complex in addition to extending its observation to February. There seems little chance of being 'rid of' these streams as Cook light-heartedly suggests would be a convenient way of removing the theoretical embarrassment attached to them.

TABLE 7.19

	a	q	e	i	Ω	π
1770 I	3.2	.67	.79	1.6°	132°	356°
6.01	2.3	.52	.77	-1.3	80	357
Scorpids	2.6	.52	.80	2	74	338

7.7 TOROIDAL METEOR STREAMS

During February intense activity was observed centred on R.A. 179° Dec. - 83°. Altogether 47 meteors were found to be associated applying the Southworth and Hawkins D criterion of $D(A,B) < 0.2$. Agreement between the orbital elements for the association (2.14) is generally good, although the range of inclinations is far greater than that normally indicative of a stream, varying from 33.6° to 106.6°. The spread in longitude of perihelion is similarly large, although some of this

spread may be attributed to the generally low values of eccentricity for the members of the association. Nevertheless there is a sharp peak at the mean value for the association of $\pi = 125^{\circ}$.

If sorting and association testing were to be based upon the meteors all satisfying a criterion of the form D(M,N) for association with a mean rather than D(A,B) for association with at least one other member of the association then it is apparent that unless D(M,N) were to be made extremely big the present association of 47 meteors would be broken into a number of smaller associations. In this case it is necessary to decide whether it is the overall distribution of the meteors which is important, or whether the smaller associations are individually important. Certainly in this regard it is worth noting that the D(A,B) criterion may find associations amongst quite diffuse orbits over a wide range of values without the likelihood of including extraneous orbits which would occur if the D(M,N) criterion were used and set large enough to include all the same orbits. In other words, where, say, a particular type of dispersing mechanism has caused a progressive spread in one or more of the orbital elements of meteors in a stream, the D(A,B) criterion can 'track down' the members of the stream, whereas the D(M,N) criterion must assume an idealized dispersing mechanism and look for streams only of a 'regular' shape.

Of course there is the possibility of 'chaining' using the D(A,B) criterion incautiously, in which the association test, if the limits are set too large, can use sporadic meteors as 'stepping stones' to link

one part of orbit space to almost any other, with rather meaningless consequences. Nevertheless, in view of the lack of similar large groups of associations in the data of other months it seems reasonably safe to assume that the broad overall association of 47 meteors is meaningful in this case, particularly in view of the general similarities in perihelion distance and eccentricities.

There is a general profusion of associations of orbits with low eccentricities and large perihelion distances with radiants at deep southern declinations during the months from and including December to March, and relatively little activity in this region during June and October. It will be interesting to observe the activity in this quarter for the months of April and May when the data is analysed. The fact that the present association of 47 meteors has not 'chained' with other associations such as 2.13 nearby gives support for its reality.

Figure 7.1 shows the observed distribution in inclination for members of this association. It can be seen that the majority of meteors have inclinations between 30° and 80° with two distinct peaks near 55° and 75°, indicating in all probability that the association is a combination of two similar broad and probably related streams.

Figure 7.2 shows the numbers of meteors of this association observed for the various days of observation during February. The equipment was operated for a few hours only on the 10th and 17th, and continuously for the days in between. There is some indication of a slow rise in the meteor rate to a broad peak over the period 13th - 15th although it is

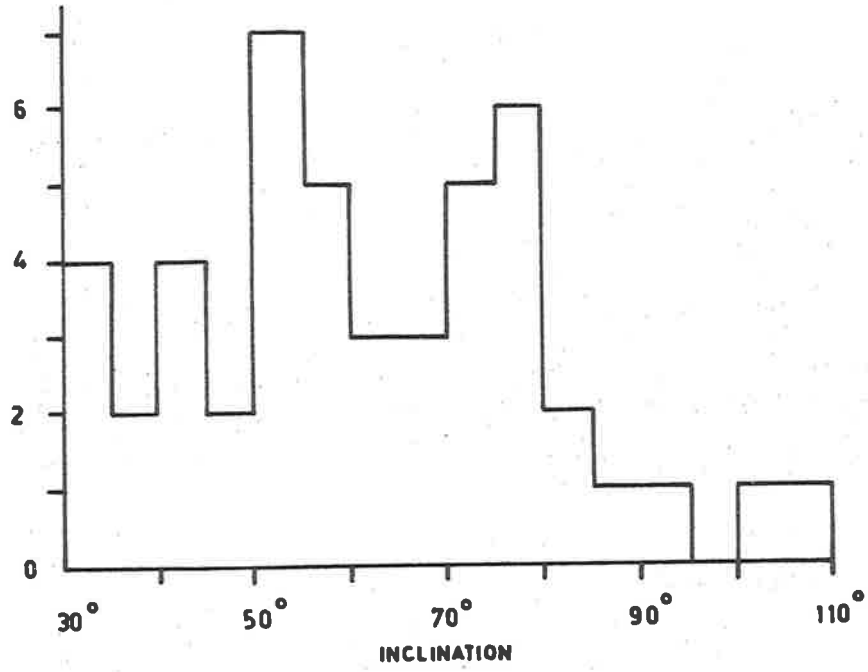

FIG. 7 · 1 DISTRIBUTION OF ASSOCIATION 2 · 14 WITH INCLINATION.

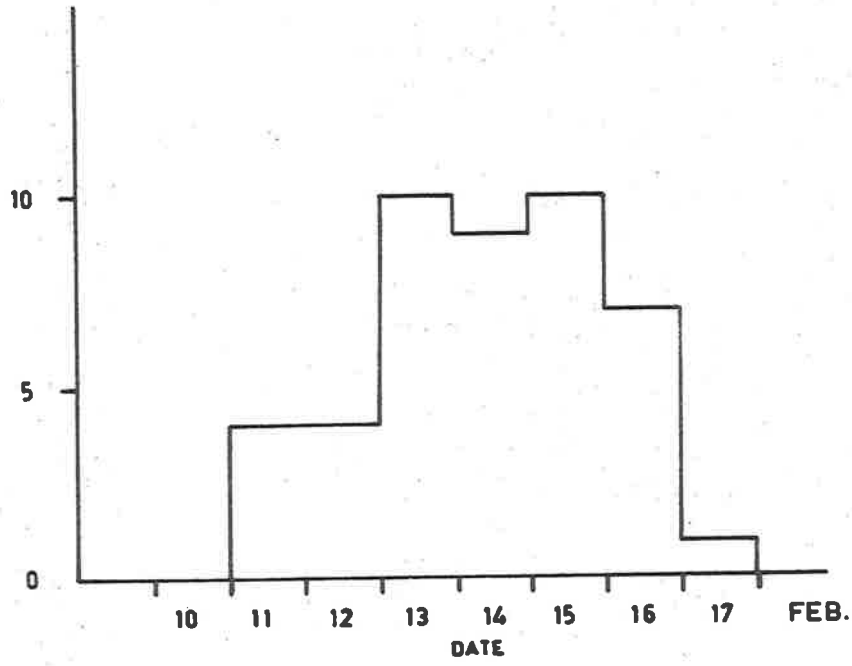

FIG. 7 · 2 DISTRIBUTION OF ASSOCIATION 2 · 14 WITH DATES OF DETECTION.

not possible to say for certain when and how suddenly the rate drops after this point.

It is interesting to note the relative lack of meteor associations of this kind amongst the data of Nilsson (1964b) which is the only available survey of individual meteor orbits covering the same range of declinations with which comparisons of the present data may be made. The Puppid shower observed by Nilsson and previously by Ellyett and Roth (1955) and Weiss (1957a,1960b) is an example of such a meteor stream. This shower probably is related to associations 12.06, 12.07, and 12.08 in this survey, although 12.06 agrees with Nilsson's elements for this stream well in e and π but not in i, whereas the two associations 12.07 and 12.08 are closer to the inclination of 70° but have exceptionally low eccentricities, so that perihelion longitude is no longer a reliable guide.

Table 7.20 compares Nilsson's determination of the Puppid radiant and orbit data for his 1960 and 1961 observations with those for the current associations 12.06, 12.07 and 12.08.

TABLE 7.20

	N	α	δ	V_∞	$\frac{1}{a}$	q	e	i	ω	Ω
Nilsson (1964b) {	5	138	-53	41	.48	.98	.53	70	354	78
	3	143	-54	40	.53	.98	.48	70	340	77
This Survey { 12,06	7	135	-63	35	.44	.97	.56	57	344	82
12.07	6	141	-48	37	.85	.99	.16	70	0	81
12.08	3	145	-45	39	.95	.98	.08	75	1	82

Radiant and Orbit of the Puppids

Few streams were detected during January although this is not surprising in view of the small number of orbits reduced for this month. The present 78 January orbits are only a sample of the data available and it will be worth reading the January (and February) film records again in more detail.

It is interesting to note in view of the meagre data for January that association 1.01 corresponds well to an association of 3 meteors with a radiant in Carina detected by Nilsson (1962). The two sets of radiant and orbit data are compared in Table 7.21. Although the present data is insufficient to draw firm conclusions it appears that this stream which we shall tentatively refer to as the Carinids may be more pronounced at $M_R \leqslant +8$ than $M_R \leqslant +6$.

TABLE 7.21

	N	α	δ	V_∞	$\frac{1}{a}$	q	e	i	ω	Ω
Nilsson (1962)	3	156	-65	40	.42	.98	.59	70	0	119
This Survey 1.01	3	160	-63	43	.34	.98	.64	74	7	122

Radiant and Orbit of the Carinids

While the Puppid and Carinid streams appear to be quite distinct they have many similarities, the greatest difference being the respective longitudes of perihelion. The Carina radiant was also observed to be active in December by Nilsson (1964b) and in February in this survey. Both of these associations have orbital similarities to the

Puppids and Carinids, and again differ most markedly in perhelion longitude. Table 7.22 lists these associations.

TABLE 7.22

	N	α	δ	V_o	$\frac{1}{a}$	q	e	i	ω	Ω
Nilsson (1964b) 60.12.7	4	154°	-61°	40	.34	.91	.69	67°	323°	76°
This Survey 2.13	9	152	-65	37	.42	.93	.60	62	33	145

Two Additional Associations in Carina

Until more data is gathered concerning all of these associations we can do little more than note their similarities. It seems reasonable to refer to them as a "family" of streams in view of their apparently similar origins. Whether their origins are more closely linked than that remains to be seen.

Nilsson (1962) did not find any shower meteors with orbits of eccentricity less than .6 although he subsequently (1964b) resolved the Puppids with eccentricity of .53 to .48 and the Carinids with eccentricity .59. From this he deduced that the short-period highly inclined orbits of low eccentricity which appear to become more prominent with smaller magnitudes (Hawkins, 1962) do not contribute to the total distribution as showers, but rather as meteors in individual and separate orbits.

It is probably due to the ability of the present survey to resolve meteors of limiting magnitude + 8 compared with Nilsson's limiting

magnitude of + 6 that the present results lead us to the reverse conclusion.

Although velocity selection effects favour the observation of short-period low eccentricity streams with high inclination rather than low inclination the relative dearth of highly retrograde orbits of similar shape in the observations suggests that the predominance of this type of orbit at high inclinations is not merely a result of observational selection. It is worth noting, too, that the astronomical collision probabilities work strongly against detecting streams of this type as can be seen from eqn 7.2, since the Earth will tend to pass through them more nearly normally rather than along the stream axis and hence in the shortest time possible.

Figure 7.3 compares the distribution in inclination of associated meteors for various ranges of eccentricity. The reality of the toroidal group is clearly apparent.

Kashcheev and Lebedinets (1967) record eleven associations of high inclination and low eccentricity, of which seven have values of $q > .87$ a.u. A number of the radiants for these associations are visible from Adelaide. Table 23 compares associations 10.06, 10.17 and 10.18 from this survey with association 40 of Kashcheev and Lebedinets. These comprise three of the four low eccentricity associations observed during October, all of which have positive declinations. Association 40 is the only association of low eccentricity meteors observed by Kashcheev and Lebedinets during October.

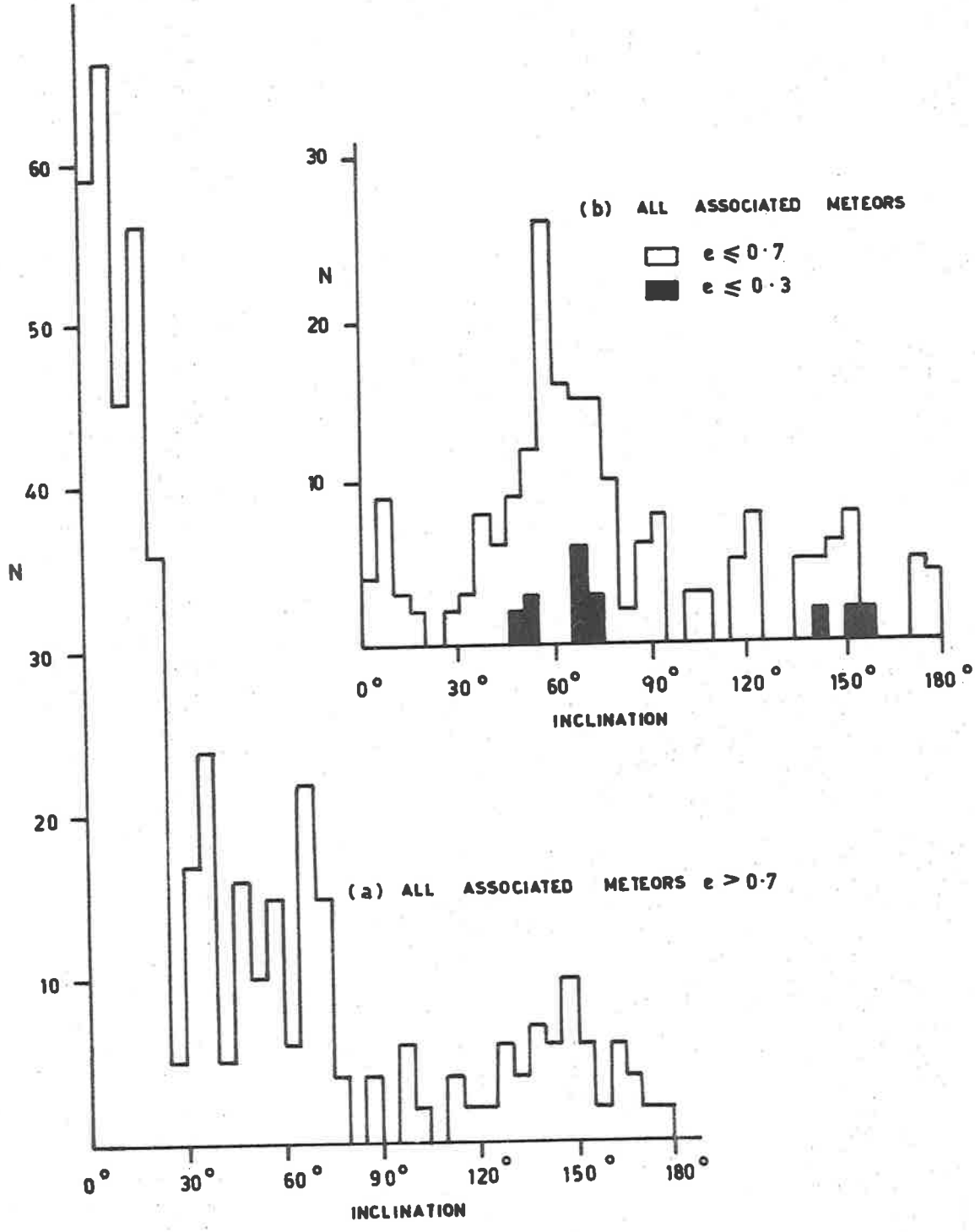

FIG. 7·3 DISTRIBUTION OF ALL ASSOCIATED METEOR ORBITS WITH INCLINATION FOR VARIOUS RANGES OF ECCENTRICITY.

TABLE 7.23

Source	N	α	δ	V_∞	$\frac{1}{a}$	e	q	i	ω	Ω
Kashcheev and Lebedinets (1967) (Assn. 40)	21	108°	15°	66	.53	.51	.94	166°	3°	23°
This Survey 10.06	3	115	17	68	.41	.58	.99	172	352	23
This Survey 10.17	2	121	5	67	.35	.67	.93	152	325	24
This Survey 10.18	2	114	6	67	.39	.61	1.00	153	359	25

The agreement between the two sets of data is sufficiently close to suggest that they are observations of the one stream. It may be significant that this stream has not been observed photographically or with less sensitive radar equipments, since this could indicate that the low value of eccentricity may be a result of prolonged action of the Poynting-Robertson effect which has reduced the orbit size for the smaller members of a meteor stream originally reaching perihelion at a distance exceeding 1 a.u.

It is understandable that the toroidal meteor streams of February have not been previously observed in view of the extremely southern radiant declinations, however the lack of published observations of streams during this month is noteworthy.

This survey has recorded a number of February streams besides those of high inclination already discussed. Of these, association 2.18 shown in Table 7.24 appears sufficiently significant to suggest that the reason it has not been detected previously may be once again because it is constituted entirely of small particles.

TABLE 7.24

	N	α	δ	V_∞	$\frac{1}{a}$	q	e	i	ω	Ω
2.18	11	346	-24	18	.44	.82	.62	2.1°	299°	144°

7.8 A COMPREHENSIVE SOUTHERN HEMISPHERE SEARCH FOR COMETARY ASSOCIATIONS WITH METEOR STREAMS

Hasegawa (1958) has predicted stream radiants for comets in the Baldet and de Obaldia catalogue (1952) which pass within 0.2 a.u. of the Earth's orbit. A search for comets associated with the streams of the present survey has been conducted by comparison first with Hasegawa's radiant data, and subsequent comparison of the orbital elements of promising associations with those for the appropriate comets given by Baldet and de Obaldia.

This constitutes the first comprehensive search for cometary associations in the Southern Hemisphere, although Nilsson (1964b) compared his survey data with the list of 19 meteor radiants for comets given by Porter (1952) and reported the association with Comet Lexell 1770 I discussed earlier.

Particular attention has been given to the streams of high inclination and low eccentricity, and a number of associations have been found with long-period comets. Differences in Ω may be expected to occur where the stream orbit is contracted markedly by the Poynting-Robertson effect. For a direct orbit such a contraction should cause Ω to increase if

perihelion occurs south of the ecliptic plane. In several cases agreement is good in most elements but not in the alignment of the line of apsides. For others only the inclinations differ significantly. Where the generating comet is of long period or parabolic and the stream of short period some small differences may arise through the differential action of secular and other perturbing forces, although such differences will rarely be sufficient to explain the discrepancies.

Larger differences may be countenanced by considering that the particles have been ejected with substantial velocities relative to the comet some time prior to perihelion. This mechanism can produce variations in all of the orbital elements, including inclination and argument of perihelion, but should have least effect upon Ω if the stream is generated near 1 a.u. from the Sun. Southworth (1963) has determined that the Perseid orbits suggest an explosive origin for this stream 1.5 a.u. from the Sun and 1.3 a.u. north of the ecliptic plane, approximately 1000 years ago. It is possible that such explosive origins for meteor streams are the rule rather than the exception, although with considerable variation in degree.

The association of Comet Mellish 1917 I with the Monocerotids has already been noted, as has that of Comet Lexell 1770 I with the Scorpid/Ophiuchid complex.

Table 7.25 lists 17 comets and associations from the present survey which may be related. In several instances the agreement is so good that no doubt arises. In others the doubt cannot be eliminated

TABLE 7.25

	Ident.	a	q	e	i	ω	Ω	π	α	δ	V_o	N
Bečvár	1947 III	-	.96	1	129.2	182	322	144	237	11	66	
	2.16	2.3	.98	.56	118.0	171	323	134	241	15	59	5
(China)	574	-	.96	1	46.5	15	128	143	111	-61	31	
	2.11	3.0	.98	.67	48.4	354	145	139	99	-76	31	5
	2.10	9.4	.98	.89	47.2	12	145	157	110	-65	32	3
	2.30	10.9	.97	.91	47.8	14	144	158	112	-64	33	2
Giacobini	1905 III	37.1	1.11	.96	40.2	358	157	155	86	-62	27	
Helfenzrieder	1766 II	2.5	.40	.85	8.0	178	76	254	157	9	27	
	2.24	2.1	.46	.78	5.3	283	323	245	154	17	27	2
Honda-Mrkos-Pajdušáková	1954 III	3.1	.56	.82	13.2	184	233	77	324	-14	25	
	2.01	2.1	.36	.82	4.5	246	144	29	316	-21	31	3
	2.19	1.4	.51	.63	1.7	75	324	38	318	-14	23	2
	2.21	1.8	.67	.63	5.1	99	323	81	326	- 4	21	2
Schwassmann-Wachmann-Peltier	1930 I	3151	1.09	1.00	99.9	325	148	113	249	-68	55	
	2.15	13.2	.95	.93	70.2	330	144	114	250	-86	44	4
	2.39	2.0	.85	.57	87.1	307	145	92	247	-71	48	2
	2.42	50	.79	1.00	101.6	307	145	92	256	-64	57	2
Brooks	1885 III	42.2	.75	.98	59.1	43	205	248	185	-75	38	
	3.06	1.6	.88	.41	65.7	57	177	234	195	-74	37	5
	3.07	2.0	.65	.65	57.3	83	179	262	184	-58	36	3
	3.09	20.6	.76	.90	59.3	58	178	236	173	-60	40	3
Gambart-Dunlop	1834	-	.51	1	6.0	50	227	277	190	- 4	29	
	3.17	3.2	.41	.86	1.2	105	177	282	183	- 3	30	2
	3.21	2.3	.46	.80	11.5	103	179	282	181	-14	28	2
	3.22	2.0	.32	.83	13.9	300	358	298	197	4	31	2
	3.23	1.6	.31	.80	18.7	122	180	303	191	-21	31	2
	3.27	16.2	.32	1.04	26.0	109	178	287	184	-19	40	2
Nakamura	1930 VII	-	.41	1	4.2	63	229	292	195	- 7	32	

TABLE 7.25 (Cont'd)

	Ident.	a	q	e	i	ω	Ω	π	α	δ	V_o	N
Gale	1938	4.9	1.18	.76	11.7	209	67	276	214	22	14	
	6.02	3.1	.93	.68	14.0	216	79	295	234	20	18	3
(Rome)	1618 II	-	.39	1	37.2	287	76	3	276	0	39	
	6.09	1.9	.15	.90	39.5	324	80	44	289	- 6	38	13
	6.10	2.6	.37	.86	43.3	292	79	11	280	6	37	4
	6.11	.9	.14	.84	66.3	333	80	53	303	3	37	5
Winnecke-Borelly-Tempel	1874 II	-	.89	1	148.4	332	274	246	20	-11	69	
	6.37	3.3	.78	.76	157.6	297	262	199	12	- 7	66	2
Sanderson	1723	-	1.00	1	130.0	331	14	316	115	- 8	66	
	10.06	2.4	.99	.58	171.6	352	23	15	115	17	68	3
	10.16	5.9	.97	.82	135.7	341	25	6	117	- 5	66	2
	10.17	2.8	.93	.67	151.6	325	24	349	121	5	67	2
	10.18	2.6	1.00	.61	153.0	359	25	24	114	6	67	2
Brooks	1888 III	9796	.90	1.00	74.2	59	101	161	130	-35	45	
	1.1	3.0	.98	.64	74.3	7	122	129	160	-63	43	3
Thiele	1906 VII	69.8	1.21	.98	56.3	9	85	93	110	-59	37	
	12.06	2.3	.97	.56	57.3	344	82	66	135	-63	35	7
Puppids/Velids	12.07	1.2	.98	.16	69.5	0	81	81	141	-48	37	6
	12.08	1.1	.98	.08	74.5	1	82	83	145	-45	39	3
Johnson	1935 I	93.2	.81	.99	65.4	18	91	109	120	-53	40	
Pons-Bouvard-Olbers	1804	-	1.07	1	56.5	332	177	149	63	-52	36	
	3.05	10.0	.98	.87	58.3	346	178	164	50	-78	38	10
	3.04	2.1	.98	.53	55.3	347	178	165	51	-81	34	11

although the similarities still are most pronounced. Nevertheless, as noted by Kashcheev and Lebedinets (1967) "if the comet's orbit passes at a large distance from the Earth's orbit, the orbit of the related stream, to be observed at the Earth, should differ noticeably from the comet's orbit."

For this reason rather than being over-cautious, all reasonable associations have been listed in the hope that some of these may stimulate further investigation. In three instances two comets are listed as possibly being associated with the one group of streams, although in each case the agreement is generally better with one comet than the other. We might well ask: if two comets why not three? Possibly the streams are associated with neither of the listed comets, but with a third, or possibly the streams are the remnants of a comet which belonged to a comet group containing the other two. Just as the complex radiant activity in December has suggested our understanding of the relation of meteor streams with comets is still over-simplified, so too might we expect that our knowledge of the relation of comets to each other might be very incomplete.

Although association 2.24 contains two meteors only some confirmation of its reality is given by the similarity of the orbit to that of Comet Helfenzrieder 1766 II. Further confirmation is given by Terenteva (1967) who describes a family of minor streams possibly associated with this comet including two, the η-Leonids and the 40 Leo Minorids, to which the present association 2.24 is intermediate.

Terenteva (1967) makes some interesting comments on the structure of 'families' of minor streams and related comets which are consistent with the observations of the present survey. In particular a number of minor streams give the appearance of a filamentous structure within a larger radiant area. Also noted is an apparent tendency for stream radiant symmetry about the ecliptic. In view of the contradictions of time-scale noted at the conclusion of this chapter, Terenteva's comment that although the minor streams are apparently in a relatively later stage of evolution in reality they might be younger (than the major streams),is worthy of serious consideration.

Among the probable cometary associations listed in Table 7.25 there are a number between long-period comets and high inclination streams which deserve special note. The agreement in Ω for associations 2.15, 2.39 and 2.42 with Comet Schwassmann-Wachmann-Peltier 1930 I is particularly close. In view of the close proximity of the inclination in each case to 90° the agreement in this element must be good if the association is to be regarded as valid.

Associations 12.06, 12.07 and 12.08 correspond to the Puppid/Velid complex already discussed. In this case the association of the complex with Comet Thiele 1906 VII is more likely than with Comet Johnson 1935 I because of the agreement in Ω. Probably more importantly the similarities in q between the meteor associations imply that the streams may have contracted under the Poynting-Robertson effect from the cometary orbit with larger q rather than having increased in q from the smaller value.

The association between 3.04, 3.05 and Comet-Pons-Bouvard-Olbers 1804 is particularly interesting. Both 3.04 and 3.05 are undoubtedly significant with 10 and 11 members respectively. 3.04 is a good example of a 'toroidal' meteor stream, and yet there is no doubt that it is related to 3.05, which certainly is not. The association with Comet 1804 is also unmistakable, and yet this comet is parabolic. It should be noted that the value of 1/a given for 3.05 is only approximate. The actual range of a for this group varies from 4.17 a.u. through to one slightly hyperbolic orbit. There is possible a case for further subdivision of this group into two groups since five of the orbits have $4.17 \leqslant a \leqslant 6.67$ a.u., while for the remainder $a \geqslant 10.1$ a.u.

Despite their strengths neither association 3.05 nor 3.04 was detected by Nilsson (1964b) during 1961 possibly because his recording period during March ended on the 17th, approximately when the March recording period for the present survey began. Although too far south for observation from the northern hemisphere the radiants of these streams are continuously observable at Adelaide. It would be interesting to determine whether any photographic meteor activity is associated with 3.05, and if so, whether 3.04 is also detectable visually or photographically.

The appearance of the toroidal class of meteors only at faint radio magnitudes is good evidence for its origin in the differential action of the Poynting-Robertson effect upon small meteors in streams. The similarities of 3.04, 3.05 and Comet 1804 give further evidence that the low

eccentricity orbits are the result of evolution rather than direct formation. Yet there is one major problem common to several of the cometary associations listed, which at present must remain unsolved. Approximate calculations show that for a "typical" low density faint radio meteor in a circular orbit near 1 a.u. from the Sun, the Poynting-Robertson effect alone will cause the meteoroid to take $\sim 10^6$ years to drift into the Sun. Yet if Comet 1804 is responsible for stream 3.04, then since it is parabolic, only 170 years have been available for 3.04 to contract from $a > 10$ a.u. to the present value of $a = 2.13$ a.u. For association 2.16 and Comet Bečvár 1947 III only 22 years have been available for a similar contraction to take place.

Possibly the streams have been ejected rear-wards from directly rotating comets. Perhaps the comets, although parabolic, have had predecessors travelling along the same orbits. Our observations even over two centuries cover only an instant in the time scale of the long-period comets. Even considering that the meteoroids are all spinning at high speed, additional drag effects such as the Yarkovsky-Radzievskii effect could not alone account for the apparent time scale discrepancies in terms of our present knowledge.

To find the answers a better understanding of cometary structure is necessary, together with the knowledge of the ways in which meteoroids may be derived from comets. The basic significance of the uncertainties underlined by the present observations indicates the need

for a comprehensive cometary space probe to obtain direct information, although in view of the variation in behaviour of comets already known the choice of comets could be as big a problem as the instrumentation.

CHAPTER VIII

DISTRIBUTIONS

8.1 INTRODUCTION

In this chapter distributions of various geocentric and astronomical quantities for the meteors of this survey are presented and their significance considered. Careful comparison of these distributions with those found in other surveys, especially for meteor populations covering different magnitude ranges, may provide us with an understanding of the 'evolutionary' factors shaping the distributions and may possibly help us to determine the origins of meteors and comets.

The observed meteor distributions are strongly influenced by a number of selection effects. In computing the true distributions allowance must be made for these.

Correction for the relative probabilities of meteors in various orbits colliding with Earth, referred to as astronomical selection, is discussed in detail in §8.2.1. Allowance must be made in corrected distributions for antenna selectivity. In the present case this is done with the assumption that all aerials are well represented by theoretical gain configurations. The adequacy of this assumption for the present case has been discussed in §4.2.2. Consideration is also given to the total observing time for which radiants are visible as a function of radiant declination. Atmospheric interaction selection, discussed in §8.2.2, arises through the dependence of meteor ionization on geocentric velocity. Since heliocentric meteor velocities near Earth are typically

of the same order of magnitude as Earth's own heliocentric velocity, the relation of the meteor orbit to that of Earth will have a strong bearing on the likelihood of detection of the meteor.

Distributions in this thesis are presented in three forms, observed, corrected for observational selection, and corrected for observational and astronomical selection. The description "observed" signifies that the distribution has not been corrected in any way for selection effects. The observational selection correction takes into account antenna selectivity as well as atmospheric interaction selection. Distributions corrected for astronomical selection, defined earlier in this section, are also corrected for observational selection.

The incidence of fragmentation amongst the observed meteoroids may introduce some form of selection effect. Fragmentation may affect the ionization profile and detectable trail length of a meteor, and could also possibly be velocity dependent. As there is insufficient knowledge regarding the structure of small meteoroids, it is not yet possible to determine the role of fragmentation in observational selection.

Several other forms of selection encountered may be peculiar to the Adelaide system, although other meteor radars will have comparable types of selection effects.

On some occasions, local interference at the St. Kilda receiving site caused the loss of a substantial fraction of the day-time meteor echoes. No attempt has been made to correct for this, as no reliable basis exists for a description of the interference, which was variable, and appeared to emanate from several sources.

The method of film reading outlined in Chapter 5 possibly favours meteors with high geocentric velocities, since, in the presence of noise, high frequency diffraction extrema seem subjectively easier to recognize than those of lower frequency and similar amplitude. As noted in §8.3.1 it has been suggested that rapid diffusion in the upper portion of the meteor region may selectively prevent a fraction of the records of high velocity meteors from being reduced. This selection effect would tend to negate that due to film reading, and since neither effect is thought to be severe, no attempt has been made to correct for them.

8.2 SELECTION EFFECTS

8.2.1 Astronomical Selection

Öpik (1951, 1961) derives expressions which may be used to find the mathematical expectation P of a collision between a particle and Earth per heliocentric revolution of the particle. Whipple (1954) uses the inverse of this expectation (eqn 8.1) as a weighting factor for the correction of observed distributions for astronomical selection effects.

$$W_{AST.} = \frac{1}{P} = \frac{\pi V_g \sin i}{R^2 V_\infty^2} \left(2 - \frac{1}{a} - p\right)^{\frac{1}{2}} \qquad (8.1)$$

where $p = q(1 + e)$ is the semi-latus rectum

q = perihelion distance

e = eccentricity

R = radius of Earth

V_g = geocentric velocity before zenith attraction

V_∞ = observed velocity before atmospheric retardation

a = semi-major axis of the meteor orbit

i = inclination of meteor orbit to the ecliptic plane.

It is important to note that the form of P in eqn 8.1 refers to the mathematical expectation of collision per heliocentric revolution of the particle and not per unit time. To correct the observed distribution over a period of time we note that the probability of collision should be directly proportional to the frequency of crossing of Earth's orbit by the particle, i.e.

$$f = \frac{1}{T} \propto a^{-\frac{3}{2}} \tag{8.2}$$

whence eqn 8.1 should be replaced by

$$W_{AST.} = \frac{\pi V_g \sin i}{R^2 V_\infty^2} \left(2 - \frac{1}{a} - p\right)^{\frac{1}{2}} \cdot a^{\frac{3}{2}} \tag{8.3}$$

As Whipple observes, the form of the weighting factor should be determined by the use to which the corrected distribution is to be put. Whipple (1954) uses eqn 8.1 rather than eqn 8.3 to compare meteor distributions with observed comet distributions, since the probability of detection of comets is, apart from other factors, similarly proportional to the frequency of perihelion passage. Nilsson (1962) and Kashcheev and Lebedinets (1967) also apply an astronomical weighting factor of the form of eqn 8.1 to their distributions.

Distributions in the present thesis are given in a number of cases for both forms of the weighting factor. Unless otherwise

stated the weighting factor used is that described by eqn 8.3. It should be noted that while it is possible to apply eqn 8.1 to hyperbolic orbits by putting $p = 2q$, $1/a = 0$, eqn 8.3 ascribes infinite weight to parabolic orbits and cannot be used above this limit. For the purpose of computing distributions with the form of the astronomical selection weighting factor of eqn 8.3 all meteors with parabolic or hyperbolic orbits have been weighted as though $a = 10^6$ a.u. and $e = 1 - 10^{-10}$.

The allowable range of the combined weighting factor (the product of all individual weighting factors used) is restricted to a maximum value of 25 for any one meteor with the distribution normalized to a mean overall weight near 5. It is prudent when considering small samples to prevent corrected distributions from being too strongly influenced by the application of very large weights to the few possibly atypical meteors which may be found in the less observable regions of the apparent distribution. The allowable variation of the combined weighting factor may be increased for larger sample sizes.

8.2.2 Atmospheric Interaction Selection

With the assumptions that,

(a) the probability of detection of a meteor is proportional to the receiver output voltage,

(b) the majority of meteors are observed near the point of maximum ionization,

(c) the number of meteors with a mass greater than m is given by $N(m) \propto m^{1-s}$ where $s \sim 2$, so that despite the

detection probability of assumption (a) the majority of meteors observed will have masses near the lower limit of the observable mass range,

we may write

$$\alpha_{max} = V_{max}^{\eta} \cdot F(\eta)^2 \cdot (1 + 2\,F(\eta)^{-3}) \cdot \cos\chi$$

$$F(\eta) = 1 + 3(2 + \eta)\xi/V_\infty^2 \qquad \text{(Weiss, 1958)}, \tag{8.4}$$

where V_∞ is the velocity of the meteor above the atmosphere, χ is the zenith angle of the radiant and ξ is the ablation energy per unit mass of the meteoroid (taken as 30 $km^2\ sec^{-2}$ after Jacchia (1949)).

For Lovell-Clegg scattering (the case in which the trail electrons are assumed to act independently of each other) the power at the receiver from an infinitely long trail is given by

$$P_R = \frac{\alpha^2 P_T G_R G_T \lambda^3}{32\pi^2 R_o^{\,3}} (e^2/mc^2)^2 \tag{8.5a}$$

and for persistent scattering (in which the trail electron line density is sufficiently great to give reflections as from a "metallic" cylinder which expands through diffusion) by

$$P_R = \frac{\alpha^{\frac{1}{2}} P_T G_R G_T \lambda^3}{54\pi^3 R_o^{\,3}} (e^2/mc^2)^{\frac{1}{2}} \tag{8.5b}$$

where e and m are respectively the charge and mass of the electron and c is the velocity of light. The transition between the two types of scattering occurs in the region of $\alpha = 10^{12}$ electrons/cm, so that both forms of scattering will contribute significantly to the numbers of meteors detected with the Adelaide system.

When ambipolar diffusion is taken into account, the power received from an underdense trail formed up to the point x_1 is given by the expression

$$P_R = \frac{P_T G_T G_R \lambda^3}{32\pi^2 R_o^3} \alpha^2 \left(\frac{e^2}{mc^2}\right)^2 \cdot \exp\left\{-2\left(\frac{2\pi r_o}{\lambda}\right)\right\} |I|^2 \qquad (8.6)$$

(Simek, 1968)

where r_o is initial trail radius, and

$$I = \frac{1}{\sqrt{2}} \int_{-\infty}^{x_1} \exp\left(-\tfrac{1}{2} i\pi x^2\right) \cdot \exp\left\{-\nabla(x_1 - x)\right\} dx \qquad (8.7)$$

with

$$\nabla = \frac{8\pi^2 D \sqrt{R_o}}{v\lambda^{3/2}} . \qquad (8.8)$$

D is the coefficient of ambipolar diffusion. In the absence of diffusion (D = 0 in eqn 8.8), I reverts to the classical form of the fresnel integral (§3.3.2).

Since the criterion for orbit determination in the present survey is that the diffraction pattern should be discernable rather than that the entire received power be above a limiting amount we may safely disregard diffusion for the determination of the physical weighting factor for the majority of echoes for the reasons outlined in §3.3.5. It has been suggested though (§8.3.1) that a small number of echoes from the upper end of the height range are lost through diffusion preventing the recording of sufficient doppler information.

The initial radius of a meteor trail decreases with increasing atmospheric density and increases with meteor velocity. For a meteor with velocity 40 km sec^{-1} at 95 km height the initial radius of the trail

is of the order of 1 metre (Kashcheev and Lebedinets, 1963; Bayrachenko, 1965). The majority of meteors are detected at Adelaide in the vicinity of 90 km height, and with λ = 11 metres the influence of initial trail radius on received signal power is quite significant.

Thus we may rewrite eqn 8.6 (following Lebedinets and Kashcheev, 1967) as

$$P_R = \frac{P_T G_R G_T \lambda^3}{32\pi^2 R_o^3} \left(\frac{e^2}{mc^2}\right)^2 |I|^2 \alpha_{eff}^2 \qquad (8.9)$$

where

$$\alpha_{eff} = \alpha \exp\left\{-\left(\frac{2\pi r_o}{\lambda}\right)^2\right\} \qquad (8.10)$$

It is apparent from eqn 8.10, considered in the light of the assumptions listed at the beginning of this section, that the variation of initial trail radius with height will impose a selection effect against the detection of fast meteors in the upper regions of the meteor height range. No attempt has been made to correct the distributions presented for this effect. Reference to Fig. 8.1, which gives the observed meteor velocity distribution as a function of height shows that orbit distributions for the present data will not be sensitive to this selection effect.

In the present survey amplitude measurements have not been determined to date and a further assumption is made that the receiver power for each echo is the minimum detectable, P_{min}. The values of $\alpha_{eff.}$ thus calculated are normalised using eqn 8.4 to an equivalent meteor of velocity 40 km sec^{-1}. The normalized received power P_n which

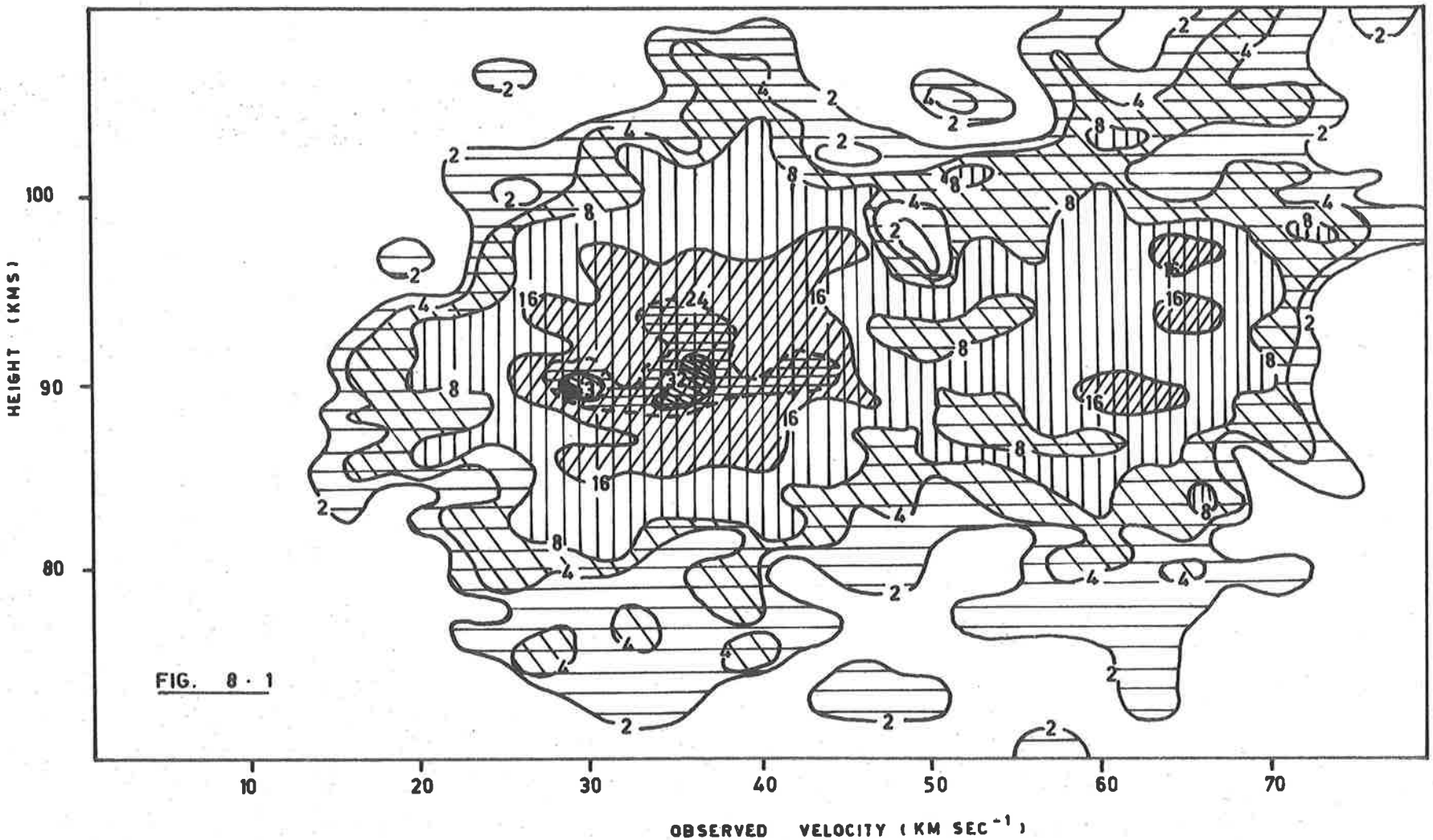
HEIGHT (KMS)
100
90
80
10
20
30
40
50
60
70
OBSERVED VELOCITY (KM SEC^{-1})

FIG. 8 · 1

may then be calculated is used to determine the weighting factor

$$W(\alpha_{eff}, V_\infty) = \left(\frac{P_n}{P_{min}}\right)^{\frac{1}{2}} .$$

Distributions have been calculated for values of $\eta = 0,2,4,5$. Several independent evaluations of η (Whipple, 1955; Hawkins, 1956; Weiss, 1957b; Verniani and Hawkins, 1964) suggest a value between 3.5 and 5.

8.2.3 Fragmentation

As mentioned in §6.4 fragmentation does not seem to be pronounced for the meteors observed. Without individual amplitude measurements it is not possible to determine whether trails are as long as would be expected theoretically. Difficulties with the operation of the long-distance South station prevent useful comparison of the (low) echo rate at this station with those at other stations. All echoes were recorded by triggering from the main station equipment.

At least we can say that fragmentation does not impose any significant selection effect on the survey. Use of the pre-t_o diffraction waveform rather than the more commonly used post-t_o pattern will render fragmentation less important, since progressive degeneration of the waveform will to some extent be matched by increasing length of the fresnel half-period zones in our case. There will also be a tendency for the diffraction information to come from earlier portions of the trail where fragmentation will be less advanced. Only in a very few cases has the pre-t_o diffraction pattern become progressively degraded towards lower order fresnel zones, while still being followed by large amplitude wind doppler information.

8.3 DISTRIBUTIONS WITH REFLECTION POINT HEIGHT

8.3.1 A Possible Velocity-Height Selection Effect

For an echo to be reduced in the present survey the radar range information and at least 1½ cycles of doppler for determination of reflection point position are required to be present in addition to at least 7 diffraction extrema on each of at least three of the 5 velocity recording traces. Nilsson (1962) in discussing the analysis of the data from the 1961 Adelaide survey suggests that there may be a selection effect against high velocity meteors being reduced since these tend to reach maximum ionization at greater heights, diffusion then being sufficiently rapid to prevent the recording of the necessary 1½ doppler cycles.

Fig. 8.1 shows the observed distribution of reflection point heights as a function of measured velocity. The solid contours represent changes in number density by factors of two, and the magnitudes denote the numbers of meteors in a region of 2 km extent in height and 4 km sec^{-1} in velocity.

The distribution suggests an increase in the mean reflection point height from 90 km for meteors of velocity 30 km sec^{-1} to 93 km in height for those with velocity near 65 km sec^{-1}. It is not possible to determine to what extent the observed distribution has been affected by a diffusion rate selection effect. It should be emphasized that a selection effect of this type would operate on the meteoroid velocity only indirectly, since it is the inability to observe sufficient body doppler

rather than inability to measure the diffraction waveform which prevents recovery of the data in these cases. Certainly use of the pre-t_o diffraction pattern available in a c.w. system enables reduction of echoes quite easily in the presence of diffusion rates which would make analysis of the post-t_o pattern from a conventional radar system virtually impossible.

8.3.2 Underdense and Persistent Echoes

In order to determine any differences in the properties of the various mass ranges of meteors contributing to this survey an attempt has been made to distinguish the meteors producing trails with underdense electron line densities from those producing overdense trails. Echoes have been divided into three classes, depending upon the nature of the doppler waveform envelope after the t_o point. Those echoes exhibiting rapid and immediate amplitude decay have been classified as underdense while those with persistent or increasing amplitudes after this point are classified as overdense. A small number of echoes will less definite intermediate characteristics have been denoted intermediate to signify this.

Fig. 8.2 shows the distribution with reflection point height for all meteors separated into these three groups. There is a slight trend apparent for the maximum at 92 km for the underdense (and overall) distribution to move to a lower height (near 90 km) for the overdense echoes. This is to be expected and is apparently a result of the variation of the rate of ambipolar diffusion as a function of height.

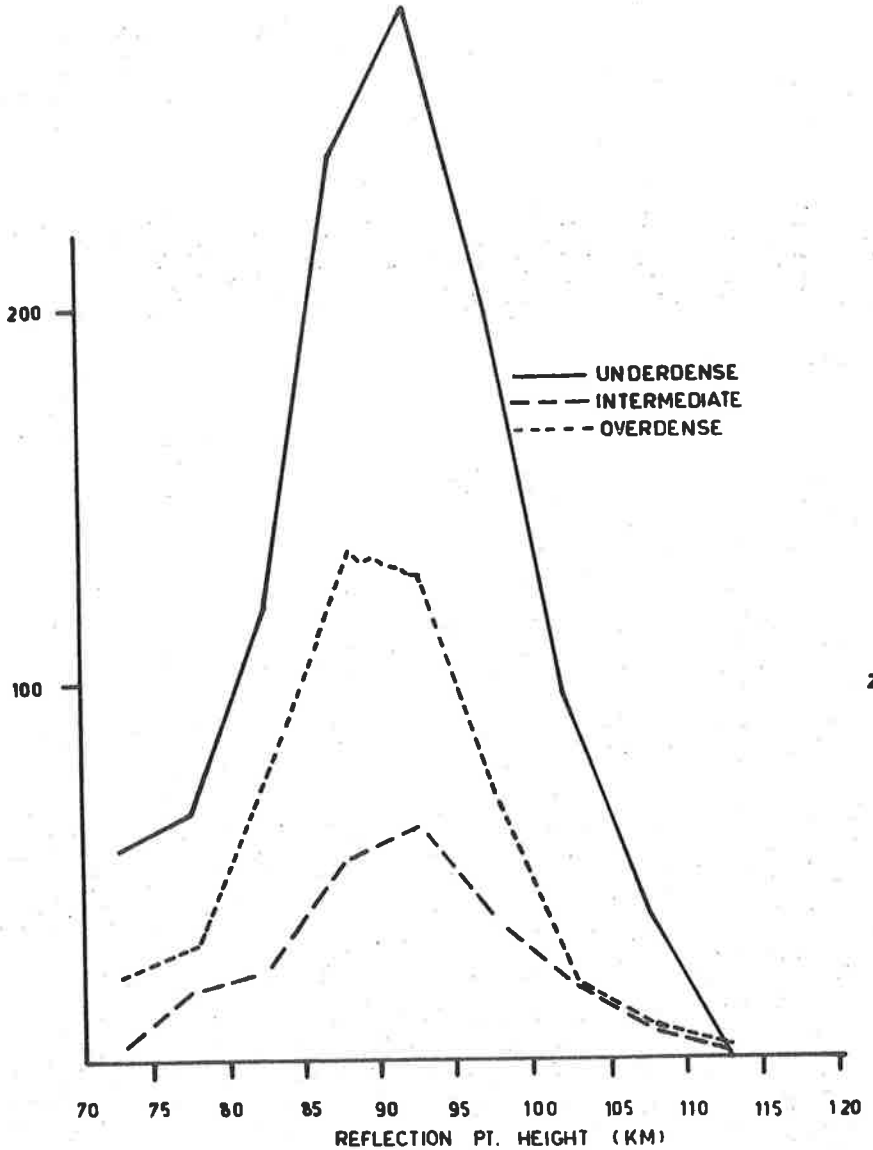

FIG. 8 · 2 OBSERVED DISTRIBUTION OF REFLECTION POINT HEIGHT FOR ALL METEORS

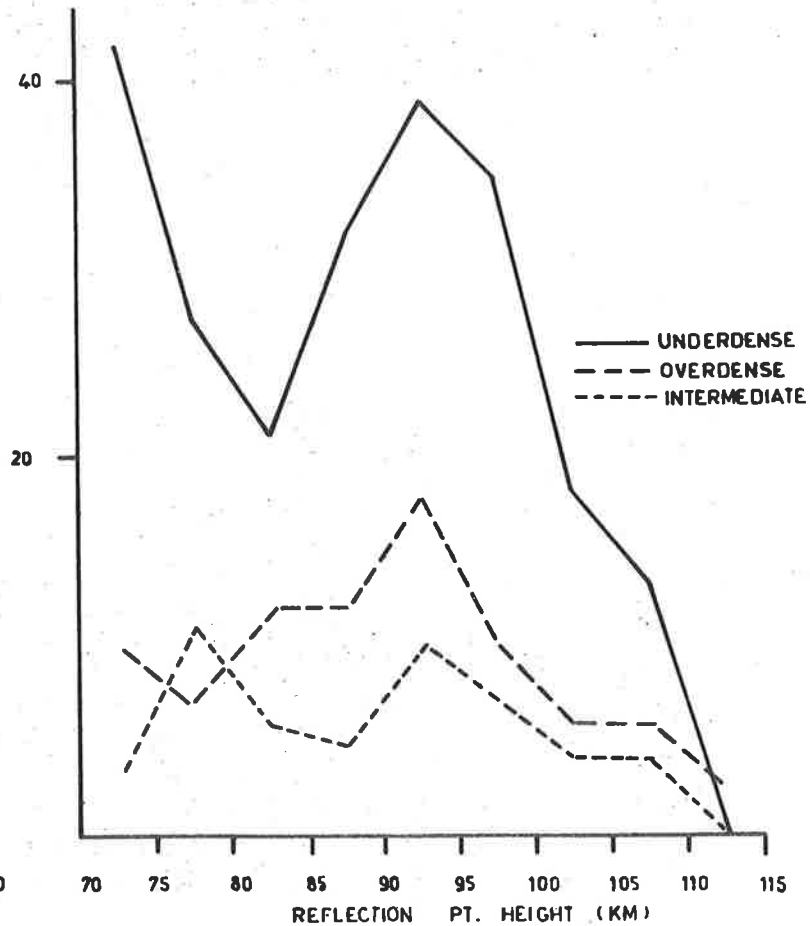

FIG. 8 · 3 OBSERVED DISTRIBUTION OF REFLECTION POINT HEIGHT FOR METEORS WITH HYPERBOLIC

8.3.3 Hyperbolic Meteors and a Check on the Atmospheric Retardation Correction

Fig. 8.3 shows the distribution of reflection point height for hyperbolic meteors only. Comparison with Fig. 8.2 indicates an anomalously high proportion of hyperbolic meteors at low reflection point heights, indicating that the retardation correction for these meteors may have been too great, and suggesting that estimates of surface area/mass ratio for these particles are too large. The larger number of over-corrected meteors amongst those producing underdense trails compared with the numbers for overdense trails is consistent with the observed mass-density variation discussed in §6.4.

8.4 RADIANT DISTRIBUTIONS

For the faint radio meteor population observed in the present survey there is no evidence to suggest that the sporadic meteors may have originated in a manner distinct from the stream component. The systematic stream search described in §7 has detected streams of undoubted significance amongst all known classes of orbits except those of low inclination with a <1. a.u. The lack of streams detected in this class of orbit is not surprising in view of the low probability of detection of orbits of this type.

The radiant distributions presented have therefore been determined for all of the meteors observed, rather than for the sporadic meteors only. The radiant distribution for stream meteors has been determined separately and is presented in Fig. 8.4. Each stream is represented by a number indicating the number of meteors in the association located at

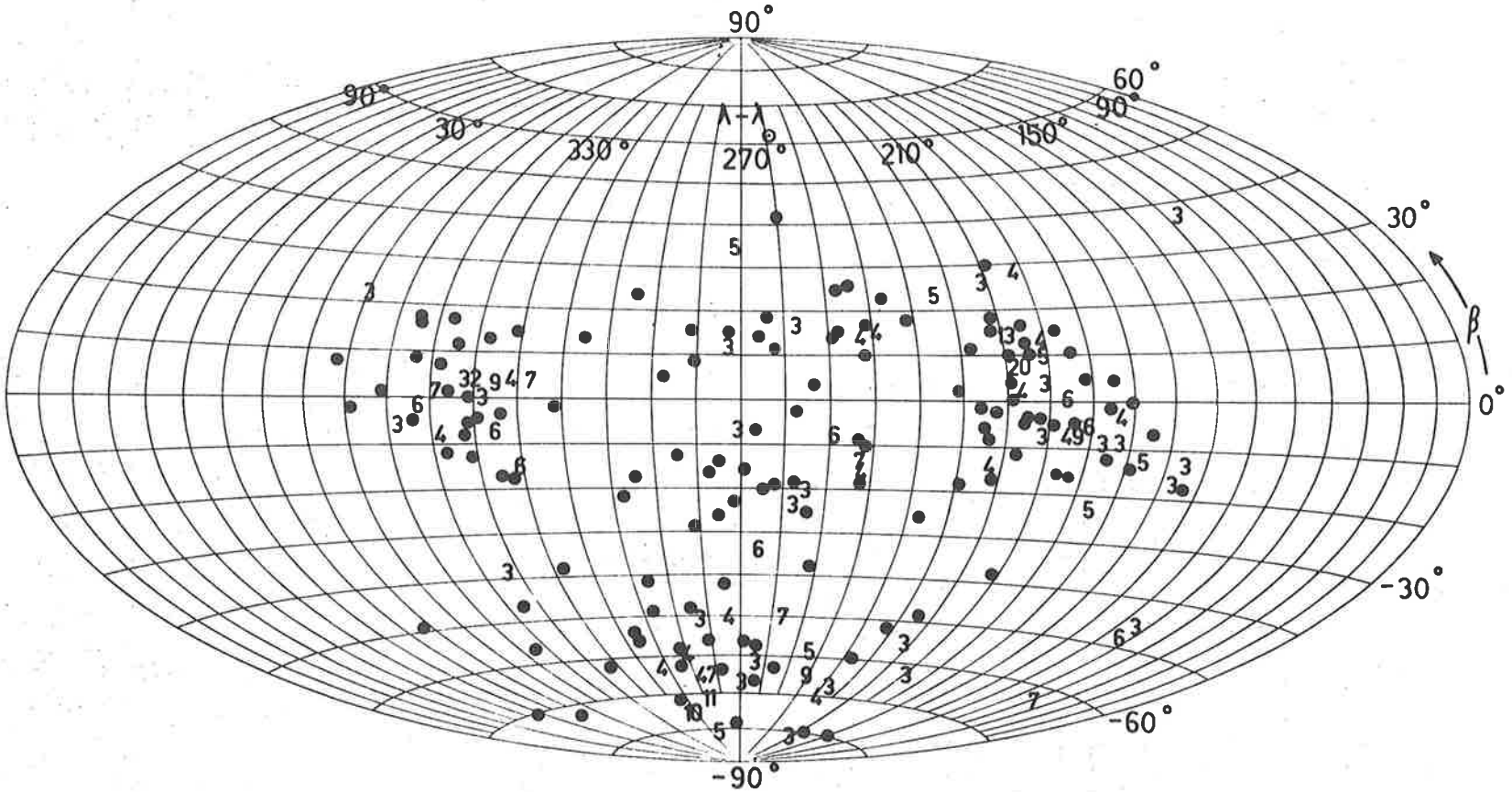

FIG. 8 · 4 RADIANT DISTRIBUTION FOR STREAM METEORS. DOT INDICATES PAIR OF METEORS. LARGER STREAMS REPRESENTED BY NUMBER OF MEMBERS.

the mean radiant position. Associations of pairs only are represented by a dot. The distributions, in ecliptic latitude and longitude relative to the longitude of the Sun, are presented on Aitoff's equal area projection of the sphere. All radiants have been corrected for zenith attraction.

It is apparent that the distribution of associated pairs in Fig. 8.4 is similar to that for larger associations. Comparison with Fig. 8.5 clearly shows the similarity between the stream radiant distribution and the observed geocentric radiant distribution for all meteors. Fig. 8.6 is a composite, comparing the Southern Hemisphere of the observed geocentric distribution of Fig. 8.5 with the Northern Hemisphere of the geocentric radiant distribution, corrected for antenna selectivity, of sporadic meteors detected at Havana, Illinois, during the period January - August, 1962 (Elford, Hawkins and Southworth, 1964). The high degree of symmetry about the equator is clearly apparent. It is interesting to note that the high latitude concentration in the Northern Hemisphere is displaced slightly in the antisolar direction from the longitude of the Apex, corresponding to a similar displacement of the equivalent Southern Hemisphere concentration towards the longitude of the Sun. Both surveys tend to favour the same months of observation. The distributions for individual months for the Havana data show considerable variation in the high latitude region and cast some doubt on the statistical significance of the displacement of the combined maximum from the longitude of the Apex. A search for this effect in data from additional surveys as

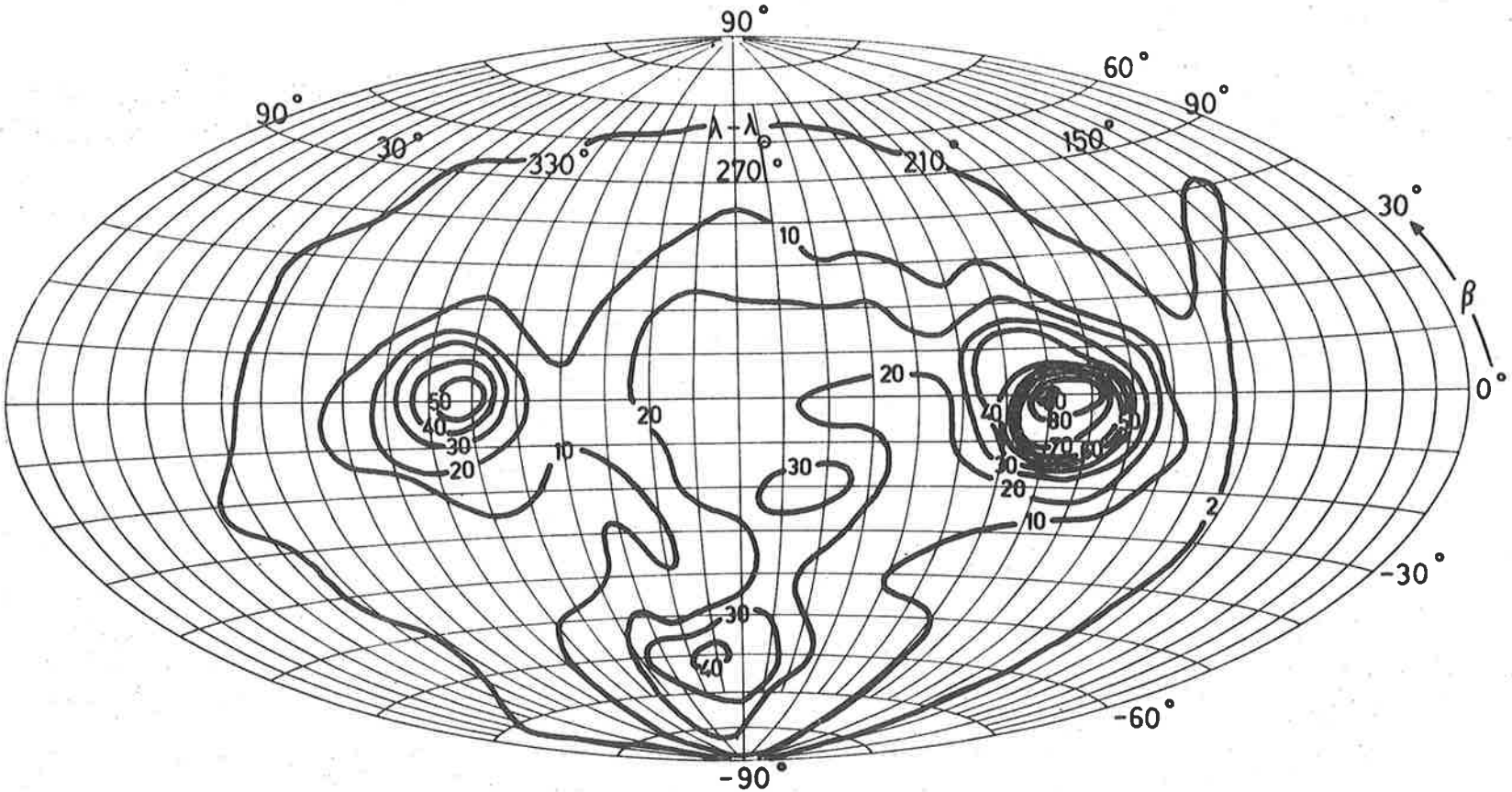

FIG. 8 · 5 OBSERVED GEOCENTRIC RADIANT DISTRIBUTION.

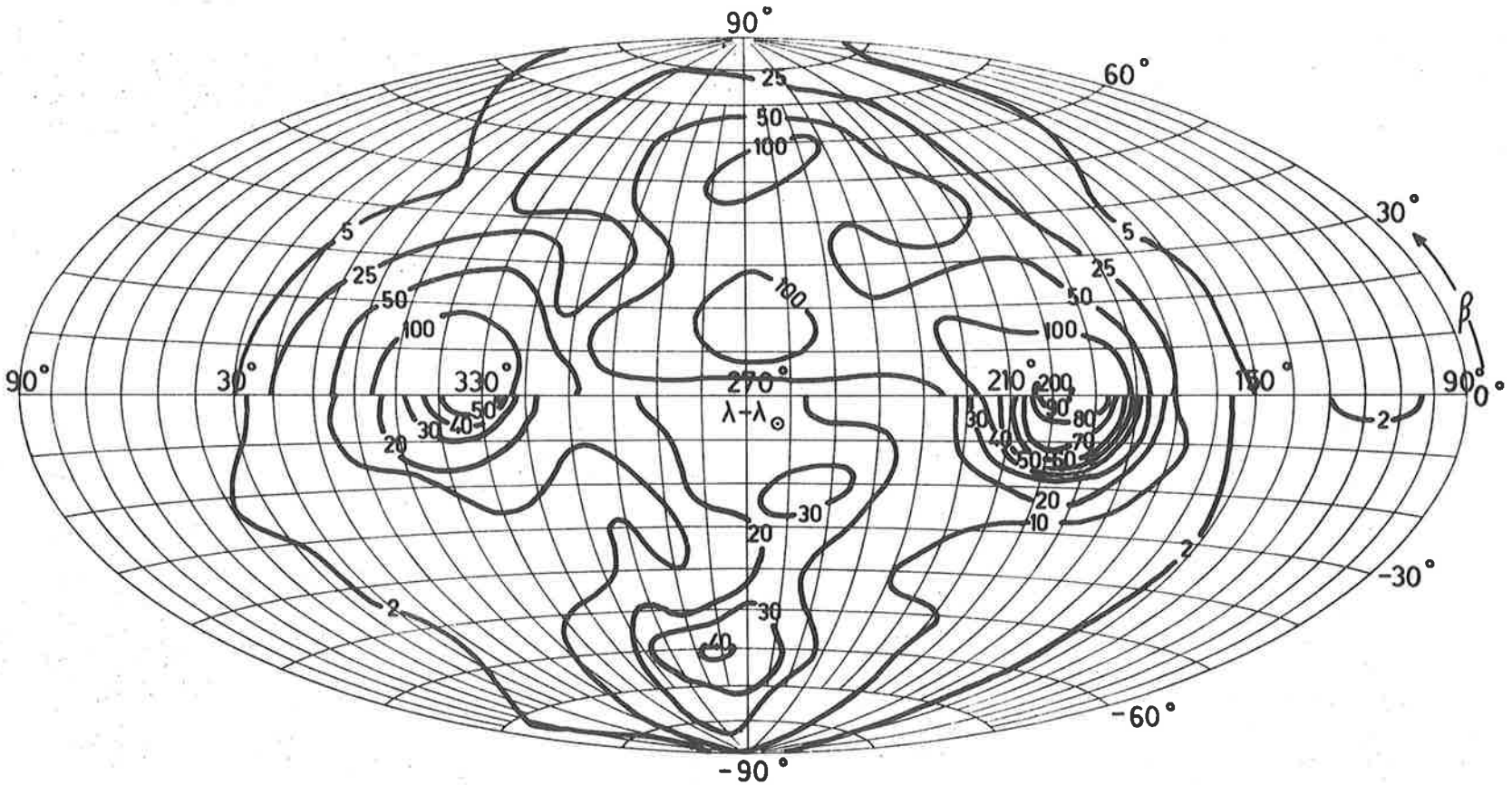

FIG. 8 · 6 A COMPOSITE, COMPARING NORTHERN HEMISPHERE DATA OF ELFORD, HAWKINS AND SOUTHWORTH (1964) WITH SOUTHERN HEMISPHERE OF FIG. 8 · 5.

well as for the remaining months of the year would be necessary to ascertain its reality.

It should be noted that there are some differences in the methods of obtaining the two distributions contributing to Fig. 8.6. Whereas the Adelaide distribution is purely as observed, without any form of correction, the Havana data has been corrected for antenna selectivity and weighted to compensate for the dependence of the duration of observability as a function of radiant declination.

In general the operating periods at Adelaide have been continuous on a 24 hour basis for durations of 6 to 10 days per month. Since the system has low gain all-sky aerials the duration of operation effectively averages the antenna selectivity and makes further correction to the distribution purely a function of radiant declination. Thus the uncorrected distribution for Adelaide will tend to emphasize the high latitude component for which the radiants are continuously visible.

A further difference in the distributions as projected is apparent. That for the Havana data has been determined by summing the weighted data over a circular area of 15° in diameter at intervals of 5° in latitude and longitude. Thus although the distribution has been presented in the form of contours on Aitoff's equal area projection of the sphere the contours represent number densities per area in multiples of square degrees rather than a true equal area distribution as implied by the projection. The distributions for the Adelaide data are true equal area representations, having been calculated similarly by averaging over a

a constant area, but in this case after projection, corresponding to a circle of 15° diameter at the Apex.

Thus the presentation of the Havana data underemphasizes the strength of the high latitude concentration, whereas the observed distribution for the Adelaide data tends to overemphasize the high latitude concentration.

Fig. 8.7 shows the diurnal variation in echo rate for the present survey. The solid line curve represents all echoes from the main station with range information and sufficient doppler for wind analysis. The broken line curve represents those multistation echoes for which velocity measurements were available. Comparison of the two curves shows a depression of the day-time multistation echo rate and a resultant shift in the times of occurrence of the rate maxima and minima. This depression, apparently caused by local day-time interference, accounts for the major portion of the difference in strengths between helion and antihelion ecliptic radiant concentrations. Reference to Figure 8.4 shows the same disproportion amongst the observed stream meteors.

Figs. 8.8(a) and (b) show the geocentric radiant distributions corrected for observational, and observational plus astronomical selection, both for $\eta = 5$. It is apparent that the weak Apex concentration of Fig. 8.5 is a result of observational selection. The high latitude concentration, on the other hand, is clearly real. The strong contribution of short-period orbits to this concentration is demonstrated by the differences between Figs. 8.8(a) and (b).

Figs. 8.9(a), (b) and (c) show the observed and corrected heliocentric radiant distributions. These are the distributions which would

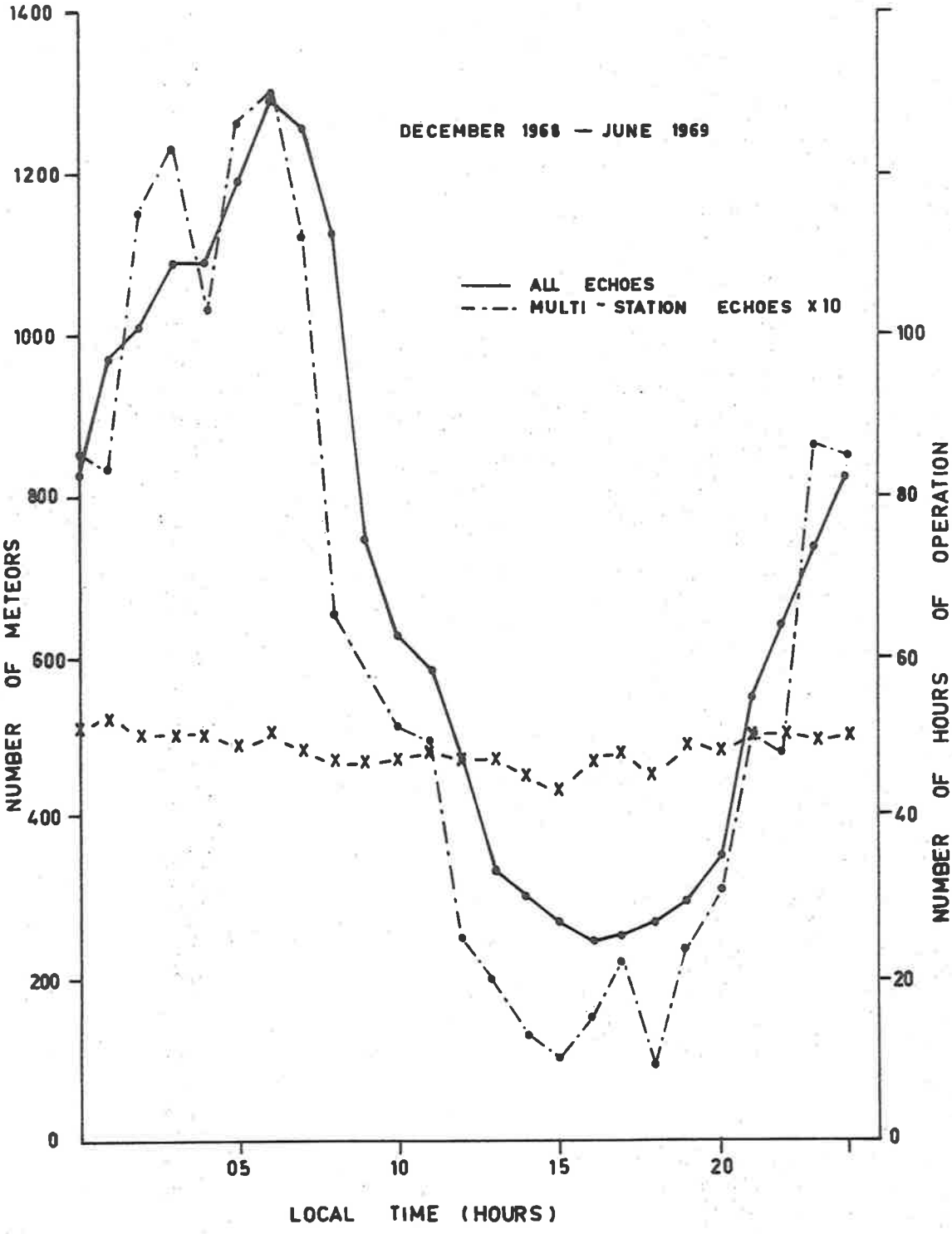

FIG. 8 · 7 : The diurnal variation in meteor rate for all echoes, and for multi-station echoes. The crosses show the number of hours of operation of the equipment for each hour of local time.

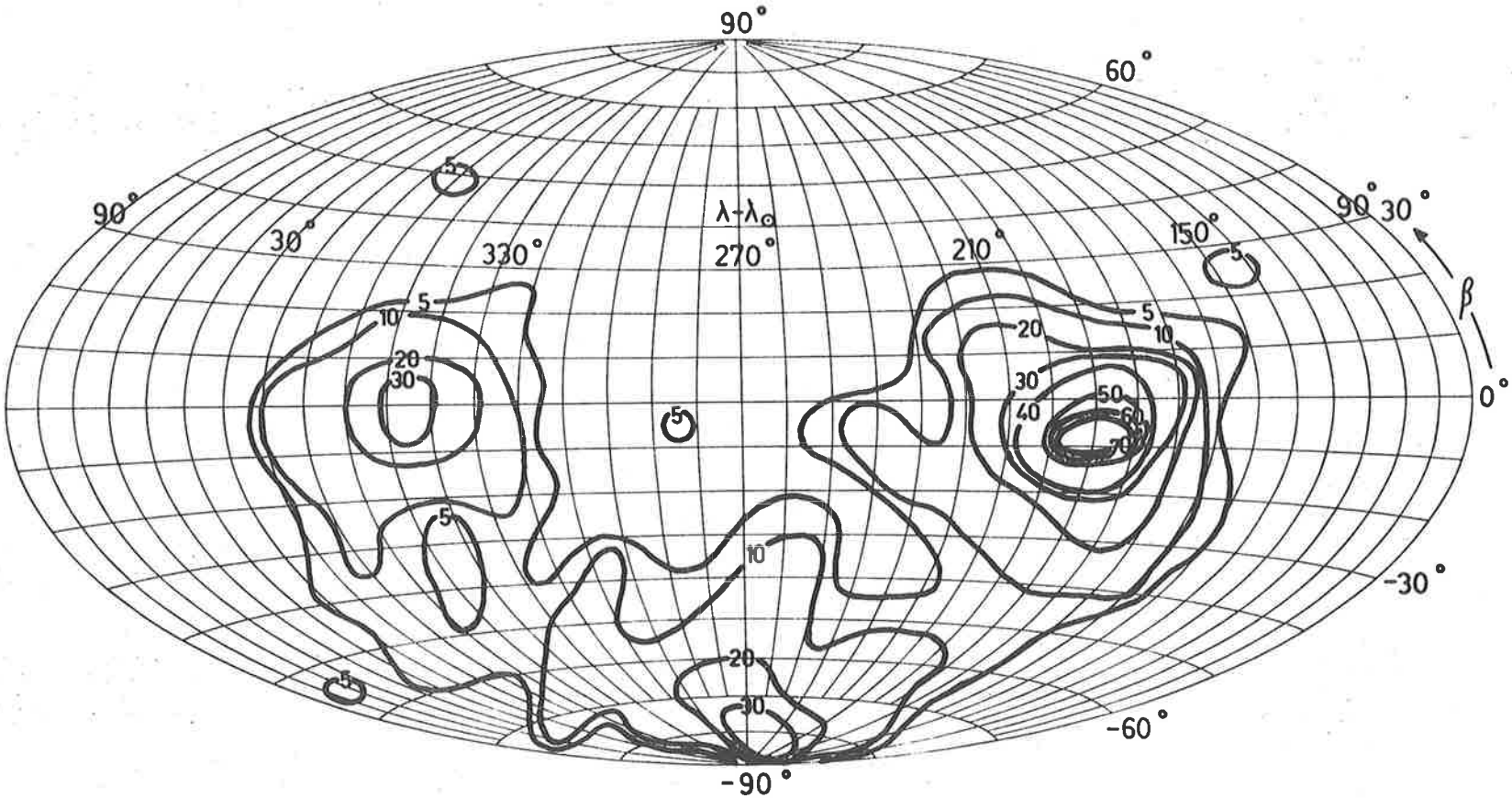

FIG. 8 · 8 (a) GEOCENTRIC RADIANT DISTRIBUTION CORRECTED FOR OBSERVATIONAL SELECTION ASSUMING $\eta = 5$.

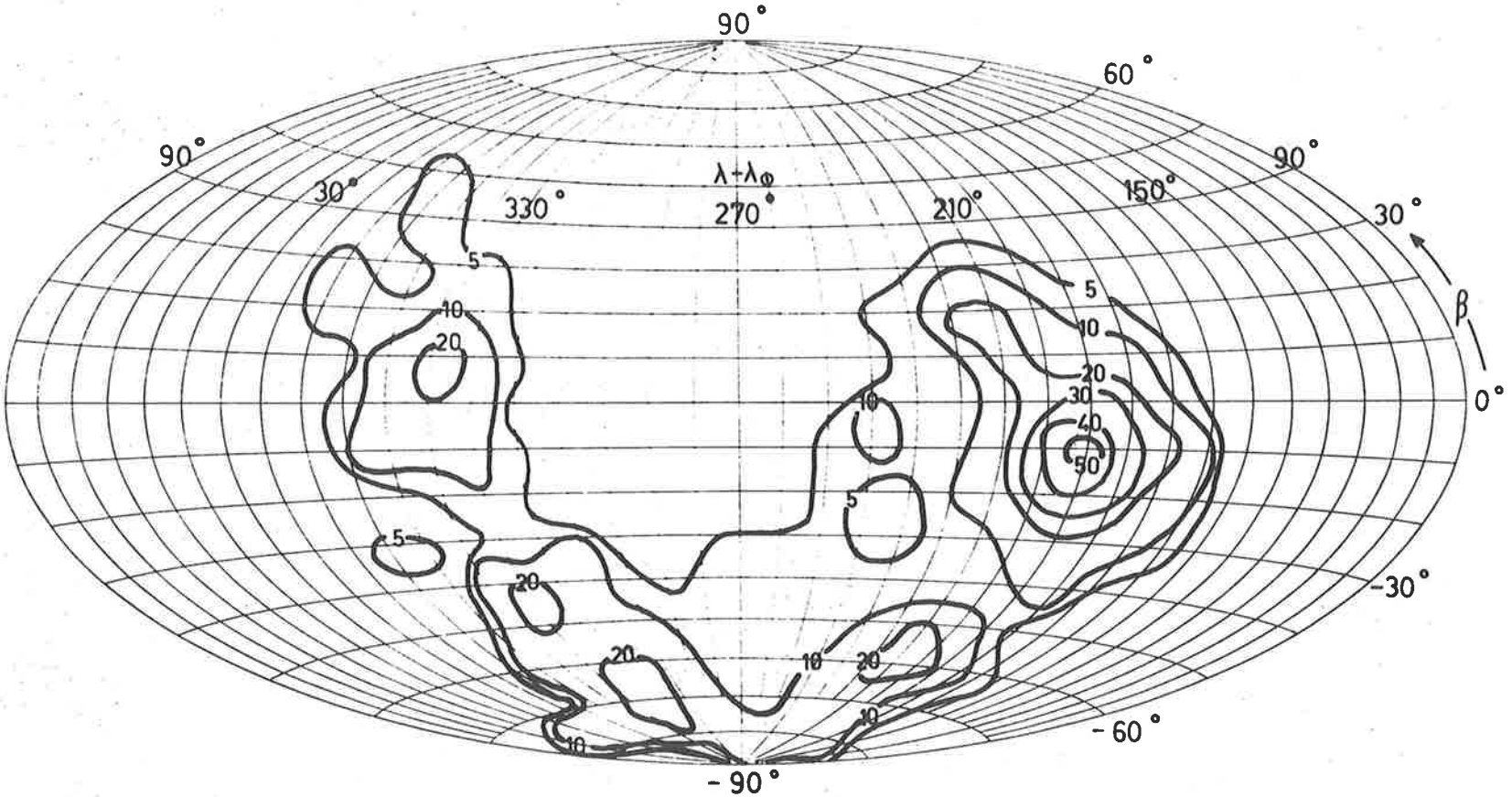

FIG. 8 · 8 (b) GEOCENTRIC RADIANT DISTRIBUTION CORRECTED FOR OBSERVATIONAL AND ASTRONOMICAL SELECTION ASSUMING $\eta = 5$.

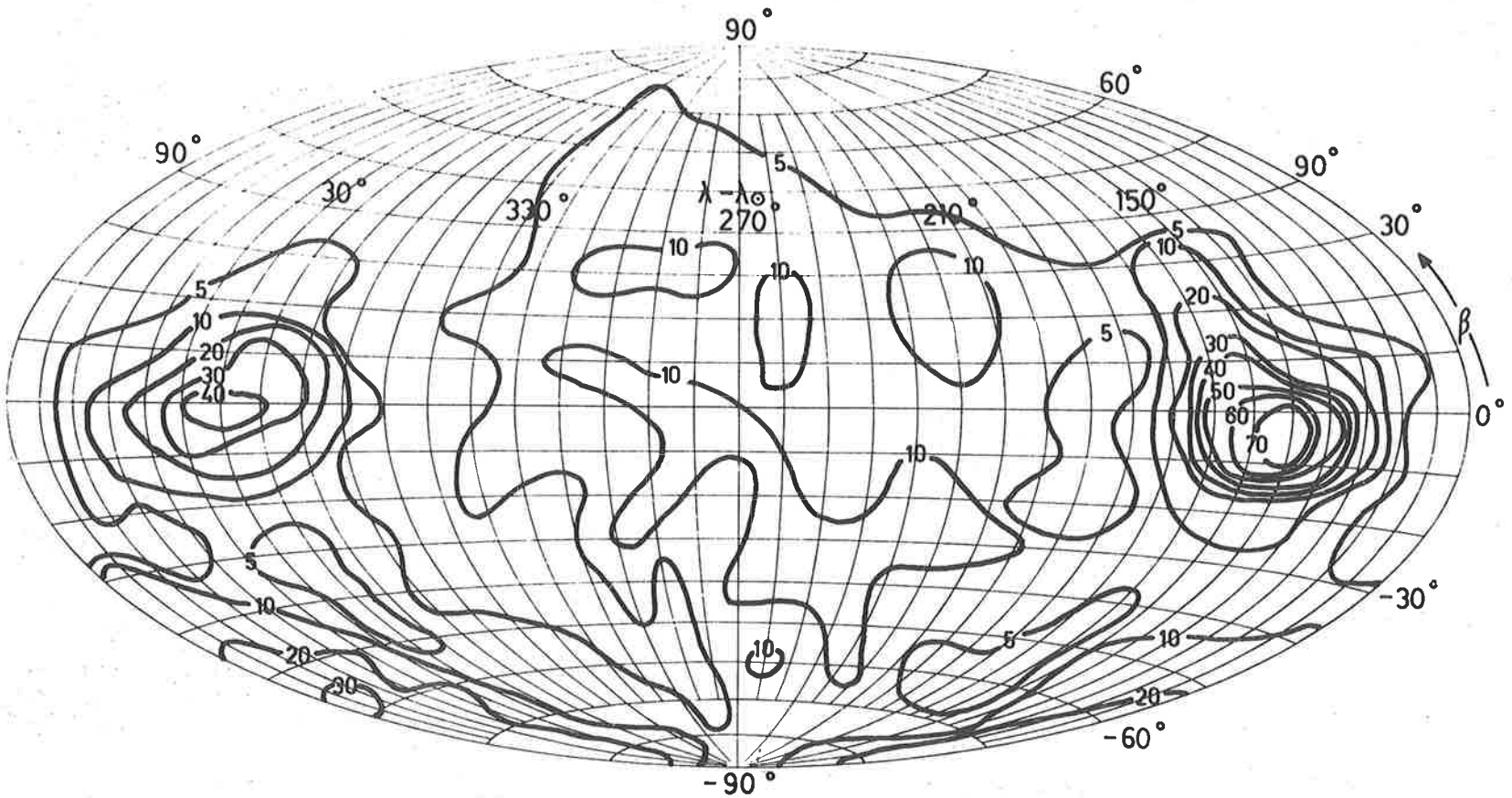

FIG. 8 · 9 (a) OBSERVED HELIOCENTRIC RADIANT DISTRIBUTION.

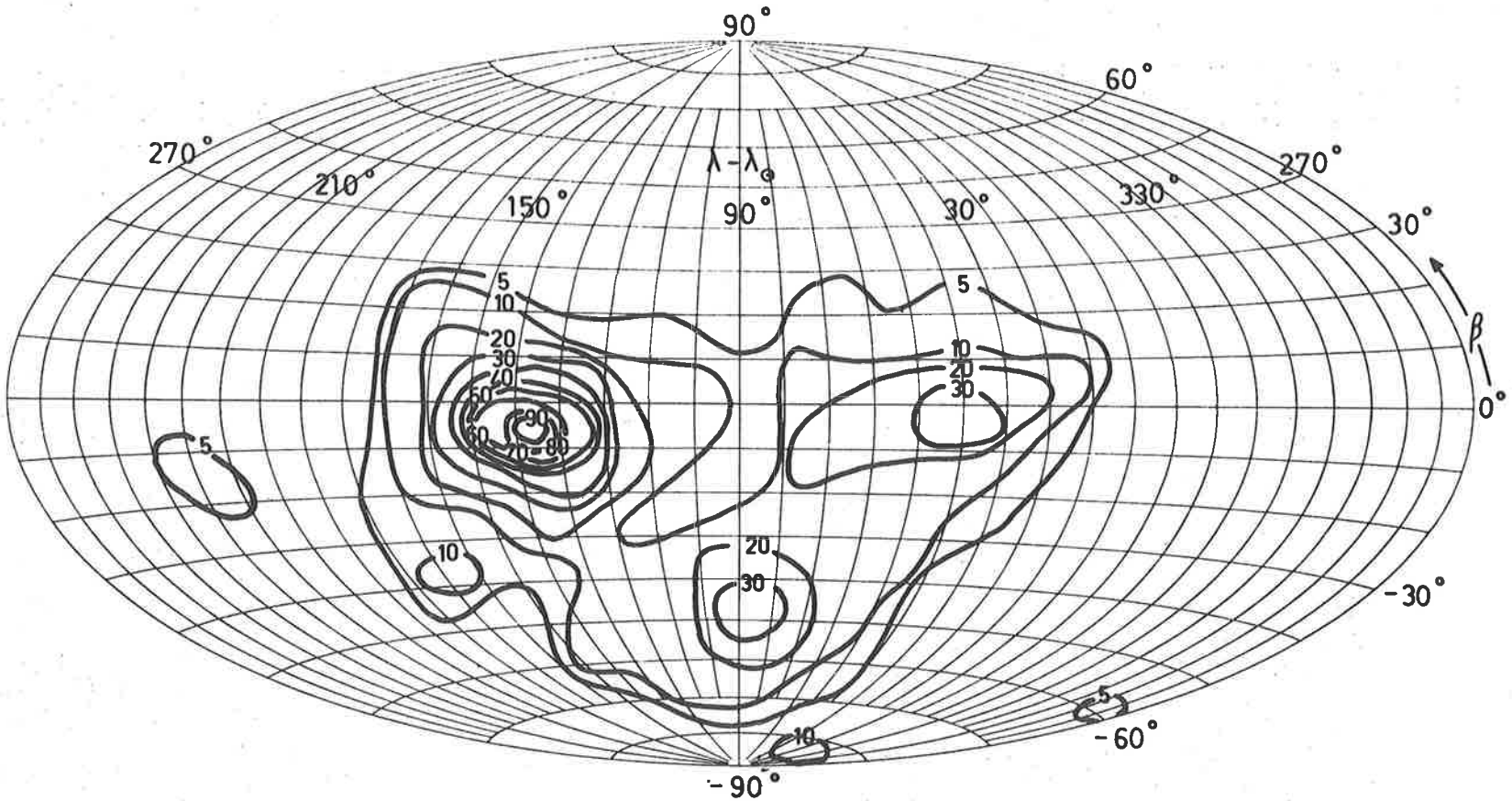

FIG. 8·9 (b) HELIOCENTRIC RADIANT DISTRIBUTION CORRECTED FOR OBSERVATIONAL SELECTION ASSUMING $\eta = 5$.

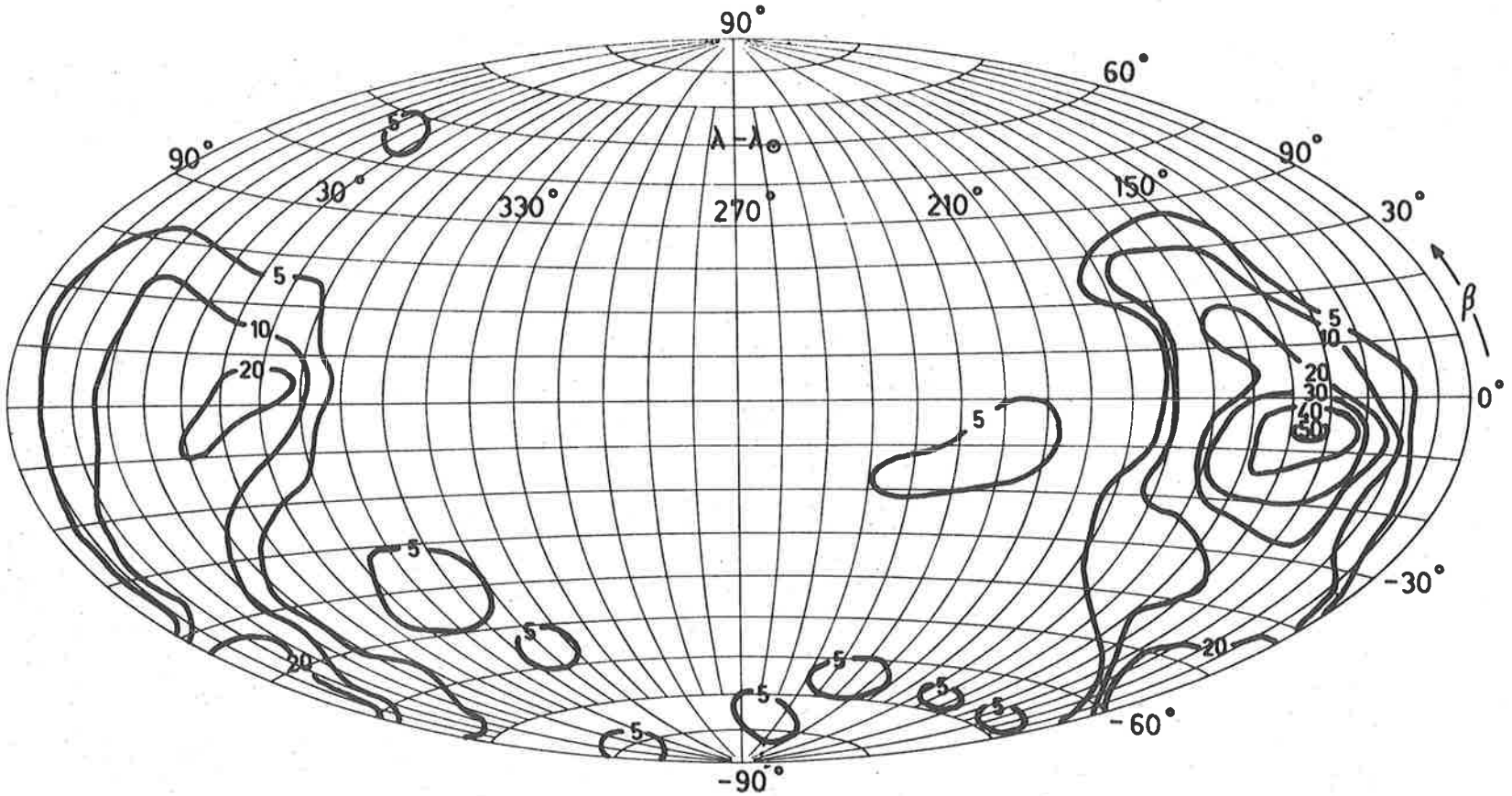

FIG. 8 · 9 (c) HELIOCENTRIC RADIANT DISTRIBUTION CORRECTED FOR OBSERVATIONAL AND ASTRONOMICAL SELECTION ASSUMING $\eta = 5$.

be seen from Earth if Earth were stationary and of zero mass (Hawkins, 1962). It should be noted that while Figs. 8.9(a) and (c) are centred on the Apex, Fig. 8.9(b) is centred on the Antapex for comparison and ease of interpretation.

The weak extended distribution of retrogade meteor radiants shown in Fig. 8.9(a) almost vanishes (Fig. 8.9(b), (c)) when account is taken of observational selection. Whilst comparison with the orbits of short period comets indicates that this might be expected amongst those meteors with orbits near the ecliptic plane, the relative lack of retrograde orbits amongst the meteors with high latitude radiants is more surprising. The significance of this is discussed in §9.

8.5 VELOCITY DISTRIBUTIONS

The meteor velocity is determined by combining the range information with a measure of the scale of the fresnel diffraction pattern from the film record, as outlined in §5. Before considering velocity distributions it is of interest to consider the diffraction data from film reading alone for estimation of film reading selection effects and errors. The quantity (x/t) is the slope of the best fit straight line to the data points obtained from the relative positions of diffraction extrema in film reading, in arbitrary units (see §5.2). Fig. 8.10 compares the distribution of observed values of this function for the present survey and the 1961 Adelaide survey.

The 1961 data contains 2000 echoes compared with 1667 for the present data. While a dip at 0.85 occurs on both curves the ratio of

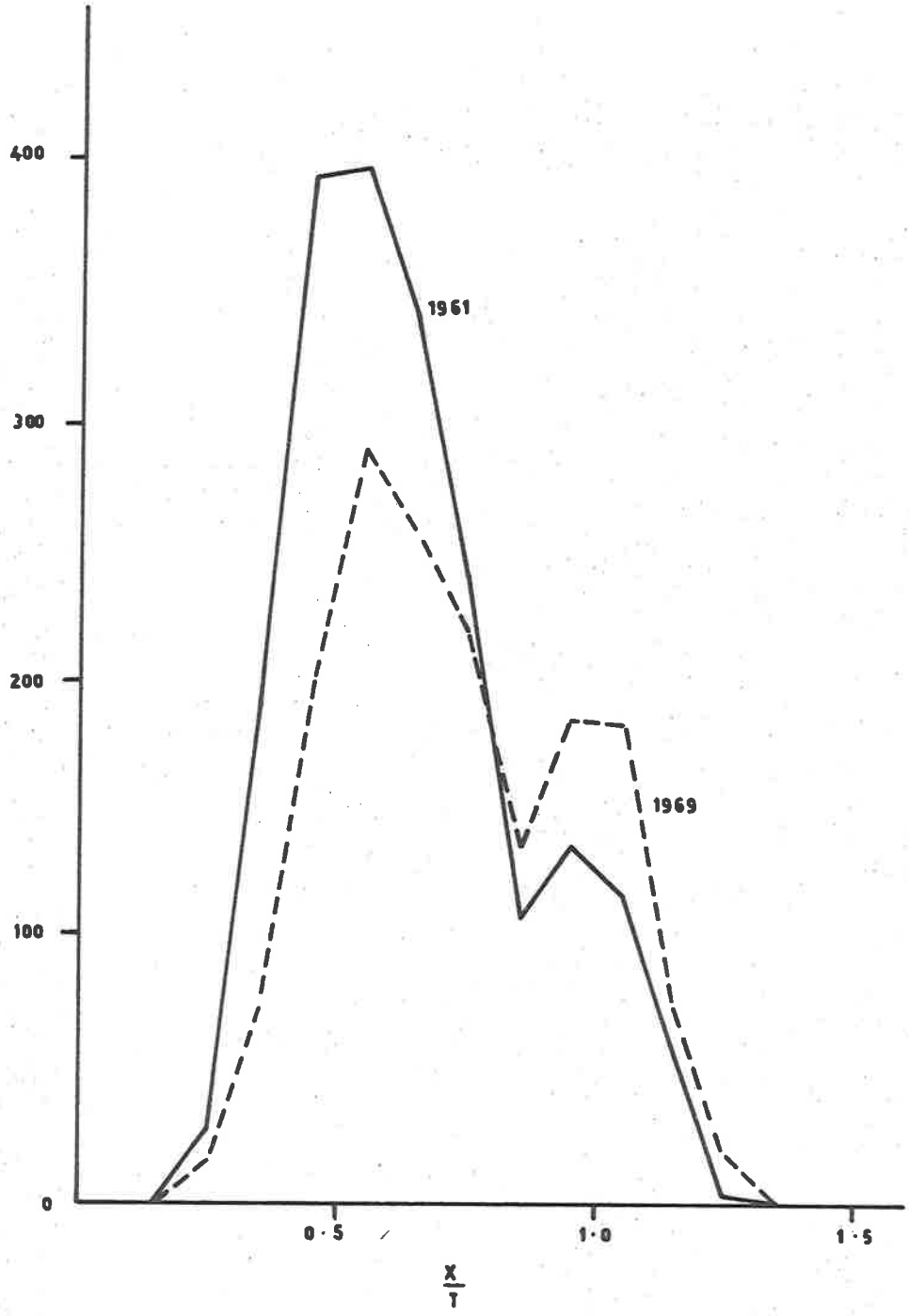

FIG. 8·10 DISTRIBUTION OF $\frac{X}{T}$

the high velocity component to the low is markedly higher for the present survey. The reason for this seems to be a selection effect in the film reading process rather than of astronomical origin. Subjectively the difference seems to be due to a greater facility to recognize and reduce the higher frequency waveforms than the lower frequency ones in the presence of noise. This effect may compensate in part for the height-diffusion selection effect already discussed. No attempt has been made to correct the observed distributions for either of these effects.

Fig. 8.11 shows the distributions of R.M.S. deviation in x/t for each trace for a sample of echoes from the February data. The x/t values contributing to Fig. 8.10 are the weighted means of at least three of the x/t values for individual traces. Thus the R.M.S. deviations of Fig. 8.11 will be an upper limit for those of the values contributing to Fig. 8.10. Fig. 8.11 also illustrates clearly that the data transmitted over the telemetry links from the North and Sheedys outstations was of similar quality to that from the main station receiver. The particularly severe interference problems encountered with the Direk outstation equipment are reflected in the higher mean value of the R.M.S. deviation for that channel.

Fig. 8.12(a) shows the observed frequency distribution of meteors with geocentric velocity compared with the distribution for the 1961 survey. This figure reflects the trend displayed in Fig. 8.10. Figs. 8.12(b) and (c) show the geocentric velocity distributions with various corrections for selection effects. It is apparent that the peak near 65

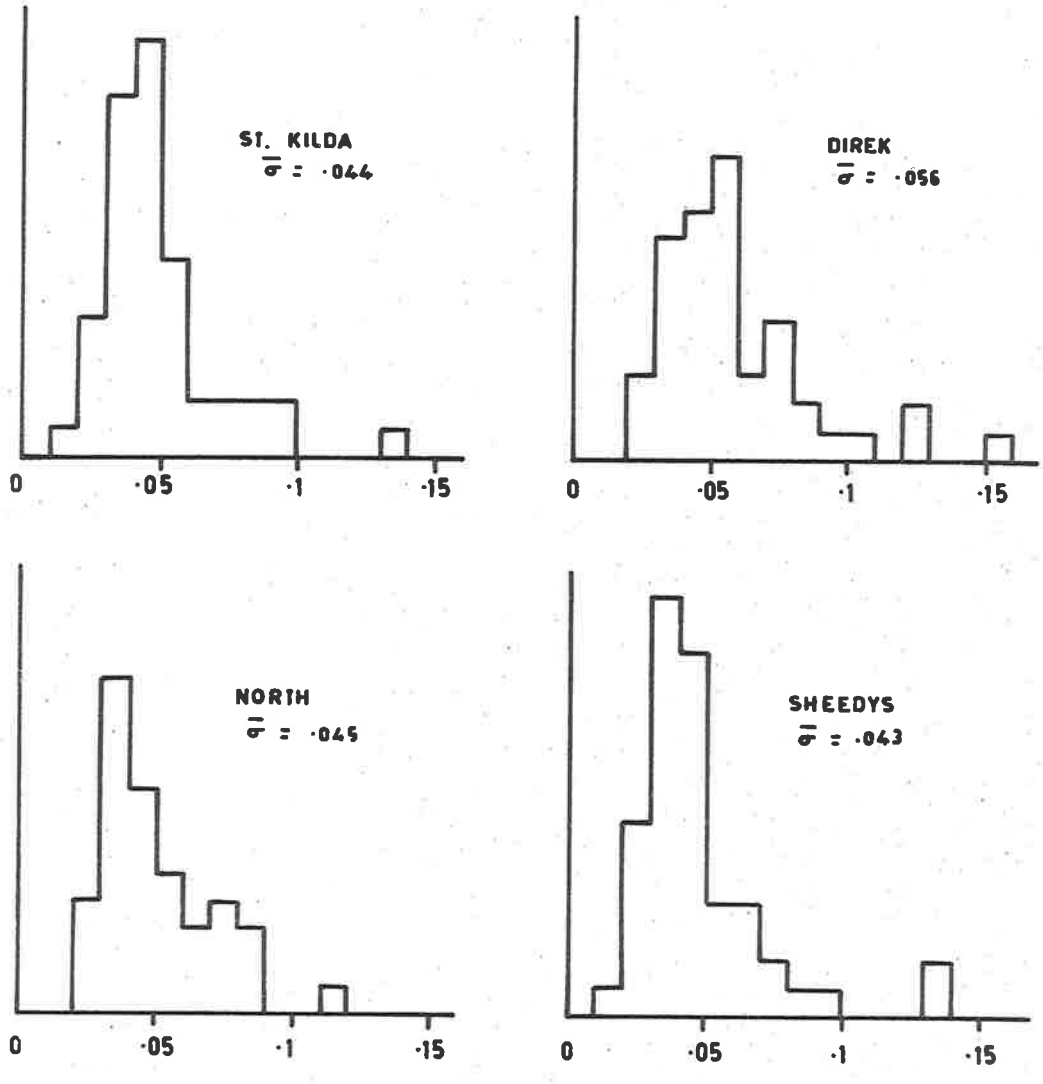

FIG. 8·11 DISTRIBUTIONS OF R.M.S. DEVIATION IN $\frac{X}{T}$ FOR THE BEST FIT LINES TO THE DATA FOR A SAMPLE OF ECHOES 20145 - 21783 FEB.

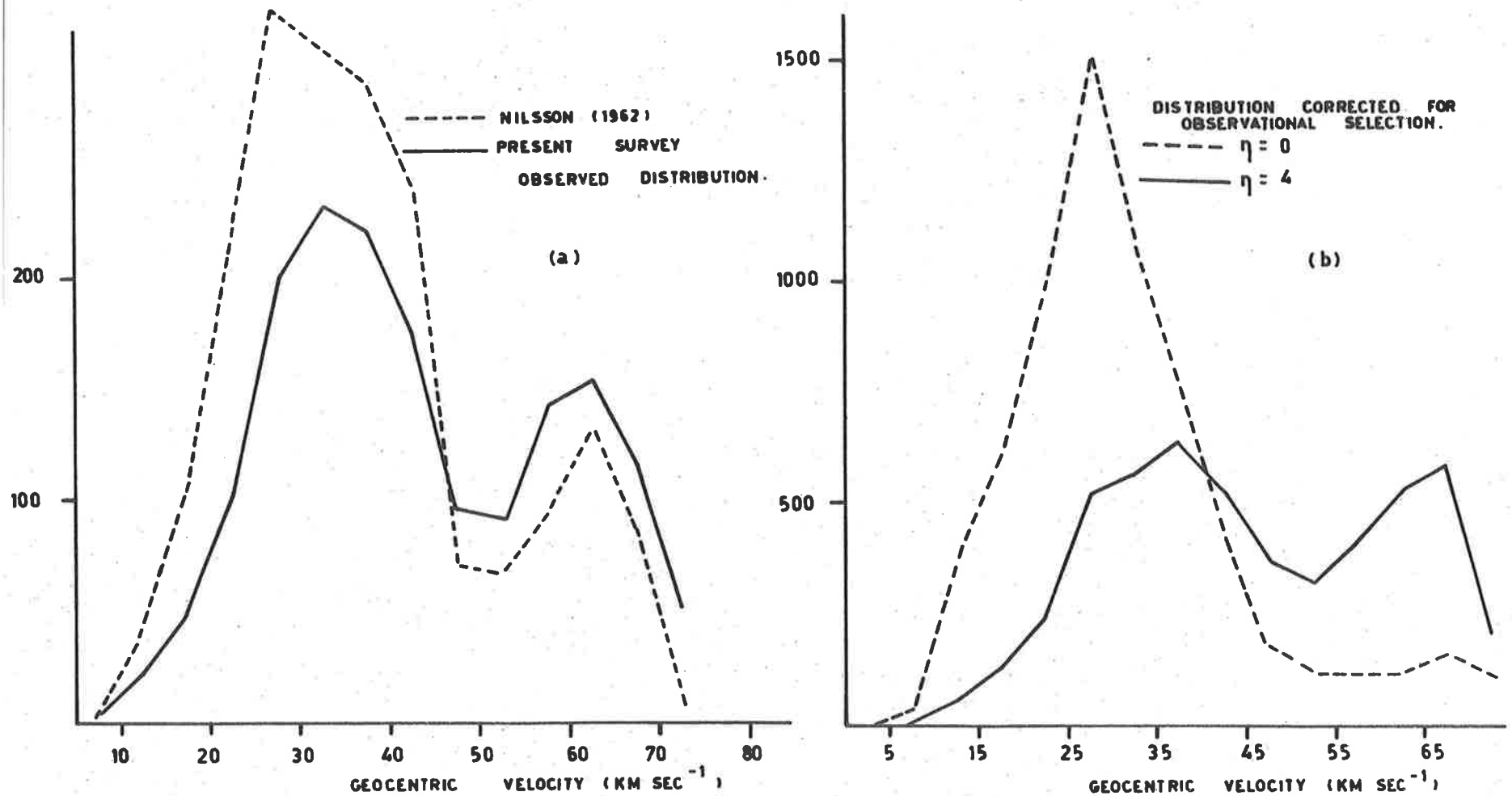
NILSSON (1962)
PRESENT SURVEY
OBSERVED DISTRIBUTION
(a)
200
100
10
20
30
40
50
60
70
80
GEOCENTRIC VELOCITY (KM SEC^{-1})
DISTRIBUTION CORRECTED FOR OBSERVATIONAL SELECTION.
$\eta = 0$
$\eta = 4$
(b)
1500
1000
500
5
15
25
35
45
55
65
GEOCENTRIC VELOCITY (KM SEC^{-1})

FIG. 8 · 12

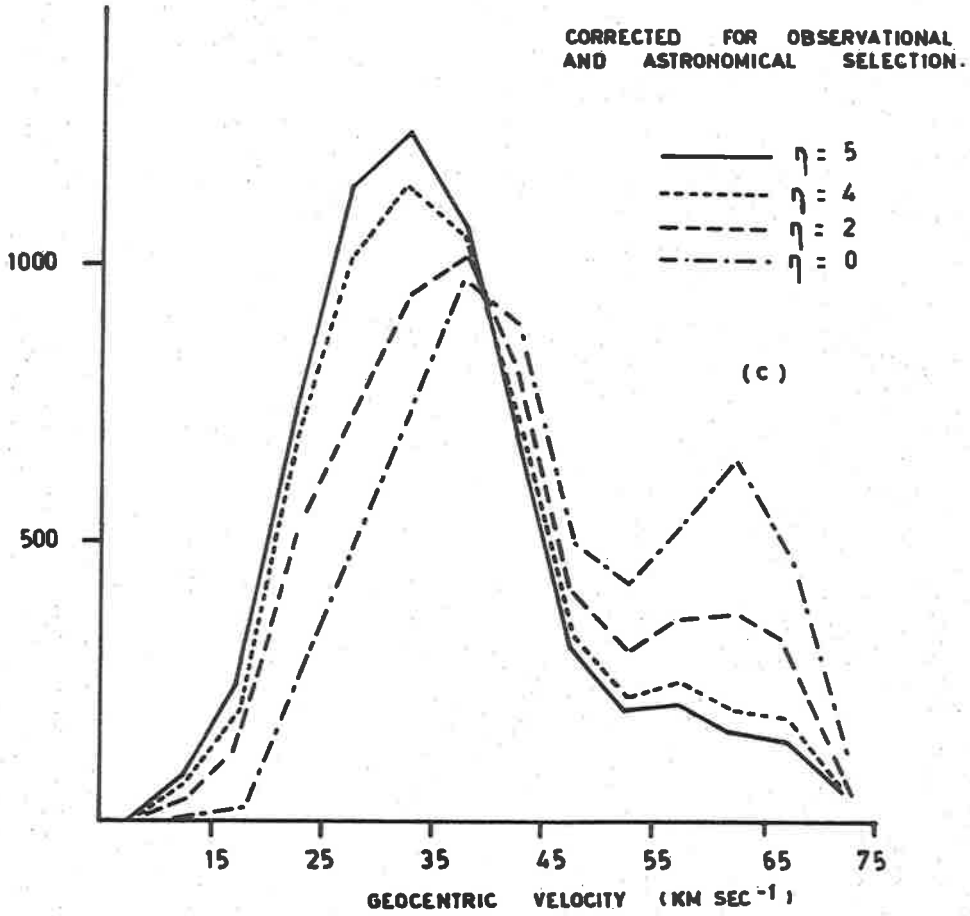
CORRECTED FOR OBSERVATIONAL AND ASTRONOMICAL SELECTION.
η = 5
η = 4
η = 2
η = 0
(c)
1000
500
15
25
35
45
55
65
75
GEOCENTRIC VELOCITY (KM SEC⁻¹)

FIG. 8 · 12 (cont.)

km sec^{-1} in the observed distribution is a result of observational selection. Fig. 8.12(c) shows clearly the gradual removal of this peak by progressive increases in the value of η, and indicates that for the present survey $\eta \sim 4$-5, in good agreement with the values obtained by other workers (§8.2.2).

Fig. 8.13(a) shows the observed heliocentric velocity distribution, again compared with that for the 1961 survey. Fig. 8.13(b) shows the heliocentric velocity distribution corrected for observational selection with $\eta = 0$ and $\eta = 4$ and observational plus astronomical selection with $\eta = 2$ and $\eta = 5$.

While at first glance the astronomical selection correction (eqn 8.3) might appear to imply an infinite number of meteors with parabolic and hyperbolic orbits, and calls to mind the 'ultraviolet catastrophe' of classical physics, it should be remembered that no unequivocal evidence exits to support the notion of interstellar meteors. If as has been suggested (Babadzhanov and Kramer, 1967) the hyperbolic component of the observed meteor distribution is generated by the action of gravitational perturbing forces or some other dynamical agent within the solar system, then in the unperturbed state no truly parabolic or hyperbolic meteors would exist. Disregarding perturbations, if, as must be the case, the true frequency distribution of heliocentric meteor velocities at 1 a.u. reaches a maximum below the parabolic limit and for higher velocities decreases with increasing heliocentric velocity more rapidly than the astronomical selection factor increases, then the corrected

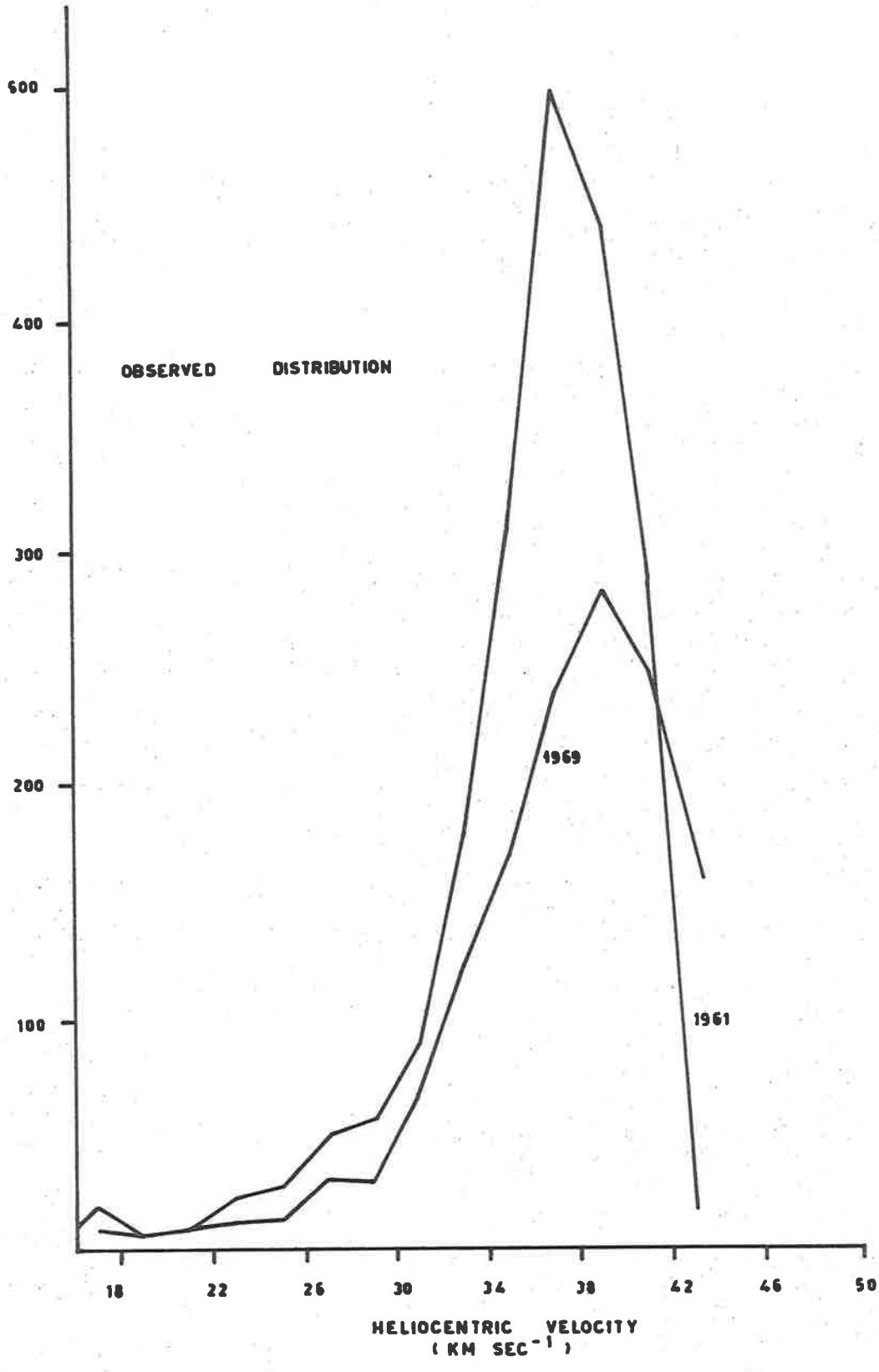
500
400
300
200
100
OBSERVED DISTRIBUTION
1969
1961
18
22
26
30
34
38
42
46
50
HELIOCENTRIC VELOCITY
(KM SEC⁻¹)

FIG. 8·13 (a)

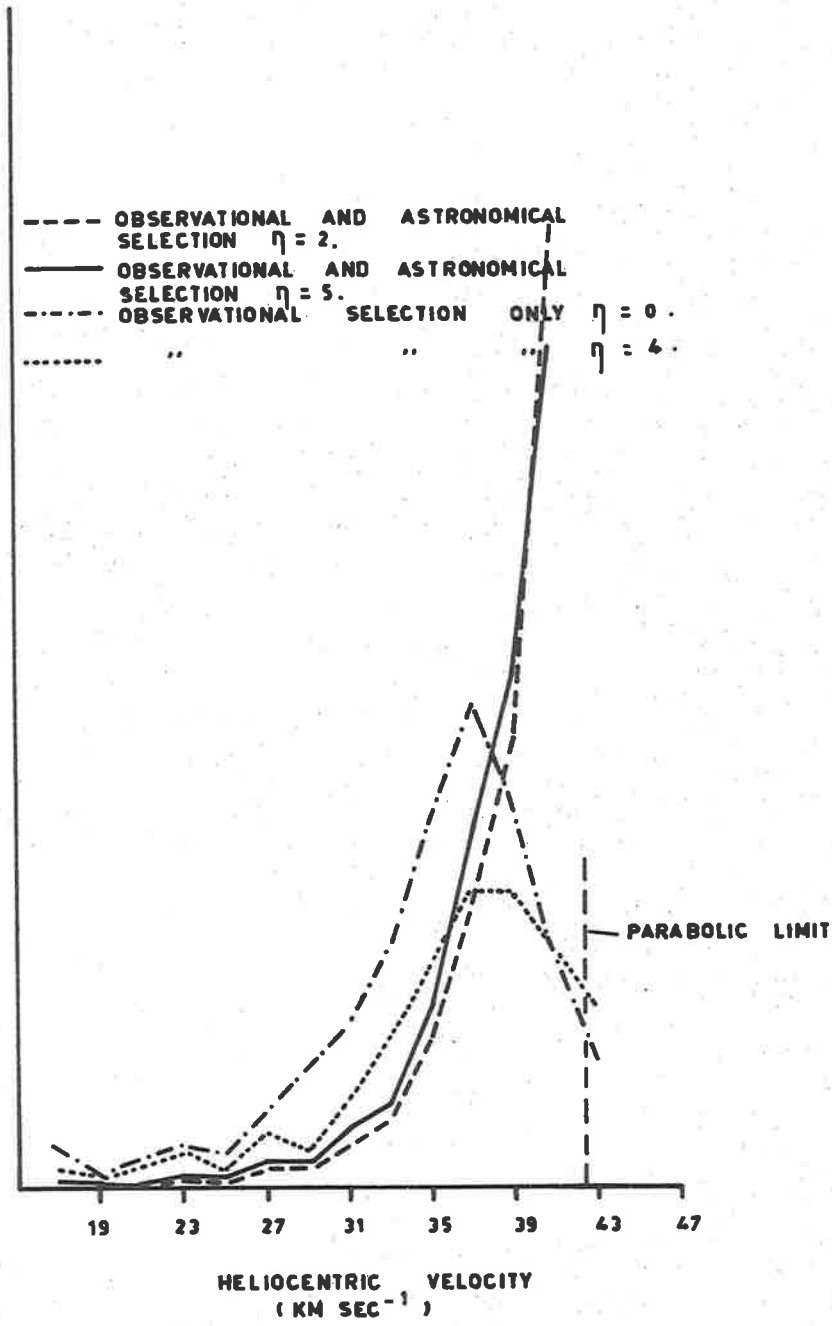
OBSERVATIONAL AND ASTRONOMICAL SELECTION η = 2.
OBSERVATIONAL AND ASTRONOMICAL SELECTION η = 5.
OBSERVATIONAL SELECTION ONLY η = 0.
" " η = 4.
PARABOLIC LIMIT
19
23
27
31
35
39
43
47
HELIOCENTRIC VELOCITY
(KM SEC⁻¹)

FIG. 8 · 13 (b)

distribution would drop properly to zero at the parabolic limit, even if showing an enormous proportion of meteors with velocities only marginally less than the limit.

If only a slight perturbation is necessary to transform a high velocity meteor from an elliptic to a hyperbolic orbit, the astronomical weighting factor which should be applied to that meteor would be close to that determined for the original unperturbed orbit. However, without knowledge of the perturbations which have affected each meteor individually there is little we can do to adjust the form of the astronomical weighting factor even on a statistical basis to compensate for this. The best we can do is to apply it to the major portion of the observed meteor distribution and note its inapplicability to meteors near the parabolic limit.

The observation in this survey of extremely hyperbolic meteor associations apparently related to the Orionid stream (§7.6.4) gives support for a perturbational origin for hyperbolic meteor orbits generally.

8.6 ORBITAL ELEMENT DISTRIBUTIONS

The orbit of a meteor is specified by five quantities, commonly taken to be

- a semi-major axis
- e eccentricity
- i inclination
- ω argument of perihelion
- Ω longitude of the ascending node

although any other five quantities which may be derived from all of these quantities may also be used. A sixth quantity, the true anomaly ν, locates the meteor in its orbit. Since in this survey meteors must collide with Earth to be detected, the observed values of true anomaly will be simply $360 - \omega^{\circ}$ or $180 - \omega^{\circ}$ depending upon whether the meteor is detected at the ascending or descending node.

Distributions of true anomaly, argument of perihelion, and longitude of the ascending node are presented for completeness in Figs. 8.14, 8.15 and 8.16. These distributions are so strongly affected by observational selection that it is pointless, in view of the uncertainties involved, to attempt to derive actual (corrected) distributions from them.

The features of Fig. 8.14 apparently reflect the observational selection effects acting rather than any particular properties of the actual distribution of true anomaly. The minimum at 180° is attributable to the low probability of detection of meteors in predominantly direct orbits near aphelion. Were this not the case, for a uniform orbit distribution one would expect to find a maximum at 180° since orbiting bodies spend most time near aphelion.

The maximum near 240° is apparently related to the antisolar ecliptic radiant concentration and the lesser maximum near 140° corresponds to the equivalent solar concentration, severely depleted as a result of the interruption of day-time recording by interference. The minor peak between $0 - 30^{\circ}$ is probably due to a large number of high inclination low eccentricity meteors detected near perihelion.

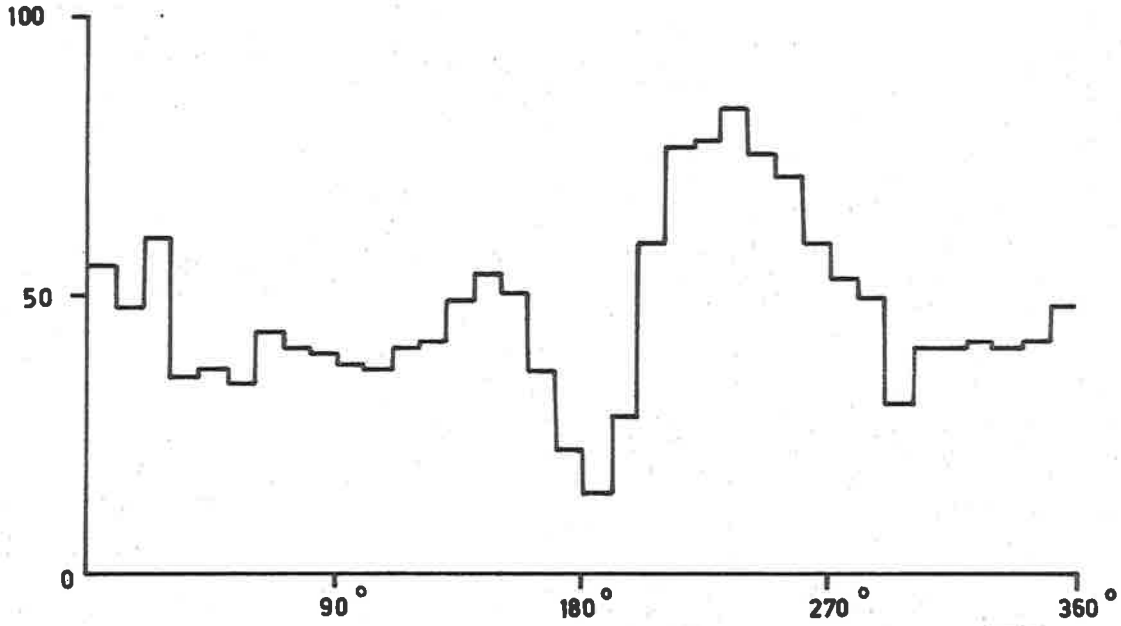

FIG. 8·14 TRUE ANOMALY.

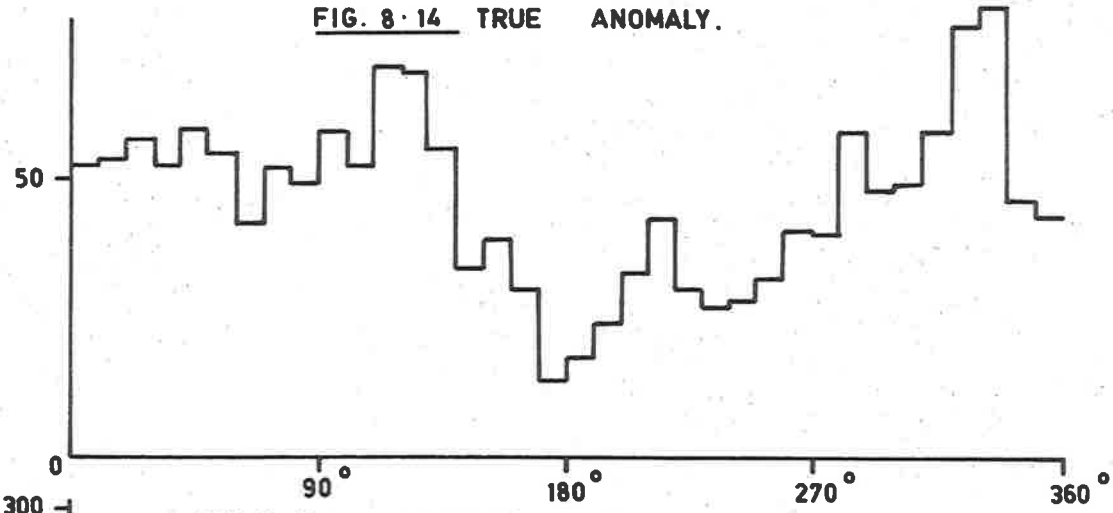

FIG. 8·15 ARGUMENT OF PERIHELION.

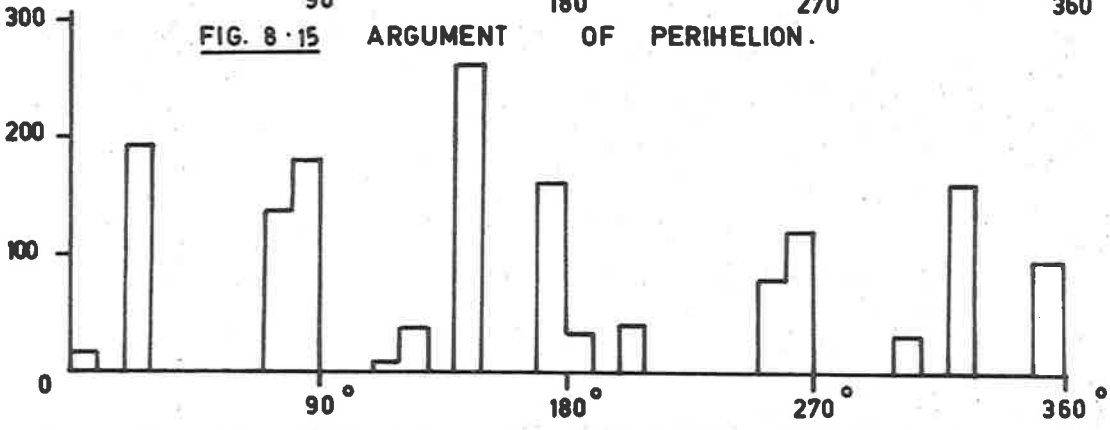

FIG. 8·16 LONGITUDE OF ASCENDING NODE.

Fig. 8.15 shows the observed distribution of the argument of perihelion ω. The simple relation already noted between this quantity and the true anomaly enables us to relate the main features of this distribution to those of Fig. 8.14.

Fig. 8.16 shows the observed distribution of the longitude of the ascending node. This distribution appears as a number of discrete groups due to the relatively short duration of the data recording periods and because only six months of the year are represented.

While a and e define the shape of an orbit, and ω defines the orientation of the major axis with the orbit plane, i and Ω are the quantities required to determine the orientation of the orbit plane in space. However, the astronomical weighting factor (eqn. 8.3) is a function of a, e, and i but not ω or Ω. Directional properties of the orbit distribution, such as, for example, a hypothetical tendency for the alignment of the line of apsides for low inclination orbits with the perihelion of Jupiter, are strongly dependent upon distributions of ω and Ω in addition to a, e, and i. In view of the severe influence of observational selection effects on the distributions of Figs. 8.14, 8.15, and 8.16, and the uncertainties in the correction factors no attempt has yet been made to look for directional tendencies of this type in the present data.

Fortunately the same problems do not prevent a meaningful analysis of the properties of meteor orbits in regard to shape, size and relation to the ecliptic plane. The remainder of this chapter is devoted to a consideration of the distribution of the present meteor sample in terms

of a, e, and i. The perihelion distance q = a (1 - e) is also considered, since this quantity is much harder to perturb significantly than either a or e by forces such as the action of the Poynting-Robertson effect, which is most pronounced near perihelion passage.

Fig. 8.17 compares the observed distributions of reciprocal semi-major axis for the present data with those for radio meteors found by Lebedinets and Kashcheev (1967) at Kharkov for $M_R < +7$, and Andrianov, Pupysev, and Sidorov (1970) at Kazan for $M_R < +8$. The distribution for the bright photographic meteors of Babadzhanov (1963) is also given for comparison.

The proportion of small orbits ($1/a > .5$ a.u.$^{-1}$) appears to increase towards fainter limiting magnitudes. Very few small orbits are found amongst the bright photographic meteors, and none for which $1/a > 1$ a.u.$^{-1}$ The $M_R < +8$ meteors of Andrianov et al. contain a much higher proportion of small orbits even than the $M_R < +7$ meteors of Lebedinets and Kashcheev. For small orbits there is quite close agreement between the distribution of Lebedinets and Kashcheev and that of the present survey, which covers meteors of $M_R < +7.5$.

For large orbits ($1/a < .5$ a.u.$^{-1}$), however, there are pronounced differences between the distributions obtained at Adelaide and Kharkov. The Kharkov distribution cuts off quite sharply near the parabolic limit for closed orbits, while that found in the present survey exhibits a relatively smooth transition from elliptical to hyperbolic orbits. In this respect the Adelaide distribution closely resembles that for the bright photographic meteors of Babadzhanov.

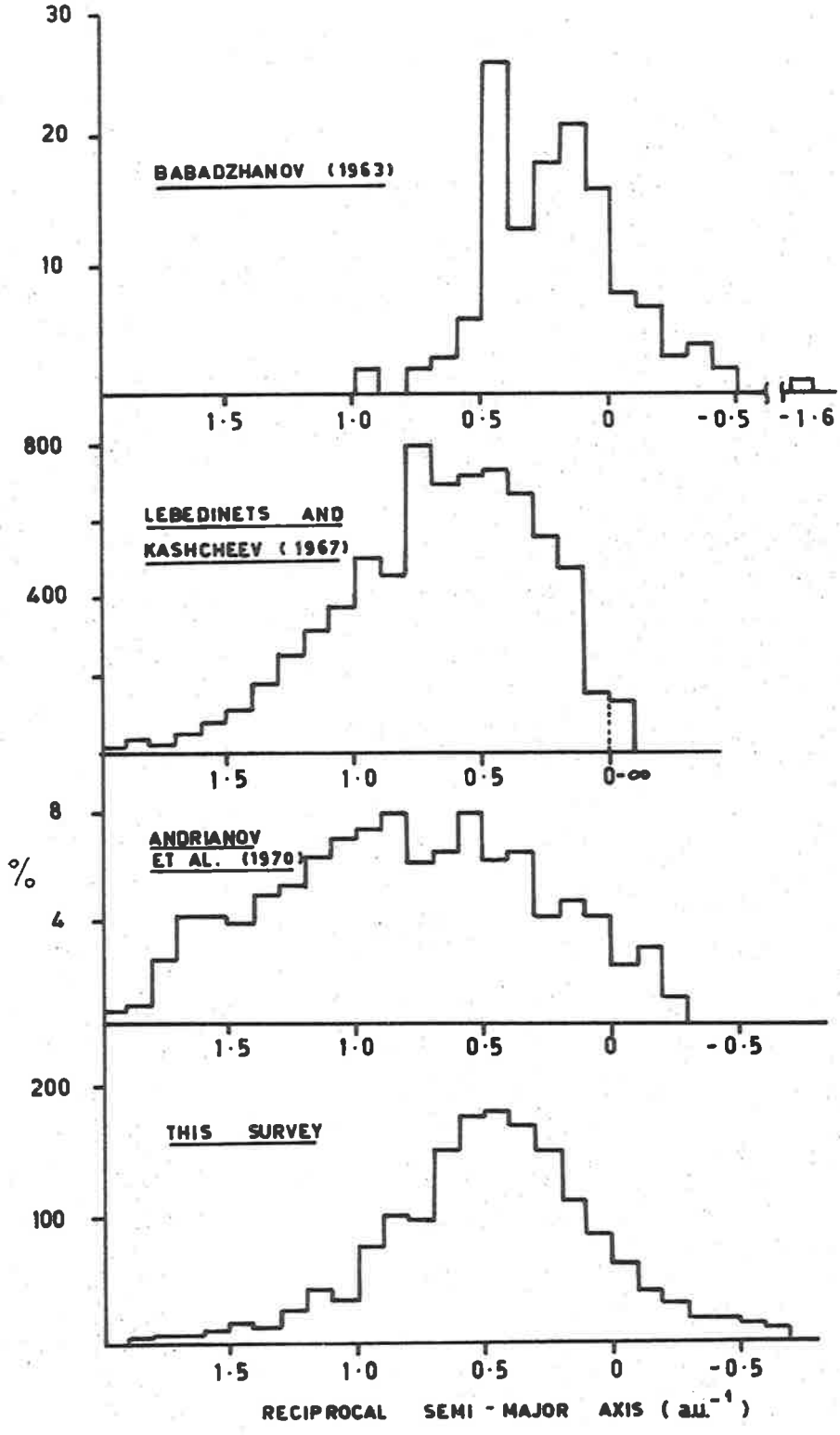
30
20
10
BABADZHANOV (1963)
1·5
1·0
0·5
0
-0·5
-1·6
800
400
LEBEDINETS AND
KASHCHEEV (1967)
1·5
1·0
0·5
0-∞
8
4
%
ANDRIANOV
ET AL. (1970)
1·5
1·0
0·5
0
-0·5
200
100
THIS SURVEY
1·5
1·0
0·5
0
-0·5
RECIPROCAL SEMI - MAJOR AXIS (a.u.$^{-1}$)

FIG. 8 · 17

The Kazan system is based on a forward-scatter communications link with a base line of 100 km. (Andrianov et al., 1968) and has radiant measurement accuracy comparable to that of the Adelaide system. Andrianov et al. (1970) claim that their radio-echo method has eliminated the low sensitivity to fast meteors arising from the rapid initial diffusion of their trains. Their distribution of reciprocal semi-major axis gives some support to this claim, since it does not show the sharp cut-off apparent in the data of Lebedinets and Kashcheev. Notwithstanding the large proportion of meteors in small orbits, the extent of the hyperbolic component of the distribution due to Andrianov et al. is not as pronounced as those of either the Adelaide distribution or that for the bright photographic meteors of Babadzhanov.

To the best of the author's knowledge pulse equipments are in use both at Kharkov and Kazan. The geometry of the Kharkov multi-station system is similar in principle to that of the Adelaide system, and the differences between the distributions for the various radio surveys shown for small 1/a are attributed to the use of a c.w. system at Adelaide instead of the more common pulse radar employed at Kharkov and Kazan. The advantages of velocity determination by the use of the pre-t_o diffraction pattern available in a c.w. system, particularly in the presence of rapid diffusion have been noted in §3.

The similarities in the Adelaide radio and the bright photographic meteor distributions for large orbits gives further support for the advantages of a c.w. system since the photographic method of velocity determination is not hampered by diffusion effects.

To test the significance of errors in velocity determination with respect to the observed distribution of reciprocal semi-major axis, distributions of 1/a have been determined for echoes satisfying various restrictions in allowable standard deviation in the determination of x/t (see §5.2). The mean value of the standard deviation for this survey is .045 (see Figs. 8.4, 8.5) compared with that for the survey of Nilsson (1962) of near .08. The difference is probably due to the preponderance of echoes in the present survey with good quality diffraction waveforms and more than sufficient extrema for reduction.

Figs. 8.18(a) and (b) show the distributions with 1/a for overdense and underdense trails for all meteors, and for meteors with standard deviations on all traces restricted to less than .07 and less than .04.

The restriction in standard deviation does not reduce the hyperbolic component and even results in a slight decrease in the mean value of 1/a in each case, indicating indeed that the higher frequency data tends to be of better quality than the low frequency data. It is interesting to note that the modal value for the overdense meteors is less than that for the underdense meteors, yet the hyperbolic component is smaller. These distributions indicate clearly that the hyperbolic component is not attributable to any major extent to error in velocity measurement.

The distributions vary in the expected manner for large values of 1/a.

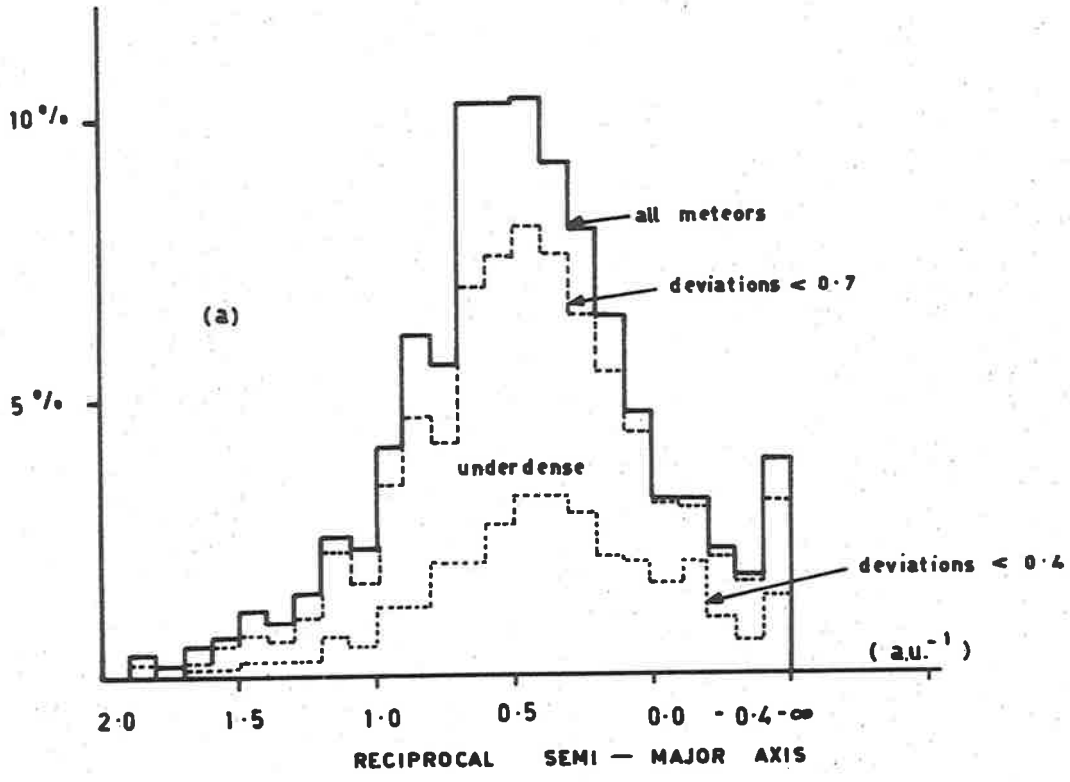
10 %
5 %
(a)
all meteors
deviations < 0·7
underdense
deviations < 0·4
(a.u.⁻¹)
2·0
1·5
1·0
0·5
0·0
- 0·4
-∞
RECIPROCAL SEMI — MAJOR AXIS

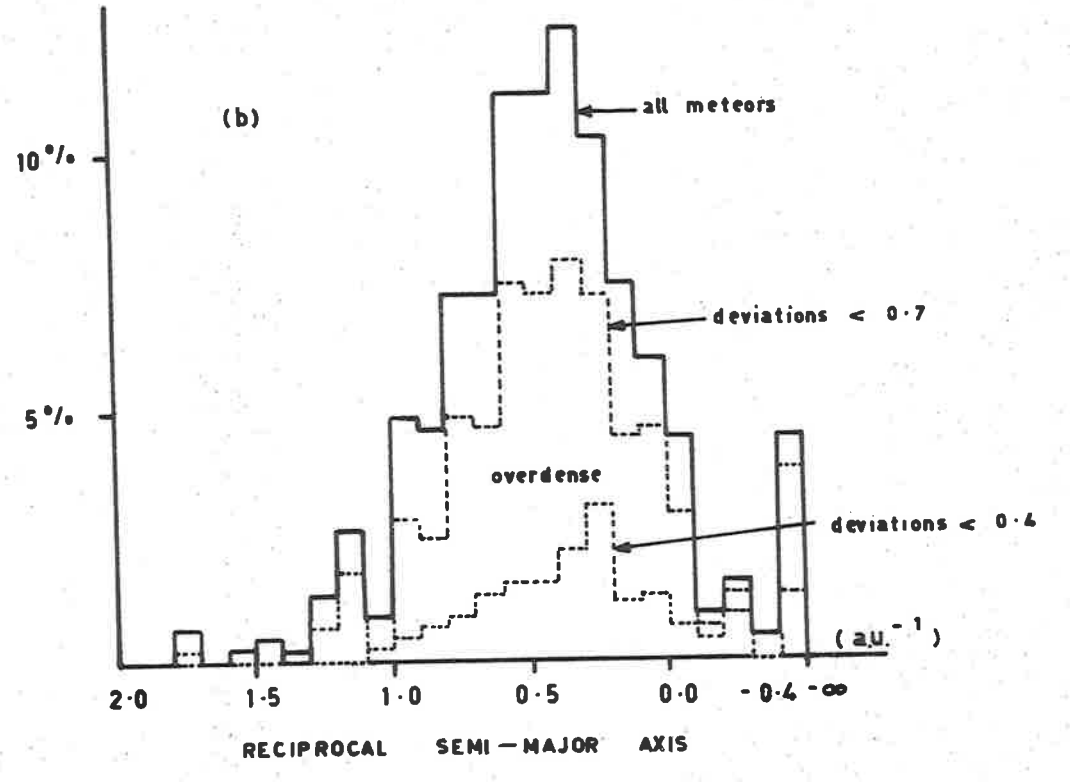
10 %
5 %
(b)
all meteors
deviations < 0·7
overdense
deviations < 0·4
(a.u.⁻¹)
2·0
1·5
1·0
0·5
0·0
- 0·4
-∞
RECIPROCAL SEMI — MAJOR AXIS

FIG. 8 · 18

Fig. 8.19 compares distributions of reciprocal semi-major axis corrected for observational selection only and observational plus astronomical selection, both for $\eta = 4$. The maximum near 0.5 a.u.$^{-1}$ for the distribution corrected for observational selection only, is similar to that for the observed distribution (Fig. 8.17) and is apparently due to the large number of low inclination meteors related to the Jupiter family of comets. When account is taken of astronomical selection, Fig. 8.19 shows that this maximum disappears and that a very large number of meteors occupy orbits of large dimensions. For reasons discussed in §8.5 the astronomical selection correction is not applied to meteors observed with parabolic or hyperbolic orbits.

Figs. 8.20 and 8.21 show the observed distributions of eccentricity and inclination for underdense, intermediate and overdense trails. Proportionately more orbits of low eccentricity are apparent for the underdense meteors, consistent with the increasing significance of the 'toroidal' meteors at fainter magnitudes. The reason for the large proportion of underdense meteors with eccentricities greater than 1.2 compared with the proportion amongst the overdense distribution is not as yet understood, and the significance of the peak at $e = 1.25$ is uncertain. This disproportion is consistent with a collisional origin for the hyperbolic meteors. Dohnanyi (1970) considers collision processes to be a major factor controlling the evolution of meteor orbit distributions. It is apparent that the fragments generated in a destructive collision between two meteoroids should be both smaller and more numerous than the

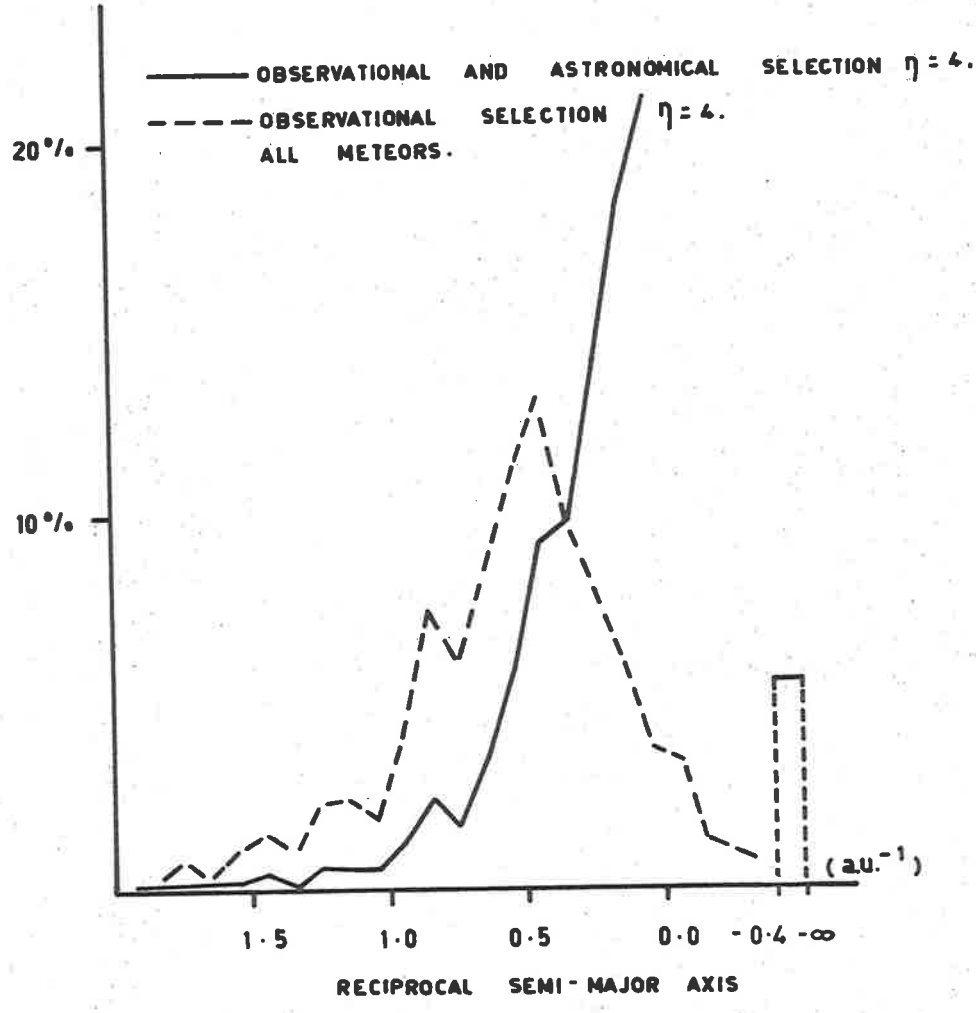
OBSERVATIONAL AND ASTRONOMICAL SELECTION η = 4.
OBSERVATIONAL SELECTION η = 4.
ALL METEORS.
20 %
10 %
(a.u.⁻¹)
1·5
1·0
0·5
0·0
-0·4
-∞
RECIPROCAL SEMI-MAJOR AXIS

FIG. 8 · 19

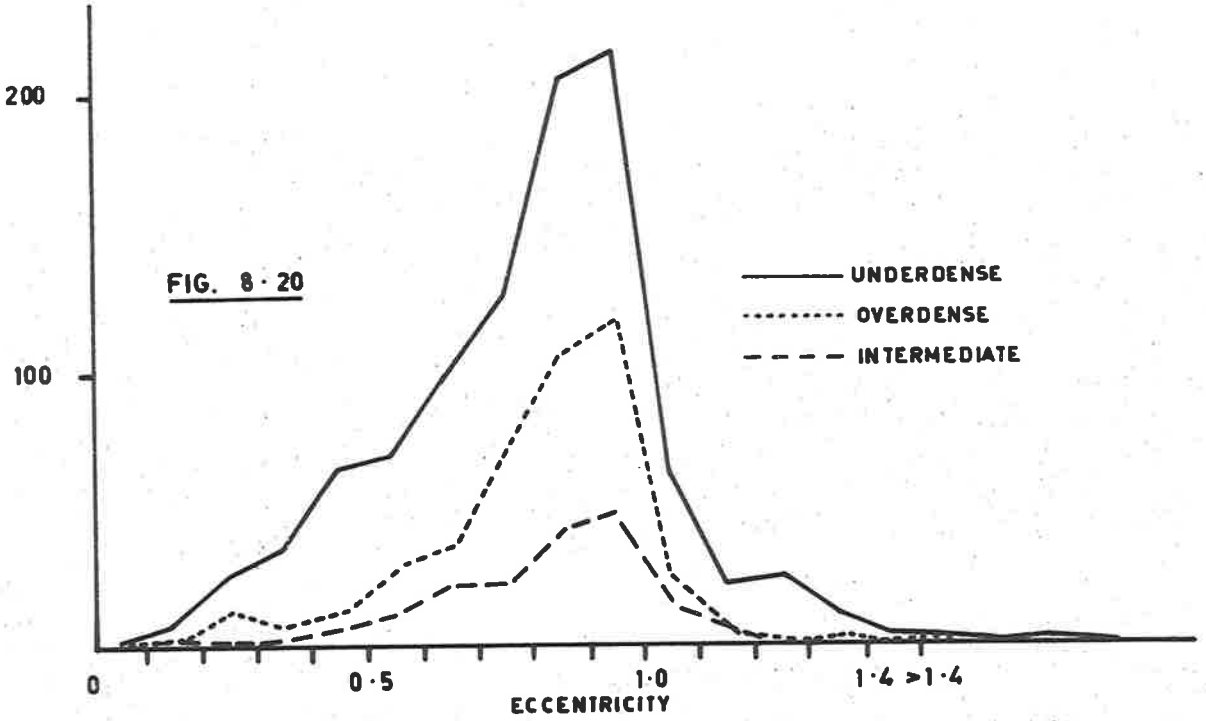

FIG. 8 · 20

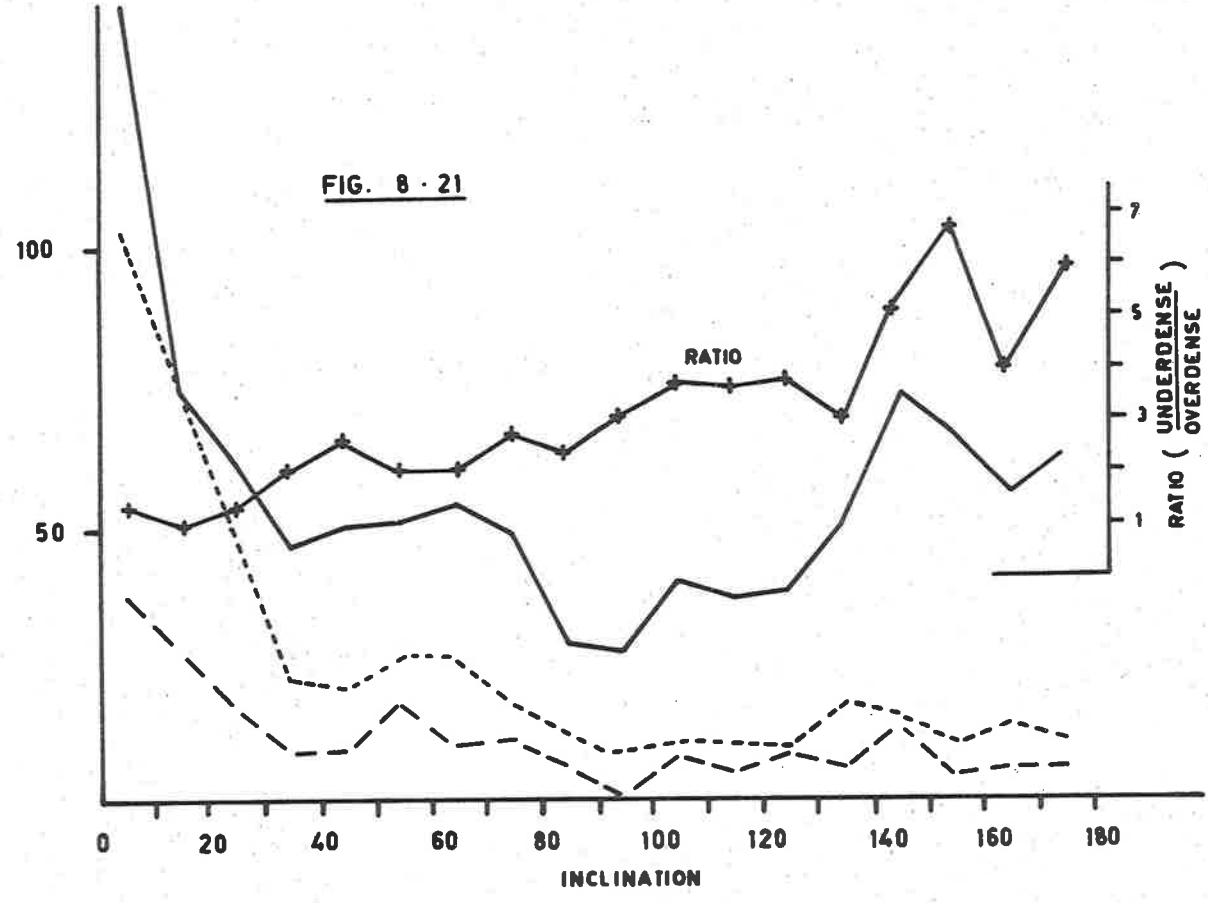

FIG. 8 · 21

parent objects, and it is conceivable that a number of these fragments could be projected into hyperbolic orbits even though the collision had occurred between two particles in elliptic orbits.

The increasing significance of the 'toroidal' meteors at fainter magnitudes is supported by Fig. 8.21 which shows the ratio of underdense to overdense meteors with inclinations near 60° to be approximately twice that for low inclination meteors. More striking is the large proportion of retrograde orbits amongst underdense meteors compared with the proportions for the intermediate and overdense trails.

Since meteors in retrograde orbits will in general have higher geocentric velocities than similar meteors in direct orbits, the dependence of ionization on velocity (§8.2.2) indicates that meteors in retrograde orbits producing trails of limiting electron line density will be of smaller mass than those in direct orbits. Thus Fig. 8.21 can be interpreted as showing that high inclination orbits become increasingly pronounced with decreasing meteoroid mass. It is apparent that were the distribution for underdense meteors to constant limiting mass rather than constant limiting electron line density, the retrograde meteor component with a maximum at 145° would be smaller than the toroidal group component with a maximum near 60°, instead of larger, as in Fig. 8.21.

Fig. 8.22 shows the observed distribution with inclination for various ranges of semi-major axis and eccentricity. The presentation is similar to that used by Davies and Gill (1960) to describe the observations of a radar survey to similar limiting magnitude. While there are

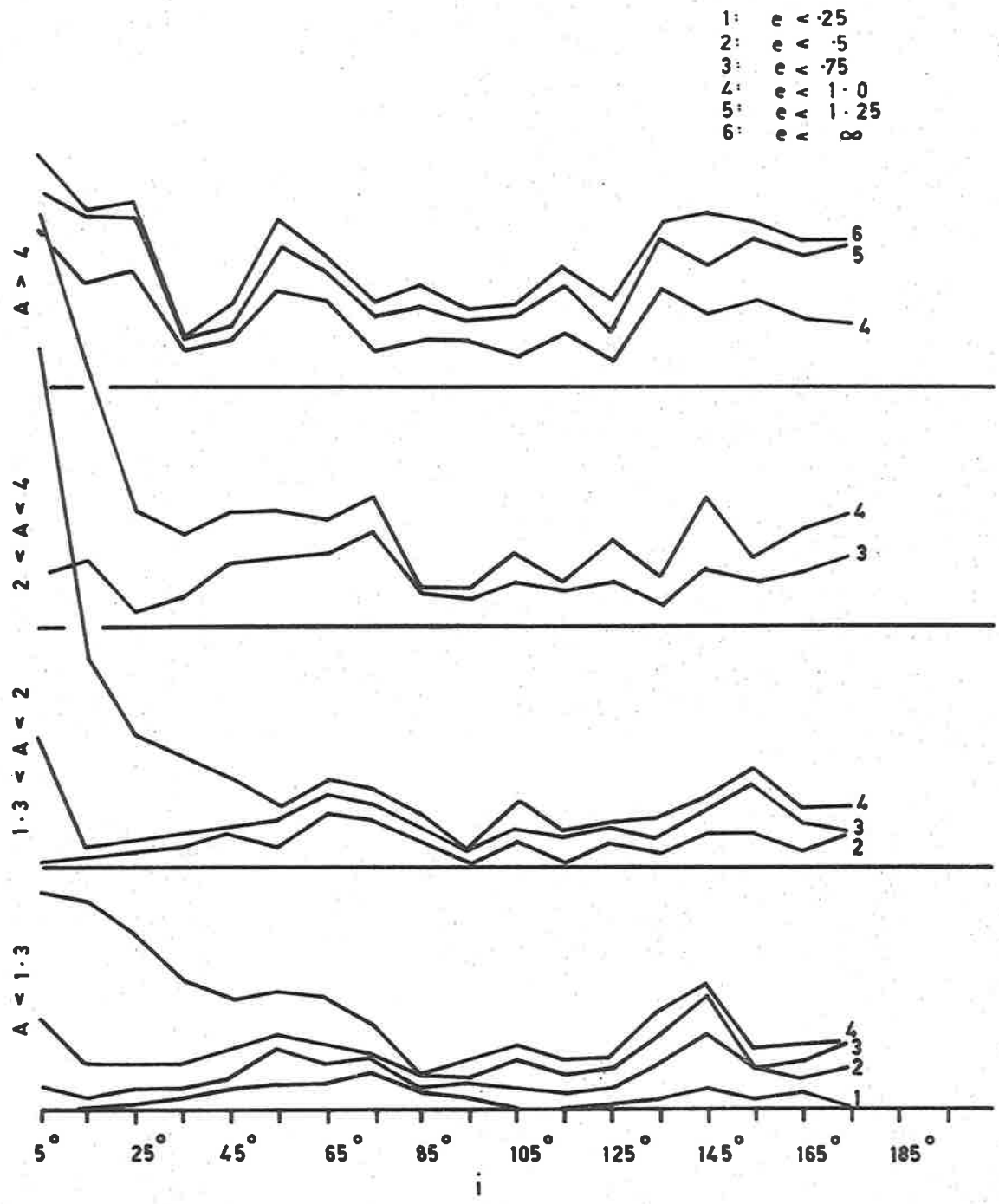

FIG. 8·22 OBSERVED DISTRIBUTION WITH INCLINATION.

similarities between the two sets of distributions there are noticeable differences as well. For $a < 1.25$ a.u. Davies and Gill observed very few low inclination orbits, most orbits with inclinations near 60° and a lesser broad maximum near 140°. High eccentricity orbits contribute little to the maximum at 60°. In contrast the present survey for $a < 1.3$ a.u. finds a large number of low inclination orbits with high eccentricities and a rather less pronounced concentration near 60° relative to the strength of the concentration near 145°. For $1.25 < a < 2$ a.u. and $2 < a < 5$ a.u. the distributions of Davies and Gill are similar, as are the distributions for $1.3 < a < 2$ a.u. and $2 < a < 4$ a.u. for the present survey. Once again, however, the Adelaide survey has detected a high proportion of low inclination orbits of high eccentricity not prominent in the data of Davies and Gill. Davies and Gill observed few retrograde orbits with $a < 5$ a.u. and found the direct orbits in this range to be uniformly distributed in inclination. The equivalent distribution of Fig. 8.22 covers the range $a < 4$ a.u. and some of the difference may possibly be attributed to meteors in the range $4 < a < 5$ a.u.. For the Adelaide data the concentration near $i = 60^{\circ}$ is still pronounced with $a > 4$ a.u. and is due to meteors with $e > .75$. The peak in the distribution for retrograde orbits is still apparent, but broader. For hyperbolic orbits there is a pronounced minimum near $i = 40^{\circ}$ but otherwise the distribution with inclination is comparatively uniform, with slight increases for both direct and retrograde orbits near the ecliptic as well as at $i = 60^{\circ}$ and $i = 145^{\circ}$. In view of the preceding discussions

of their significance (§6.5, §8.3.3) it appears that about one third of the hyperbolic orbits present may be due to over-correction of the atmospheric retardation for higher density meteors detected at low reflection point heights. The majority of the remaining two thirds are considered to be real. If the real component is generated by perturbation of elliptic orbits it is apparent that the hyperbolic orbits whether real or generated by error should be distributed in a similar manner to the large elliptic orbits. The observed distribution shows this to be the case and gives no evidence for an interstellar origin of hyperbolic meteors with either random or preferred directions of arrival.

Consideration of Fig. 8.22 shows that we may reasonably class meteors according to inclination in three distinct groups, namely

(i) $i \leqslant 30^{\circ}$

(ii) $30 < i \leqslant 90^{\circ}$

(iii) $i > 90^{\circ}$

Figs. 8.23(a), (b), (c) show the observed distributions with perihelion distance q for these three groups, calculated separately for sporadic and associated meteors from the present survey. In each inclination range there is a close correspondence between the distributions for sporadic and associated meteors, although quite distinct differences are apparent between the various ranges of inclination. This gives further support to the adequacy of consideration for most purposes of the faint radio meteor distribution as a whole without prior removal of the stream component (§8.4).

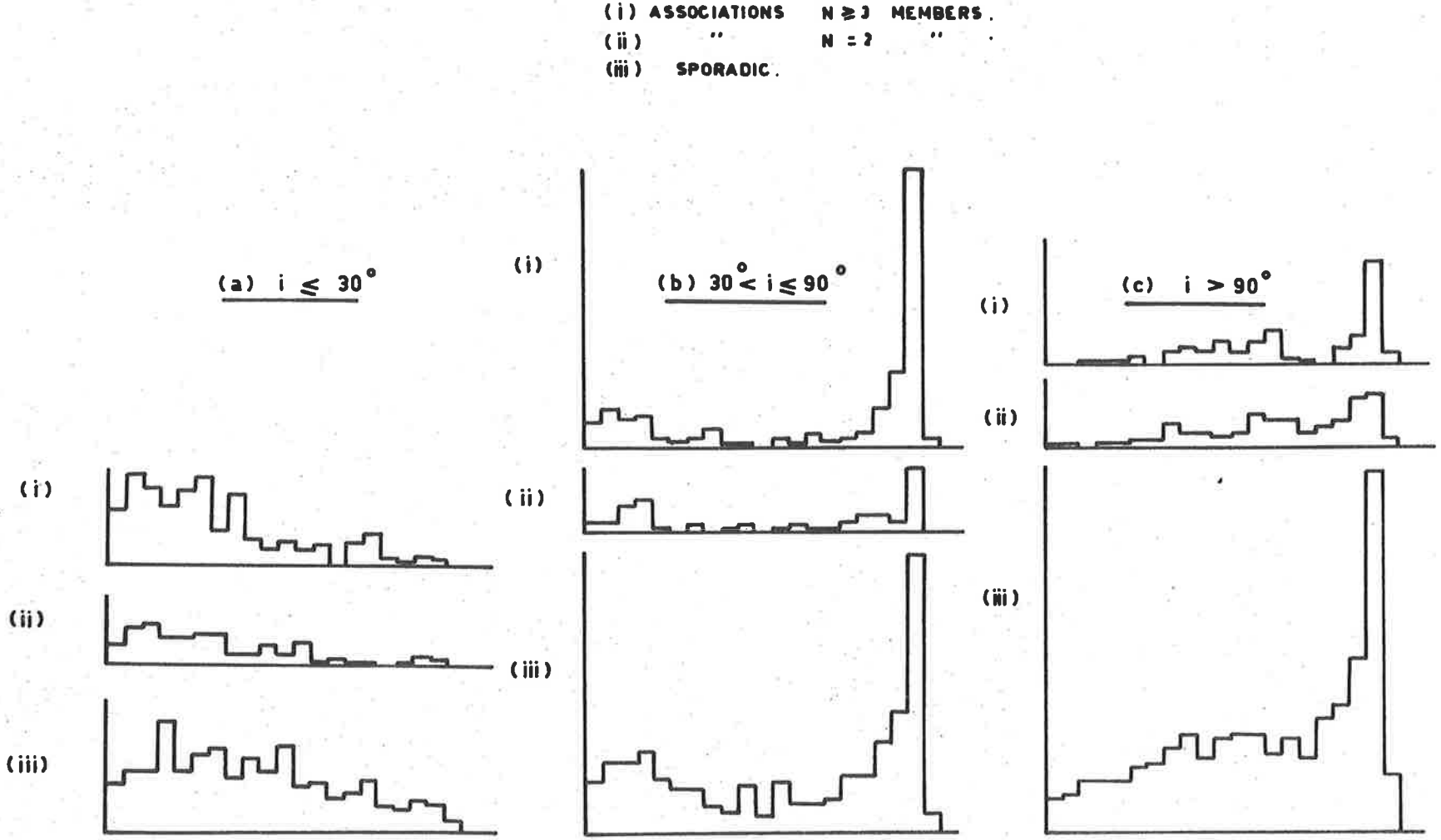

FIG. 8·23 OBSERVED DISTRIBUTION OF PERIHELION DISTANCE (q).

The most noticeable differences in the distribution of perihelion distance are

(i) Both high inclination ranges show sharp peaks near q = 1 a.u. In contrast the $i \lesssim 30^{\circ}$ range has a minimum for q = 1 a.u.

(ii) The $i \lesssim 30^{\circ}$ distribution is broad with a preference for orbits of small q. There is a more pronounced concentration of small q orbits for $30 < i \lesssim 90^{\circ}$ with a minimum in the vicinity of q =.5 a.u. On the other hand the $i > 90^{\circ}$ distribution has few small q orbits and a steady increase with increasing q. There is a suggestion of a broad maximum near q = .6 a.u.

The significance of the main features of these distributions are better understood when considered in conjunction with information on orbit size and shape, specified by the semi-major axis and eccentricity.

Following Kresák (1967) we consider the foregoing distributions in the form of two-dimensional a-e diagrams, one for each of the three ranges of inclination discussed above. Kresák has calculated the distributions for a number of related quantities in terms of the a-e diagram, and has demonstrated the usefulness of this presentation for comparison of meteor orbit distributions with those of short-period comets and asteroids, as well as for displaying the evolutionary paths which would be followed by orbits under the action of such influences as the Poynting-Robertson effect.

The a-e diagram, besides being an alternative way of presenting the information contained in Fig. 8.22, also yields directly the distribution

of orbits in terms of perihelion distance, eccentricity and inclination since $q = a(1-e)$.

Fig. 8.24 shows the relation of a, q and e as an a-e diagram for ease of reference. The heavy boundaries correspond to the extreme conditions necessary for an earth-crossing orbit (neglecting the earth's own eccentricity) of $a(1-e) = 1$, and $a(1+e) = 1$.

Figs. 8.25(a), (b) and (c) show the observed a-e distributions for all meteors of the present survey, according to inclination range. It is interesting to compare these distributions with those of Kresák (1967) for bright and faint photographic sporadic meteors. For low inclinations Kresák finds a concentration of meteors for $1.5 \lesssim a \lesssim 3.5$ a.u. near $q = 1$ a.u. for both bright and faint meteors. The faint photographic meteors show an extension of this concentration into the region $a \simeq 1$ a.u., $e \lesssim .2$ which Kresák (1967) suggests is the area which would be reached by asteroidal meteors under the action of the Poynting-Robertson effect. Due to a much smaller sample of bright meteors, comparison of this region for the faint and bright photographic meteors is not possible. In contrast Fig. 8.25(a) shows few orbits with $q \sim 1$ a.u., particularly near $a = 1$ a.u., and has a strong concentration in the region $1 < a < 2$ a.u., $.75 \lesssim e \lesssim 1$.

A similar distinction has been noted by Lebedinets and Kashcheev (1967) who found the orbits of faint radio meteors with small inclinations to the ecliptic to be concentrated preferentially for $q < .25$ a.u. in contrast to the preference for $q > .5$ a.u. shown by photographic

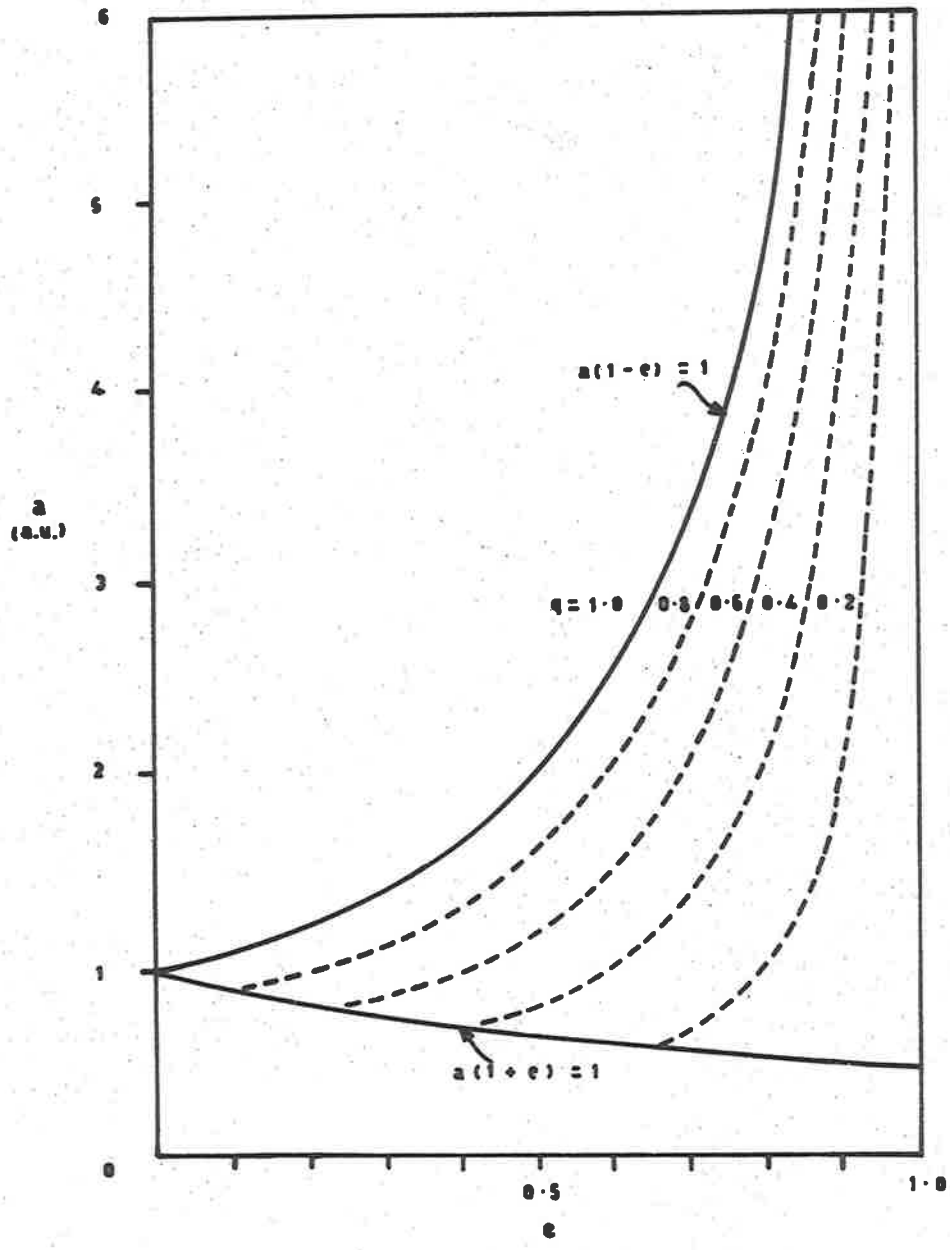

FIG. 8·24 THE a - e DIAGRAM. THE LINES a(1 - e) = 1, a(1 + e) = 1 ARE THE LIMITING CONDITIONS FOR AN EARTH - CROSSING ORBIT. DASHED LINES ARE ISOPLETHS OF PERIHELION DISTANCE.

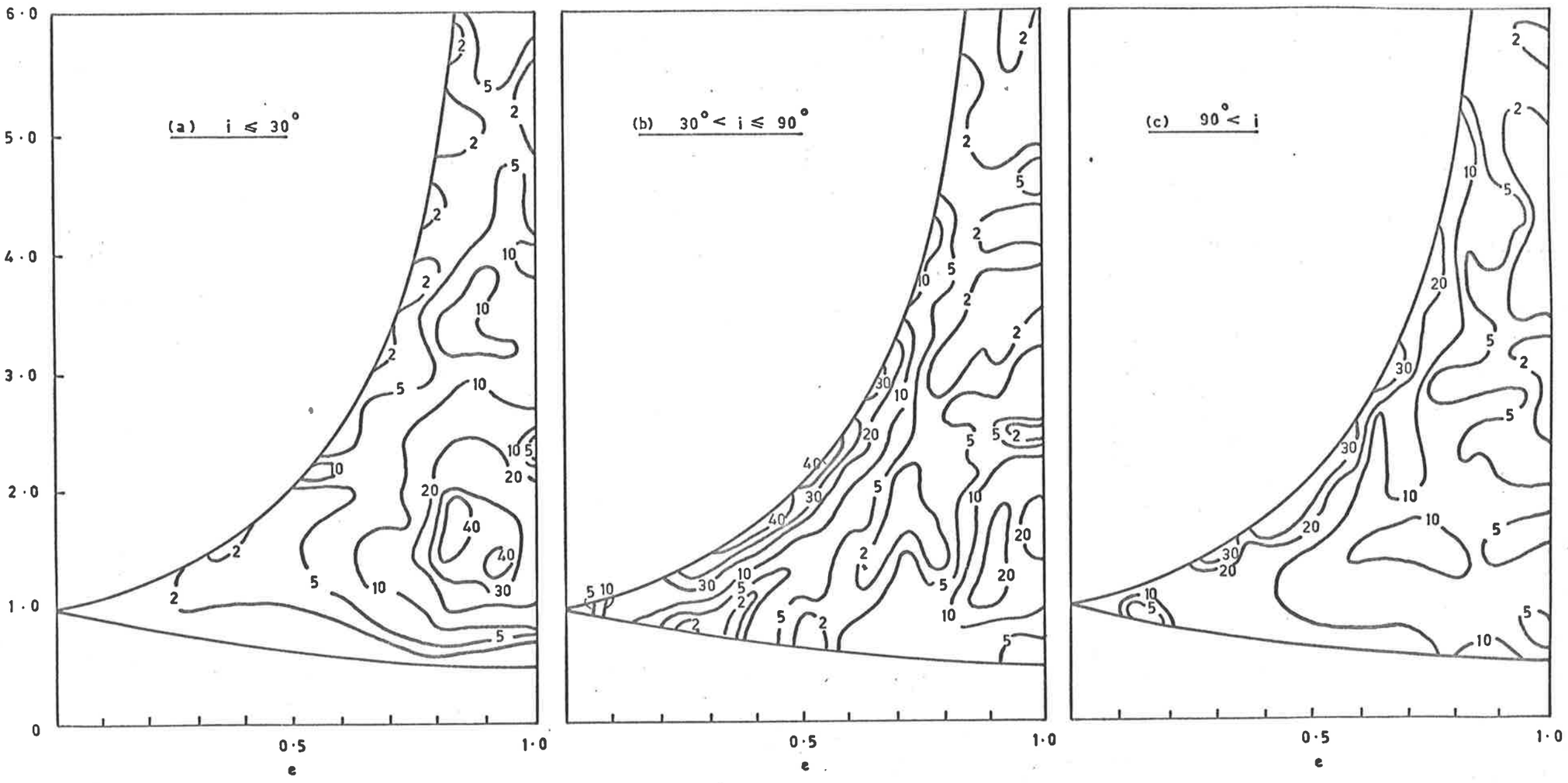

FIG. 8·25 a - e DIAGRAMS FOR VARIOUS INCLINATION RANGES OBSERVED DISTRIBUTIONS. CONTOURS REPRESENT ORBIT DENSITIES IN ARBITRARY UNITS.

meteors of low inclination. More recently Kresák (1969) has considered the relative merits of a number of criteria for distinguishing between cometary and asteroidal orbits, and finds that the zone for probable detection of asteroids lies close to q = 1 a.u. and extends up to a ≃ 2.8 a.u. Kresák predicts a peak near a = 1.5 a.u. due to drag effects bringing the meteoroids into contact with Earth, and a peak near a = 2 a.u. for collisional and perturbational ejection into an Earth-crossing orbit.

Fig. 8.25(a) does exhibit a local concentration of orbits near a = 2.2 a.u., q ≃ 1 a.u., but shows no sign of the predicted concentration at a ≃ 1.5 a.u., q ≃ 1 a.u.

The radio meteor a-e diagram for $30 < i \lesssim 90^\circ$ (Fig. 8.25(b)) shows some similarity to the equivalent distribution for faint photographic meteors, although the concentration near $1 \lesssim a \lesssim 2$ a.u. and $0.8 \lesssim e < 1$ is still again stronger for the radio meteors. The concentration of orbits near q = 1 a.u. occurs for $1 \lesssim a \lesssim 4.4$ a.u. compared with $2 \lesssim a \lesssim 6$ a.u. for the photographic meteors, consistent with the smaller meteors being in a more advanced stage of evolution through action of the Poynting-Robertson effect.

For $i > 90^\circ$ (Fig. 8.25(c)) the radio meteor a-e distribution shows much closer agreement with the equivalent faint photographic meteor distribution given by Kresák, even to the extent of showing a minor concentration of orbits with $1 \lesssim a \lesssim 2$ a.u. and $0.6 \lesssim e \lesssim 0.8$. It does, however, show a loose concentration of orbits along the a(1+e) = 1 boundary as well as for $e \lesssim .4$, a ≃ 1 a.u. not present in the photographic sample.

Fig. 8.26(a), (b), (c) shows the a-e distributions for the present survey corrected for observational and astronomical selection assuming $\eta = 4$ and using the astronomical weighting factor of eqn. 8.1.

As might be expected, the strong orbit concentrations near the $q = 1$ a.u. boundary of Figs. 8.25(b) and (c) result from selection effects and are substantially removed in the corrected distributions of Figs. 8.26(b) and (c). The remaining concentration near $a = 2$ a.u., $e = 0.5$ in Fig. 8.26(b) corresponds to the 'toroidal' group of meteor orbits. Lack of time has prevented the calculation of corrected a-e distributions using an astronomical correction factor of the form of eqn. 8.3. The differences between the two for the purposes of the a-e diagram amounts simply to a weighting difference of $a^{3/2}$ in the direction of the a-axis.

Kresák (1967) employs an astronomical weighting factor similar to that described by eqn. 8.3 to compare distributions in space with observed distributions of comets and asteroids. This is certainly reasonable for asteroids, however, as mentioned in §8.2 Whipple (1954) considers eqn. 8.1 the more appropriate form of the astronomical weighting factor for comparison with comets.

The correction factor of the form of eqn. 8.3 is perhaps the more appropriate form for use in considering meteor orbit evolution. Where short-period orbits are thought to have evolved from long-period orbits the use of eqn. 8.3 is necessary for determination of the true proportions of meteors in various orbit ranges. Possibly the toroidal

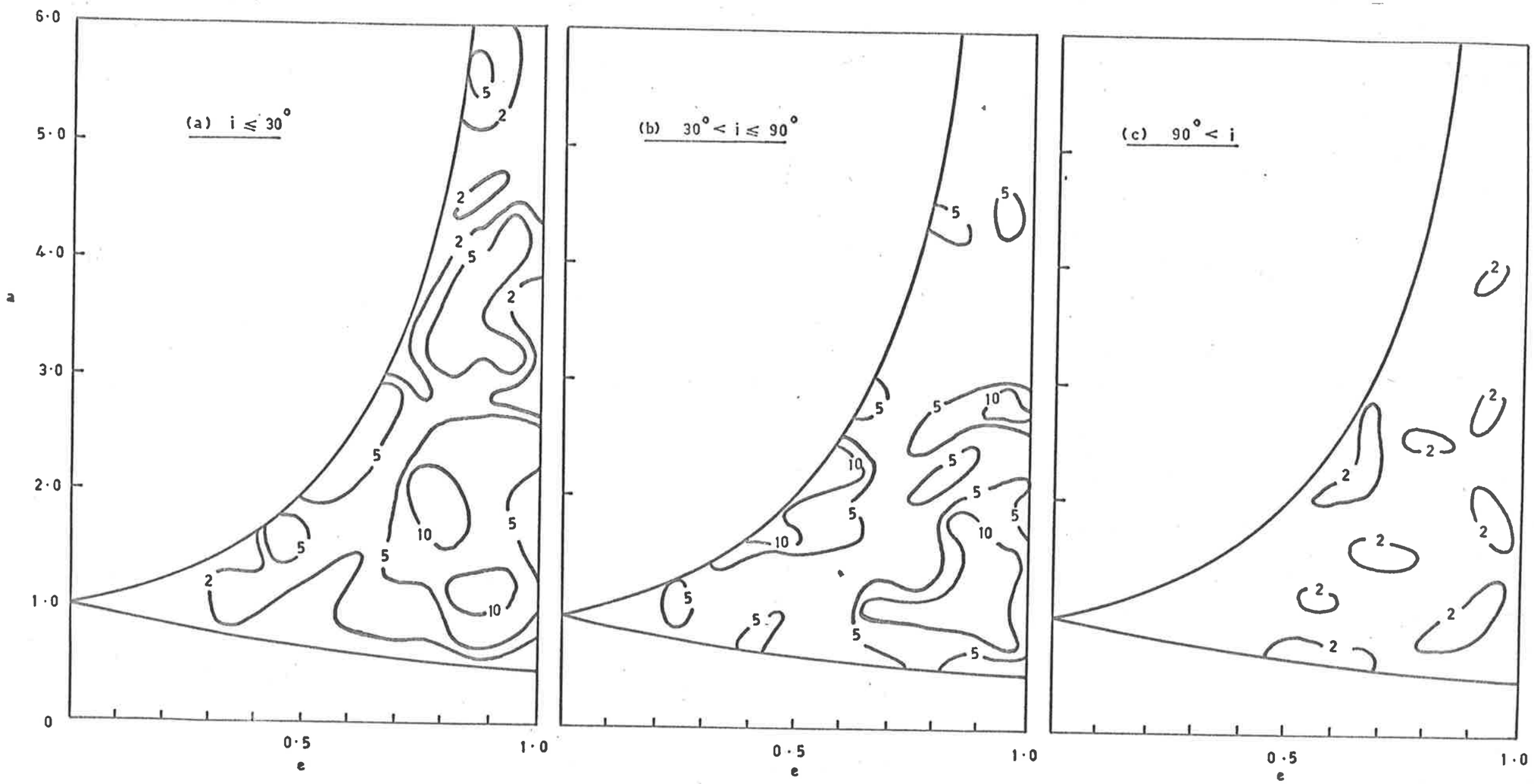

FIG. 8·26 a - e DIAGRAMS FOR VARIOUS INCLINATION RANGES CORRECTED FOR OBSERVATIONAL AND ASTRONOMICAL SELECTION ASSUMING $\eta = 4$. CONTOURS REPRESENT ORBIT DENSITIES (ARBITRARY UNITS).

meteor group of Fig. 8.26(b) would extend smoothly along the q = 1 a.u. boundary towards large a, if eqn. 8.3 were used, instead of terminating as at present near a = 2.5 a.u. through the use of eqn. 8.1.

The significance of the features of the corrected distribution for retrograde orbits (Fig. 8.26(c)) is doubtful, although the agreement between the observed distribution (Fig. 8.25(c)) and that of Kresák's photographic meteors is good. Detection of meteors in retrograde orbits is strongly enhanced by observational selection effects, and the corrected distributions show relatively few meteors in retrograde orbits.

Possibly the most significant feature of the a-e diagrams presented, when compared with those of Kresák (1967) for photographic meteors, is that they indicate the probable evolutionary history of a meteor orbit concentration. Thus, as has already been pointed out, the low eccentricity high inclination meteors apparent at radio magnitudes may well have evolved from orbits like those of the equivalent, more eccentric concentration of photographic meteors.

The strong concentration of low inclination meteors centred on a = 1.5, e = .85 on the other hand shows no signs of having evolved from orbits of larger dimensions, and appears to represent a distinct class of radio meteors. The Geminids and δ-Aquarids are exceptional photographic streams with similar orbits. No comets have been observed with orbits of this type, leading Kashcheev and Lebedinets (1967) to postulate that they are generated by a class of very short-lived comets with similar orbits.

An alternative suggestion is tentatively put forward as a result of the apparent relation of the Geminids to a complex of streams including the Monocerotids (§7.5). Perhaps orbits of this type may arise directly from ejection of material from comets of longer periods than those suggested by Kashcheev and Lebedinets. Such a possibility cannot be discounted without more knowledge of cometary processes. One argument against this seems to be the relative lack of photographic meteors with this type of orbit, implying some selective evolution has also taken place. This argument also mitigates against the source proposed by Kashcheev and Lebedinets.

It does seem, however, that such streams must be young. With such small perihelion distances they should age rapidly. This does not suggest an 'extinct' class of comets, but rather one which should still be active at the present time. Thus the lack of sightings of comets with orbits corresponding to this class of meteor orbits should perhaps indicate that such comets do not exist, and that the derivation of these meteors from the presently known comets may be more likely.

CHAPTER IX

SOME CONCLUSIONS FROM THE PRESENT SURVEY AND AN EXPLANATION OF SOME APPARENT ANOMALIES IN TERMS OF A HYPOTHETICAL ORIGIN FOR COMETS

9.1 RECAPITULATION

This survey has been the first in the Southern Hemisphere to measure orbits of individual meteors down to a limiting magnitude of $M_R = +8$. It has confirmed and extended the results of surveys by a number of other workers and has given some degree of coherence to a variety of observations of the meteoric complex. Where the survey has not been able to provide definitive answers to some questions it has hopefully at least given a clearer idea of what those questions should be.

Before considering their implications, the main findings of this study are summarized.

9.1.1 Atmospheric Deceleration Measurements

Direct measurements of meteoroid deceleration in the atmosphere, combined with what are thought to be reasonable assumptions about meteoroid shape and the ablation process, have enabled computation of the surface area/mass ratio for individual meteoroids. Further assumptions regarding the meteor magnitude and ionising efficiency enable estimates to be made of meteoroid mass and bulk density. While the scatter in individual measurements is considerable, clear trends in the data are apparent when the meteors are grouped according to height range of observation. A selection effect relating meteoroid bulk density to height of

observation (hence height of maximum ionization) is evident, with the highest densities corresponding to the lowest height range.

A similar density - height selection effect has been noted for photographic meteors by Verniani (1964). To the best of the author's knowledge this survey is the first to recognise the effect amongst radio meteors. The data of Evans (1966) shows a similar trend, but Evans has not placed any interpretation on this.

A mean value for meteoroid bulk density of 0.65 gm cm^{-3} has been found for the meteors observed near 90 km height in this survey. This measurement is in good agreement with those of Verniani (1966) and suggests that the meteoroids have either an agglomeritic or pumice-like structure. The apparent densities of the meteors observed at the lowest heights are sufficiently great to confirm that the low densities recorded at greater heights are real, since proportionate scaling of all densities to increase the smaller values would produce densities at lower height ranges which are physically unattainable.

9.1.2 Meteor Streams and Cometary Associations

The orbit data has been systematically searched for associations using the D-criterion method of Southworth and Hawkins (1963). Altogether 40% of the orbits were found to be associated, or 30% if pairs of meteors only were excluded. Some methods of estimating the significance of associations have been critically examined, and it is concluded that associations observed between pairs of orbits at high inclinations are probably significant.

In addition to delineating some well-known major streams, the present stream search has found a number of significant streams not previously observed, and in particular has observed a class of low eccentricity 'toroidal group' meteor streams with radiants at deep Southern declinations. The mean radiant positions for the detected associations have been compared with the predicted radiants for streams possibly associated with comets, listed in the general index-list of Hasegawa (1958), and subsequently checked against the Baldet and de Obaldia (1952) catalogue of comet orbits. Possible associations occur between 34 of the meteor associations and 17 comets.

This survey has found what appear to be indisputable relationships between low and high eccentricity meteor streams, and also between low eccentricity streams and long-period comets. While it seems certain that these meteor streams have been generated by comets, difficulties are encountered in several cases when attempts are made to reconcile the time scale of evolutionary processes with elapsed time since perihelion passage of the parent comets. These difficulties arise from the commonly held notion that meteors originating from a comet should have orbits virtually identical to that of the comet. This notion is questioned later in the chapter in an attempt to resolve the problem.

9.1.3 Orbit Distributions

In contrast to the larger photographic meteors, distributions of stream and sporadic meteors in the present survey show marked similarities. This appears to be due to the decrease in significance of the

major streams at fainter magnitudes, combined with the increased number of minor streams resolved from what would formerly have been considered as sporadic meteors.

Unlike a number of radio meteor surveys to similar limiting magnitude, the present survey has found the distribution of hyperbolic orbits for small meteors to coincide well with that observed for bright photographic meteors. The present equipment is well suited to the detection of high velocity meteors, and their paucity in other radio surveys may be due to limitations of the observing technique rather than due to any distinct differences in the distribution of large orbits between radio and photographic meteors. The hyperbolic orbits are thought to arise from elliptic orbits through perturbation or collisions between particles, and are not considered to indicate that the meteors are of interstellar origin.

Similarities between distributions of shower and sporadic meteors in terms of radiant coordinates and perihelion distance suggest that sporadic meteors probably arise from stream decay, rather than having a distinctly sporadic origin.

Orbital distributions have been presented for various inclination ranges on a-e diagrams, following the use of this effective method of presentation by Kresák (1967) for photographic meteor orbits. Probable evolutionary paths on these diagrams suggest that 'toroidal' radio meteors may have evolved from photographic meteors in more eccentric orbits, while indicating that the short-period orbits of high

eccentricity and low inclination common amongst radio meteors have been generated directly and have not evolved from some other form.

Comparison of orbit distributions for meteors producing underdense, intermediate, and overdense trails shows that the 'toroidal' class of orbit is most pronounced for the underdense meteors, and that high inclination orbits become increasingly important with decreasing meteoroid mass. When distributions are corrected for observational and astronomical selection effects, it is found that very few of the meteors are in retrograde orbits (those which are have a high probability of detection), and that the true number of meteors increases with increasing semi-major axis out to very large orbit dimensions.

9.2 THE RELATION OF METEORS IN ORBITS OF HIGH INCLINATION TO THE SYSTEM OF LONG-PERIOD COMETS

Richter (1963) in the opening paragraph to his book 'The Nature of Comets' is certainly succinct, if rather modest, when he says:

> "If a present-day astrophysicist were asked the question 'What is a comet?', he could summarize the whole of our existing knowledge of these objects in the brief reply:
>
> 'A comet is a cloud of meteors, surrounded (at times) by a gaseous envelope, the whole system moving round the Sun in a path having the form of a conic-section.'"

Certainly our direct knowledge of cometary structure is rather sparse. Nobody is sure whether comets in general have solid nuclei, or whether they are made up of particles moving in individual orbits. A number of theories have been proposed to account for the observed behaviour of

comets, and perhaps the most successful of these is that due to Whipple (1950,1951) known as the 'icy comet model' in which it is suggested that comets may have nuclei consisting of a conglomerate of particles cemented together with ices of such substances as H_2O, NH_3, CH_4 etc.

Comets may be divided into two distinct classes, according to orbital characteristics. One such class corresponds to the short-period comets, which generally have orbits of low inclination. In this class the Jupiter family (those comets with aphelia close to Jupiter's orbit) predominates.

The other class comprises the long-period comets and those observed to have parabolic orbits and is more evenly distributed in inclination (Porter, 1952). The distinction between asteroids and comets is not always clear. Objects have been observed with characteristics of both. This point will be amplified later.

Both asteroids and comets as classes of objects have been proposed as sources of meteoroidal material, and while it is generally agreed that each will contribute to the meteor population, the relative proportions of the meteors arising from each is a matter of some doubt (Kresák, 1969). The author has no wish to enter this controversy, which applies chiefly to meteors with direct orbits near the ecliptic plane, so the following remarks will be mainly confined to a consideration of the highly inclined (and in particular the 'toroidal') meteor orbits which are best observed at faint radio magnitudes.

The large numbers of highly inclined low eccentricity 'toroidal' meteor streams observed in this survey have indicated that this class of meteors, formerly thought to be possibly intrinsically sporadic (Hawkins, 1962) has originated from streams in the normal manner. A comprehensive cometary orbit search has revealed several indisputable associations between such streams and long-period (which for this discussion includes parabolic) comets, with a particularly significant intermediate high eccentricity stream also observed in one case, and a similar relation between smaller associations observed in another case.

Possibly 'toroidal' meteor orbits may arise in other ways as well, for example through the action of perturbing forces as described by Hamid and Youssef (1963), but certainly the present survey has demonstrated that such orbits are in some cases derived from those of the parabolic and near-parabolic long-period comets.

The relation between long-period comets and toroidal group meteors is not altogether unexpected, although one major question at least awaits an answer. There are relatively few retrograde meteors even amongst the high inclination meteors only, whereas the long-period comets are fairly evenly distributed in inclination. One simple explanation of the discrepancy is proposed, but at present is only a hypothesis requiring observational verification. Before considering this problem further, however, it is timely to outline a separate problem which was noted briefly at the end of §7, in regard to the time-scale for evolution of meteor streams. The explanation proposed to explain the retrograde

orbit proportion problem may also provide an answer to the second problem.

The occurrence of toroidal meteor orbits only at faint magnitudes suggests that these orbits may well be the result of evolutionary forces acting differentially on the meteor mass range. On the other hand as mentioned earlier the time scale for such evolutionary processes is quite incompatible with elapsed time since perihelion passage of associated comets for almost all the cometary associations found. If we disregard the possibility of some undiscovered strong drag force existing, capable of massive aphelion contraction in only several revolutions of a particle, two possible explanations of the apparent time scale discrepancy remain.

(i) We may need to study the mechanics of ejection of particles from comets in much greater depth. Long-period comets do not show the preference for the ecliptic plane exhibited by most other members of the solar system so that the relation of their origin to that of the other bodies is not clear. If we suppose, despite this, that the majority of long-period comet nuclei rotate in the direct sense irrespective of whether their orbital motion is direct or retrograde, then there will be two major consequences.

Solar heating on the sunward side of a comet near perihelion in a direct orbit will result in the ejection of material with a velocity component towards the antapex of the comet's way and

into an orbit of lower eccentricity. For a directly rotating comet in a retrograde orbit the ejection of material will be displaced towards the cometary apex. For a long-period or parabolic comet such a displacement would result in the meteors created having hyperbolic orbits in a large number of cases. This model could thus explain at once the dearth of retrograde meteors and the observed tendency for meteor stream orbits to have lower eccentricities than the associated comets. The model is not suggested to be the sole cause of the low eccentricity orbits of the toroidal group. The lack of meteors of photographic size amongst the toroidal group indicates that a mass-dependent process has also contributed.

(ii) A second explanation of the apparent time-scale discrepancies, not mutually exclusive but rather complementary to the comet rotation hypothesis already discussed, is that long-period comets may frequently occur in comet groups. Such groups may possibly have been generated by the disintegration of giant comets at some long past perihelion passage. If this were so then it would be possible that the low eccentricity streams observed to be associated with recent comets may actually be derived from previous members of a comet group.

Rotational motion of comet nuclei is an idea originally considered by Whipple (1950). Observations of cometary motion for a number of short-period comets confirm the action of non-gravitational forces

generally acting strongly away from the Sun with a smaller transverse component in the orbit plane. This is apparently the result of reaction to ejection of gas and/or solid material from the comet, since the degree of the non-gravitational behaviour of the comet tends to decrease with time and is not apparent at all for comets of asteroidal appearance (Marsden, 1969).

Marsden (1968, 1969) has studied the effect of non-gravitational forces on a number of short-period and one long-period comet. For the short-period comets the distribution of the non-gravitational forces suggests generally small rotations, with direct and retrograde sense being about equally probable. The long-period Comet Burnham 1960 II was observed to be accelerating slightly. This implies retrograde spin since the comet has a retrograde orbit. The observations are, however, uncertain and inconclusive, and cannot be considered as representative of the class of long-period comets.

Marsden's calculations which show the transverse component of the non-gravitational force acting on a comet to lie in the orbital plane are all for comets with orbits close to the ecliptic plane. It remains to be seen whether this still applies to orbits of high inclination.

Some problems arise when trying to reconcile the present arguments with the findings of Dohnanyi (1970) (see §2). While these observations give support to Dohnanyi's conclusion that sporadic meteors may be derived from shower meteors and hence from comets, they also indicate at first sight that some form of radiation damping may have resulted in the

streams of low eccentricity observed, whereas according to Dohnanyi collisional processes should have predominated to destroy the stream.

On the other hand, as Dohnanyi himself recognizes, collisional processes will have the highest probability of occurrence near stream perihelion, when the space density of particles within the stream is greatest. Collisions at perihelion could thus result in the creation of lower eccentricity orbits associated with the main stream, in addition to higher eccentricity orbits to balance the conservation laws. The higher eccentricity orbits could in a number of cases be hyperbolic, and thus have a low probability of detection. Such a collision mechanism seems to be the most likely explanation of the definitely hyperbolic orbits observed in the Orionids of this survey (§7.5).

The low eccentricity orbits would be more apparent at fainter magnitudes, since the range of particle sizes amongst collision products should cover smaller particles than the primary cometary ejecta.

It is also apparent that the greatest space density of particles must occur within the comet itself and in its immediate environs, so that collision probabilities may be many orders of magnitude higher at this stage in the life of a stream than subsequently. Consideration should be given to the likelihood of low eccentricity orbits being directly created by collision during stream formation, and the likely relative mass distributions to be encountered in such orbits. Such a process would not only be consistent with Dohnanyi's model of stream dispersal but would remove

the apparent discrepancy in time-scales noted already in regard to the action of the Poynting-Robertson effect in the creation of low eccentricity streams.

9.3 AN INTRA-SOLAR SYSTEM ORIGIN FOR THE SYSTEM OF LONG-PERIOD COMETS

9.3.1 Meteoroid Density

The correlation between meteoroid bulk density and height of observation in the atmosphere discussed in §9.1.1 indicates that the frothing mechanism proposed by Allen and Baldwin (1967) does not contribute significantly for the present meteors. In the course of other work (unpublished) the author has noted that frothing is a common occurrence when a variety of materials are heated in vacuo, and may be caused by the release of even minute quantities of adsorbed or occluded gases under these conditions. The present density-height variation therefore does not show the frothing mechanism of Allen and Baldwin to be unreasonable, for a dense particle but merely that their supposition that the basic meteoroid before ablation is compact is untenable. A reverse mechanism of progressive melt collapse has been proposed (§6.4) for an initially extended or porous structure to explain the observed density-height variation, although height-frequency distributions suggest that this variation may simply reflect a meteoroid bulk density probability distribution consistent with inhomogeneous agglomeritic or pumice-like composition.

Further support for the pumice-like extended structure of the majority of meteors comes from studies of the Arietid/δ-Aquarid

stream complex, the meteors of which have an unusual appearance, being sharp, showing no wakes, and giving off no sparks (Terenteva, 1963). The exceptionally small perihelion distance of this stream (q = 0.06 a.u.) suggests that the meteors may undergo melting near perihelion, in which case a mechanism such as the 'capillary' melt collapse already proposed for an extended porous object might take place near the Sun rather than in the Earth's atmosphere, giving the meteors the greater than usual cohesion observed in their atmospheric flight. Terenteva (1963) considers that meteors will reach temperatures comparable with the melting point of silicates ($\sim 1100^{\circ}K$) near the perihelion distance of the δ-Aquarid stream. Thus the frothing mechanism would be inapplicable to the process of meteor formation from comets near perihelion for the majority of meteors observed, perihelion generally occurring at much larger distances than 0.06 a.u.

It seems more likely that frothing will occur, if at all, earlier in the history of the meteoroid, probably in the formation of the proto-meteoroids belonging to comets.

9.3.2 Cometary Cosmogony

Lyttleton's theory of aggregation of interstellar particles has already been mentioned in §6.4, and has been considered to be consistent with the low densities observed for the majority of meteors. It is in inescapable consequence of solar system dynamics that some particles must be perturbed into hyperbolic orbits from time to time. Evidently this will occur for other planetary systems besides our own, and inter-

stellar particles must result. Lyttleton's theory is basically sound and his mechanism must therefore operate. Whether it accounts for the observed system of long-period comets, though, remains to be proven.

Alternatively, it is possible that the long-period comets may have originated within the Solar System. The origin of the solar system may have been accompanied by an explanation (or series of explosions) which projected material in all directions from the centre with a spread in energies such that an appreciable quantity was in hyperbolic orbits and escaped, while the remainder has condensed into the present long-period comet system.

An explosive origin seems necessary for the generation within the Solar System of material not confined to the ecliptic plane, and it seems that such an event would probably have been distinct from that which generated the system of planets which is virtually confined to the ecliptic plane.

Oort (1950) has suggested that a large cloud may exist at great distances from the Sun, and postulates that such a cloud may have originated as the result of explosion during the disintegration of a planet between Mars and Jupiter, the same explosion also generating the asteroid belt.

This origin for the necessary explosion is possibly more acceptable in terms of total mass distributions than a more primordial explosion, and has the advantage of not implying a catastrophic origin for the Solar System, in keeping with the more widely accepted theories

of Solar System cosmogony. There is, however, no apparent reason in this model for the comets of Oort's cloud to require perturbations by nearby stars to send them towards the Sun. It would appear more reasonable to suggest that they may be in their initial highly eccentric orbits, resulting from the explosion, and because of large orbit dimensions spend very large portions of their time near aphelion.

Such comets may also undergo condensation and gravitational compaction from originally fairly nebulous concentrations of matter. The genesis of such cometary material at the same time as the asteroids is consistent with the disintegration of a planet with a molten core such as the primeval Earth. The already solid and compact crust would form the asteroids, whereas the molten material in such an explosion would have been initially under pressure and containing dissolved gas. Explosion in this case would be analogous to a volcanic eruption with the creation of vast quantities of ash and pumice-like material due to rapid cooling of the magma.

Comparison with other planets shows that we could expect a large planet between Mars and Jupiter to have an enveloping ocean or ice cover composed of such substances as H_2, H_2O, CO_2, CH_4, NH_3, which could provide a source for the cometary ices of Whipple's model.

To account for the vastly different orbital properties of the asteroids and the long-period comets it is only necessary to consider that the final disintegration of the hypothetical planet between Mars and Jupiter was only the last stage of a continuing series of major volcanic

eruptions on the planet. The early eruptions could thus have produced the matter for the long-period comets, while the final disintegration, spreading the energy more evenly between the various fragments, gave rise to the asteroids and a supply of rapidly cooling magma from which the short-period comets originated.

The number of asteroidal bodies observed with cometary orbits is quite large when consideration is taken of the low probability of detection, and the existence of many more such bodies is implied. The notion of dense cometary nuclei at least in some cases is consistent with the idea of asteroidal material being present, and the Apollo asteroids have been suggested by Öpik (1963) to be extinct comets. This would seem to imply for these bodies an origin distinct from the asteroids, since comets with asteroidal orbits are apparently far less prevalent than asteroids with cometary orbits. It may be that many asteroids are surrounded by dust clouds but have no visible coma.

Objections to an eruptive origin for cometary material have been made on the grounds that the necessary escape velocities for particles to leave a planet's gravitational field are improbably high, yet these objections appear to be based upon caution rather than any comprehensive knowledge of the dynamics of volcanic processes.

Vsekhsvyatskii (1967) finds evidence to suggest a separate eruptive origin in relatively recent times for the system of short-period comets and considers that the long-period and parabolic comet system may have originated in more ancient and more intense volcanic

activity. He considers it probable that short-period comets are still being formed from time to time, and suggests that the first appearances of Comets 1965b, 1965c, and 1966 VIII, which "emerged nearly simultaneously from Jupiter's sphere of influence in 1961" are connected with the formation of a dark equatorial belt around the planet at that time. This belt, which did not diappear completely until the end of 1965, he suggests is an ash cloud arising from volcanic activity.

If the long-period comet system has originated within the Solar System in an explosive or eruptive manner, the projected material would carry with it some of the angular momentum from the original system. Angular momentum would be conserved in any subsequent condensation or agglomeration by appropriate changes in the angular velocities of the systems of particles. It could also be re-distributed by collision processes. With predominantly direct rotation apparent amongst the major members of the Solar System it is reasonable to expect that the total angular momentum of the cometary system would result in an excess of comets exhibiting direct rotation. Conversely if one could show that there was a preference for direct rotation amongst long-period comets, this would give support to an eruptive intra-solar system origin for these objects.

9.3.3 Conclusions

Reliable determinations of non-gravitational motion in some comets (Marsden, 1968,1969) have indicated that those comets are rotating. It seems probable that cometary rotation is the rule rather than the

exception, and it is certain that astronomers will be searching for this effect amongst other comets with keen interest.

In view of our scant knowledge of cometary structure, it is not surprising that little is known of the mechanics of meteoroid ejection from comets. In any model the effects of inter-particle collisions and cometary rotation should be included.

In §9.2 it was indicated that a discrepancy between the numbers of highly inclined meteors in retrograde orbits, and the distribution with inclination of long-period comets could be reconciled with a cometary origin for the meteors if the comets could be shown to have predominantly direct angular momentum. Observations of comets in future will no doubt provide further evidence of rotational motion. Whether such observations will be sufficiently general to show any overall preference for direct or retrograde rotation, or the lack of it, amongst long-period comets remains to be seen. Direct observation of a number of comets near perihelion with a series of space-probes seems most desirable, and could find the answers to a number of important questions.

In the meantime we may find out a great deal from the study of meteors as products of cometary decay. This survey has demonstrated that at least some of these meteors do originate from the long-period comets.

In §9.3.1 it was argued that the low densities observed for the present meteoroids are real, and cannot arise from frothing in the atmosphere. These densities are consistent with those of volcanic pumices.

In §9.3.2 a possible eruptive or explosive origin for the system of long-period comets was proposed. Two pieces of circumstantial evidence support this hypothesis, namely the pumice-like densities of the observed meteoroids and the low number of retrograde meteors. The cometary rotation link remains to be shown, and even then would not give positive proof of the proposed origin. Nevertheless, the above line of argument certainly illustrates clearly the importance of a thorough investigation of the properties of meteoroids to our understanding of cosmogony.

9.4 FUTURE WORK

It seems likely that many of the low eccentricity, high inclination streams observed in this survey should be annual if their shape is attributable to the Poynting-Robertson effect, since their apparent age implies that the members should be spread fairly uniformly around their orbits. Lack of annual periodicity, on the other hand, would indicate a recent origin, conceivably linked with collision processes or rotation at the time of ejection of the material from the parent comet. Further study of these streams in the Southern Hemisphere, as well as a search for similar streams in the Northern Hemisphere, should add considerably to our knowledge.

A theoretical investigation of the importance of collision processes at the time of stream formation from comets would be worthwhile. This could be undertaken by measuring meteoroid flux densities to different limiting masses in known streams, and extrapolating these

back in time to a particle volume number density in a small region near the generating comet at perihelion. Assumptions regarding the initial mass distribution, and the particle loss rate from the comet-stream system between formation and the present, would enable estimates of collision probabilities for meteoroids at stream formation to be made.

The deceleration measurements carried out in this survey, while presently yielding interesting information, are certainly capable of refinement. Due to operational difficulties encountered with the long-distance outstation, the measurements for this survey were generally over trail lengths of 6 km or less. Satisfactory operation of the long-distance outstation would enable routine measurements of deceleration over distances of up to 20 km, and should greatly improve the resolution of the determinations of meteoroid surface area/mass ratio.

The study of streams is of great importance to our understanding of meteor origins, in view of the common origin implied for members of a stream. As noted in §7 a number of quite well-defined streams appear to belong to less well defined stream complexes, and through common membership of such complexes such apparently distinct streams as the Geminids and the Monocerotids may possibly be related. Further investigation of this possibility is certainly warranted.

While radio meteor surveys at fainter magnitudes are of great importance, dispersion may be more advanced and streams less easily determined.

The present survey has contributed significantly to our knowledge of radio meteor astronomy and has indicated the desirability of further studies of radio meteors to a similar limiting magnitude.

APPENDIX

Meteor Associations

Ident.	Mean Date	No.	$\frac{1}{a}$ (a.u.$^{-1}$)	q (a.u.)	e	i (deg.)	ω (deg.)	Ω (deg.)	α (deg.)	δ (deg.)	V_o (km sec^{-1})	$\overline{D(N,N)}$	
DECEMBER													
12.01	13	4	.69	.09	.93	2.0	331	261	111	23	38	.05	
12.02	14	6	.37	.33	.85	7.1	117	82	95	18	32	.14	
12.03	14	3	.22	.74	.77	9.4	65	82	71	5	23	.12	
12.04	12	5	.33	.50	.83	20.4	95	80	88	2	30	.13	
12.05	14	20	.74	.13	.90	18.2	327	261	112	30	36	.12	Geminids
12.06	15	7	.44	.97	.56	57.3	344	82	135	-63	35	.19	
12.07	13	6	.84	.98	.16	69.5	0	81	141	-48	37	.14	
12.08	13	3	94	.98	.08	74.5	1	82	145	-45	39	.05	
12.09	13	3	.13	.19	.98	39.9	130	82	106	6	42	-	Monoc-erotids
12.10	12	2	.65	.12	.92	9.4	146	80	108	19	38	.03	
12.11	11	2	.52	.15	.92	8.0	141	80	104	19	37	.02	
12.12	12	2	.41	.89	.63	19.4	318	80	294	-79	20	.07	
12.13	13	2	.85	.23	.80	17.6	44	261	237	- 8	31	.09	
12.14	12	2	.54	.95	.47	29.0	333	81	84	-84	21	.09	
12.15	11	2	.52	.14	.93	30.9	322	259	109	34	40	.04	
12.16	13	2	.60	.11	.93	38.2	33	261	232	- 6	40	.06	
12.17	12	2	.48	.79	.62	38.6	299	80	212	-74	28	.04	
12.18	15	2	35	.45	.84	75.9	260	83	203	-50	46	.05	
12.19	14	2	-.17	.36	1.09	110.8	102	82	126	- 6	60	.05	
12.20	13	2	.82	.44	.64	122.4	65	261	204	16	54	.10	
12.21	14	2	.02	.99	.98	169.3	6	83	169	- 2	73	.08	
12.22	13	2	.09	.86	.92	149.4	137	260	190	14	69	.06	

Meteor Associations (Cont'd)

Ident.	Mean Date	No.	$\frac{1}{a}$ (a.u.$^{-1}$)	q (a.u.)	e	i (deg.)	ω (deg.)	Ω (deg.)	α (deg.)	δ (deg.)	V_o (km sec^{-1})	$\overline{D(N,N)}$	
JANUARY													
1.01	22	3	.34	.98	.64	74.3	7	122	160	-63	43	.13	Carinids
1.02	22	2	.36	.19	.93	8.8	133	122	143	10	38	.05	
1.03	21	2	.24	.96	.77	30.4	340	121	37	-68	24	.06	
1.04	22	2	.43	.98	.57	50.9	358	122	123	-71	32	.05	
1.05	22	2	.35	.59	.79	145.4	264	302	195	11	64	.07	
1.06	21	2	.59	.37	.78	155.4	296	301	188	7	60	.05	
FEBRUARY													
2.01	13	3	.48	.36	.82	4.5	246	144	316	-21	31	.07	
2.02	15	6	.54	.27	.85	1	125	147	164	6	32	.06	
2.03	14	3	.21	.60	.87	18.0	98	325	320	7	29	.10	
2.04	15	3	.49	.19	.90	7.8	315	326	169	9	35	.05	
2.05	12	5	.48	.61	.69	8.1	86	143	148	25	24	.08	
2.06	14	3	.68	.20	.86	12.2	137	145	167	- 2	33	.05	
2.07	14	4	.62	.23	.85	20.4	313	325	174	16	33	.07	
2.08	14	3	1.11	.04	.96	33.6	13	326	284	-16	37	.09	
2.09	12	3	.14	.36	.93	49.9	43	143	133	-50	35	.10	
2.10	14	3	.11	.98	.89	47.2	12	145	110	-65	32	.05	
2.11	13	5	.34	.98	.67	48.4	354	145	99	-76	31	.13	
2.12	14	3	.76	.99	.25	54.1	3	146	155	-77	31	.05	
2.13	14	9	.42	.93	.60	62.0	33	145	152	-65	37	.19	
2.14	14	47	.56	.93	.44	61.9	340	145	179	-83	36	.39	
2.15	13	4	.08	.95	.93	70.2	330	144	250	-86	44	.13	
2.16	12	5	.44	.98	.56	118.0	171	323	241	15	59	.13	
2.17	13	3	1.24	.46	.43	141.5	322	323	225	1	54	.11	
2.18	14	11	.44	.82	.62	2.1	299	144	346	-24	18	.23	

Meteor Associations (Cont'd)

Ident.	Mean Date	No.	$\frac{1}{a}$ (a.u.$^{-1}$)	q (a.u.)	e	i (deg.)	ω (deg.)	Ω (deg.)	α (deg.)	δ (deg.)	V_o (km sec^{-1})	$\overline{D(M,N)}$	
2.19	13	2	.72	.51	.63	1.7	75	324	318	-14	23	.05	
2.20	12	2	.61	.08	.95	.9	27	323	296	-21	40	.03	
2.21	11	2	.56	.67	.62	5.1	99	323	326	- 4	21	.04	
2.22	15	2	.71	.09	.93	4.0	331	327	177	3	37	.04	
2.23	15	2	.60	.37	.78	5.3	296	326	162	13	28	.04	
2.24	12	2	.48	.46	.78	5.3	283	323	154	17	27	.03	
2.25	14	2	1.17	.03	.97	15.0	348	325	188	0	37	.04	
2.26	15	2	1.13	.25	.72	12.6	323	327	181	12	25	.05	
2.27	13	2	.25	.25	.93	18.1	123	144	158	- 2	37	.04	
2.28	14	2	.63	.10	.93	23.8	330	324	178	10	38	.05	
2.29	12	2	.73	.84	.39	44.2	297	143	339	-81	28	.08	
2.30	13	2	.09	.97	.91	47.8	14	144	112	-64	33	.03	
2.31	14	2	.65	.15	.90	48.4	322	325	186	18	40	.08	
2.32	15	2	.10	.52	.97	53.8	87	146	153	-31	41	.10	
2.33	15	2	.63	.70	.56	61.1	79	146	161	-50	37	.10	
2.34	12	2	.70	.79	.45	63.7	290	143	272	-79	37	.05	
2.35	11	2	.45	.98	.55	65.5	4	143	161	-74	39	.08	
2.36	16	2	.21	.98	.78	73.6	13	147	170	-72	44	.07	
2.37	12	2	-.23	.94	1.24	76.0	337	144	224	-85	49	.09	
2.38	14	2	.70	.98	.31	76.3	11	145	191	-70	41	.04	
2.39	15	2	.50	.85	.57	87.1	307	146	247	-71	48	.09	
2.40	15	2	.06	.97	.92	86.6	345	147	215	-75	51	.05	
2.41	12	2	.19	.94	.82	96.8	332	143	227	-67	54	.04	
2.42	14	2	.02	.79	1.00	101.6	307	145	256	-64	57	.06	
2.43	15	2	.40	.97	.61	105.0	344	146	223	-61	55	.09	
2.44	14	2	.49	.94	.53	104.1	210	324	235	24	54	.07	
2.45	15	2	.20	.87	.81	114.7	43	146	202	-48	60	.10	
2.46	12	2	.46	.22	.90	119.9	311	323	201	11	54	.06	
2.47	13	2	.40	.51	.79	131.8	265	144	258	-44	60	.08	
2.48	13	2	.43	.42	.81	138.8	288	324	210	6	60	.09	
2.49	13	2	.60	.92	.48	145.4	39	144	218	-35	64	.06	

Meteor Associations (Cont'd)

Ident.	Mean Date	No.	$\frac{1}{a}$ (a.u.$^{-1}$)	q (a.u.)	e	i (deg.)	ω (deg.)	Ω (deg.)	α (deg.)	δ (deg.)	V_o (km sec^{-1})	$\overline{D(M,N)}$	
2.50	14	2	.32	.64	.77	152.8	260	324	217	- 1	65	.09	
2.51	14	2	.56	.96	.46	153.4	205	325	232	- 4	65	.04	
2.52	16	2	.19	.97	.82	155.6	165	327	242	- 7	70	.07	
2.53	10	2	.43	.05	.98	174.7	202	141	273	-24	54	.05	
2.54	14	2	.44	.96	.58	178.8	159	145	236	-20	68	-	
MARCH													
3.01	19	7	.59	.18	.89	1.8	42	359	338	- 8	35	.08	
3.02	19	3	.08	.75	.91	7.3	62	178	159	- 5	23	.09	
3.03	19	5	.61	.23	.86	19.4	312	358	203	3	33	.07	
3.04	18	11	.47	.98	.53	55.3	347	178	51	-81	34	.22	
3.05	19	10	.10	.98	.87	58.3	346	178	50	-78	38	.17	
3.06	18	5	.63	.88	.41	65.7	57	177	195	-74	37	.17	
3.07	19	3	.49	.65	.65	57.3	83	179	184	-58	36	.10	
3.08	17	3	.04	.93	1.00	61.9	28	177	154	-73	40	.13	
3.09	19	3	.05	.76	.90	59.3	58	178	173	-60	40	.09	
3.10	17	4	.35	.95	.67	73.6	332	177	332	-79	43	.11	
3.11	19	3	.71	.93	.34	85.2	317	179	297	-72	45	.11	
3.12	19	7	.37	.94	.62	92.8	29	178	241	-71	50	.22	
3.13	21	4	.22	.99	.76	95.9	353	181	281	-72	53	.12	
3.14	19	6	.22	.98	.62	121.6	13	178	262	-56	60	.18	
3.15	20	3	.85	.66	.43	137.4	97	179	250	-43	57	.11	
3.16	19	4	.12	.42	.93	141.8	282	359	240	- 4	62	.13	
3.17	17	2	.32	.41	.86	1.2	105	177	183	- 3	30	.03	
3.18	19	2	.40	.10	.96	8.0	148	178	202	-12	40	.05	
3.19	19	2	.16	.76	.88	10.3	61	178	157	-10	23	.04	
3.20	18	2	.27	.56	.85	10.7	88	177	172	-11	27	.03	

Meteor Associations (Cont'd)

Ident.	Mean Date	No.	$\frac{1}{a}$ (a.u.$^{-1}$)	q (a.u.)	e	i (deg.)	ω (deg.)	Ω (deg.)	α (deg.)	δ (deg.)	V_o (km sec^{-1})	$\overline{D(M,N)}$	
3.21	20	2	.43	.46	.80	11.5	103	179	181	-14	28	.03	
3.22	19	2	.50	.32	.84	13.9	300	358	197	4	31	.04	
3.23	21	2	.62	.31	.81	18.7	122	180	191	-21	31	.03	
3.24	19	2	.44	.29	.86	23.8	302	358	201	9	34	.05	
3.25	18	2	1.04	.06	.94	21.4	162	178	211	-19	37	.09	
3.26	17	2	.27	.33	.91	24.6	66	357	337	8	36	.05	
3.27	19	2	.06	.32	1.04	26.0	109	178	184	-19	40	.09	
3.28	18	2	.89	.34	.70	37.8	308	357	215	17	30	.07	
3.29	21	2	.30	.98	.70	39.8	17	180	114	-65	27	.05	
3.30	19	2	.15	.63	.88	52.5	282	178	0	-50	38	.10	
3.31	18	2	-.40	.20	1.08	49.9	58	357	330	7	49	.03	
3.22	20	2	.56	.24	.87	39.5	27	0	329	13	36	.05	
3.33	18	2	.87	.87	.25	49.4	291	179	3	-75	29	.05	
3.34	21	2	.73	.13	.89	51.8	211	177	330	-32	39	.08	
3.35	19	2	.40	.13	.93	54.0	324	0	216	4	42	.09	
3.36	18	2	.28	.85	.75	65.8	48	178	180	-69	40	.08	
3.37	19	2	.49	.99	.51	68.4	349	178	324	-86	39	.04	
3.38	18	2	.49	.08	.94	67.7	26	356	318	- 1	44	.08	
3.39	18	2	.31	.83	.74	73.4	307	178	341	-69	44	.07	
3.40	18	2	.35	.93	.68	76.0	328	177	328	-77	44	.04	
3.41	18	2	-.03	.98	1.03	88.8	2	178	263	-79	53	.08	
3.42	18	2	.79	.34	.73	128.3	125	178	232	-39	54	.07	
3.43	18	2	.05	.71	.96	130.3	245	357	247	4	64	.07	
3.44	19	2	.67	.99	.33	138.8	348	177	270	-46	61	.09	
3.45	21	2	.78	.95	.26	141.1	40	181	266	-44	60	.07	
3.46	19	2	.32	.85	.72	145.4	49	179	253	-41	65	.07	
3.47	19	2	.49	.96	.53	146.3	205	359	264	- 5	64	.09	
3.48	17	2	.91	.83	.24	154.4	279	176	274	-36	60	.10	
3.49	20	2	.85	.68	.42	173.6	86	0	77	22	61	.08	
3.50	20	2	.42	.74	.69	177.4	292	179	285	-24	67	-	

Meteor Associations (Cont'd)

Ident.	Mean Date	No.	$\frac{1}{a}$ (a.u.$^{-1}$)	q (a.u.)	e	i (deg.)	ω (deg.)	Ω (deg.)	α (deg.)	δ (deg.)	V_o (km sec^{-1})	$\overline{D(X,Y)}$	
6.01	11	4	.44	.52	.77	1.3	97	260	262	-25	26	.04	
6.02	10	3	.33	.93	.68	14.0	216	79	234	20	18	.11	
6.03	13	3	.28	.04	.98	2.4	18	82	47	18	42	.05	Arietids
6.04	11	9	.54	.02	.99	18.0	14	81	44	19	43	.09	
6.05	11	32	.36	.08	.96	17.4	28	81	49	23	41	.19	
6.06	11	4	.67	.02	.99	30.9	11	80	39	19	43	.06	
6.07	12	6	.65	.06	.96	38.2	203	261	48	9	41	.09	
6.08	10	4	.87	.11	.90	33.5	152	259	297	-34	35	.10	
6.09	11	13	.54	.15	.90	39.5	224	80	289	- 6	38	.19	
6.10	9	4	.39	.37	.86	43.3	292	79	280	6	37	.09	
6.11	10	5	1.10	.14	.84	66.3	333	80	303	3	37	.11	
6.12	11	6	.51	.12	.92	65.3	214	261	47	- 2	43	.13	
6.13	11	3	.12	.29	.96	68.1	297	80	290	5	46	.09	
6.14	12	3	.20	.90	.81	171.0	317	261	4	- 4	68	-	
6.15	11	3	.15	.27	.59	145.3	6	80	349	10	48	.11	
6.16	13	4	.03	.42	.98	166.4	280	80	323	- 9	65	.12	
6.17	11	8	.19	.99	.79	177.7	165	80	354	- 1	69	-	
6.18	13	3	.14	.51	.89	177.8	266	262	16	6	65	-	
6.19	12	2	.79	.22	.82	1.1	43	80	56	21	31	.04	ζ-Perseids
6.20	12	2	.56	.06	.96	12.7	336	81	292	-19	40	.10	
6.21	12	2	.58	.31	.82	4.8	237	261	65	18	30	.05	ζ-Perseids
6.22	11	2	.46	.26	.88	5.8	127	260	278	-27	33	.04	
6.23	12	2	.84	.13	.89	11.8	217	261	52	13	34	.03	
6.24	10	2	.56	.07	.96	13.1	205	259	48	14	40	.05	

Meteor Associations (Cont'd)

Ident.	Mean Date	No.	$\frac{1}{a}$ (a.u.$^{-1}$)	q (a.u.)	e	i (deg.)	ω (deg.)	Ω (deg.)	α (deg.)	δ (deg.)	V_o (km sec^{-1})	$\overline{D(M,N)}$
6.25	11	2	.20	.26	.95	16.3	57	80	60	30	37	.05
6.26	12	2	.72	.02	.99	18.6	191	261	43	14	42	.04
6.27	13	2	.51	.22	.89	20.5	228	261	61	9	35	.05
6.28	13	2	.98	.18	.82	20.4	215	261	53	7	30	.05
6.29	11	2	.04	.17	1.00	21.5	44	80	55	28	43	.05
6.30	13	2	.45	.10	.95	24.0	212	262	54	11	40	.02
6.31	13	2	.28	.12	.97	28.4	322	82	287	-13	42	.01
6.32	14	2	1.07	.17	.81	33.1	211	263	51	- 0	31	.05
6.33	9	2	.56	.18	.90	37.9	318	78	285	- 6	38	.04
6.34	11	2	.92	.10	.90	61.6	153	259	307	-37	39	.09
6.35	10	2	.75	.13	.91	69.6	213	259	44	- 4	42	.04
6.36	12	2	.29	.42	.85	123.6	286	81	314	6	57	.09
6.37	13	2	.34	.64	.78	126.5	261	82	321	12	59	.04
6.38	11	2	.26	.92	.76	128.1	321	260	14	-25	62	.08
6.39	12	2	.20	.27	.94	143.0	59	81	20	22	59	.09
6.40	11	2	.74	.48	.64	145.1	290	80	326	2	58	.06
6.41	13	2	.31	.78	.76	157.6	297	262	12	- 7	66	.04
6.42	9	2	1.05	.69	.27	158.0	301	78	338	2	57	.09
6.43	10	2	.59	.93	.50	162.3	118	79	356	8	64	.08
6.44	8	2	.30	.71	.79	167.3	108	78	3	8	66	.08
6.45	12	2	.28	.53	.85	179.9	267	261	80	23	28	-
6.46	10	2	.40	.71	.64	173.3	257	79	334	- 7	64	.06
OCTOBER												
10.01	16	3	.24	.47	.90	8.2	96	23	28	3	31	.05
10.02	17	3	.31	.43	.86	8.9	104	24	32	4	31	.03
10.03	17	3	.15	.92	.85	138.2	34	23	101	- 0	66	.13
10.04	17	4	.29	.51	.84	145.0	94	20	87	8	63	.15
10.05	17	6	.14	.65	.85	161.8	76	24	94	14	67	.13

Meteor Associations (Cont'd)

Ident.	Date	No.	$\frac{1}{a}$ (a.u.$^{-1}$)	q (a.u.)	e	i (deg.)	ω (deg.)	Ω (deg.)	α (deg.)	δ (deg.)	V_o (km sec^{-1})	$\overline{D(M,N)}$	
(b) Double Intersections													
D.01	6.09-14	6	.58	.30	.82	7.1	69	81	65	27	30	.15	ζ- Perseids Southern Taurids
	10.15-19	49					129	24	44	11	31		
D.02	2.12	1	.60	.39	.76	.6	54	323	308	-21	30	.09	
	6.10-13	6					114	261	271	-24	28		
D.03	12.14-16	2	.50	.61	.67	54.2	276	79	288	25	34	.13	
	6.10-11	2					277	83	210	-62	37		
D.04	12.13-13	2	.22	.57	.86	144.8	88	81	142	- 2	64	.11	
	6.12	1					98	81	8	21	63		
D.05	12.12	1	.34	.54	.82	.4	91	80	81	24	27	.03	
	6.11-14	2					84	81	81	23	27		
D.06	6.10	1	.82	.44	.63	1.9	65	78	64	24	23	.03	
	10.16	1					118	23	35	12	23		
D.07	6.12	1	.53	.59	.68	3.7	269	261	80	18	23	.01	
	12.12	1					269	261	80	29	23		
D.08	2.10	1	.53	.31	.83	3.4	119	141	156	8	31	.04	
	10.17	1					58	204	189	- 1	31		
D.09	6.12	1	.58	.65	.62	154.4	259	81	330	4	62	.10	
	12.16	1					269	84	187	- 4	63		
D.10	6.12	1	.96	.94	.09	152.3	166	81	347	10	60	.08	
	12.16	1					131	84	167	-10	59		
D.11	6.14	1	.61	.62	.60	104.7	97	263	343	-45	51	.10	
	12.13	1					95	261	209	23	52		

REFERENCES

Allen, H. J., and Baldwin, B. S. Jr., 1967, J. geophys. Res. 72, 3483.

Andrianov, N. S., Kurganov, R. A., Nasirov, A. M. and Sidorov, V. V., 1968, I.A.U. Symposium No. 33 "Physics and Dynamics of Meteors", Kresák and Millman (eds), D. Riedel Co., Dordrecht, Holland, 14.

Andrianov, N. S., Pupysev, U. A., and Sidorov, V. V., 1970, Mon. Not. R. astr. Soc., 148, 227.

Babadzhanov, P., 1963, Smithson. Contr. Astrophys. 7, 287.

Babadzhanov, P., and Kramer, E. N., 1967, Smithson. Contr. Astrophys. 11, 67.

Baker, K., and Forti, G., 1966, Harvard Radio Meteor Project Res. Rep. No. 14.

Baldet, F., and De Obaldia, G., 1952, Catalogue Général des Orbites des Cometès de l'an -466 à 1952. Observatoire de Paris, Section d'Astrophysique de Meudon.

Barber, D., Sutcliffe, H. K., and Watkins, C. D., 1962, J. atmos. terr. Phys. 24, 585.

Bayrachenko, I. V., 1965, Geomag. Aeron. 5, 460.

Berg, O. E., and Secretan, L., 1967, Smithson. Contr. Astrophys. 11, 271.

Bertaux, J. -L., and Blamont, J., 1970, C.R. Acad. Sc. Paris, Ser. B270, 1581.

Brown, N., and Elford, W. G., 1970, Research Rep. No. ADP93, Physics Dept., University of Adelaide.

Ceplecha, Z., 1967, Smithson. Contr. Astrophys. 11, 35.

Ceplecha, Z., 1968, Smithson. Astrophys. Obs. Spec. Rep. No. 279.

Ceplecha, Z., 1970, Rep. Comm. 22 I.A.U., in 'Reports on Astronomy', D. Riedel Co., Dordrecht, Holland, 207.

Cook, A. F., 1970, Smithson. Astrophys. Obs. Spec. Rep. No. 324.

Davies, J. G., and Gill, J. C., 1960, Mon. Not. R. astr. Soc. 121, 437.

Dohnanyi, J. S., 1970, J. geophys. Res. 75, 3468.

Elford, W. G., Hawkins, G. S., and Southworth, R. B., 1964, Harvard Radio Meteor Project Res. Rep. No. 11.

Elford, W. G., 1967, Smithson. Contr. Astrophys. 11, 121.

Ellyett, C., and Roth, K., 1955, Aust. J. Phys. 8, 390.

Eshleman, V. R., and Gallagher, P. B., 1962, Astr. J. 67, 245.

Evans, J. V., 1966, J. geophys. Res. 71, 171.

Gartrell, G., 1971, Research Report No. ADP104, Physics Dept., University of Adelaide.

Gill, J. C., and Davies, J. G., 1956, Mon. Not. R. astr. Soc. 116, 105.

Greenhow, J. S., and Hall, J. E., 1960, Mon. Not. R. astr. Soc. 121, 183.

Hajduk, A., 1970, Bull. astr. Insts Csl. 21, 37.

Hamid, S. E., and Youssef, M. N., 1963, Smithson. Contr. Astrophys. 7, 309.

Hasegawa, I., 1958 (Revis. 1962), General Index-List. 'Theoretical Radiant-Points of Meteors Associated with Comets'. Institut d'Astrophysique; Documentation des Observateurs. Bull. 11, No. 1 (Fasc. 3).

Hawkins, G. S., 1956, Astrophys. J. 124, 311.

Hawkins, G. S., and Southworth, R. B., 1958, Smithson. Contr. Astrophys. 2, 349.

Hawkins, G. S., Southworth, R. B., and Steinon, F., 1959, Astr. J. 64, 183.

Hawkins, G. S., 1962, Astr. J. 67, 241.

Hawkins, G. S., and Southworth, R. B., 1963, Harvard Radio Meteor Project Res. Rep. No. 2.

Herlofson, N., 1948, Rep. Prog. Phys. 11, 444.

Herlofson, N., 1951, Ark. Fys. 3, 247.

Hicks, G. T., Barton, G. G. Jr., and Dambeck, W. J., 1967, Smithson. Contr. Astrophys. 11, 95.

Hindley, K. B., and Houlden, M. A., 1970, Nature 225, 1232.

Jacchia, L. G., 1949, Harvard Reprint Series II-31.

Jacchia, L. G., 1958, Harvard Reprint Series II-122.

Jacchia, L. G., and Whipple, F. L., 1961, Smithson. Contr. Astrophys. 4, 97.

Jacchia, L. G., Verniani, F., and Briggs, R. E., 1965, Smithson. Astrophys. Obs. Spec. Rep. No. 175.

Jones, J., and Kaiser, T. R., 1966, Mon. Not. R. astr. Soc., 133, 411.

Kaiser, T. R., and Closs, R. L., 1952, Phil. Mag. (7) 43, 1.

Kaiser, T. R., 1955, Spec. Supp. J. atmos. terr. Phys. 2, 55.

Kashcheev, B. L., and Lebedinets, V. N., 1961, Resultaty Issled. MGG-Ionosfera i Meteory 7, 1.

Kashcheev, B. L., and Lebedinets, V. N., 1963, Smithson. Contr. Astrophys. 7, 19.

Kashcheev, B. L., and Lebedinets, V. N., 1967, Smithson. Contr. Astrophys. 11, 183.

Kashcheev, B. L., Lebedinets, V. N., and Lagutin, M. F., 1967, Resultaty Issled. MGP-Issled. Meteorov, No. 2, 1.

Kresák, L., 1967, Smithson. Contr. Astrophys. 11, 9.

Kresák, L., 1968, I.A.U. Symposium No. 33 "Physics and Dynamics of Meteors", Kresák and Millman (eds), D. Riedel Co., Dordrecht, Holland, 391.

Kresák, L., 1969, Bull. astr. Insts Csl. 20, 177.

Lebedinets, V. N., and Kashcheev, B. L., 1967, Soviet Astr. 10, 683.

Lebedinets, V. N., 1968, I.A.U. Symposium No. 33 "Physics and Dynamics of Meteors", Kresák and Millman (eds), D. Riedel Co., Dordrecht, Holland, 241.

Lebedinets, V. N., and Sosnova, A. K., 1968, I.A.U. Symposium No. 33 "Physics and Dynamics of Meteors", Kresák and Millman (eds), D. Riedel Co., Dordrecht, Holland, 27.

Lebedinets, V. N., and Sosnova, A. K., 1969, Geomag. Aeron. 9, 550.

Lindblad, B. A., 1970, Smithson. Contr. Astrophys., in press.

Lovell, A. C. B., and Clegg, J. A., 1948, Proc. Phys. Soc. 60, 491.

Lovell, A. C. B., 1954, "Meteor Astronomy", Clarendon Press: Oxford.

Lyttleton, R. A., 1948, Mon. Not. R. astr. Soc. 108, 465.

Mainstone, J. S., 1960, Mon. Not. R. astr. Soc. 120, 517.

Manning, L. A., Villard, O. G., and Peterson, A. M., 1949, J. appl. Phys. 20, 475.

Manning, L. A., Villard, O. G., and Peterson, A. M., 1952, J. geophys. Res. 57, 387.

Marsden, B. G., 1967, Astr. J. 72, 1170.

Marsden, B. G., 1968, Astr. J. 73, 367.

Marsden, B. G., 1969, Astr. J. 74, 720.

McCrosky, R. E., and Posen, A., 1961, Smithson. Contr. Astrophys. 4, 15.

McCrosky, R. E., and Soberman, R. K., 1963, Smithson. Contr. Astrophys. 7, 199.

McCrosky, R. E., and Ceplecha, Z., 1969, Smithson. Astrophys. Obs. Spec. Rep. No. 305.

McIntosh, B. A., 1962, J. atmos. terr. Phys. 24, 311.

McIntosh, B. A., 1963, Can. J. Phys. 41, 355.

McKinley, D. W. R., 1961, "Meteor Science and Engineering", McGraw-Hill, New York.

Millman, P. M., 1968, I.A.U. Symposium No. 33 "Physics and Dynamics of Meteors", Kresák and Millman (eds), D. Riedel Co., Dordrecht, Holland, 3.

Nicolet, M., 1955, Spec. Supp. J. atmos. terr. Phys. 2, 99.

Nilsson, C. S., 1962, Ph.D. Thesis, University of Adelaide.

Nilsson, C. S., 1963, Observatory 83, 934.

Nilsson, C. S., 1964a, Aust. J. Phys. 17, 158.

Nilsson, C. S., 1964b, Aust. J. Phys. 17, 205.

Nilsson, C. S., 1966, Science 153, 1242.

Nilsson, C. S., and Alexander, W. M., 1967, Smithson. Contr. Astrophys. 11, 301.

Oort, J. H., 1950, Bull. astr. Insts Neth. 11, 91.

Öpik, E. J., 1934, Circ. Harv. Coll. Obs. No. 389.

Öpik, E. J., 1951, Proc. R. Ir. Acad A54, 165; Armagh Obs. Contrib. No. 6.

Öpik, E. J., 1958, "Physics of Meteor Flight in the Atmosphere", Interscience Publishers Inc., New York.

Öpik, E. J., 1961, Ann. Acad. Scient. Fennicae, Series A, III Geologica - Geographica 61, 185; Armagh Obs. Contrib. No. 34.

Öpik, E. J., 1963, Adv. Astr. Astrophys. 2, 219.

Paddack, S. J., 1969, J. geophys. Res. 74, 4379.

Pokrovskiy, G. I., 1964, Meteoritika 20, 95.

Poole, L. M. G., 1967, Smithson. Contr. Astrophys. 11, 157.

Porter, J. G., 1952, "Comets and Meteor Streams", Chapman and Hall, London.

Poynting, J. H., 1903, Phil. Trans. R. Soc. A202, 525.

Radzievskii, V. V., 1954, Dokl. Akad. Nauk SSSR 97(1), 49.

Richter, N. B., 1963, "The Nature of Comets", Methuen, London.

Robertson, D. S., Liddy, D. T., and Elford, W. G., 1953, J. atmos. terr. Phys. 4, 255.

Robertson, H. P., 1937, Mon. Not. R. astr. Soc. 97, 423.

Roper, R. G., 1962, Ph.D. Thesis, University of Adelaide.

Roper, R. G., 1965, (Editor) Laboratory Report, Physics Dept., University of Adelaide.

Simek, M., 1968, Can. J. Phys. 46, 1563.

Soberman, R. K., Hemenway, C. L., Ryan, T. G., Chrest, S. A., Frissora, J., Fullam, E. F., Balsamo, J. J., Cole, J., Hallgren, D., Yedinak, P., Goodman, A., and Hoff, G., 1963, Smithson. Contr. Astrophys. 7, 89.

Southworth, R. B., and Hawkins, G. S., 1963, Smithson. Contr. Astrophys. 7, 261.

Southworth, R. B., 1963, Smithson. Contr. Astrophys. 7, 299.

Southworth, R. B., 1968, I.A.U. Symposium No. 33 "Physics and Dynamics of Meteors", Kresák and Millman (eds), D. Riedel Co., Holland, 264.

Srirama Rao, M., Rama Rao, P. V. S., and Ramesh, P., 1969, Aust. J. Phys. 22, 767.

Stone, B. J., 1966, Laboratory Report, Physics Dept., University of Adelaide.

Terenteva, A. K., 1963, Smithson. Contr. Astrophys. 7, 293.

Terenteva, A. K., 1967, Smithson. Contr. Astrophys. 11, 109.

Terenteva, A. K., 1968, I.A.U. Symposium No. 33 "Physics and Dynamics of Meteors", Kresák and Millman (eds), D. Riedel Co., Dordrecht, Holland, 408.

U.S. Standard Atmosphere, 1962, U.S. Govt. Printing Office, Washington, D.C.

Verniani, F., 1961, Nuovo Cim. 19, 415.

Verniani, F., 1964, Nuovo Cim. 33, 1173.

Verniani, F., and Hawkins, G. S., 1964, Harvard Radio Meteor Project Res. Rep. No. 5.

Verniani, F., 1966, J. geophys. Res. 71, 2749.

Verniani, F., 1967, Smithson. Contr. Astrophys. 11, 61.

Verniani, F., 1969, Space Sci. Rev. 10, 230.

Vsekhsvyatskii, S. K., 1967, Soviet Astr. 11, 473.

Weiss, A. A., 1957a, Aust. J. Phys. 10, 299.

Weiss, A. A., 1957b, Aust. J. Phys. 10, 397.

Weiss, A. A., 1958, Aust. J. Phys. 11, 591.

Weiss, A. A., 1959, Aust. J. Phys. 12, 320.

Weiss, A. A., 1960a, Aust. J. Phys. 13, 532.

Weiss, A. A., 1960b, Mon. Not. R. astr. Soc. 120, 387.

Weiss, A. A., and Elford, W. G., 1963, Proc. Instn Radio Engrs Aust. 24, 197.

Whipple, F. L., 1950, Astrophys. J. 111, 375.

Whipple, F. L., 1951, Astrophys. J. 113, 464.

Whipple, F. L., 1954, Astr. J. 59, 201.

Whipple, F. L., 1955, Astrophys. J. 121, 241.

Whipple, F. L., and Hawkins, G. S., 1959, Handb. Phys. 52, 519.

Whipple, F. L., 1961, Astr. J. 66, 375.

Wright, J. W., 1967, J. geophys. Res. 72, 4821.

Wyatt, S. P., and Whipple, F. L., 1950, Astrophys. J. 111, 134.

Young, J. M., Johnson, C. Y., and Holmes, J. C., 1967, J. geophys. Res. 72, 1473.